The Role of STAT3 in the Pathogenesis of Chronic Lymphocytic Leukaemia

Sarah Brophy, B.A. (Mod)

A thesis submitted to Trinity College Dublin for the degree of Doctor of Philosophy

2018

Declaration

I declare that this thesis has not been submitted as an exercise for a degree at this or any other university and it is entirely my own work.

I agree to deposit this thesis in the University's open access institutional repository or allow the Library to do so on my behalf, subject to Irish Copyright Legislation and Trinity College Library conditions of use and acknowledgement.

_____

Sarah Brophy

September 2017

Acknowledgements

Firstly, I would like to thank my two supervisors Prof. Elisabeth Vandenberghe and Dr. Tony McElligott who gave me the opportunity to pursue this PhD. I am extremely grateful for their support, input and the opportunities they've provided to me over the past four years. I cannot say how much I appreciate how generous they were with their time and knowledge.

To Tony, words can't express how grateful I am to you for the amount of effort, time and technical training you've provided me. You were always there no matter what the issue and this thesis would not exist without you. If only you had a euro for every comma inserted in this thesis you could retire a millionaire!

Thanks to the Bone Marrow for Leukaemia Trust who funded this study and to the patients and staff of St. James's Hospital who participated in this study.

To Fiona, again, words cannot express how thankful I am to you for all of the time and knowledge you've given me. For introducing me to the world of diagnostics and molecular biology, not forgetting keeping my nails in shape! To Dave and everyone else in CMD who helped me at every turn, I really appreciate it. To Dr. Larry Bacon and Prof. Paul Browne and everyone who took time out to provide pointers and advice, thank you.

To everyone from 0.72 over the years, the friendships got me through those cold winters in the basement and you guys lit it up (even if there were no windows). To Eamon, for getting me out of the basement to the best office in the building. Thanks for all of your help along the way and for taking FlowJo when I couldn't bear to…You can have it forever! To everyone else in TTMI, especially Eoin, who was there to lend an ear for a rant or an idea in a time of need, thanks for helping me through.

To my friends and family, thanks for supporting me & always being there through this. To my mum, I cannot express to you how much I appreciate all that you have done for me, it would be longer than this thesis, and to my brothers, thanks for making sure there was always ink in the printer!

To Anne-Marie, you are my rock, thanks for the tea, hot water bottles and long nights listening to me talk about this thesis. I'm sure you never want to hear the word STAT3 again for as long as you live……. And as for apoptosis…….

This thesis is dedicated to my Dad.

Summary

Chronic Lymphocytic Leukaemia (CLL) is characterized by the accumulation of CD5/19+ B cells in the blood, bone marrow and lymph nodes. The tumour microenvironment of the bone marrow and secondary lymphoid organs promotes cell proliferation, survival and protection from drug induced apoptosis. Selectins, integrins and chemokines mediate the trafficking of CLL cells to these protective niches. An important adhesion molecule in this process is L-selectin (CD62L) which is involved in initial tethering and rolling of CLL cells in the high endothelial venules (HEV), allowing migration between the blood and the secondary lymphoid organs. Within the tumour microenvironment, the B-cell receptor (BCR) signalling pathway is the most important pathway involved in microenvironmental crosstalk and CLL cell survival, and has recently been shown to interact with the Signal Transducer and Activator of Transcription 3 (STAT3) signalling pathway. STAT3 is a transcription factor that regulates a number of genes involved in cell survival, proliferation and migration. Elucidating how CLL cells traffic to, and their interactions within, the tumour microenvironment may provide new avenues for therapeutic intervention in CLL. In this thesis, the role of STAT3 in the trafficking and microenvironmental interactions of CLL cells, and its potential as a therapeutic target, was investigated.

The role of STAT3 in CLL pathogenesis is unclear; however, it is constitutively phosphorylated on serine residue 727 (serine pSTAT3) in CLL cells. Phosphorylation on tyrosine residue 705 (tyrosine pSTAT3) was seen in 6 out of 28 CLL samples isolated from the peripheral blood of patients, and correlated with poor prognostic indicators (unmutated immunoglobulin heavy chain variable (IGVH) genes and NOTCH1 mutated patient samples). STAT3 targeting agents, Cucurbitacin and S3I-201, had a divergent effect on CLL cell survival, being pro-apoptotic in some and pro-survival in others. Cucurbitacin induced apoptosis was concurrent with a downregulation in serine pSTAT3. The upstream JAK inhibitor Ruxolitinib had no effect on serine pSTAT3 and apoptosis of CLL cells.

We investigated the role of STAT3 in the regulation of a panel of adhesion molecules involved in the migration of lymphocytes. Pharmacologically targeting STAT3, using Cucurbitacin ($p<0.0001$, $n=29$) and S3I ($p<0.0001$, $n=21$), and siRNA mediated STAT3 knockdown, resulted in a significant decrease in the cell surface expression of CD62L in CLL cells. The effect of Cucurbitacin on CD62L downregulation was greater in patient samples positive for the expression of the poor prognostic marker CD38.

We investigated the adhesion of CLL cells to human umbilical vein endothelial cells (HUVEC) under fluid shear flow conditions to model the interactions of CLL cells with endothelial cells in the HEV. We found that that blocking CD62L, using and anti-CD62L antibody, and treatment with Cucurbitacin resulted in a decrease in the adhesion of CLL cells to HUVECs under fluid shear flow ($p<0.001$, $n=5$). In addition to inhibition of CLL cell adhesion, pharmacological targeting of STAT3 using Cucurbitacin and S3I resulted in a significant decrease in CLL cell migration in response to the chemokine CXCL12 ($p<0.001$, $n=8$).

We investigated the effect of microenvironmental stimuli on the activation of STAT3 and the regulation of CD62L in CLL cells. Hs5 bone marrow stromal cell (BMSC) co-cultures resulted in an increase in tyrosine pSTAT3 and a significant increase in CD62L positive CLL cells ($p<0.01$, $n=7$). However; this did not overcome Cucurbitacin and S3I downregulation of CD62L.

The BCR is the most prominently activated pathway in CLL cells from the lymph node compartment. Stimulation of the BCR induced significantly increased tyrosine and serine phosphorylation of STAT3 in CLL cells with unmutated immunoglobulin (IGVH) genes compared to cells with mutated IGVH genes ($p<0.05$, $n=26$) . We show that BCR stimulation-mediated STAT3 phosphorylation is prolonged and suggest that it is a key target of the BCR signalling pathway. Stimulation of BCR also resulted in a significant increase in CD62L expression in patient samples, with increased upregulation seen in samples with UM-IGVH compared to M-IGVH ($p< 0.05$, $n=23$). Gene expression studies showed BCR stimulation also resulted in an upregulation of CD62L gene expression in CLL cells with unmutated IGVH genes. BCR stimulation-induced tyrosine pSTAT3 and upregulation of CD62L was abrogated by pre-treatment with the Janus kinase (JAK)/STAT3 inhibitor Ruxolitinib and the BCR inhibitor Ibrutinib ($p<0.05$, $n=5$).

In conclusion, this thesis shows a role for STAT3 in the pathogenesis of CLL. We have shown that STAT3 is an important regulator of the key adhesion molecule CD62L and is an important downstream mediator of the BCR signalling pathway. The down-regulation of CD62L expression, through BCR signalling pathway inhibition using Ibrutinib, and inhibition of STAT3 activation using Ruxolitinib, may have implications for the trafficking of CLL cells and present new potential therapeutic avenues for targeting CLL.

Abbreviations

AF	Alexa Fluor
ALL	Acute lymphoblastic leukaemia
AML	Acute myeloid leukaemia
APC	Allophycocyanin
APS	Ammonium persulfate
ATM	Ataxia telangiectasia mutated
AV	Annexin V
B2M	β2 Microglobulin
BCL2	B-cell lymphoma 2 protein
BCR	B cell receptor
BIRC3	Baculoviral IAP repeat-containing protein 3
BMSC	Bone Marrow stromal cell
BSA	Bovine serum albumin
BTK	Bruton tyrosine kinase
CLL	Chronic lymphocytic leukaemia
CML	Chronic myeloid leukaemia
C_t	Cycle threshold
DLBCL	Diffuse Large B-Cell Lymphoma
DMEM	Dulbecco's Modified Eagle's medium
DMSO	Dimethyl sulfoxide
dNTP	Deoxynucleotide Triphosphates
DTT	Dithiothreitol
EBV	Epstein Barr virus
EC_{50}	Half maximal effective concentration
ECM	Extracellular matrix
EDTA	Ethylenediaminetetraacetic acid
FACS	Fluorescence-activated cell sorting
FAM	6-carboxyfluorescein
FBS	Fetal bovine serum
FDC	Follicular dendritic cell
FISH	Fluroesence *in-situ* hybridisation
FITC	Fluorescein isothiocyanate
FRC	Fibroblastic reticular cell
GFP	Green Fluorescent protein
HCL	Hydrochloric acid
HEPES	4-(2-hydroxyethyl)-1-piperazineethanesulfonic acid
HEV	High Endothelial Venules
HM	Haematopoietic malignancies
HPRT1	Hypoxanthine Phosphoribosyltransferase 1
HRP	Horseradish Peroxidase
HSC	Haematopoietic stem cell
HSCT	Hematopoietic stem cell transplantation

HUVECS	Human umbilical vein endothelial cells
Ig	Immunoglobulin
IGVH	Immunoglobulin variable heavy chain
IL-4	Interleukin 4
IL-6	Interleukin 6
ITAM	Immunoreceptor tyrosine-based activation motif
JAK	Janus kinase
M-IGVH	Mutated Immunoglobulin variable region heavy chain
MCL1	Myeloid cell leukaemia 1
MDS	Myelodysplastic syndromes
MPN	Myeloproliferative neoplasms
MSC	Mesenchymal stromal cell
MTT	(3-(4,5-Dimethylthiazol-2-yl)-2,5-Diphenyltetrazolium Bromide
NFκB	Nuclear factor kappa-light-chain-enhancer of activated cells
NLC	Nurse like cell
PAGE	Polyacrylamide gel electrophoresis
PBMC	Peripheral blood mononuclear cells
PC	Proliferation centres
PCR	Polymerase chain reaction
PE	Phycoerythrin
PECAM1	Platelet endothelial cell adhesion molecule 1
PI	Propidium iodide
PI3K	Phosphoinositide 3-kinase
PIAS	Protein inhibitor of activated STAT
PVDF	Polyvinylidene difluoride
RIPA	Radioimmunoprecipitation assay buffer
RPMI	Roswell Park Memorial Institute
RQ	Relative change in expression
RT	Room temperature
SDS	Sodium dodecyl sulfate
SELL	Selectin L (CD62L)
SF3B1	Splicing factor 3B subunit 1
SHM	Somatic hypermutation
SHP	SH2-containing phosphatase 1
siRNA	Small interfering RNA
SOCS	Suppressor of cytokine signalling
STAT	Signal transducer and activator of transcription
TBS	Tris-buffered saline
TBST	Tris-buffered saline + 0.1% (v/v) Tween
TEMED	Tetramethylethylenediamine
UM-IGVH	Unmutated Immunoglobulin variable region heavy chain
VEGF	Vascular endothelial growth factor
VLA4	Very Late Antigen-4

Table of Contents

List of Figures

List of Tables

Chapter 1

Introduction

1.1 Haematological malignancies and Chronic Lymphocytic Leukaemia

Haematological malignancies (HM) comprise a group of heterogeneous diseases with varied epidemiology and prognosis. Accounting for 9% of all cancers, HMs are the fourth most common diagnosed cancer in developed countries according to Globocan 2012 Cancer Incidence, Mortality and Prevalence Report (Ferlay et al., 2010). The estimated prevalence of haematological malignancies in Ireland is in concordance with this, accounting for 8% of all cancers (Ferlay et al., 2010). The World Health Organisation (WHO) classifies haematological malignancies into two main groups, myeloid and lymphoid neoplasms shown in Figures 1.1 and 1.2. Myeloid neoplasms, derived from cells of the myeloid lineage, include acute myeloid leukaemia, myeloproliferative neoplasms (MPNs) and chronic myeloid leukaemia and myelodysplastic syndromes (MDS) (Arber et al., 2016). MPNs are a subgroup of diseases that are characterised by hyper proliferation of myeloid derived cells while MDS are a group of diseases affecting immature 'blasts' or stem cells leading to ineffective haematopoiesis. These disorders can progress to acute myeloid leukaemia (Huang et al., 2008, Lichtman, 2008). Lymphoid neoplasms, derived from cells of the lymphoid lineage, comprise mature B cell neoplasms, mature T and NK cell neoplasms, Hodgkin's lymphoma and multiple myeloma (Swerdlow et al., 2016). Mature B cell neoplasms include chronic lymphocytic leukaemia (CLL), one of four main leukaemia types. Other leukaemias include acute lymphocytic leukaemia (ALL), acute myeloid leukaemia (AML) and chronic myeloid leukaemia (CML). Acute leukaemias consist of non-functioning immature blasts that increase rapidly and are aggressive while chronic leukaemias are more mature cells that can retain some function and develop more slowly. A table of incidence and survival rates for each leukaemia type are shown in Table 1.1. Chronic lymphocytic leukaemia, a biologically complex haematological malignancy, is the most common leukaemia in the western world, accounting for ~40% of all adult leukaemia's (Howlader, 2013) and is the focus of this thesis. The incidence of CLL is higher in older people with 54% of CLL diagnoses in those 70 and older and occurring twice as much in men as in women (Nabhan et al., 2014, Pulte et al., 2015). These haematological malignancies occur when cells of haematopoietic origin undergo malignant transformation.

[1] Source: National Cancer Registry Report Dec 2010, http://www.ncri.ie/sites/ncri/files/pubs/CancerTrendsNo.6-Leukaemia.pdf. Accessed: 20/09/2017

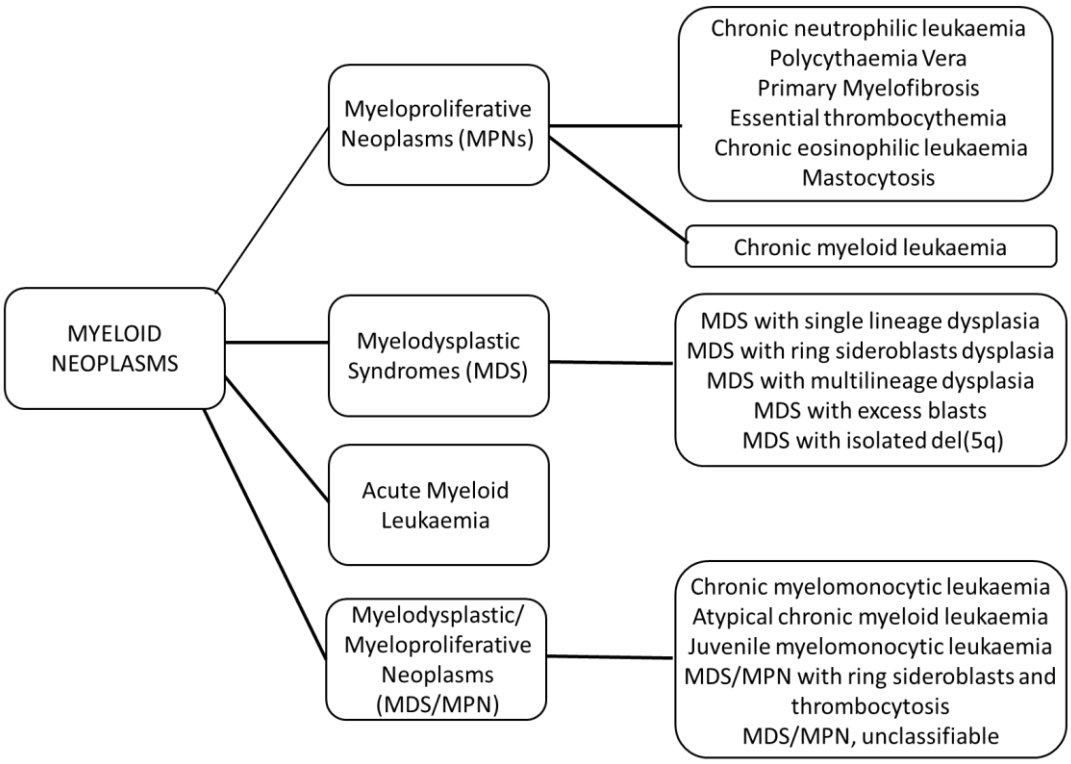

Figure 1. 1 World Health Organisation (WHO) classification of Myeloid Neoplasms WHO myeloid neoplasm classification based on information from (Arber et al., 2016)

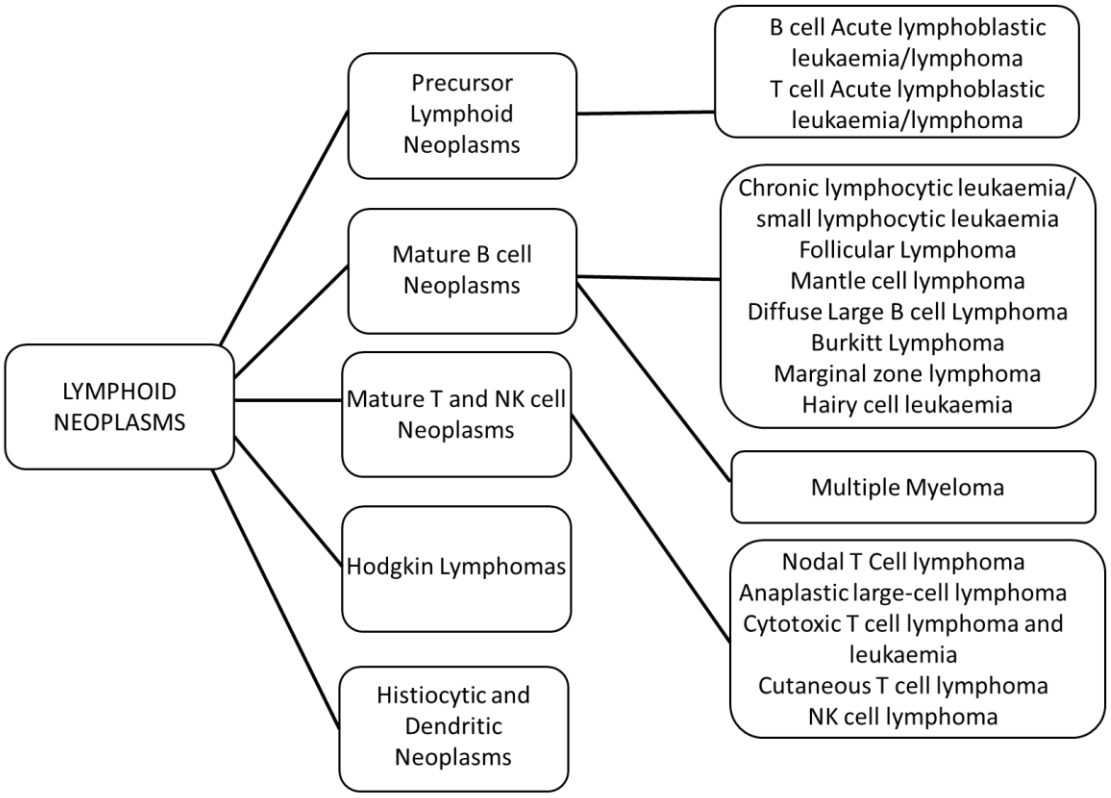

Figure 1. 2 World Health Organisation (WHO) classification of Lymphoid Neoplasms WHO lymphoid neoplasm classification based on information from (Swerdlow et al., 2016)

Table 1. 1 Incidence and survival rates for leukaemia subtypes in the UK and Ireland

Leukaemia	Incidence (per 100,000)[1]	5 year survival rate[2]
Acute lymphocytic leukaemia	1.38	66%
Acute myeloid Leukaemia	3.24	15%
Chronic myeloid leukaemia	0.85	51%
Chronic lymphocytic leukaemia	4.1	70%

1(Sant et al., 2010) ; 2 (De Angelis et al., 2015)

1.1.1 Haematopoiesis and the development of B cell malignancies

Haematopoiesis is the process through which a multipotent haematopoietic stem cell (HSC) commits to a particular lineage of cell through a number of differentiation steps (Figure 1.3). All cellular components of the blood are derived from HSCs in the bone marrow. These cells give rise to two types of progenitor cells; the myeloid progenitor which is the precursor cell of mast cells, eosinophils, basophils, neutrophils and macrophages, and the lymphoid progenitor; the precursor cell to natural killer cells and lymphocytes. The two main types of lymphocyte are T cells and B cells. These lymphocytes are part of the adaptive immune system that mounts specific responses to various antigens.

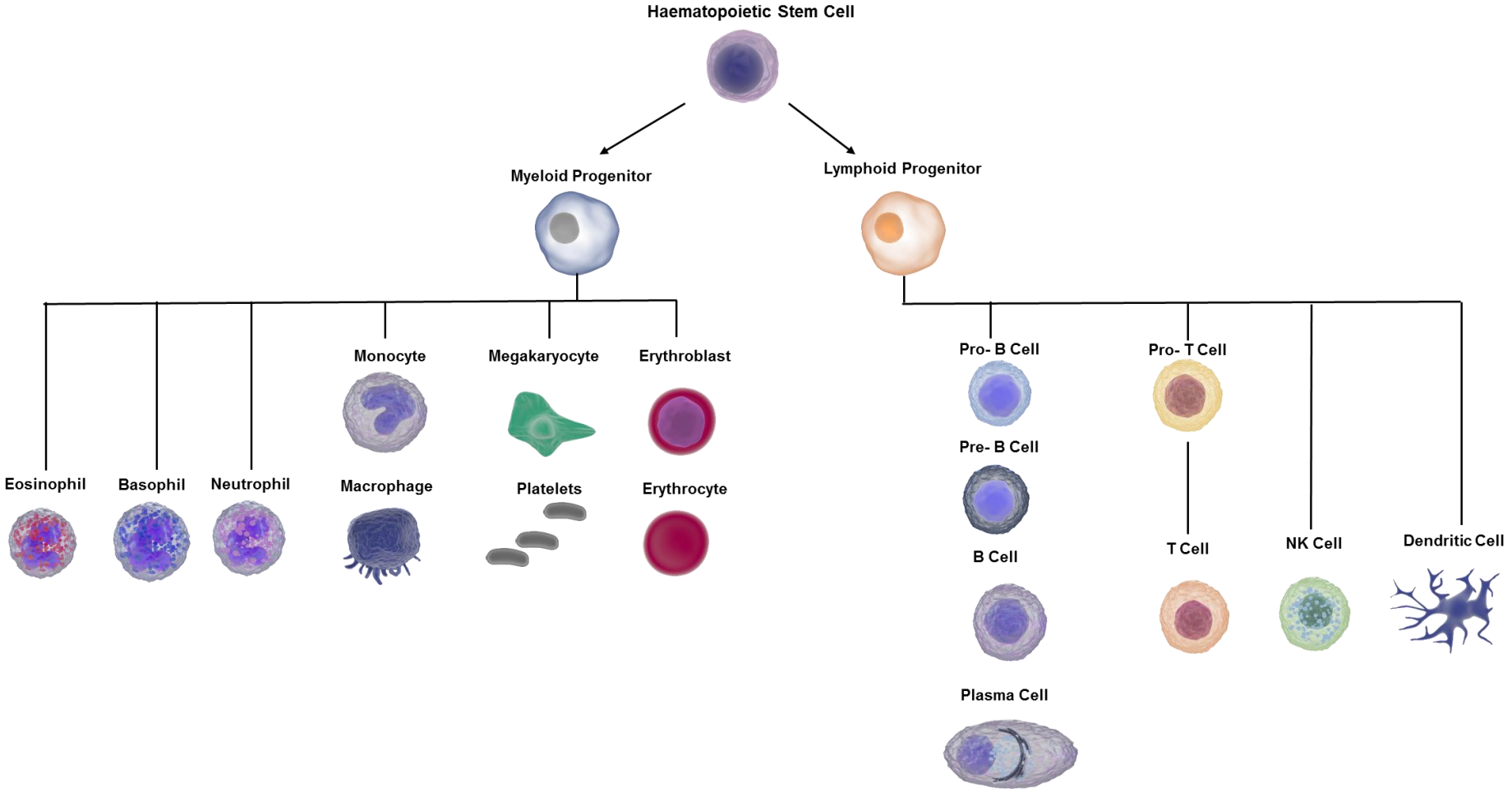

Figure 1. 3 The process of Haematopoiesis. All cells of the blood are derived from one common haematopoietic stem cell (HSC). The HSC differentiates into a myeloid progenitor which gives rise to the myeloid lineage of cells, eosinophils, basophils, neutrophils, macrophages, platelets and erythrocytes and a lymphoid progenitor which gives rise to cells of the lymphoid lineage, B and T cells, NK cells and dendritic cells.

B and T cells both originate in the bone marrow; T cells mature in the thymus, while B cells initially remain in the bone marrow and complete their maturation in the spleen and lymph nodes in order to become mature cells expressing immunoglobulins that recognise non-self antigens (Shortman, 1984, Campana et al., 1985, Osmond, 1990). The maturation process facilitates the development of a large number of different immunoglobulins allowing recognition of discrete epitopes. The initial steps of B cell development occur in the bone marrow independent of antigen where the pro-B cell undergoes heavy chain immunoglobulin gene rearrangement. The immunoglobulins consist of two heavy chains and two light chains that have constant regions and variable regions held together by disulphide bonds as shown in figure 1.4. The Variable (V) Diversity (D) and Joining (J) (VDJ) immunoglobulin gene segments code for the variable region of the immunoglobulin, which will engage with antigen. Rearrangement of the VDJ immunoglobulin gene segments enables the generation of highly variable antigen receptors, pre-B cell receptors (BCR), that are capable of recognising numerous different antigens. Enzymes called RAG1 and RAG2 initiate this process by introducing double strand breaks in the DNA which is then repaired by non-homologous end joining (Oettinger et al., 1990). Large pre-B cells downregulate the expression of the pre-BCR in order to progress to a resting small pre-B cell. Light chain rearrangement occurs and expression of a functional BCR with both a heavy and light chain, known as an immature B cell exits the bone marrow to the peripheral blood and secondary organs. There are two classes of light chain that can be selected by the B cell; kappa (κ) or lambda class (λ). Mature, naive B cells circulate until they are exposed to antigen within the microenvironments of the lymph nodes and spleen which trigger their maturation into B cell subsets including germinal centre, follicular and marginal zone B cells (Figure 1.5).

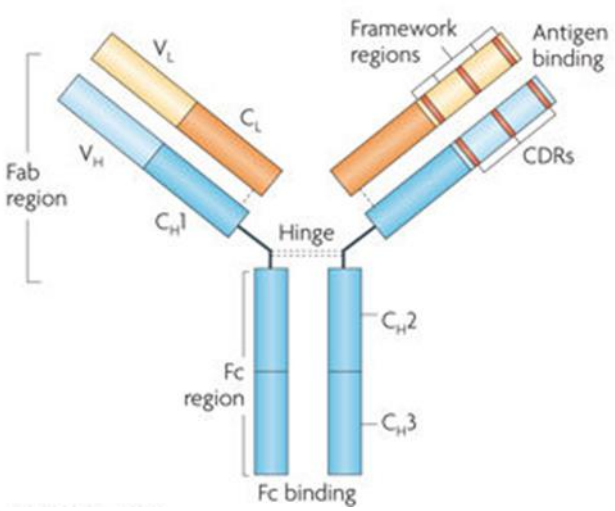

Figure 1. 4 The structure of an immunoglobulin molecule. The immunoglobulin is composed of two light (orange) and two heavy (blue chain) chains. These chains combine to create a Fab region linked to a constant Fc region by disulphide bonds. The light and heavy chain have constant (C_H and C_L) and variable (V_H and V_L) regions. The complementarity-determining regions (CDRs) of the variable regions bind antigen (adapted from (Hansel et al., 2010)).

The lymph node is composed of a cortex that contains primary follicles. When B cells encounter antigen and begin to proliferate, these primary follicles become secondary follicles or germinal centres. Signals received from the germinal centre B cells gives rise to activated and differentiated memory B cells and plasma cells (Klein and Dalla-Favera, 2008). Signal transduction through the BCR, T cell interactions and cytokines triggers class-switch recombination. Nine functional heavy chain (CH) switch gene regions are located downstream from the VDJ loci which encode separate domains, termini or hinges. Different expression of these CH gene segments can result in a switch of immunoglobulin isotype from IgM/IgD to IgG, IgE or IgA while maintaining the specificity for antigen. The choice of isotype is dependent on the type of antigen, signalling pathways activated by the antigen and signals from the microenvironment. Different isotypes determine the mode of antigen capture and mechanism of elimination, for example IgM is involved in the primary immune response to pathogen and is secreted as a pentamer that can opsonize or coat pathogens for killing by complement (Bjornson and Detmers, 1995). After exposure to antigen, B cells also undergo somatic hypermutation (SHM) which involves the introduction of a large number of point mutations in the V genes of both the heavy and light chains at a frequency of 10^{-3} to 10^{-4} base pairs per generation (Honjo et al., 2002). This results in B cells with a hugely diverse immunoglobulin repertoire (Liu et al., 1989). Although rare, it has also been reported that SHM can occur independent of T cell interaction, outside

of the germinal centres (William et al., 2002). Stimulated B cells rapidly respond to antigen and differentiate into antibody producing plasma cells or memory B cells.

Malignant transformation can occur at different steps in this maturation process resulting in different disease types (Fig 1.5). Genetic mutations and chromosomal translocations in the pre-B cell can result in B-cell derived acute lymphocytic leukaemia (ALL) (Iacobucci et al., 2012). Malignant transforming events in circulating mature B cells within the follicle that have not encountered antigen is thought to result in mantle cell lymphoma (MCL) (Kuppers, 2005). While germinal B cells that have encountered antigen give rise to a number of Non-Hodgkin's lymphomas, including diffuse large B cell lymphoma (DLBCL), Burkitt's lymphoma and follicular lymphoma, and are characterized by mutations in the V gene segments of the immunoglobulin heavy chain genes. Multiple myeloma is derived from antibody secreting plasma cells of the germinal centre.

Although the cell of origin for CLL is controversial, CLL is thought to develop at two points of B cell development resulting in two different subtypes of the disease (Ghia and Caligaris-Cappio, 2006, Chiorazzi and Ferrarini, 2011). As discussed, B cells that encounter antigen undergo somatic hypermutation of their immunoglobulin heavy chain variable region (IGVH). CLL with mutated IGVH is thought to be derived from germinal or post-germinal centre B cells that have undergone SHM (Stevenson et al., 2001) while unmutated IGVH CLL is derived from circulating mature B cells within the follicle that have not encountered antigen or undergone SHM.

Figure 1. 5 B cell development and the occurrence of B cell malignancy. Large pre-B cells develop from lymphoid progenitor cells in the bone marrow. The pre-B cell undergoes light chain rearrangement and differentiation steps to exit the bone marrow as a mature B cell. The B cell enters the lymph node and here the mature BCR expressing B cell is exposed to antigen and undergoes class switching and somatic hypermutation. Antigen stimulation results in activation and differentiation into memory B cells and antibody producing plasma cells. Green boxes indicate the points in this development where different B cell malignancies develop.

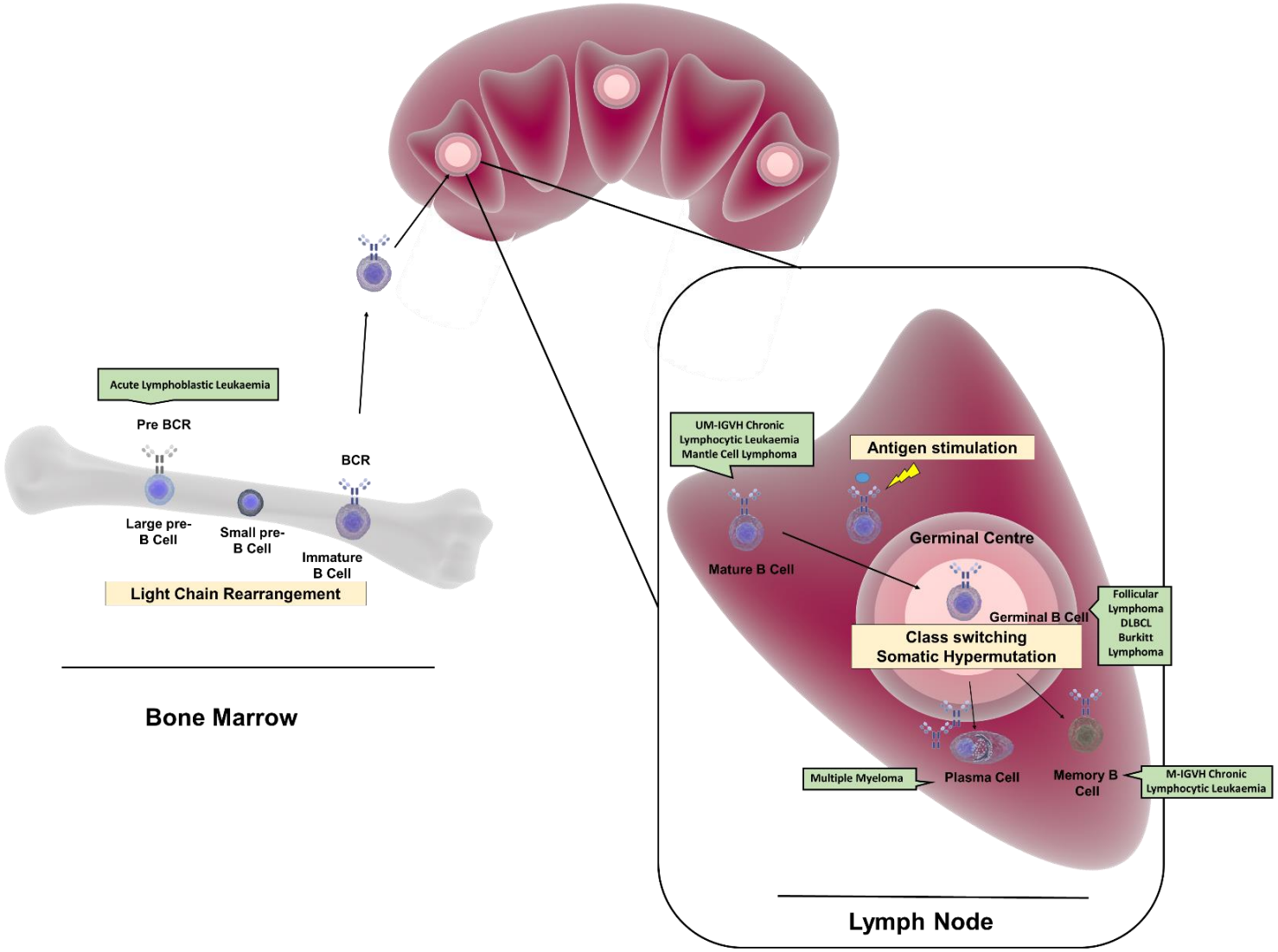

1.2 Chronic Lymphocytic Leukaemia

Chronic lymphocytic leukaemia (CLL) is classified clinically as a lymphoproliferative disorder characterised by the accumulation of small, round, immunophenotypically distinct B-lymphocytes in the peripheral blood, bone marrow, lymph nodes and spleen. The age and sex adjusted incidence rate of CLL in Europe is 4.92 per 100,000 with over 12,000 cases being diagnosed each year (Sant et al., 2010). CLL is diagnosed through blood counts, immunophenotyping and blood smears. A count of >5000/µl B lymphocytes in the peripheral blood with specific immunophenotypic signature, including the expression of antigens CD19, CD23 and CD20, the T cell antigen CD5 and clonal light chain restriction to kappa or lambda on B cells, are the diagnostic criteria for CLL (Scarfo et al., 2016). CLL cells also express lower levels of B cell receptor signalling subunit CD79b, CD20 and immunoglobulin than their normal counterparts (Eichhorst et al., 2015, Alapat et al., 2012). Additional cell surface markers detected by flow cytometry used in CLL prognostication include CD38 and CD49d. CD38 is a surface glycoprotein whose expression in CLL is associated with a poorer prognosis (Damle et al., 1999). CD49d is the α4 subunit of the α4β1 integrin, a molecule involved in adhesion and its expression is associated with unfavourable prognosis in CLL (Gattei et al., 2008). A cut-off of 30% is applied to both CD38 and CD49d expression in CLL (Zucchetto et al., 2012, Bulian et al., 2014, Gattei et al., 2008, Matrai, 2005).

Lymphocytes in the blood smear appear small and mature with very little cytoplasm, compacted nuclei, aggregated chromatin and no discernible nucleoli. Larger prolymphocytes are also present with the presence of >10% associated with a more aggressive disease (Hallek et al., 2008, Melo et al., 1986, Eichhorst et al., 2015). Monoclonal B lymphocytosis is a precursor condition of CLL that progresses to CLL at a rate of 1-2% per year (Rawstron et al., 2008). MBL can be defined as ‘high count MBL’ or ‘low count MBL’ depending on lymphocyte count in the peripheral blood in the absence of lymphadenopathy, organomegaly or cytopenias from bone marrow infiltration by the 2016 WHO Classification guide (Marti et al., 2005, Swerdlow et al., 2016). High count MBL requires routine follow up and is similar to very early stage CLL in phenotype and genetic profile.

Clinically, CLL can present as a stable, indolent form of the disease requiring no immediate intervention to an aggressive life-threatening form requiring treatment (Zenz et al., 2010). The Rai and Binet clinical staging systems are used to describe three major prognostic groups with distinct clinical outcomes (Rai et al., 1975, Binet et al.,

1977). These systems centre on two parameters, physical examination and complete blood cell count. The Rai system classifies patients according to: low, intermediate and high risk: low risk presenting with lymphocytosis in the peripheral blood and or bone marrow infiltration; intermediate risk also with the presence of lymphadenopathies or splenomegaly; and high risk with thrombocytopenia and or anaemia. The Binet staging system introduced in 1977 determines 3 risk categories based on complete blood cell counts and lymph node involvement by physical exam. Binet stage A includes patients with up to 2 lymphoid sites involved but no thrombocytopenia or anaemia, stage B greater than 2 lymphoid sites involved with no thrombocytopenia or anaemia and stage C the presence of anaemia and or thrombocytopenia aside from the involvement of lymphoid sites. Generally newly diagnosed asymptomatic patients (Rai 0, Binet A stage) are monitored with no intervention until there is evidence of disease progression. In patients that are Rai intermediate or high risk and Binet B or C treatment is usually initiated; however, some may be monitored until their disease progresses or they become symptomatic. 5-10% patients with CLL will progress to Richter's transformation, the development of aggressive lymphoma, normally diffuse large B cell lymphoma (DLBCL), which is associated with very poor prognosis (Jamroziak et al., 2015).

The cause/causes of CLL have not been identified however some risk factors have been suggested. Genetic predisposition is a known risk factor with a family history of haematological malignancies increasing relatives' risk of developing CLL by 2-to-8 fold (Slager et al., 2013, Slager et al., 2014). Lifestyle and occupational factors have also been suggested to have a link to increased risk of CLL diagnosis, including exposure to chemicals such as formaldehyde and benzene, working in the rubber manufacturing industry (Baan et al., 2009) and farming (Slager et al., 2014).

1.3 The Biology of CLL

A major breakthrough in determining the prognosis of CLL came with the discovery of two prognostic subgroups based on the mutational status of the immunoglobulin. The immunoglobulin complexes noncovalently to signal transducing heterodimers CD79a and CD79b to form the B cell receptor (Dylke et al., 2007). As described in section 1.1.1, normal, mature B cells express a BCR composed of a pair of heavy chain and light chain immunoglobulins. The class of heavy chain (α, δ, ε, γ, σ) determines the isotype of the antibody (IgA, IgD, IgE, IgG, IgM), which in the case of normal B cells is usually IgG or IgM expressed on the surface. The immunoglobulins express a unique

antigen binding site as a result of somatic hypermutation and rearrangement of immunoglobulin VJD genes. Analysis of IGVH gene rearrangements in CLL show unmutated IGVH genes (UM-IGVH) are found in 45-50% of CLL patients and are associated with a poorer prognosis and mutated IGVH genes (M-IGVH) being associated with indolent disease which normally requires less treatment and is less aggressive (Hamblin et al., 1999, Oscier et al., 2002, Hamblin et al., 2000, Damle et al., 1999). >98% sequence homology with the germline is used to distinguish between M-IGVH CLL and UM-IGVH CLL. The exact mechanism by which the BCR is stimulated in CLL and the type of antigen that activates it is not known but a number of antigens have been suggested. UM-IGVH have been shown to have polyreactive BCRs that can recognise and bind multiple motifs on apoptotic cells and bacteria (Herve et al., 2005, Catera et al., 2008, Lanemo Myhrinder et al., 2008), while M-IGVH have more restricted reactivity and recognise motifs from yeast and fungi (Hoogeboom et al., 2013).

The importance of the BCR and a role for antigen recognition in CLL pathogenesis is suggested by the fact that 1% of CLL have identical immunoglobulins and ~30% of CLL carry stereotyped BCRs, whereby BCRs from completely unrelated patients have similar gene segment usage in their antigen receptors (Agathangelidis et al., 2012, Messmer et al., 2004). Furthermore, certain subsets of stereotyped BCR respond to specific antigen, such as subset 6 which responds to myosin heavy chain II expressed in apoptotic cells (Chu et al., 2010), and certain viral antigens are associated with specific subsets, such as hepatitis C with subset 13 (Kostareli et al., 2012) and Epstein-Barr with subset 4 (Kostareli et al., 2009) These subsets can further inform on prognosis, for example M-IGVH that are subset 2 carrying IGHV3-21, show an aggressive clinical course similar to UM-IGVH CLL (Baliakas et al., 2015a).

Tonic signalling also contributes to CLL pathogenesis as several kinases remain activated in the absence of antigen stimulation; it been suggested that stimulation occurs autonomously by recognition of an epitope within the BCR itself (Binder et al., 2013) (Duhren-von Minden et al., 2012). The role of this autonomous signalling is not clear and does not reconcile with the differences in clinical outcome between M-IGVH and UM-IGVH CLL; however, autonomous signalling may work in combination with signalling by non-self antigens.

In normal B-cells, the BCR is utilized to promote proliferation, differentiation and the production of antibodies (Tsubata and Wienands, 2001). In comparison to normal B cells, BCR expression in CLL is considerably lower (Vuillier et al., 2005). In addition to this, the several subunits that comprise the BCR complex undergo dysfunctional folding and assembly in CLL cells compared to normal B cells (Payelle-Brogard et al., 2002). A

cascade of signalling events are triggered through activation of the BCR, discussed further in section 1.7.2, initiating a number of pro-survival pathways that result in cell proliferation, survival, migration and inhibition of apoptosis (Herishanu et al., 2011). Studies have shown that the ability of CLL subsets to signal through the BCR is different from normal B cells. M-IGVH CLL have a decreased signalling capacity and typically BCR signalling results in anergy (Packham et al., 2014). UM-IGVH retain capability to signal through the BCR and engagement of the BCR by antigen enables strong signalling that can result in anergy or proliferation.

1.4 The genetic landscape in CLL

In addition to IGVH mutational status, a plethora of prognostic markers can inform on prognosis, including cytogenetic abnormalities and genetic mutations. Fluorescence *in situ* hybridization (FISH) studies have revealed cytogenetic abnormalities in ~80% of CLL cases (Dohner et al., 2000). The most common cytogenetic abnormality is deletion 13q14 (del(13q)), occurring in in 50% of CLL cases resulting in loss of MIR15A and MIR16A, which function in the regulation of expression of apoptotic and cell cycle genes BCL2, cyclinD1 and cyclinD3 (Cimmino et al., 2005). Del (13q) alone is normally characterized by a benign course of the disease and favourable prognosis. Deletions in the long arm of chromosome 11, 11q23 (del (11q)) occur in 10-20% of patients, depending on disease stage, and are a negative prognostic marker in CLL. This aberration results in deletion of the DNA damage response kinase and tumour suppressor encoding ATM gene (Dohner et al., 1997, Stankovic et al., 1999). Larger deletions of 11q can also cover areas encoding for the negative regulator of NFκB, BIRC3, located near the ATM gene at 11q22. Loss of BIRC3 is associated with a loss of sensitivity to chemotherapy and poor prognosis (Rossi et al., 2012). Trisomy 12 is the third most frequent chromosomal abnormality, detected in 5-20% of CLL. Initial studies associated trisomy 12 with an aggressive clinical course (Matutes et al., 1996, Oscier et al., 1990); however, further studies have classified it as a marker of intermediate and even low risk disease (Dohner et al., 2000, Rossi et al., 2013c, Gunnarsson et al., 2011). Trisomy 12 occurs early in CLL evolution and is thought to be a driver mutation facilitating secondary mutations in genes such as TP53 (Landau et al., 2013, Falisi et al., 2014). Although the functional effects of Trisomy 12 are not fully known, it is thought to effect the expression of cell cycle regulators p27, and CDK4 and the negative regulator of p53, MDM2 (Winkler et al., 2005). Deletions in 17p13 (del(17p)) are found in 5-8% of treatment-naïve patients, increasing to 30% in

refractory CLL and results in deletion of the *TP53* tumour suppressor gene. Del(17p) is the poorest prognostic marker for CLL (Dohner et al., 2000). Del(17p) is one of the most commonly acquired abnormality after treatment and patients who acquire the deletion have a worse survival outcome compared to those with the de novo deletion (Tam et al., 2009). Patients with del(17p), in most cases, do not respond to DNA damaging chemotherapy agents, such as fludarabine and cyclophosphamide (Dohner et al., 1995), and also have shorter responses to monoclonal antibody treatments (Hallek et al., 2010) and kinase inhibitors (Farooqui et al., 2015, Byrd et al., 2013). The only current potentially curative option for patients with high-risk del(17p) that do not respond to therapy is haematopoietic stem cell transplantation (HSCT) (Dreger et al., 2007). Due to the discovery of a number of these biological and genetic variables that can add prognostic information, recently a new prognostic index, CLL international prognostic index (CLL-IPI) has been developed. CLL-IPI defines four groups, low, intermediate, high and very high risk groups based on five independent factors: clinical stage, using Rai and Binet classification; age; β2 microglobulin concentration; IGVH mutational status and TP53 status (Hallek, 2017).

Whole genome/exome sequencing has recently revealed additional mutations leading to a larger genetic signature for CLL. These include mutations in *TP53*, *NOTCH1*, *SF3B1, MYD88* and *BIRC3* (Puente et al., 2011). Although the poor prognosis associated with del(17p), mentioned above is well known, it has also emerged that mutations in TP53 are equally as unfavourable as deletions in CLL (Rossi et al., 2009). Mutations in the TP53 gene have been found in 4-35% of CLL cases (Zenz et al., 2008) and are an independent predictor of chemorefactoriness, rapid disease progression and poor survival. (Rossi et al., 2009). Although the other mutations have been used to predict prognosis, their role in predicting response to therapy is still being investigated

NOTCH1 mutation distribution varies across the clinical phases of CLL, increasing with disease aggressiveness, being found in 12% of patients with newly diagnosed CLL patients, increasing to 20% of patients with relapsed and progressive CLL, and further to 30%-40% in CLL patients progressing to Richter's syndrome. NOTCH1 mutations are indicative of a poor prognosis with shorter time to treatment and overall survival (Puente et al 2011, Oscier et al 2013, Rossi et al 2013, Fabbri et al 2011). NOTCH1 is a member of a family of type1 transmembrane receptors that are activated by Delta and Serrate/Jagged (DSL) ligands, cleaved by ADAM and γ-secretase proteases and, upon translocation of the intracellular portion to the nucleus, alter target gene

expression, including transcription factors, c-myc and NFκB (Vilimas,T. et al. 2007) and cell cycle genes p21 and Cyclin D1 (Ronchini,C. et al. 2001). 80% of NOTCH1 mutations in CLL are represented by a two base pair frameshift deletion (c.7544-754 5delCT). This two base pair deletion results in a NOTCH1 protein lacking a C-terminal PEST domain, a region involved in the proteasomal degradation and signal suppression of the protein, thought to result in a stable active isoform of NOTCH1 (Puente et al 2011, Di Ianni et al 2009, Sportoletti et al 2010, Willander et al 2013). Mutations in non-coding regions of NOTCH1 occur in 2% of untreated patients (Larrayoz et al., 2017). A number of studies show NOTCH1 mutations correlate with high CD38 expression, trisomy 12 and UM-IGHV genes (Balatti et al 2011, Oscier et al 2013, Jeromin et al 2014). Studies have reported different results on the occurrence of NOTCH1 in combination with other mutations. The association of NOTCH1 and TP53 is controversial. Jeromin et al (2014) and Weissmann *et al* (2013) reported a significant association between NOTCH1 and TP53 mutations. However, Rossi *et al* (2012) reported that NOTCH1 mutations tend not to occur in those patients with TP53 mutations. This difference may be due to different patient cohorts or different methods for detecting NOTCH1 and TP53 mutations. Rossi *et al* (2012) showed the effect of NOTCH1 mutations on overall survival was similar to patients carrying a mutation or deletion in TP53.

The occurrence of Splicing Factor 3b subunit 1 (*SF3B1)* mutations ranges across studies with incidence of 3%-10% in newly diagnosed, untreated CLL patients and is associated with poor prognosis in CLL (Jeromin et al., 2014, Quesada et al., 2012). SF3B1 mutations effect subunits of the spliceosome which removes intron sequences from pre-mRNA transcripts to produce mature mRNA resulting in abnormal splicing in CLL (van der Feltz et al 2012). (Schwaederlé et al 2013, Quesada et al 2012, Oscier et al 2013). SF3B1 mutations are associated with the 11q chromosomal deletion (Quesada et al 2012, Jeromin et al 2014), correlate with unmutated immunoglobulin status and are mutually exclusive to TP53 mutations (Schwaederlé et al, Rossi et al 2011(Jeromin et al., 2014).

Mutations in Baculoviral IAP repeat-containing protein 3 (BIRC3) are relatively rare in CLL occurring in 2-4% newly-diagnosed CLL cases (Rossi et al., 2013b) increasing to 25% of cases in fludarabine chemorefractory CLL. BIRC3 disruption is associated with unfavourable prognosis in CLL (Rossi et al., 2012). BIRC3 regulates the NFκB pathway through negative regulation of MAP3K14, an activator of non-canonical NFκB pathway. Inactivation of BIRC3 results in proliferation and resistance to apoptosis (Zarnegar et

al., 2008, Conze et al., 2010). BIRC3 mutations are associated with del(11q) and trisomy 12 and occur mutually exclusively to del(17p) and TP53 mutations (Cortese et al., 2014, Baliakas et al., 2015b).

MYD88 mutations are found in 3-5% of CLL (Puente et al., 2011), and are associated with a favourable outcome (Martinez-Trillos et al., 2014, Landau and Wu, 2013). MYD88 is an adaptor protein for the IL1 receptor, IL1R. Signalling through the IL1-R/TLR signalling pathway results in the phosphorylation of MYD88 and ultimately the activation of NFκB. Mutations in MYD88 are associated with M-IGVH and low CD38 expression.

These mutations (table 1.2) do not occur in isolation and patients carrying multiple mutations have a poorer prognosis (Guieze et al., 2015). CLL cells can undergo clonal evolution, developing additional mutations leading to heterogeneous populations of genotypically distinct CLL cells after drug treatment. These additional mutations can lead to relapse and give rise to subclones that can be more aggressive and treatment resistant. Clonal evolution has been investigated in CLL and two common types of clonal evolution have been described, one in which a single subclone acquires additional driver mutations over time and secondly branched clonal evolution where two or more genetic subclones co-exist. In branched clonal evolution, some of the subclones that develop have been shown not to be present at diagnosis (Schuh et al., 2012, Ojha et al., 2015, Ouillette et al., 2013, Landau et al., 2013).

Table 1. 2 Cytogenetic abnormalities and mutations in Chronic Lymphocytic Leukaemia.

Cytogenetic abnormality/ Mutation	Occurrence in CLL at diagnosis	Prognosis	References
Del(13q)	50%	Favourable if sole cytogenetic aberration detected	(Dohner et al., 2000)
Del(11q)	10-20%	Poor	(Dohner et al., 1997)
Trisomy 12	5-20%	Controversial, poor, intermediate and low risk	(Matutes et al., 1996, Oscier et al., 2002, Rossi et al., 2013a, Gunnarsson et al., 2011)
Del(17p)	5-8%	Poor	(Dohner et al., 2000)
TP53 mutation	4%	Poor	(Rossi et al., 2009)
NOTCH1 mutation	12%	Poor	(Puente et al., 2011, Oscier et al., 2013)
SF3B1 mutation	3-10%	Poor	(Quesada et al., 2012, Jeromin et al., 2014)
MYD88 mutation	3-5%	Favourable	(Landau and Wu, 2013, Martinez-Trillos et al., 2014, Rossi et al., 2012)
BIRC3 mutation	2-4%	Poor	(Rossi et al., 2012)

1.5 B-cell homing and migration

B-cell trafficking to and from the blood vessels into the secondary lymphoid organs is a multistep process which involves a network of molecules, chemokines, integrins and selectins. This recirculation process is crucial to maintaining effective immune surveillance as it facilitates the search for, and presentation of, foreign antigens. (Gowans and Knight, 1964) and (Marchesi and Gowans, 1964) first showed evidence of this recirculation by transfusing radioactively labelled lymphocytes into rats and tracking their migration to the lymph nodes across the high endothelial venues (HEVs). Dendritic cells and naive T and B cells enter via the HEVs, specialised blood vessels containing a thick basal lumina, prominent perivenular channel and a plump and tall endothelial cell layer (von Andrian, 1996). These morphological features along with the expression of a distinct set of genes distinguish these vessels from normal venules and allow for the trafficking of lymphocytes to the secondary lymphoid organs. HEVs are normally only found in lymphoid organs (excluding the spleen) but malignancy can cause their development in non-lymphoid tissues, resulting in the infiltration of high numbers of lymphocytes to these tissues (Martinet et al., 2011). After exposure to antigen, activated dendritic cells enter through the HEVs in response to chemokines, especially CCL21 where they reside in the paracortex, close to the HEVs. It is thought that here they present antigen to naïve T and B cells coming through the HEVs (Wendland et al., 2011, Moussion and Girard, 2011). Lymphocyte trafficking to the secondary lymphoid organs through the HEVs occurs broadly in three steps, entry to the HEVs, migration to T- and B-cell zones and exit from the lymphatic system. A number of protein families, in particular selectins and integrins expressed on the homing lymphocytes, and sialylated carbohydrates, integrin ligands and chemoattractants expressed in the HEVs are crucial to the migration process. Initial adhesion and migration to the HEVs occurs as a multistep adhesion cascade (Figure 1.6). Carbohydrate and mucin-like molecules line the HEVs and are recognized by selectin molecules expressed on homing lymphocytes. Mucins are heavily O-glycosylated serine- and threonine-rich proteins that are sulphated, fucosylated and sialyated then expressed in the HEVs. These include glycosylation-dependent cell adhesion molecule 1 (GLYCAM1), CD34, nepmucin, podocalyxin and endomucin (Rosen, 2004, Umemoto et al., 2006). The initial interactions between lymphocytes and HEVs occur through the binding of CD62L to its recognised ligands CD34, GlyCAM1 or nepmucin and in particular to the carbohydrate moiety 6-sulpho siayl Lewis X. This interaction allows the slowing and rolling of lymphocytes along the endothelial layer and is the start of a multistep migration cascade. Chemokines within the HEV activate

integrins which mediate the sticking of lymphocytes to HEV endothelial cells. Follicular dendritic cells (FDC) and fibroblastic reticular cells (FRC) express CXCL12 and CXCL13 which form a chemokine gradient to attract lymphocytes towards the lymph nodes. Naive B cells express both CXCR4 and CXCR5, the receptors for CXCL12 and CXCL13 (Miyasaka and Tanaka, 2004). Engagement with these chemoattractants results in the activation of integrins, such as lymphocyte function-associated antigen- 1 (LFA-1 or CD11a/CD18), which causes lymphocyte arrest by binding to intracellular adhesion molecule- 1 and 2 (ICAM-1 and ICAM-2) expressed on endothelial cells (Lawrence and Springer, 1991). After initial adhesion, additional integrins that strengthen the adhesion of lymphocytes to the endothelial cells include integrins CD11b/18, CD11c/18 and CD49d. Lymphocytes then transmigrate between endothelial cells in a process called diapedesis using later adhesion molecules including CD38 and CD31 (Kinashi, 2005). T cells migrate to the paracortex, directed by CCL21 and CCL19 expressed by T cell zone FRC, allowing T cell accumulation. B cells also interact with FCR of T cell zone and migrate towards CXCL13 produced by FDC before entering B cell follicles (Bajenoff et al., 2006). Follicular B cells roll along FDCs in the centre of the follicle, which present antigens to the B cells, or travel along the marginal reticular stromal cells, spending approximately 24 hours in the lymph node in mouse models (Mueller and Germain, 2009, Roozendaal et al., 2009). Immature lymphocytes that have not experienced their specific antigen leave the lymph node through the efferent lymphatic system and return to the circulation. The trafficking of CLL cells between the peripheral blood and secondary lymphoid organs is important in the pathogenesis of CLL. CLL cells are found to migrate to structures similar to secondary follicles (where normal B cells differentiate and proliferate), but these structures are called pseudofollicles or proliferation centres (PC) and they differ morphologically to their normal counterpart (Ratech et al., 1988). Although the mechanism of CLL cells recirculation between these microenvironments is not as clearly defined as normal B cell migration, a number of studies have emerged, modelling CLL migration. These studies suggest there are phenotypically distinct subpopulations of CLL cells primed to home to lymph node microenvironment. Calissano et al. showed, using in-vivo deuterium labelling of CLL cells, that subclones of CLL cells exist, a proliferative compartment that are $CXCR4^{dim}$ $CD5^{bright}$ that have just emigrated from the lymph node and a resting compartment that are $CXCR4^{bright}$ $CD5^{dim}$. In addition to this, a shear force model of CLL cells interaction with endothelial cells and showed subpopulations of CLL cells with a propensity to migrate below the endothelial cell layer had higher levels of CD38 and CD69 (Walsby et al., 2014). They also showed that expression of CD49d correlated with CLL cells propensity to migrate and a better ability to activate T cells.

They suggest these cells are a subpopulation of CLL cells, similar to cells taken directly from the lymph nodes, that are primed to migrate (Pasikowska et al., 2016). As discussed below, the molecules mentioned here that are key to normal B cell migration are also thought to control CLL cell migration to the pseudofollicules within the lymph nodes.

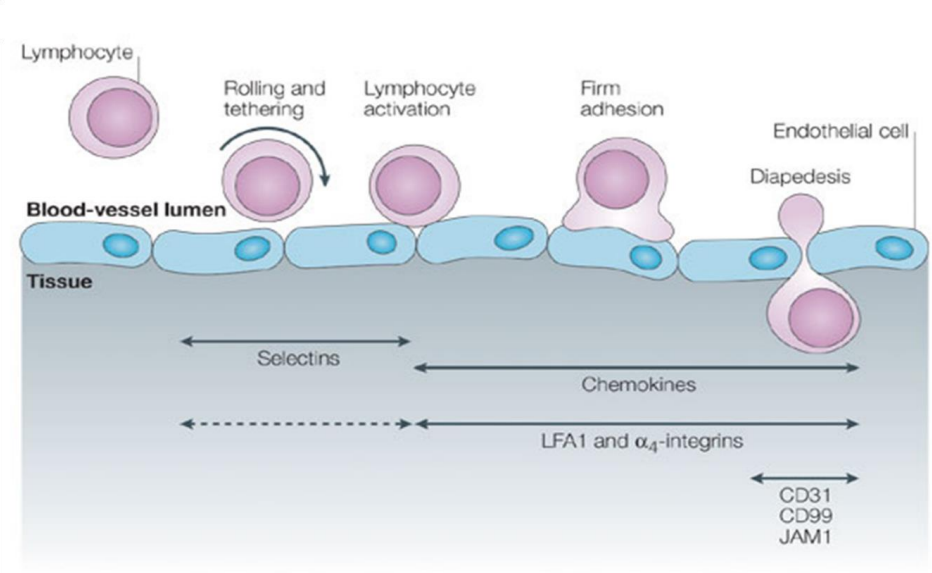

Figure 1. 6. Multistep process of lymphocyte adhesion and migration. Lymphocytes under shear flow initially begin to roll and tether using selectin molecules such as the selectin, CD62L. After adhering to the endothelial cell layer chemokines (CXCL12) activate integrins and integrins (CD49d) and further adhesion molecules (CD31) enable the adhesion and transmigration of lymphocytes (Kinashi, 2005).

1.5.1 Important Molecules in CLL cell homing and migration

1.5.1.1 Chemokines

Chemokines and their respective receptors are key factors in the organization, homing and communication between CLL and accessory cells. Chemokines have two important roles in creating the tumour microenvironment. Firstly, chemokines secreted by CLL cells, in response to external signals, such as CCL3, CCL4, CCL22 and IL8 can recruit accessory cells, such as T-cells and other immune cells, which support the proliferation and survival of CLL cells. Secondly, chemokines are secreted by stromal cells which play an important role in the chemotaxis and organization of CLL cells in the microenvironment. Important chemokines in the homing of CLL cells include CCL19, CCL21, CXCL9, CXCL10, CXCL12 and CXCL13. (Burger et al., 2009) (Davids and Burger, 2012). A characteristic chemokine receptor profile is seen on CLL cells and two of the most characterised of these are CXCR4 and CXCR5 and their

respective ligands CXCL12 and CXCL13. CXCL13 is a ligand known to act through the CXCR5 receptor (Widney et al., 2010). CLL cells express high levels of CXCR5 on their surface. Stromal cells in the lymph node secrete CXCL13, recruiting CLL and normal lymphocytes to the lymph node (Allen et al., 2004). CXCR5 and CXCL13, along with CCL19/CCR7 have been shown to play a role in the inhibition of apoptosis of B-CLL cells (Chunsong et al., 2006) through the inhibition of ERK1/2 and AKT/GSK3 pathways (Ticchioni et al., 2007). The engagement of CXCR5 activates downstream pathways involving PI3Kinase and MAP kinases which, results in actin polymerization and activation of integrins allowing chemotaxis to occur (Burkle et al., 2007).

CXCL12 is a ligand that elicits its effect via the CXCR4 receptor. CXCR4 is a G-coupled protein receptor involved in the normal processes of haematopoiesis, development and organisation of the immune system. CXCR4 is expressed on a number of cells, haematopoietic and non-haematopoietic (Murphy et al., 2000). CLL cells in the peripheral blood express CXCR4 at high levels on the cell surface and have been shown to migrate underneath CXCL12 secreting stromal cells in coculture. CXCR4 expression in CLL cells is lower in the lymph nodes and bone marrow because CXCL12 stimulation mediates CXCR4 endocytosis (Ghobrial et al., 2004). Bone marrow stromal cells secrete CXCL12 to form a gradient and activate CXCR4 on CLL cells. Activation of CXCR4 initiates downstream pathways involved in cell growth, such as MAP kinase-(ERK1/2), PI3K and STAT3 to increase the survival of CLL cells in addition to actin polymerization and migration across vascular endothelium (Burger et al., 1999, Bleul et al., 1996). CXCL12 functions in controlling the trafficking of mature B lymphocytes through the HEV to the lymph nodes and positions them within germinal centres (Allen et al., 2004), and also in directly inducing a prosurvival effect in CLL cells (Burger et al., 2000). Due to its role in CLL cell protection and chemotaxis, CXCR4 has been considered as a therapeutic target (Burger et al., 2005). CXCR4 antagonists such as Plerixafor (AMD3100) and T140 analogs, can mobilize leukaemia cells from their protective microenvironment by disrupting this pathway (Burger et al., 2009).

1.5.1.2 Selectins

Selectins are crucial molecules in the initiation of the multistep adhesion cascade that enables the migration of lymphocytes through the HEVs to the lymph nodes. The selectin family are single chain glycoproteins composed of an N-terminal C-type lectin domain, an epidermal growth factor-like domain, a transmembrane domain, a series of tandem repeats and a cytoplasmic tail (Kansas, 1992). The selectin family consists of

CD62P (P-selectin), CD62E (E- selectin), and CD62L (L-selectin). CD62P is expressed on activated platelets, both CD62P and CD62E are expressed on endothelial cells, and CD62L is expressed by all leukocytes. The three selectins bind to siayl Lewis X moieties on their respective ligands. CD62P and CD62L are very efficient at tethering cells under high fluid velocities while CD62E mainly supports rolling at very low flow rates (Kunkel and Ley, 1996).

The most important selectin in initiating the adhesion and migration of lymphocytes is CD62L. CD62L mediates cell-cell interactions through shear and catch bonds with its ligands GlyCAM-1, Spg200, CD34, MADCAM-1, ESL1 and PSGL1 expressed on endothelial cells (Mebius et al., 1993, Baumheter et al., 1993, Berg et al., 1993, Nicholson et al., 1998). CD62L can be soluble or membrane bound and contains a unique cleavage site that is cleaved by ADAMS17/TACE (Tu et al., 2002, Zhao et al., 2001). CD62L also functions as a signal-transducing molecule, mediating the activation of integrins that increase adhesion to the endothelium further (Steeber et al., 1997). There is variable expression of CD62L on CLL cells and it has been shown to be aberrantly glycosylated (Long et al., 2010, Prystas et al., 1993). In CLL, a critical role for CD62L in the adhesion of CLL cells to the walls of the HEV and migration to the lymph nodes has been demonstrated *in vivo* (Lafouresse et al., 2015). CD62L has also been shown to have a potential prosurvival role in CLL as CD62L blocking antibodies resulted in the induction of apoptosis in CLL cells (Burgess et al., 2017). It appears CD62L has a key role in CLL cell migration to the lymph nodes and interfering with CD62L-mediated CLL trafficking could therefore represent a novel therapeutic strategy in CLL.

1.5.1.3 Integrins

Integrins are a family of glycoproteins composed of α and β subunits that are expressed on CLL cell surface and are activated after chemokine and stromal cell contact, mediating CLL cell migration (Maffei et al., 2012). Key integrins in CLL cell migration include VLA4 and the CD11/CD18 family of integrins. VLA4, a heterodimer of α4 (CD49d) and β1(CD29) adheres to VCAM-1 on endothelial cells and fibronectin, a component of the extracellular matrix (ECM) (Elices et al., 1990) (Guan and Hynes, 1990) (Yago et al., 1997). CLL cells express variable but reduced VLA4 expression compared to normal B cells (Hartmann et al., 2009) but, despite its lower expression, VLA4 is functional in CLL. VLA4 plays a key role in mediating the adhesion of CLL cells to other accessory cells such as bone marrow stromal cells and the ECM resulting in their retention in the microenvironment (Burger et al., 2001). This VLA-4 dependent migration has been shown to be driven by autocrine VEGF production, a critical

requirement for CLL but not normal chemokine-mediated B cell migration (Till et al., 2005). Engagement of VLA4 by its ligands activates CLL cell signalling pathways cells resulting in the expression of transcription factors which promote cell-cycle progression, cell survival and reorganization of the cytoskeleton (Kumar, 1998).

Integrin alpha subunits (CD11a, CD11b and CD11c) dimerizes with the β2 subunit (CD18) to form molecules that bind fibrinogen (Postigo et al., 1991), ICAM-1 (Blackford et al., 1996) and ICAM-4 (Ihanus et al., 2007) which are expressed on endothelial cells (Berlin-Rufenach et al., 1999). CLL cells express this family of proteins and high expression of CD11c has been seen in CLL patients with splenomegaly suggesting it may have a role in migration of CLL cells to or retention within the spleen (Hanson et al., 1990).

1.6 The microenvironment in CLL

The protective tumour microenvironment encompasses the bone marrow and secondary lymphatic tissues, including the lymph nodes and spleen. Most of the cells located in the peripheral blood are arrested in G0/G1 stages of the cell cycle and proliferation occurs in pseudofollicles in the microenvironments of the lymph nodes or bone marrow. The importance of the microenvironment is shown by the fact once removed from the body, CLL cells undergo rapid apoptosis *in vitro* (Collins et al., 1989); however, this spontaneous apoptosis can be inhibited by a variety of coculture models such as stromal cells or fibroblasts (Shanafelt et al., 2008, Lagneaux et al., 1998). Clinically, it is often observed that, in response to chemotherapy, CLL cells in the lymph nodes and bone marrow are protected and persist (Burger et al., 2009, Burger and Gribben, 2014). It is thought that the subset of malignant cells that persist, protected in the microenvironment, are subjected to the stress and selective pressure of therapies, resulting in the recurrence of more complex, resistant and aggressive disease (Meads et al., 2009, Shain et al., 2015). CLL cells within the lymph nodes and bone marrow interact with the stromal cells, T-cells and the extracellular matrix (ECM) in a number of complex interactions whereby CLL cells influence and shape their microenvironment (Figure 1.7). These protective niches provide pro-survival signals, enable the cells to survive, proliferate and replenish while also conferring drug resistance, (Burger et al., 2009) making targeting microenvironmental interactions a promising therapeutic target in CLL.

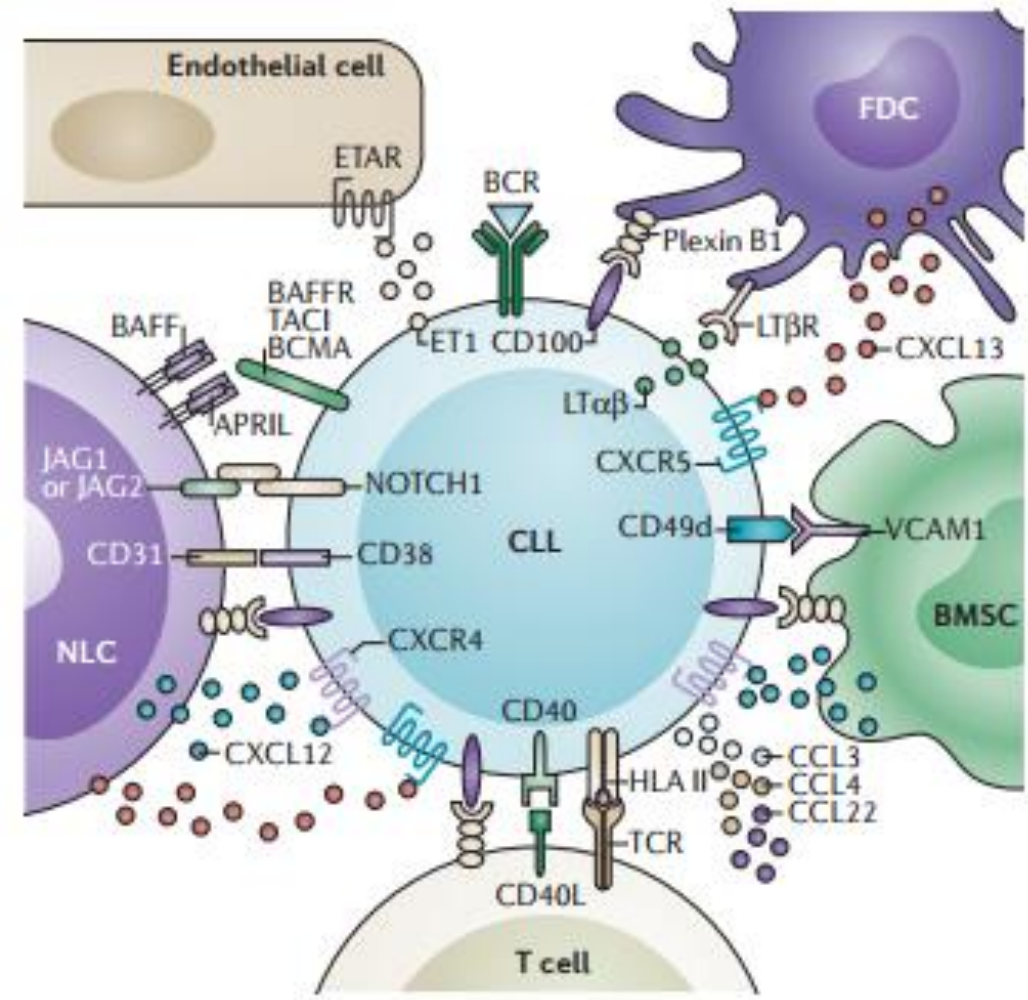

Figure 1. 7 The microenvironment in CLL. The microenvironment is composed of bone marrow stromal cells (BMSC), monocyte-derived nurse like cells (NLC), T cells, Follicular Dendritic Cells (FDC) and endothelial cells. Complex bi-directional crosstalk between CLL cells and cells of the microenvironment occurs through chemokine networks (CXCL12/CXCR4) and adhesion molecules (CD49d/VCAM) and other signalling molecules such as the B Cell Receptor (BCR) (Fabbri et al, 2016).

1.6.1 Cellular components of the CLL microenvironment

The main cellular players of the CLL microenvironment include bone marrow stromal cells (BMSC), monocyte-derived nurse like cells (NLC), T cells (Burger, 2011) and NK cells. Mesenchymal stromal cells (MSC), such as bone marrow stromal cells (BMSC), were the first stromal cell type found to contribute to CLL cell survival and proliferation (Panayiotidis et al., 1996). In CLL, BMSC provide growth factors and attachment sites to hematopoietic precursor cells to create this protective environment for the CLL cells. CLL cells have a high affinity for BMSC and contact with BMSC has been shown to protect CLL cells from both spontaneous and drug-induced apoptosis (Lagneaux et al., 1998). Pseudoemperipolesis, the rapid adhesion and migration of CLL cells beneath BMSC, is seen with the co-culture of CLL cells and BMSC (Burger et al., 1999). CLL

cell cross-talk with BMSC is bi-directional and contact with CLL cells (Ding et al., 2010) (Lutzny et al., 2013) results in the activation of NFkB and PKCβ, signalling molecules critical to BMSC function of supporting CLL cell survival. CLL secreted exosomes containing protein and mRNA can also activate BMSC, resulting in an increase proliferation and cytokine production (Paggetti et al., 2015). MSC are also present outside of the bone marrow in other lymphoid organs (Ruan et al., 2006) and provide protective, pro-survival signals that prevent apoptosis of CLL cells (Kurtova et al., 2009) through the upregulation of the BCL2 family proteins. MSC also upregulate surface receptors such as CD38 involved in cell migration and adhesion. Similar to BMSC, MSC crosstalk with CLL cells is bidirectional as CLL cells causes an increase in the production of vascular endothelial growth factor (VEGF) and platelet-derived growth factor (PDGF) while decreasing thrombospondin-1 in MSC, which is indicative of an angiogenic switch (Ding et al., 2009, Baeriswyl and Christofori, 2009). MSCs have also been shown to have a possible immunosuppressive role in their ability to suppress non-malignant T-cell proliferative responses, potentially contributing to the immune dysfunction seen in patients with CLL (Pontikoglou et al., 2013).

Nurse like cells (NLC) were found, initially, to function in thymocyte maturation and differentiation in the thymus (Wekerle and Ketelsen, 1980). *In vitro,* monocytes differentiate into nurse-like cells when co-cultured with CLL cells (Burger et al., 2000) and their importance has been shown in CLL animal models (Reinart et al., 2013). These NLC are round, large, fibroblast-like cells which CLL cells adhere to. They are found in the lymphoid tissues and spleen in patients with CLL (Tsukada et al., 2002). CLL cells attach to NLC and are protected from spontaneous and drug-induced apoptosis through expression of survival and proliferation regulating proteins, APRIL and BAFF, CD31 (Cols et al., 2012) and CD14 (Seiffert et al., 2010). NLC also induce expression of genes associated with BCR and NFκB signalling pathways in CLL (Burger et al., 2009). Cross talk is bidirectional and CLL cells secrete CCL3 and CCL4 to recruit NLC precursors, which in turn mature and produce CXCL12 and CXCL13 to attract more CLL cells to the protective niche of the lymph node and bone marrow (Burger et al., 2009).

The role of T lymphocytes in CLL is controversial. T cells have been proposed to have a range of different roles in the progression of CLL; they can either stimulate or suppress the CLL clone expansion. Certain T cell subsets (T-regulatory and γδ-Tcells) may overcome the anti-tumour effect of other subsets, to aid progression of the disease (Beyer et al., 2005). The absolute number of T cells (CD4 and CD8) is

increased in patients with CLL and higher numbers are associated with poor prognosis (Gonzalez-Rodriguez et al., 2010). Although higher in number, T cells from CLL patients have defects in their normal immune function resulting in a lack of cytotoxicity. T cells show chronic activation (upregulation of CD69, HLA-DR and CD57) and exhaustion markers (CD244, CD160 and PD1). CLL cells recruit T cells to the lymph node through the secretion of CCL2, 3 and 4 (Audrito et al., 2013). CLL cells can then influence T cells through immune checkpoint molecules, CTLA-4 and PDL1, (McClanahan et al., 2015) to change gene expression profiles inducing defective actin polymerization and reduced migratory capacity. CLL cell contact with T cells also results in an impaired formation of the immunologic synapse and this dysfunction can be repaired upon treatment with the immunomodulatory agent Lenalidomide (Ramsay et al., 2008, Serrano et al., 1997). Bagnara et al. (2011) have shown, in a murine CLL-transfer model, that CD4 T-cells adoptively transferred into the bone marrow and lymph nodes support CLL cell proliferation by releasing IL2, IL4, IFN-α and –γ and interacting with CD40 to inhibit the apoptosis of CLL cells (Buske et al., 1997, Fluckiger et al., 1992). T cells also produce IL2 and TNFα providing additional prosurvival signals to CLL cells (Riches et al., 2013, Plander et al., 2009), The reprogramming of autologous T cells to target tumour antigens, such as CD19, is currently under investigation in CLL and yielding promising results (Turtle et al., 2017)

CLL cells associate with Follicular Dendritic Cells (FDC) and Natural Killer (NK) cells in the bone marrow and lymph nodes. FDC interact with CD44 on the surface of CLL cells resulting in upregulation of anti-apoptotic MCL1 and protection from spontaneous apoptosis(Pedersen et al., 2002). NK cells within the CLL microenvironment have a lack of cytoplasmic granules and are defective in their ability to lyse CLL cells, in addition to cytoskeletal dysfunction and an inability to form immune synapses (Kay and Zarling, 1987). They express low levels of the activating receptor NKp30 and do not respond to the activation BAG6 ligand from CLL cells (Reiners et al., 2013). CLL cells exert similar effects on T cells and NK cells, inhibiting their cytotoxic functions and are thought to reshape their environment in order to evade immune detection and killing (Maki et al., 2008).

1.7 Microenvironmental mediated signalling pathways in CLL

The interaction of CLL cells with cells of the microenvironment activates a number of downstream signalling pathways critical to the survival of CLL cells and progression of the disease.

1.7.1 T cell signalling pathway

T cells within the germinal centres provide important prosurvival signals to CLL cells. CD40 is a member of the TNF superfamily of receptors and it is expressed on CLL cells, while its ligand CD40L is expressed on T cells in the germinal centres in CLL patients (Pizzolo et al., 1983) (Walker et al., 2000, Burger et al., 2009). Activation through CD40 results in the activation of PI3K and NFκB pathway, an increase in surface molecules CD95 and CD80 expression and an upregulation of antiapoptotic genes MCL-1 and BCL-2 (Scielzo et al., 2011, Cuni et al., 2004), inducing CLL cell proliferation and protection from apoptosis (Buske et al., 1997, Granziero et al., 2001, Douglas et al., 1997). It has also been shown that there is responsive heterogeneity to CD40L engagement and not all clones respond *in vitro (*Scielzo et al., 2011*)*. In addition to the CD40/CD40L interaction, IL4 is a prosurvival signal provided by T cells. CLL cells express higher levels of IL4 receptor than non-malignant B cells (Mainou-Fowler et al., 2001). Binding of IL4 to its receptor is known to activate JAK1/3 which phosphorylates STAT6. This further activates downstream mediators resulting in the expression of a number of apoptotic proteins including Bcl-XL and MCL1 (Steele et al., 2010). Higher levels of T cells expressing IL4 is associated with aggressive disease (Rossmann et al., 2002). IL4 administration has been shown to result in an increase in lymphocyte blood count indicating that IL-4 may have a stimulatory or an antiapoptotic effect on CLL cells in the peripheral blood (Lundin et al., 2001). These signals are of particular importance as CLL cells are primarily in contact with T cells expressing CD40L and IL4 in the protective niche of proliferation centres (Walker et al., 2000, Burger et al., 2009)

1.7.2 B-cell Receptor signalling pathway

The importance of the BCR in CLL pathogenesis, discussed in section 1.3, is demonstrated by the very different clinical course of the disease depending on the mutational status of the BCR. Functionally, cross-talk between CLL cells and the microenvironment occurs through downstream signalling pathways. The BCR signalling pathway, shown in figure 1.8, has been determined as the most prominently activated

pathway in CLL cells isolated from lymphatic tissue (Herishanu et al., 2011) and has been shown to be integral in CLL cell survival and proliferation. The lymphatic tissue in particular the lymph nodes, are the suggested primary site for BCR activation for both normal B cells and CLL cells; however, pseudofollicles in CLL differ from the germinal centres of normal lymph nodes. BCR expression is lower in CLL cells and assembly of the BCR differs in CLL cells compared to normal B cells. In addition to dysfunction in the assembly of the BCR in CLL, dysregulation is also seen in signalling pathways downstream of the BCR (Figure 1.8).

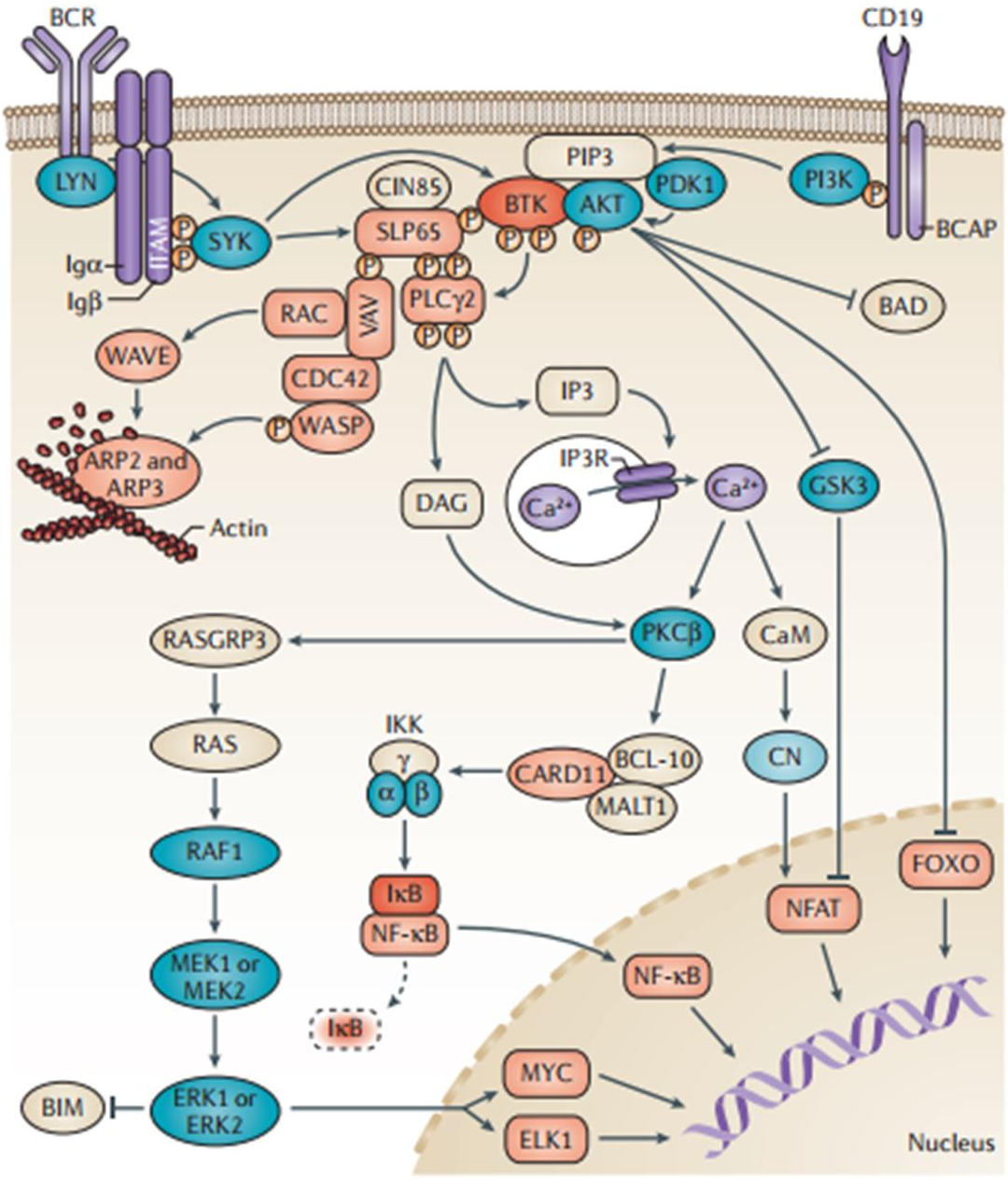

Figure 1. 8 The B cell receptor (BCR) Signalling Pathway. The BCR is stimulated resulting in the phosphorylation of the ITAM domain of the BCR by Lyn and Lck. This activation recruits Syk which in turn activates the formation of the signalosome. The signalosome is a multi-protein complex composed of PI3K, Btk PLCγ2 in addition to a number of other proteins. Downstream signalling results in the activation of a number of pathways including the MEK/ERK and NFκB pathways. Btk also activates Wiskott - Aldrich syndrome Protein (WASP) protein which alters the cytoskeleton. PI3K activates the Akt signalling pathway resulting in calcium mobilization. A number of pathways culminate in the activation of transcription factors such as forkhead box O (FOXO), Nuclear receptor of activated T Cells (NFAT) and MYC which effect the expression of genes involved in cell survival, proliferation and migration (Hendriks et al., 2014).

As discussed in section 1.1.1, the BCR is composed of the membrane immunoglobulin which binds antigen, and the signalling subunit of disulphide linked CD79a and CD79b. Antigen binding to the BCR results in BCR aggregation and initially activates upstream kinases Lyn or Lck which phosphorylate the cytoplasmic immunoreceptor tyrosine-based activation motif (ITAM) domains of CD79a and CD79b (Iacovelli et al., 2015, Burger and Chiorazzi, 2013, Bernal et al., 2001, Kurosaki, 1999). This provides a docking site for recruitment of further signalling proteins such as Syk (Liu et al., 2010, Rowley et al., 1995). BCR associated CD19 enhances the activation of ITAMs by enhancing the recruitment of Lyn and Syk (Fujimoto et al., 2000). Lyn and Syk are tyrosine kinases that have both been shown to be up-regulated in CLL cells and their activity amplified to the level of being constitutively activated in the case of Lyn (Buchner et al., 2010a). Inhibition of these kinases with known inhibitors has been shown to induce apoptosis, indicating their pro-survival role in CLL (Baudot et al., 2009). After phosphorylation of the ITAM motifs and recruitment of Syk the first step in BCR signalling is formation of the signalosome. Downstream of Syk and Lyn cytoskeletal protein HS1 is activated and F-actin polymerises. Syk activation is a critical step leading to the formation of the plasma membrane associated signalosome, assembling phospholipase-Cγ2, PI3K, Bruton tyrosine Kinase (Btk), BLNK, VAV and RAC. PI3K recruitment to the plasma membrane leads to the production of phosphatidylinositol 3,4,5-triphosphate (PIP_3), resulting in the activation of Btk and subsequent activation of Akt (Stevenson et al., 2011) The deregulation of the PI3K/Akt pathway also contributes to CLL cell survival.

PI3K family of proteins are divided into three classes and further into different isoforms. Class I has four isoforms, PI3K α, β, γ and δ. The γ and δ isoforms are expressed in haematopoietic cells with the δ isoform having an important role in B-cell function (Jou et al., 2002). PI3K, and resulting downstream Akt activation, can occur constitutively in CLL cells. In addition to this, many signals from the microenvironment, such as CXCR4 activation and adhesion to mesenchymal stromal cells cause PI3K activation. This results in the expression of antiapoptotic BCL2 family members such as MCL1, and the anti-apoptotic protein XIAP, all of which contribute to the survival of the CLL cell (Burger et al., 1999, Ringshausen et al., 2002, Edelmann et al., 2008). In addition toPI3K activation the Akt signalling pathway results in calcium mobilisation required for the phosphorylation of further protein kinases.

Btk is mainly expressed in haematopoietic cells, primarily in B-cells, not T cells or plasma cells (Genevier et al., 1994). In normal cells, Btk plays a role in the PI3K/Akt pathway and has also been shown to activate IκB, leading to the phosphorylation and translocation of NFκB to the nucleus (Petro et al., 2000). Btk also activates Wiskott -

Aldrich syndrome protein (WASP) which affects the cytoskeleton (Hendriks et al., 2014, Sharma et al., 2009). Btk interacts with CXCR4 and CXCR5 chemokine receptor signalling pathways and integrin activation, which function in cell migration and adhesion (de Gorter et al., 2007, Spaargaren et al., 2003). PLCγ-2 activates IP3 and DAG which also lead to calcium mobilisation and activation of PKCβ (Saijo et al., 2002). Following the activation of PI3K, Btk and PKCβ the signal is propagated through distal molecules such as MAPKs and NFκB. The activation of MAPK leads to the subsequent regulation of a variety of transcription factors, including c-Jun and ATF2 through p38 MAPK, and c-myc through Erk (Johnson and Lapadat, 2002). In normal B cells, activation of MAPK pathways leads to the phosphorylation of I-κB. I-κB is a kinase complex that attaches to NFκB in the cytoplasm, keeping NFκB in its inactive form. Upon its phosphorylation, I-κB is broken down leading to the translocation of NFκB to the nucleus where it exerts its effect on gene transcription. Both the MAPK and NFκB pathways are deregulated in CLL. Components of the MAPK pathway, Erk1 and Erk2, are upregulated in CLL, affecting CLL cell proliferation and survival (Krysov et al., 2012) .The dysfunction in NFκB leads to an upregulation of antiapoptotic genes resulting in increased survival of CLL cells (Furman et al., 2000). Signalling through these pathways culminates in calcium signalling and the activation of transcription factors NFκB, forkhead box O (FOXO) (Szydlowski et al., 2014), nuclear receptor of activated T cells (NFAT) (Antony et al., 2003) and MYC that control cell activation, proliferation, survival and migration. Regulation of BCR signalling intensity and duration involves tight control of signalosome activation by transmembrane receptors such as CD5, CD22, CD72 and FcγRIIB. These receptors, when activated by Lyn, control BCR signalling by recruiting phosphatases, such as SHPs, through their immunoreceptor tyrosine-based inhibition motif (ITIMs) to halt BCR signalling (Billadeau and Leibson, 2002).

BCR signalling is extremely complex due to these downstream pathways being in constant crosstalk with one another and the existence of multiple mechanisms for activation and repression of the multiple downstream targets. These pathways are tightly controlled in non-malignant cells by a number of regulatory cascades; however, as described, they are deregulated and amplified in CLL (Woyach et al. 2012) making them ideal therapeutic targets. Newer agents in use for the treatment of CLL that interfere with the BCR signalling pathway are discussed in section 1.9.

1.8 JAK-STAT Signalling Pathway

In addition to the signalling pathways discussed above, the JAK/STAT3 pathway has been shown to be activated by BCR stimulation (Rozovski et al., 2014). Signal transducer and activator of transcription (STAT) proteins are a seven member family (STAT 1, 2, 3, 4, 5a, 5b and 6) of proteins that function in a variety of cellular processes. STAT proteins have different functions but, broadly, STAT 2, 4 and 6 are mainly involved in interferon signalling and the development of T cells while STAT 1, 3 and 5 are involved in embryogenesis. In normal cells, latent cytoplasmic STATs are activated in response to cytokines and growth factors through tyrosine phosphorylation. STATs are phosphorylated on a single tyrosine residue towards the proteins' carboxyl terminus. Tyrosine phosphorylation of STATs leads to their dimerization, forming hetero- or homo-dimers, and translocation to the nucleus. In the nucleus, STATs bind DNA through specific DNA binding sites, resulting in increased transcription of target genes that regulate a number of cellular processes, including control of cell cycle progression, proliferation and apoptosis (Bromberg and Darnell, 2000). STAT activation normally occurs through receptor tyrosine kinases (cytokine receptor associated kinases e.g. JAKs) or growth factor tyrosine kinases and non-receptor tyrosine kinases e.g. *abl*. Each member of the STAT family responds to a specific set of cytokines and, in turn, regulates a group of defined genes. STATs often function in a feed forward loop whereby their downstream target genes encode cytokines and growth factors which then signal back through the same STATs enabling autocrine and paracrine STAT activation.

Some STATs also have a second phosphorylation site, on a serine residue in their carboxyl-termini. This serine phosphorylation is normally seen in addition to tyrosine phosphorylation. The biologic role of serine phosphorylation is not clear but has been shown to modulate STAT function. Studies have reported that phosphorylation on both tyrosine and serine residues can enhance transcription and is sometimes required for maximal activity (Chung et al., 1997, Wen et al., 1995) while others demonstrate that serine phosphorylation induces inhibitory activity (Lim et al., 1999). A number of kinases and signal transducers have been seen to play a role in serine phosphorylation, including MEK1/2, ERK1/2, p38 MAPK, PI3Kinase and JNK pathways (Decker and Kovarik, 2000).

1.8.1 STAT3

STAT3 is the only STAT family member required for embryonic survival (Takeda et al., 1997). Initially, it was discovered as an acute phase response protein activated in response to the IL-6 cytokine family (Zhong et al., 1994, Akira et al., 1994, Raz et al., 1994). STAT3 is involved in a number of physiological processes, including immune suppression, glycolysis and inflammation (Levy and Lee, 2002). STAT3 has the typical structure of a STAT family protein with an N-terminal coiled-coiled domain, involved in protein-protein interactions; a Src homology-2 (SH-2) domain, involved in stabilising STAT dimer interactions; a DNA-binding domain and a c-terminal transactivation domain. The transactivation domain contains the two phosphorylation sites; tyrosine residue 705 and serine residue 727. The STAT3 gene is located in chromosome 17 and has four known isoforms, STAT3α, STAT3β, STAT3γ and STAT3δ. STAT3α is the most predominant isoform while STAT3β is alternatively spliced to yield a protein with no C-terminal domain, lacking amino acids 723-770 (Maritano et al., 2004, Yoo et al., 2002, Zammarchi et al., 2011). While STAT3α is the main isoform involved in tumour development, the inactivated β form also translocates to the nucleus at high levels and remains phosphorylated for longer periods than the more transient STAT3α. However, the two isoforms regulate different sets of genes. STAT3β can also cross-regulate STAT3α, prolonging its phosphorylation and retention in the nucleus (Ng et al., 2012, Ng et al., 2014). The STAT3β isoform a has no serine phosphorylation site at residue 727 due to its truncated carboxyl-terminus (Schuringa et al., 2001, Huang et al., 2007). Few studies have investigated STAT3γ and STAT3δ but it is known that both STAT3γ and STAT3 δ are truncated isoforms of STAT3α and STAT3γ has been shown to play a role in neutrophil activation (Chakraborty and Tweardy, 1998), while STAT3δ has been shown to have a role in pancreatic cancer (Dettlaff-Pokora, 2010). STAT3 expression levels and activation vary from cell type to tissue type. The neutrophils of the bone marrow, leukocytes of the peripheral blood and the digestive tract have high basal STAT3 levels. In normal cells, ligand binding to a cytokine or growth factor receptor initiates the activation of glycoprotein130 or Src which dimerizes with the α subunit of the specific receptor. This complex can recruit and activate JAK2 which then phosphorylates tyrosine residue of the receptor, allowing the docking of STAT3 through its SH2 domain. STAT3 can also be activated directly by non-receptor tyrosine kinases, including Src and *abl* (Figure 1.9). Normally, within 30-60 minutes of exposure to stimuli tyrosine phosphorylation of STAT3 reaches its peak and STAT3 activation begins to decline, even when being continually exposed to the stimulus. In addition to phosphorylation, STAT3 can be acetylated, methylated and ubiquitinated at a number of sites. (Yuan et al., 2005). STAT3 is the only STAT family member that can also

translocate to the nucleus in its inactivated form, using nucleoporin transmembrane proteins (Herrmann et al., 2007). STAT activation is terminated by a number of mechanisms, including regulatory proteins such as the SOCS family of proteins and the protein tyrosine phosphatases (PTPs) (Croker et al., 2008). SOCS3 is an inhibitor of STAT3 that is controlled transcriptionally by STAT3, providing a negative feedback mechanism. The Src-homology domain-containing phosphatases (SHPs), protein inhibitor of activated STAT (PIAS) and protein tyrosine phosphatase receptor T (PTPRT) families also regulate STAT3 activation (Xu and Qu, 2008, Chung et al., 1997). This negative regulation of STAT3 is extremely important is preventing neoplastic transformation as continuous activation is characteristic of malignant cells.

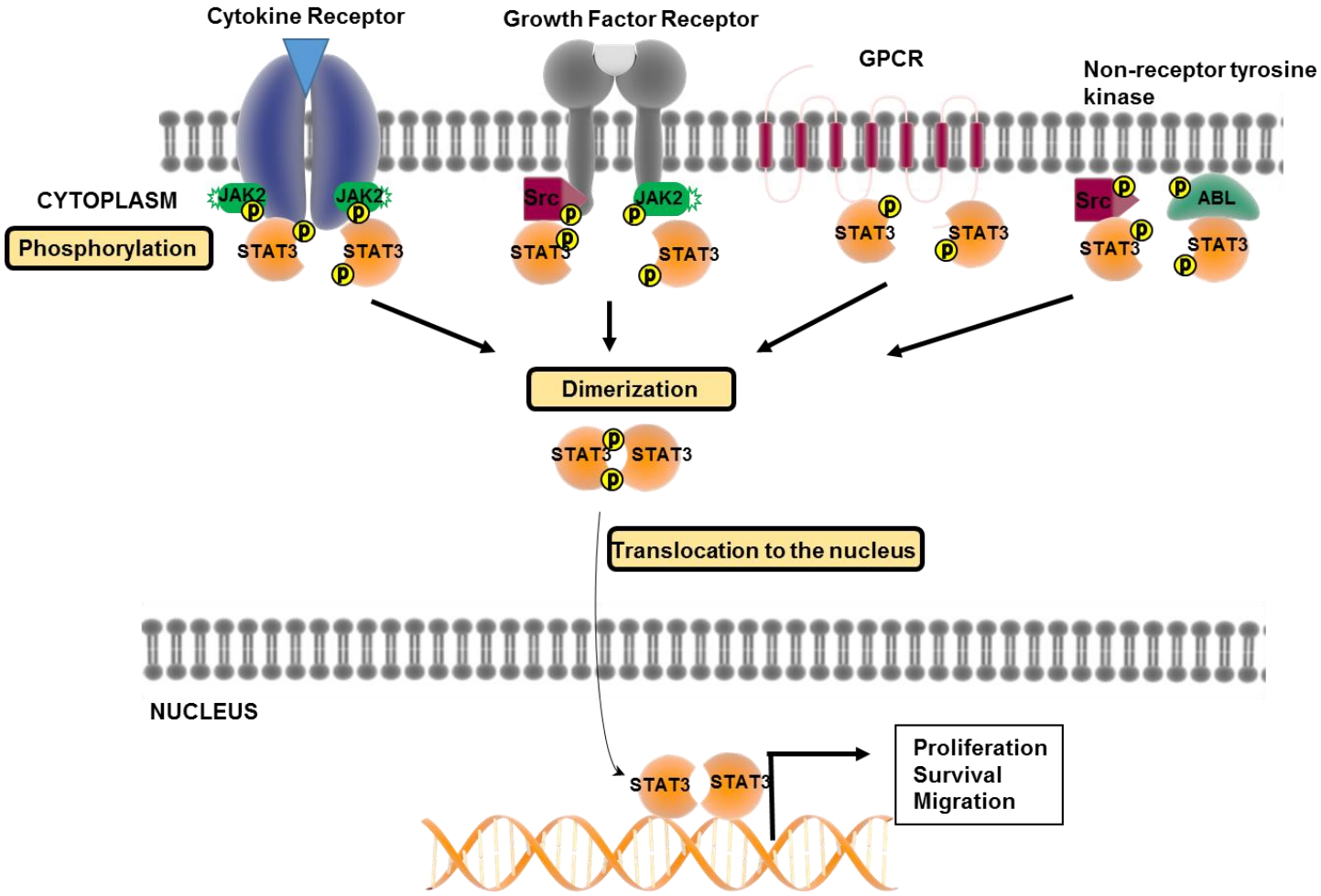

Figure 1. 9 **The JAK2/STAT3 Signalling Pathway.** STAT3 can be activated, normally by JAK2, through the phosphorylation of a tyrosine residue after engagement of cytokine receptor, growth factor receptors; G-protein coupled receptors and non-receptor tyrosine kinases. Activated STAT3 dimerizes and translocates to the nucleus. In the nucleus STAT3 binds to DNA and effects the expression of a number of different genes involved in proliferation, survival and migration.

1.8.2 The role of STAT3 in cancer

STAT3 has been has been shown to be overexpressed or constitutively active in a number of human cancers including lung (Jiang et al., 2011), prostate (Lou et al., 2000), breast (Garcia et al., 1997), ovarian (Wen et al., 2014), head and neck (Cattaneo et al., 1998), melanoma (Pansky et al., 2000) and lymphomas and leukaemias (Frank et al., 1997, Gouilleux-Gruart et al., 1996, Koskela et al., 2012, Mangolini et al., 2013, Zhang et al., 1996). This persistent activation has a number of effects in cancer cells, including an increase in proliferation, survival, angiogenesis and metastasis, while exerting an inhibitory effect on anti-tumour immunity (Frank, 2007, Bromberg and Darnell, 2000). Persistent activation can be maintained by positive feedback loops, disruption in negative feedback loops or genetic mutations. The upstream factors that are involved in positive feedback and contribute to the constitutive activation of STAT3 include the epidermal growth factor receptor, the IL-6 type cytokine receptor family that form complexes with JAKs and a number of G-coupled protein receptors (GCPRs). The deregulation of tyrosine phosphorylation in cancer has been well investigated. Signalling components that promote tyrosine STAT3 phosphorylation have been seen to be elevated or constitutively active in a number of tumour types and are usually associated with poor prognosis (Silva, 2004). Common deregulations of the negative mechanisms that regulate the STAT3 response in tumour cells include a decrease in the negative regulator SOCS protein (Chim et al., 2004). Lastly mutations in STAT3 that lead to its persistent activation have been found in chronic lymphoproliferative disorders of natural killer cells (CLPD-NKs), T-cell large granular lymphocytic leukaemias (T-LGLs) (Koskela et al., 2012) and diffuse large B-cell lymphoma (DLBCL) (Lohr et al., 2012, Hu et al., 2013).

The target genes of STAT3 are signature genes which contribute to the attributes of a tumour cell and are implicated in a number of events contributing to neoplastic cell development, including proliferation, survival, self-renewal angiogenesis and invasion (Hanahan and Weinberg, 2011). STAT3 targets Jun B, Egr-1 and cyclin D1 function in cell cycle entry and allow continued progression of the cell cycle. STAT3 allows cancer cells to survive and avoid apoptosis by upregulating the anti-apoptotic genes MCL1, BCL2, BCL-xl (Nielsen et al., 1999). STAT3 target genes play a role in invasion and metastasis of tumours with the potent pro-angiogenic vascular endothelial growth factor (VEGF) being regulated by STAT3. STAT3 also regulates the matrix metallo-proteinases which play a role in tumour invasion (Teng et al., 2014). The transcription of these genes can also be affected by other transcription factors, not just STAT3.

Additional studies have suggested STAT3 may have a tumour suppressive function in some tumour types. In mouse models of colorectal cancer, STAT3 inactivation results

in later tumour progression and this tumour suppressor role has also been shown in colorectal cancer cell lines (Musteanu et al., 2010, Couto et al., 2012). The oncogenic or tumour suppressive role of STAT3 is hypothesised to be due to different STAT3 isoforms, different post translational modifications and certain biochemical and genetic attributes of the cell. This has been shown in liver cancer, glioblastoma and oesophageal squamous cell carcinoma. Constitutively active STAT3 has a tumour suppressive role in ras-transformed hepatocytes lacking p19 but constitutively active STAT3 acts as an oncogene in liver tumours with p19 expression, while unphosphorylated STAT3 is oncogenic in the p19 knockout but tumour suppressive in the presence of p19 (Schneller D1, 2011). Similarly in glioblastoma, in tumours expressing the epidermal growth factor receptor (EGFR) but with low expression or a loss of PTEN, STAT3 has a tumour suppressive role while in the presence of both EGFR and PTEN, STAT3 drives tumour progression (de la Iglesia et al., 2008). STAT3β expression level is hypothesised to dictate the role of STAT3 as a driver or suppressor of tumour progression in oesophageal squamous cell carcinoma independently and through its interactions with STAT3α (Zhang et al., 2016).

1.8.3 The role of STAT3 in CLL

STAT3 pathway is involved in leukaemogenesis and its deregulation has been seen in a variety of haematological malignancies. Dysregulation is seen in both lymphoid and myeloid leukaemia including acute lymphoblastic leukaemia (ALL), multiple myeloma, acute myeloid leukaemia (AML) and CLL (Benekli et al 2003, 2009). STAT3 has been shown to be constitutively activated in ALL, as a downstream result of the TEL-AML1 signalling pathway, and cells with this translocation are sensitive to STAT3 inhibition (Mangolini et al 2013). Patients with constitutively activated STAT3 in AML also exhibit shorter disease-free progression than those without (Benekli et al., 2002). STAT3 has also been shown to be constitutively active in multiple myeloma cells (Catlett-Falcone et al 1999) and its down regulation disrupts the tumour microenvironment, causing a decrease in cell adhesion to bone marrow stromal cells, cytokine secretion and cell survival (Bharti et al 2004). Constitutive activation of STAT3 has been seen in AML (30%-100% of patients) and is associated with poor prognosis and short disease free survival (Benekli et al 2002).

Constitutive phosphorylation of tyrosine residue 705 has been commonly seen in a variety of haematological malignancies and solid tumours. However, Frank et al (1997) and Hazan- Halevy et al (2010) have shown STAT3 to be constitutively phosphorylated

on serine residue 727 in the absence of tyrosine phosphorylation in CLL. While the biologic role of this constitutive serine phosphorylation of STAT3 (pSTAT3) remains to be elucidated, CK2-BLNK-CD5 complex has recently been implicated in the induction of this serine phosphorylation of STAT3 in CLL (Rozovski et al., 2017a). Studies so far have indicated different roles for serine pSTAT3, some suggesting that the serine phosphorylation enhances transcriptional activity while others report contradictory results: that serine phosphorylation acts in an inhibitory fashion (Chung et al., 1997). The overall effect of serine pSTAT3 is probably dependant on cell type, extracellular stimulus and activation status of the cell. While constitutive serine pSTAT3 has been shown in CLL, transient tyrosine phosphorylation can be induced when cells are exposed to endogenous factors such as IL-6 and CXCR4 (Burger et al., 2005). Tyrosine phosphorylation is not required for serine pSTAT3 to bind DNA and serine pSTAT3 has been shown to translocate to the nucleus and bind to STAT3 specific DNA binding sites. Downstream, serine pSTAT3 was found to affect the transcription of STAT3 regulated genes such as BCL2, Pim-1, BCL-X_L and c-myc (Hazan-Halevy et al., 2010). It is most likely that serine pSTAT3 has an important role in the pathogenesis of CLL, enhancing survival of these cells through its activation of proliferation and survival genes (Frank et al., 1997). Roles for serine pSTAT3 have been demonstrated in CLL in the induction of VEGF (Badoux et al., 2011, Lee et al., 2005) and the regulation of the expression of a number of microRNAs (Rozovski et al., 2013) in CLL. It has also been shown to have a possible role in the regulation of MCL1 in CLL cells (Allen et al., 2011). NF-κB is constitutively activated in CLL cells and unphosphorylated STAT3 binds to and forms a DNA-binding complex with NF-κB, activating NF-κB regulated genes (Liu et al., 2011). Pharmacological inhibition and knockdown of STAT3 has been shown to result in the apoptosis of cancer cells including multiple myeloma and ALL cells (Redell et al., 2011, Bar-Natan et al., 2012) (Zhao et al., 2011, Han et al., 2014, Konnikova et al., 2003). In CLL, both shRNA targeting STAT3 (Hazan-Halevy et al., 2010) and pharmacological targeting, using JSI-124 (Cucurbitacin I), induced apoptosis in CLL cells and also to sensitized the cells to treatment with fludarabine (Ishdorj et al., 2011, Ishdorj et al., 2010).

1.9 Treatment of CLL

The treatment choice for CLL depends on a number of factors including the fitness and age of the patient and the progression and genetic profile of the disease. The front-line treatment for CLL in younger, fit patients with progressive disease is combination chemoimmunotherapy of purine analogue fludarabine, alkylating agent cyclophosphamide and anti-CD20 antibody rituximab (FCR) which was shown to have higher overall response rates than fludarabine and cyclophosphamide (FC) alone (Hallek et al., 2010). Unfit patients are given monotherapy, typically single cytostatic agents such as cyclophosphamide or chlorumbacil (Hallek et al., 2010, 1999, Fischer et al., 2016) or these agents with or without anti-CD20 antibodies Obinutuzumab or Ofatumumab (Frustaci et al., 2016, Hillmen et al., 2015, Goede et al., 2014) (Figure 1.10). Both FCR and single agents can have low response rates in patients with high risk del (17p) and/or mutated TP53. In addition to this, some patients do not respond to the therapy at all and others relapse quickly after treatment (Riches et al., 2011). Given the lack of response in these patient groups more targeted therapies have been investigated. Due to their restricted expression to B cells and key role in BCR signalling in CLL, Bruton tyrosine kinase (Btk) and PI3K have been targeted in CLL.

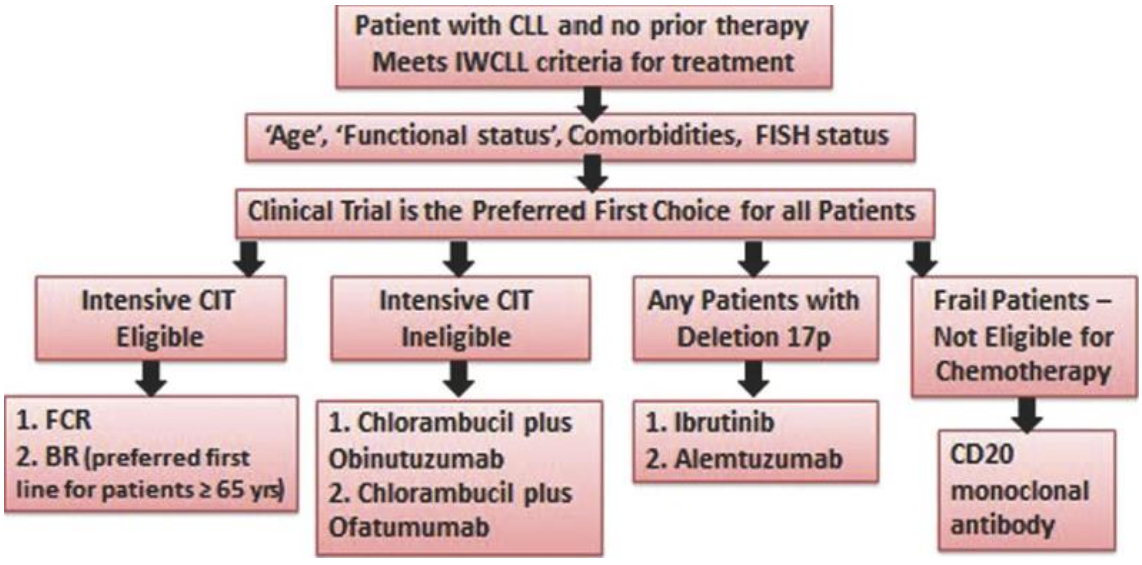

Figure 1. 10 Algorithm for the treatment of first-line CLL patients. CIT=Chemoimmunotherapy; FISH= Fluorescence *in situ* hybridisation (Jain et al, 2015).

Ibrutinib (PCI-32765) is a small molecule that inhibits Btk by irreversibly binding to cysteine-481 in the ATP-binding domain (Dubovsky et al., 2013). Ibrutinib is FDA approved for use in untreated and relapsed patients with CLL (Byrd et al., 2013, Burger et al., 2015). *In vitro*, Ibrutinib induces apoptosis in CLL cells alone and in culture with stromal cells and pro-survival soluble factors IL-4 and CD40L (Herman et al., 2011). Ibrutinib has also been shown to inhibit CLL cell migration towards CXCL12 and CXCL13 and prevent the release of CCL3 and CCL4 by CLL cells inhibiting the recruitment of T cells and monocytes to support the CLL cell (Ponader et al., 2012). Ibrutinib related toxicities include bleeding, diarrhoea, fatigue and infections (Byrd et al., 2013). Bleeding complications have been shown to be due the inhibition of platelet aggregation and other toxicities have been postulated to be due to off target effects on other kinases (Kamel et al., 2015) (Levade et al., 2014, Berglof et al., 2015, Gao et al., 2014).

Idelalisib (5-fluoro-3-phenyl-2-[(S)-1-(9H-purin-6-ylamino)-propyl]-3H-quinazolin-4-one) is a reversible inhibitor of the p110δ isoform of PI3K that has been FDA approved for the treatment of CLL (Coutre et al, 2014). *In vitro*, Idelalisib blocks survival signals through the B-cell receptor and induces caspase-dependent apoptosis in CLL cells alone and in culture with stromal cells and pro-survival factor CD40L (Herman et al., 2011), in addition to inhibiting migration towards CXCL12 and CXCL13 (Hoellenriegel et al., 2011). The most common toxicities seen with Idelalisib include pyrexia, neutropenia, pneumonia, diarrhoea and colitis (Furman et al., 2014). Clinically, both Ibrutinib and Idelalisib can cause a decrease in lymph node and spleen size and lymphocytosis, indicating a role for BCR signalling in CLL cell homing and migration (Woyach et al., 2012, Herman and Johnson, 2012, de Rooij et al., 2012, Ponader et al., 2012).

Resistance to Ibrutinib, in the form of C481S mutations in the binding site, have been described and mutations downstream of Btk leading to gain-of function been reported (Woyach et al., 2014b). Combination strategies may offer more options for durable responses and prevent the emergence of resistance and relapse, and a number of options are being investigated. In addition to this Ibrutinib carries a very high economic burden that is not sustainable as it is not a cure with the estimated per-patient lifetime cost of CLL treatment in the USA is predicted to increase 310% increase as targeted therapies such as Ibrutinib and Idelalisib become the first-line treatment (Chen et al, 2017). For these reasons, combinations of BCR inhibitors with other, considerably cheaper agents are being investigated. Ibrutinib and Idelalisib are undergoing

combination studies with chemotherapeutic agents and monoclonal antibodies (Chanan-Khan et al., 2016). Trials with Ibrutinib and CD20 targeting Rituximab in patients with del(17p) or TP53 mutation resulted in a 95% response rate. Combinations of Idelalisib with rituximab have proved effective in relapsed and older CLL patients (Furman et al., 2014, O'Brien et al., 2015). In addition, lymphocytosis as a result of treatment resolved quicker with two agents than with Ibrutinib alone (Burger et al., 2014). Novel, experimental agents are also being explored to prevent resistance, including second and third generation Btk inhibitors, for example ONO-4059 and Acalabrutinib (ACP-196) are more potent and selective Btk inhibitors than Ibrutinib that have shown durable responses in high-risk relapsed CLL (Walter et al., 2016) (Wu et al., 2016, Byrd et al., 2016). The second generation PI3K inhibitor Duvelisib (IPI-145) which targets the γ and δ isoforms is in Phase III clinical trials in relapsed/refractory CLL (O'Brien, 2014).

Other signalling molecules within the BCR pathway have also been targeted. The SYK inhibitor Fostamatinib had promising effects in a Phase II trial in relapsed/refractory CLL and a number of patients exhibited similar treatment induced lymphocytosis as seen with Ibrutinib and Idelalisib (Herman et al., 2013). A Lyn inhibitor Dasatinib has also undergone a small phase II trial for CLL in which 20% of patients responded (Amrein et al., 2011).

Novel agents, aside from targeting the BCR pathway, include BCL2 targeting agents such as Venetoclax (ABT-199), the first BCL2 inhibitor in routine clinical practice, which was FDA approved for use in previously treated patients with del(17p) after Phase II trials (Roberts et al., 2016, Roberts et al., 2017). Studies are ongoing on the first-line use of Venetoclax in unfit or elderly patients, as well as Venetoclax in combination therapy, particularly their possible use in combination with Ibrutinib and Idelalisib (Seymour et al., 2017, Flinn IW, 2015) (Deng et al., 2017). The development of these novel agents with emerging knowledge on the genetic landscape and prognostic indicators of CLL aim to find least-toxic, optimal combination of therapy. Given that TP53 deletion/mutation is currently the only response predictor clinically used, the identification of specific molecular and genetic features and will hopefully identify CLL subsets that will benefit from tailored treatment interventions and improved methods to target residual and subclonal disease.

1.10 Targeting STAT3 as a therapeutic strategy in CLL

This biologically significant role played by STAT3 presents it as a potential therapeutic target in the treatment of cancer. A key issue when considering a therapeutic target is the ability to use the target to treat malignant cells only, leaving normal cells unharmed. STAT3 is dispensable for normal cells and tissues, due to redundancies in signalling cascades. A loss of STAT3 in normal cells confers a decreased susceptibility to neoplastic transformation in a number of different types of cells (K. Schlessinger, 2005). Neoplastic cells are often characterized by constitutive STAT3 activation or require it continually and are said to have 'oncogene addiction', potentially making STAT3 an ideal therapeutic target (Demaria et al., 2010). While STAT3 is crucial for embryonic development, studies in mice have found it to be more dispensable to the function of normal, terminally differentiated cells (Takeda and Akira, 2001, K. Schlessinger, 2005). Inhibition of STAT3 in mice and humans results in moderate side effects in non-cancerous differentiated tissues (Park et al., 2014, Sen et al., 2012). STAT3 inhibition has also been shown to sensitize some cancer cells to chemotherapeutic agents, suggesting a role for STAT3 inhibitors in combination therapy (Alas and Bonavida, 2003, Spitzner et al., 2014). It is known that the inhibition of STAT3 is detrimental to tumours; however, attempts to develop a direct STAT3 inhibitor for clinical use has proved challenging. These agents mainly target the SH2 domain, N-terminal coiled-coil domain to disrupt STAT dimerization, or the DNA-binding domain. Problems arise with targeting these sites as they are large planar sites that are difficult for small molecules to bind to. Most small molecule inhibitors that are FDA approved bind the ATP binding cleft which STAT3 lacks (Fontaine et al., 2015). STAT family proteins are also highly homologous making targeting STAT3 specifically very difficult. A number of techniques have been implemented to identify direct STAT3 targeting agents, including compound library screens, virtual computer-based screening using STAT3 crystal structure, fragment-based drug design and alteration of natural STAT3 inhibiting compounds (Schust and Berg, 2004, Siddiquee et al., 2007, Li et al., 2011). These have resulted in the development of different types of STAT3 inhibitors including peptides and peptidomimetics, small molecules and oligonucleotides.

Despite a number of agents in preclinical studies showing efficacy across different cancer types few direct STAT inhibitors are in clinical trials and none are FDA approved for clinical use. A recently described STAT3 decoy oligonucleotide NSC-741763, has been shown to improve the survival of head and neck squamous cell

carcinoma in phase 0 clinical trials and a number of agents are undergoing clinical trials including OPB-31121, a novel STAT3 inhibitor (NCT00955812, NCT00511082, NCT1406574) (Oh et al., 2015, Hong et al., 2015).

Given the difficulty in the development of a direct STAT3 inhibitor, upstream targets of STAT3 have been investigated as an alternative to direct STAT3 inhibition. There are many protein tyrosine kinases that can phosphorylate STAT3 but a large area research has focused on JAK inhibitors. Clinical trials for JAK inhibitors have resulted in the FDA approval Ruxolitinib, a JAK1/2 inhibitor for myelofibrosis (Mascarenhas and Hoffman, 2012), and Tofacitinib, a JAK 1/2/3 inhibitor for rheumatoid arthritis and psoriasis (Hodge et al., 2016). Limitations to the use of JAK1/2 inhibitors include associated toxicities including anaemia and thrombocytopenia (Tefferi and Pardanani, 2011).

1.11 Aims and objectives

A number of signalling pathways, in particular the BCR signalling pathway, have been well studied in CLL; however, the role of the STAT3 pathway has been less investigated. Although new therapies have been developed there is a need for new therapeutic options for this disease (Roberts et al., 2017, Woyach et al., 2014b). Here, we seek to investigate the role of STAT3 in CLL pathogenesis and its potential as a therapeutic target in CLL. Initially, we will assess the phosphorylation status of STAT3 in CLL cells and the effect of pharmacological agents on this phosphorylation of STAT3 and CLL cell survival. Given the importance of cell trafficking and the tumour microenvironment in CLL, we particularly wish to investigate the role of STAT3 on the migration process, by assessing its effects on a panel of adhesion markers, in addition to chemotaxis and adhesion under the fluid shear flow conditions found in the high endothelial venules. Given the importance of crosstalk within the tumour microenvironment in CLL we will assess the role of STAT3 in this crosstalk with emphasis on the key BCR signalling pathway. Using a well characterized patient cohort the aim of the project is to better understand the role of STAT3 in the context of CLL heterogeneity. The specific aims of this study are to investigate:

Chapter 3: the role of STAT3 and the effect pharmacological inhibition of STAT3 on CLL cell survival.
Chapter 4: The role of STAT3 in the regulation of CLL cell adhesion; in particular, its role in regulating expression of the selectin CD62L, and the role of STAT3 in the chemotaxis of CLL cells and their adhesion under shear flow.
Chapter 5: The role of STAT3 in microenvironmental cross talk, in particular its function as a key downstream effector of BCR signalling.

Chapter 2

Materials and Methods

2.1 Materials and Patient Characteristics

2.1.1 Laboratory Reagents and Cell culture materials

All reagents were of analytical standard and were obtained from Sigma-Aldrich (St Gallen, Switzerland) or Thermo Fisher Scientific (Darmstadt Germany) and stored as per the manufacturer's instructions unless otherwise stated. All plastics were purchased from Thermo Fisher Scientific (Darmstadt Germany), unless otherwise stated. The EBV-transformed CLL cell lines I83 and HG3 were obtained from Prof. Anders Rosén (Linköping University, Linköping, Sweden) (Lanemo Myhrinder et al., 2008). Hs5 bone marrow stromal cells (BMSC) were obtained from American Type Culture Collection (ATCC®) (Manassas, VA, USA). Human Umbilical Vein Endothelial Cells (HUVECs) and Endothelial Cell Media were obtained from PromoCell (Heidelberg, Germany). Roswell Park Memorial Institute-1640 (RPMI) medium, Dulbecco's Modified Eagle's medium (DMEM), Trypsin (0.025% trypsin and 0.01% EDTA in Phosphate Buffered Saline (PBS)), Fetal Bovine Serum (FBS) Penicillin-Streptomycin (10,000 units/mL penicillin, 10,000 µg/mL of streptomycin) and phosphate buffered saline (PBS) were obtained from Gibco, Life Technologies (Darmstadt, Germany).

2.1.2 Reagents for Western blotting, immunofluorescent microscopy and flow cytometry

Rabbit polyclonal STAT3, pSTAT3 (Ser727), pSTAT3 (Tyr705) were obtained from Cell Signalling Technology (Leiden, Netherlands) and secondary goat anti-mouse used for western blotting were obtained from Santa Cruz Biotechnology (Heidelberg, Germany). Secondary HRP-linked anti-rabbit was from Sigma Aldrich (St Gallen, Switzerland). Hoechst 33342, Rhodamine Phalloidin and secondary Alexa Fluor 488 and Alexa Fluor 647 used for confocal microscopy were from Thermo Fisher Scientific (Darmstadt, Germany). Flow Cytometry antibodies were obtained from BD Biosciences (Nyon, Switzerland) (Section 2.2.6.1, Table 2.7). Annexin V-FITC was obtained from IQ Products (Groningen, Netherlands), Annexin V-PE was obtained from Immunotools (Friesoythe, Germany) and Propidium Iodide (PI) was obtained from Sigma-Aldrich. 25mg of PI was reconstituted in 25ml of sterile H_20 to give a stock solution of 1mg/ml.

2.1.3 Inhibitors and Proteins

Cucurbitacin I (Cucurbitacin) was obtained from Tocris Bioscience (Bristol, UK). 1mg of Cucurbitacin was dissolved in 193.3µl of DMSO to make a 10mM stock. S3I-201 (S3I), Ruxolitinib, Ibrutinib, and Idelalisib were obtained from Selleck Chemicals (Munich,

Germany). They were supplied as a 10mM solution in 1ml DMSO that was aliquoted and stored at -80°C. $F(ab')_2$ anti-human IgM fragments from MPbio (Alsace, France) were reconstituted in sterile H_2O up to a concentration of 3.5mg/ml. Recombinant human rh-CXCL12, rh-Fibronectin, rh-TNFα, rh-IL-4 and rh-IL-6 were obtained from R&D systems (Oxfordshire, UK). 10µg of CXCL12 and IL-4 were reconstituted in 100µl PBS containing 0.1% BSA to give stock concentrations of 100µg/ml. 50µg of Fibronectin was reconstituted in 50µl of sterile H_2O to give a stock concentration of 1mg/ml. TNFα and IL-6 were reconstituted in 100µl PBS containing 0.1% BSA to a stock concentration of 100µg/ml. CD40L was obtained from PeproTech (London, UK). 50µg was reconstituted in 100µl Sodium Phosphate Buffer (pH 7.4). This 0.5mg/ml stock was diluted 1:5 in PBS + 0.1% BSA to give a stock concentration of 0.1 mg/ml. Anti-CD62L antibody and isotype control were obtained from BD Biosciences (Nyon, Switzerland)).

2.1.4 SiRNA

ON-TARGET plus non-targeting control siRNA and SMARTPOOL STAT3 siRNA were obtained from GE Dharmacon (Cambridge, UK). 5nmol of siRNA was reconstituted in 250µl of 1X siRNA buffer as per manufacturer's instructions to make a 20µM stock that was stored at -80°C.

2.1.5 PCR Primers

Primers for mycoplasma detection, forward primer (5′-TGCACCATCTGTCACTCTGTTAACCTC-3′) and reverse primer (5′-GGGAGCAAACAGGATTAGATACCCT-3′) were obtained from Sigma-Aldrich (MO, USA). Primers for wild-type consensus NOTCH1 (5' GTG ACC GCA GCC CAG TT – 3'), forward primer for mutant NOTCH1 (5' TCC TCA CCC CGT CCC GA – 3') with reverse primers for NOTCH1 (5' AAG GCT TGG GAA AGG AAG -3') were obtained from Eurofins Genomics (Bavaria, Germany). TaqMan Gene Expression Assays (Section 2.2.14, Table 2.12) were obtained from Applied Biosystems (Netherlands).

2.1.6 Patient Sample Characteristics

CLL cells were isolated from patients following informed consent and their use for this project was approved by the St James's Hospital and Adelaide and Meath incorporating the National Children's Hospital Joint Ethics Committee. For patients presenting with elevated blood cell counts, lymphocytosis or symptoms such as fever, night sweats or weight loss, a peripheral blood sample was sent for immunophenotyping to the Immunophenotyping Laboratory, Department of Haematology in St. James's Hospital. Diagnosis of CLL requires monoclonal B cells with a characteristic immunophenotype based on guidelines by the European Society of Medical Oncology, National Comprehensive Cancer Network and International Workshop on Chronic Lymphocytic Leukaemia (Eichhorst et al., 2015, Hallek et al., 2008). In the Immunophenotyping Laboratory, samples are processed and stained by whole-blood staining and the following characteristics of the B cell population are indicative of CLL: CD200 positive, IgM weak to negative expression, FMC7 negative, CD20 weak, CD10 negative, CD22 weak, CD23 positive and CD79b negative expression.

The clinical characteristics, IGVH mutational status, CD38 and CD49d expression, NOTCH1 mutational status cytogenetics (del13q, trisomy 12, del11q, and del17p), Binet stage, bulky disease and treatment for the patient cohort used in this study are shown in table 2.1. PCR was performed as per section 2.2.2.3 for the detection of NOTCH1 mutations. Detection of IGVH mutational status was performed in collaboration with Dr. Fiona Quinn and the Cancer Molecular Diagnostics, St. James's Hospital as described in section 2.2.2.1 according to Ghia et al. (2007). Whole Blood staining of fresh CLL samples for flow cytometry was performed by Mr. David O'Brien, Immunophenotyping Laboratory, Department of Haematology, St. James's Hospital as described in section 2.2.2.2. Clinical information was supplied by Prof. Elisabeth Vandenberghe.

Table 2. 1 Clinical Characteristics for CLL patient samples

CLL Number	Binet Stage	WBC (10^9/L)	CD19+	CD19+/CD5+	IGVH		NOTCH1	Flow cytometry Markers		Cytogenetics			
					Mutation %	M/UM		CD38	CD49d	Del13q	Trisomy 12	Del11q	Del17p
2	A	50.1	92	98	100	UM	M	N	ND	N	N	N	N
4	B	169.2	96	99	95.00	M	UM	N	N	N	N	N	N
5	B	37.6	98	100	94	M	UM	N	N	P	N	N	N
6	A	69.7	91	99	98	UM	M	N	N	N	N	N	N
7	C	94.3	93	61	100	UM	M	N	ND	N	N	N	P
8	B	34	97	99	100	UM	M	P	P	N	N	N	P
9	A	30.6	76*	92	88.54	M	UM	N	P	ND	ND	ND	ND
11	A	NA	92	99	94.39	M	UM	N	ND	ND	ND	ND	ND
13	B	47.9	93	97	100	UM	M	P	ND	N	N	P	N
17	C	45.5	92	100	100	UM	M	N	P	ND	ND	ND	ND
19	A	183.5	97	94	ND	ND	UM	N	P	N	N	P	N
21	C	105.8	94	96	95.07	M	UM	N	ND	ND	ND	ND	ND
24	C	96	95	99	100	UM	M	N	P	P	N	P	N
26	A	139.4	93	100	100	UM	UM	P	N	P	N	P	N
27	A	28.1	97	96	99.51	UM	UM	N	P	N	N	N	P
28	A	103.7	96	51	ND	ND	ND	ND	N	ND	ND	ND	ND
29	C	138.6	97	99	95.79	M	UM	N	P	ND	ND	ND	ND
30	C	387	93	100	100	UM	UM	P	N	P	N	P	N
31	C	19.9	61*	98	100	UM	M	P	P	N	N	N	N
32	C	74.7	97	97	99.5	UM	M	N	N	N	N	N	N
33	A	58.3	94	100	94.17	M	M	N	ND	P	N	N	N
35	A	33	99	95	ND	UM	UM	N	ND	P	N	N	N
37	A	63.4	95	96	100	UM	UM	P	P	N	N	N	N
38	C	141.7	97	100	100	UM	M	P	ND	P	N	N	N
39	B	171	97	99	99.5	UM	UM	P	ND	N	N	P	N
40	A	NA	92	58	100	UM	UM	N	N	P	N	N	N
42	A	33.1	95	98	92	M	UM	N	ND	P	N	p	N
44	A	80.1	95	99	ND	ND	UM	ND	ND	P	N	N	N
45	A	38	92	99	96.01	M	M	N	N	P	N	N	N
48	C	32.5	97	44	99.05	UM	UM	N	N	N	N	N	N
50	B	132.8	93	100	98.21	UM	M	P	P	P	N	N	N

M= mutated; UM= Unmutated; ND= Not defined; P= positive, defined as >30% expression for CD38 and CD49d; N= Negative; Y= Yes; N= No; * B-Cell Isolation performed FCR= Fludarabine, Chlorambucil, Rituximab; Benda=Bendamustine; Alem= Alemtuzumab; Ritux= Rituximab; OFA= Ofatumumab; IDELA= Idelalisib

2.2 Methods

2.2.1 CLL patient samples

2.2.2 CLL cell characterisation

2.2.2.1 Detection of IGVH Somatic Hypermutation

Detection of IGVH somatic hypermutation was performed by Cancer Molecular Diagnostics, St. James's Hospital. Gene rearrangements of the antigen receptor occur during B cell development and are unique in sequence and length for each cell. PCR can be used to detect these individual V-J arrangements within the antigen receptor loci by using multiple consensus DNA primers that target conserved genetic regions within the immunoglobulin heavy chain gene. IGVH mutational status was assessed by PCR amplification of the V-J region followed by bidirectional sequencing and interrogation of the international ImMunoGeneTics (IGMT) database. The presence of IGVH somatic mutation is defined as greater than or equal to 2% difference from the germline variable gene sequence of the immunoglobulin heavy chain. Unmutated samples have > 98% similarity to the germline sequence.

PCR

A PCR Mastermix was prepared by combining 22.875µl of AmpliTaq Gold PCR Mastermix and 0.8µl MgCl2 Solution, 3µl 25mM dNTP Mix and 1.125µl of AmpliTaq Gold per sample in an Eppendorf. 50ng in 2µl of patient DNA or controls were added to the relevant tubes. Each run contained a 20% positive control, a 100% polyclonal control and a negative control. Tubes were run in an AB2720 thermocycler (MJ Research). After amplification, PCR reactions were stored at -20°C until electrophoresis was ready to be performed.

Samples were prepared to be analysed by an ABI 3130xl Genetic Analyser. A mastermix was prepared by adding 10µl HiDi formamide and 0.5µl of GS400HD size standard per sample and vortexing. 10µl of prepared mastermix was added to each well of a 96 well plate followed by 1.2µl of PCR sample. Samples were denatured by heating to 95°C for 3 minutes on a thermocycler (MJ Research). The plate was assembled in the ABI 3130xl Genetic Analyser plate holder and the ABI 3130xl was run and GeneMapper software was used to view unanalysed sample files. Positive, polyclonal and negative controls were checked. Using the controls, each patient was determined as clonal, biallelic/biclonal or polyclonal. A clonal peak was determined as one that appears within the expected size range at amplitude well above the polyclonal distribution. A biallelic/biclonal sample was determined as one in which two peaks

occur within the expected size range. A polyclonal distribution is characterized as a variety of peaks usually at low amplitudes within the expected size range. Biclonal/Biallelic samples, where more than one clone is evident, are then further analysed by performing IGVH somatic hypermutation analysis in cDNA that is generated from RNA from the sample. cDNA is prepared by creating a mastermix by combining 5µl of 5X Superscript first strand buffer, 1µl of 25mM dNTPs, 1.5µl H20, 2.5µl of 100mM DTT, 1µl of Random primers in addition to 12µl of RNA per sample in a 0.2ml PCR tube. Tubes were heated to 96°C for 2 minutes and chilled on ice for 5 minutes. 1µl of RNase Out and 1µl of Superscript II was added to each sample and samples were mixed. Samples were placed at 42°C for 90minutes, heated to 96°C and chilled on ice for 5 minutes. 1µl of cDNA and 1µl of H_20 were used to carry out PCR as described previously.

For samples showing a monoclonal peak post PCR, PCR products are cleaned up using the QIAquick PCR purification Kit (Qiagen, Netherlands) according to manufacturer's instructions

Sequencing of cDNA with Big Dye Terminators v3.1

In each sequencing run, a positive sequencing control which is a PCR product already identified as having a defined V region, a positive PCR control and an NTC control was run alongside the samples. Sequencing reactions were prepared by combining 4µl of Ready reaction mix (2.5X), 2µl Big Dye sequencing buffer (5X), 1.6µl primer (2pmol/µl), 5µl of purified PCR product and 7.4µl of sterile dH20 and ran in the ABI2720 Thermocycler.

Sequencing products were cleaned using Dyex spin columns (Qiagen, Netherlands) as per manufacturer's instructions and were used immediately or stored at -20.

Drying sequencing products

Sequencing products were placed in a heated vacuum centrifuge at 30°C for 20 minutes or until dry. When dry, 10µl of HiDi formamide was added to each dried reaction and left at RT for 5 minutes.

Electrophoresis of sequencing reactions

10µl of each sequencing reaction was added to wells of a 96 well plate and the rubber septa plate cover was placed on the plate. The plate was placed on the PCR thermocycler (MJ Research) and set to a 95°C soak program for 3 min without heated lid. The plate was placed on ice for 5 minutes and the white plastic plate cover was placed over the plate and the plate was run on the ABI3130xl. Results were analysed using LaserGene CoreSuite- Seqman Pro software and V Quest search engine in the IMGT database.

2.2.2.2 Whole Blood Flow Cytometry Diagnostic Panel

Whole Blood Flow cytometry was performed by the Immunophenotyping Laboratory, St. James's Hospital. This method allows the staining of leukocytes from fresh, whole blood. 5 15ml Falcon tubes were labelled and antibody mixes were prepared as per table 2.2. The peripheral blood was diluted to $2x10^6$ cells/ml in CellWASH (BD, Switzerland) and 100µl of whole blood was added to each tube. Tubes were placed in a BD FACS Sample Prep Assistant III and cells were washed by adding 2ml of CellWASH was added to tubes 1 and 2 from table 2.2 (IgM, kappa/lambda) and vortexed and centrifuged. The supernatant was removed and this was repeated twice more. The appropriate monoclonal antibodies (Table 2.2) were added to each individual tube and cells were vortexed and incubated at room temperature in the dark for 5 minutes. Tubes were then placed in the BD FACS Lyse Wash Assistant and 2ml of Pharm Lyse (10X buffered ammonium chloride diluted 1:10 with distilled water) (BD, Switzerland) was added to each tube, vortexed and incubated, in the dark at room temperature for 15 min. 1ml of Cell WASH was added to the tubes and they were vortexed and centrifuged to remove lysed antibody and unbound Fluorochrome. The supernatant was removed and cells were resuspended in 0.5ml CellWASH before running on the BD FACS Canto II flow cytometer (BD, Switzerland).

Table 2. 2 Chronic B Lymphoproliferative flow cytometry Panel

Tube	Antibody	Fluorochrome	Volume (µl)
1	CD5 FITC	FITC	20
	CD3 PE	PE	20
	CD19 PerCP-Cy5.5	PerCP-Cy5.5	20
	CD45 APC-H7	APC-H7	5
2	Kappa /Lambda	FITC/PE	20
	CD19	PerCP-Cy5.5	20
	CD38	APC	5
3	CD43	FITC	20
	CD200	PE	20
	CD19	PerCP-Cy5.5	20
	IgM	APC	20
4	FMC7	FITC	20
	CD20	PE	20
	CD19	PerCP-Cy5.5	20
	CD10	APC	5
5	CD22	FITC	20
	CD23	PE	20
	CD19	PerCP-Cy5.5	20
	CD79b	APC	20

2.2.2.3 NOTCH1 mutational Status

Activating NOTCH1 mutations are found in 10% of CLL at diagnosis with higher frequencies in chemorefractory and advanced CLL. 80% of NOTCH1 mutations are represented by a two basepair frameshift deletion (c.7544-754 5delCT). This deletion results in a premature stop codon and the production of a shorter protein lacking an ubiquitination site, thought to allow the protein to remain transcriptionally active for longer. We used a PCR assay with primers designed to amplify the wild type and this mutant allele of NOTCH1. Two mastermixes containing either forward primers for consensus NOTCH1 (5' GTG ACC GCA GCC CAG TT – 3') or forward primer for mutant NOTCH1 (5' TCC TCA CCC CGT CCC GA – 3') with reverse primers for NOTCH1 (5' AAG GCT TGG GAA AGG AAG -3') (Eurofins Genomics (Bavaria, Germany)) were prepared by combining the reagents in table 2.3. dNTPS were diluted from a stock of 25mM to 1mM by performing a 1:25 dilution in nuclease free H_20. Primers were diluted from a stock of 100pM to 10pM by performing a 1:10 dilution in nuclease free H_20 prior to adding to the mastermix.

Table 2. 3 Reagents and volumes required for NOTCH1 PCR Mastermix

Reagent	Volume for 1X reaction
AmpliTaq Gold 10X PCR Buffer (Applied Biosystems)	2µl
$MgCl_2$ Solution 25mM (Applied Biosystems)	0.8µl (1mM final conc)
dNTP Mix	3µl (150µM final conc)
Forward Primer	1µl (10 pmol/µl final conc)
Reverse Primer	1µl (10 pmol/µl final conc)
AmpliTaq Gold 5U/ul DNA Polymerase (Applied Biosystems)	0.3µl
Nuclease Free H_20	9.9µl
Total	18µl

18µl of mastermix was added to a separate 0.2ml PCR tube for each patient. 2µl containing 100ng of patient DNA was added to each tube. The tubes were vortexed and centrifuged briefly before amplifying in an ABI 2720 Thermocycler under the conditions in table 2.4.

Table 2. 4 PCR conditions for amplification of NOTCH1

Cycles	Temperature (°C)	Time
1	95	3 minutes
34	95	30 seconds
34	58	30 seconds
34	72	30 seconds
1	72	5 minutes

After amplification, a 2% agarose gel was prepared by adding 2g of agarose (Panreac Applichem, Germany) to 100ml of 1X TAE buffer (10X Tris Acetate-EDTA buffer diluted 1L in 10L H_20)(Sigma Aldrich, Switzerland). The gel was heated in a microwave for approximately 2 minutes or until clear and 5µl of SYBER Safe DNA gel Stain (Invitrogen, UK) was added per 50ml of gel. 100ml was poured into a tray containing a 15 well comb and bubbles were removed. The gel was allowed to set for 20 minutes. After PCR amplification, samples were centrifuged and 3.3µl of 6X Loading dye was added to each sample. 22µl of each sample was loaded per well as well as a 100bp ladder at each end of the gel in a Bio-Rad Wide Mini Sub Cell GT Gel Dock (Basel, Switzerland). A negative polyclonal control with wild type NOTCH1, a positive control with a known NOTCH1 mutation and a no template control was ran with each PCR. The gel was run at 100V, 500mA for 45 minutes using a Hybiad PS250 power pack. A Syngene ingenius 3 UV Gel Dock was used to take an image of the gel under UV light.

2.2.3 CLL patient sample processing and treatment

CLL cells were isolated from patients following informed consent and their use for this project was approved by the St James's Hospital and Adelaide and Meath incorporating the National Children's Hospital Joint Ethics Committee.

Peripheral Blood Mononuclear Cells (PBMCs) were isolated from CLL patients by density gradient centrifugation using Lymphoprep® (Axis-Shield, UK). The blood samples were diluted by adding an equal volume of RPMI and layered on top of 15ml of Lymphoprep. The tubes were capped and centrifuged at 800xg with no brake for 30 minutes at room temperature. After centrifugation, the cells were removed from the sample/medium interface using a Pasteur pipette. The harvested cells were diluted 1:1 with RPMI, centrifuged at 250xg for 10 minutes at RT and resuspended in RPMI media containing 10% FBS or cryopreserved at a cell density of ~$1x10^7$/mL in FBS containing 10% dimethyl sulfoxide (DMSO) (Sigma Aldrich, Switzerland). Cryopreserved samples were rapidly thawed at 37°C , resuspended in RPMI media containing 10% FBS and incubated at ~ $1x10^7$ cells/ml for at least 1 hour, to allow cells to recover prior to use.

CLL cell selection was performed on bone marrow samples and peripheral blood samples that were <90% CD19 positive as identified by immunophenotyping (Table 2.1). Selection was performed using EasySep™ Human B Cell Enrichment Kit without CD43 Depletion (Stemcell Technologies). After isolation of PBMCs, cells were counted and resuspended in the recommended buffer (PBS, 1mM EDTA, 2% FBS) at a concentration of $5x10^7$ cells/ml. 50µl of selection cocktail was added per ml of sample

and incubated at room temperature for 10 minutes. 50µl of magnetic particles was added per ml of sample and incubated at room temperature for ten minutes. The required volume of buffer was added to a final volume of 2.5ml and the tube was incubated in the EasySep Magnet (Stemcell Technologies) for 5 minutes. The enriched cells were poured into a new tube by inverting the magnet and 2.5ml of buffer was added to the tube. The remaining cells were added to the new tube. Cells were stained with CD19 antibodies and purity was confirmed using flow cytometry on an aliquot of enriched cells.

2.2.3.1 Cell count and viability using Acridine Orange and Ethidium Bromide

Cell count and viability were assessed by staining with acridine orange and ethidium bromide and using a haemocytometer. 10mg/ml Ethidium Bromide and 100ug/ml Acridine Orange were diluted 1:100 in PBS to make the staining solution. Prior to use, an aliquot of cell suspension was diluted 1:20 or 1:50 with PBS and stained with acridine orange/ethidium bromide. 10µl of cell suspension was loaded onto a haemocytometer and placed under the blue light of a fluorescent microscope. Cell count and viability were noted in 4 squares with live cells appearing green and dead cells appearing orange under the fluorescent microscope.

2.2.3.2 Culture and Treatment of CLL cells

CLL cells were cultured in RPMI medium supplemented with 10% (v/v) Fetal Bovine Serum, 100units/ml Penicillin and 0.1mg/ml Streptomycin at a density of 3-5x10^5 cells/100µl in a 96 well plate for all flow cytometry experiments and 3x10^5 cells/chamber slide for confocal microscopy unless otherwise stated. Cells were cultured at 4-5x10^6 cells/500µl RPMI in 24 well plates for protein and RNA extraction experiments. Stimulation of the BCR was performed by incubating CLL cells with 10µg/ml F (ab)$_2$ anti-human IgM fragments. IgM immobilization was performed by diluting F (ab)$_2$ anti-human IgM fragments to 10µg/ml in PBS and placing 150µl per well of a flat-bottomed 96 well plate overnight at 4°C. Remaining liquid was removed and the plate was blocked using 0.5% BSA in PBS for one hour. Stimulations using IL-4, IL-6, CXCL12 and CD40L were performed after serum starving cells for one hour in unsupplemented RPMI followed by incubating CLL cells with 10ng/ml IL-4, 50ng/ml IL-6, 1µg/ml CD40L or 100ng/ml CXCL12. Experiments using drug treatments were performed by incubating CLL cells with Cucurbitacin, S3I, Ruxolitinib, Ibrutinib or Idelalisib for the times and concentrations specified in the figure legends.

2.2.3.3 Bone marrow stromal cells and conditioned media

Patient derived BMSC were expanded from the mononuclear cell fraction of bone marrow aspirates following density gradient centrifugation as described in section 2.2.3. 1 x10^6 mononuclear cells were incubated in in DMEM supplemented with 10% (v/v) FBS and 100units/ml Penicillin and 0.1mg/ml Streptomycin and the BMSC were allowed to adhere to the culture vessel surface overnight. Non-adherent cells were washed off and the BMSC were allowed to expand until confluent and harvested by removing the media and washing gently with PBS before trypsin was added to the flask and left in the incubator for 5 minutes or until cells had lifted. Cells were then cryopreserved as described above. Hs5 BMSC cells were grown in DMEM supplemented with 10% (v/v) FBS and 100units/ml Penicillin and 0.1mg/ml Streptomycin. HUVEC were maintained in Endothelial Cell Media with added supplement. The cells were maintained in a humidified atmosphere containing 5% CO_2 at 37 ℃. The cells were split when the monolayer was 70-80% confluent. Cells were split by removing the media and cells were washed gently with PBS to remove any floating cells, debris and excess media. Trypsin was added to the flask and left at 37°C for 5 minutes or until cells had lifted.10ml of media was added to the flask to inhibit the enzymatic activity of the trypsin and the cells were centrifuged. The cells were split 1:3 and added to a new cell culture flask.

For coculture experiments, Hs5 BMSC, patient derived BMSC and HUVECs were seeded at 2.5 x10^4 cells per well in 96-well plate and incubated overnight to reach a confluent monolayer and washed 3 times with RPMI before the addition of CLL cells.

For conditioned media, fresh DMEM was placed in 70% confluent flask of Hs5 cells was incubated overnight. The DMEM was removed and centrifuged at 400g for 3 minutes to remove debris before incubation with CLL cells.

2.2.4 CLL Cell Line Culture

The human I83 cells are characterized by $CD19^+$, $CD5^+$ and IgMδ with mutated IGVH genes. The HG3 cells are characterized by $CD19^+$, $CD5^+$ and IgMδ with unmutated IGVH genes. The cells were grown in RPMI medium supplemented with 10% (v/v) Fetal Bovine Serum, 100units/ml Penicillin and 0.1mg/ml Streptomycin. Both cell lines were split 1 in 3, three times a week to maintain a sub-confluent cell suspension. Cells were harvested for use in the log phase of growth. Both cell lines were cultured at 3-4x10^5 cells/500µl in 24 well plate.

2.2.5 Mycoplasma Testing

Mycoplasma are a simple genus of bacteria that are distinguishable by their lack of cell wall. Mycoplasma commonly infects cell cultures and can alter cells behaviour leading to unreliable results (Miller et al., 2003). Mycoplasma testing of HG3, I83 and Hs5 cells was performed by PCR according to (Young et al., 2010). 1ml of supernatant was taken from a confluent T75 flask and debris was pelleted by centrifuging at 200xg for 1 minute. A PCR mix was set up by adding the reagents in table 2.5 to 0.2ml PCR tubes.

Table 2. 5 Reagents and volumes required for mycoplasma PCR mastermix

Reagent	Volume for 1X reaction
Green GoTaq Mastermix	25µl
Forward Primer (20µM)	1µl
Reverse Primer (20µM)	1µl
Nuclease Free H_20	22µl

The forward primer (5′-TGCACCATCTGTCACTCTGTTAACCTC-3′) and reverse primer (5′- GGGAGCAAACAGGATTAGATACCCT-3′) were obtained from Sigma-Aldrich (St.Gallen, Switzerland). 1µl of cell culture supernatant was added to each PCR tube and a positive control with known mycoplasma and a negative control with water. Tubes were vortexed and centrifuged briefly before being ran under the conditions in table 2.6 on a PTC-100 thermocycler (MJ Research).

Table 2. 6 PCR conditions for mycoplasma amplification

Cycles	Temperature	Time
1	95˚C	5 minutes
40	94˚C	30 seconds
	55˚C	30 seconds
	72˚C	1 minute
1	72˚C	10 minutes

A 2% gel was prepared by adding 1g of agarose to 50ml 1X TBE buffer and microwaving for 2 minutes. 5µl of SyberSafe Dye was added per 50 ml gel before pouring. Gel was left to set for 20 minutes. 20µl of sample was added per well and 20µl of a 100 base pair ladder was added to the first and last well of the gel. The gel was run at 100V for 30 minutes and imaged using a Fusion FX Gel Dock (Vilber, France). Cells tested negative for mycoplasma as shown in appendix 1.

2.2.6 Flow Cytometry

Flow Cytometry was used to analyse surface molecule expression, intracellular protein expression, cell cycle and cell viability.

Gating Strategy

For all surface molecule flow cytometry experiments cells were gated on single, live (using live/dead stain propidium iodide), CD19 positive cells live/dead stain propidium iodide was used to gate on live cells as shown in figure 2.1 plots (i)-(iv). For apoptosis, and intracellular staining cells were gated on single, CD19+ cells as shown below in figure 2.1 plots (i)- (iv). Fluorescence minus one (FMOs) were used for positioning gates for surface antigen expression.

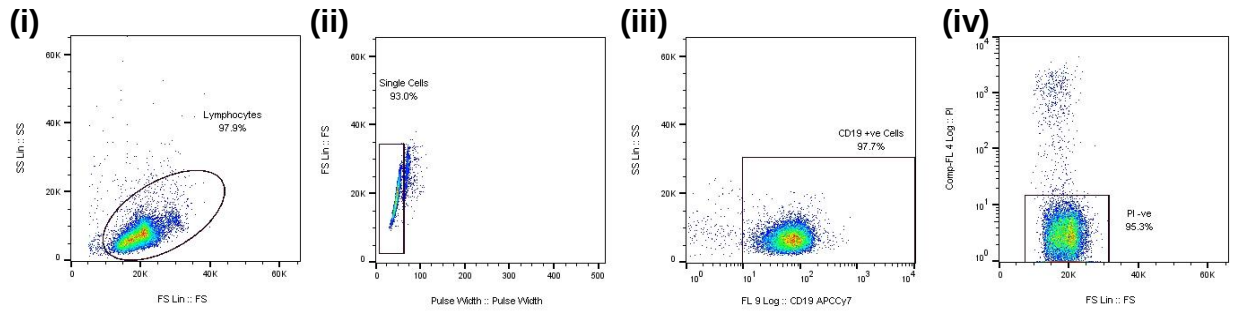

Figure 2. 1 Gating strategy for flow cytometric analysis of surface adhesion molecules (i) **SS Lin vs FS Lin plot is used to gate on the lymphocyte population.** (ii) **FS Lin vs Pulse Width is used to gate on single cells and remove doublets from analysis** (iii) **SS Lin vs CD19 which is identified using FL9 is used to gate on CLL B cells.** (iv) **PI identified by FL4 vs FS Lin is used to gate on viable cells. Gates for CD19 and PI are set using an unstained sample.**

Compensation and controls

Compensation matrices were created using compensation beads (BD Biosciences). 100µl of flow cytometry staining buffer (PBS, 1mM EDTA, 2% FBS, 0.09% Sodium Azide) was added 5ml flow tubes. Negative and positive beads were vortexed and one drop (60µl) was added to the tube. 1µl of flurochrome-conjugated antibody was added to the tube and incubated in the dark at 4℃ for 20 minutes. 1ml of staining buffer was added to the tube and centrifuged at 400g for 5 minutes. Beads were resuspended in 600µl staining buffer for acquisition on the Cyan ADP.

An aliquot of cells (3x105) was used as compensation controls for dyes Annexin V (AV) and Propidium Iodide (PI). For Annexin V, cells were washed with 1ml of AV binding buffer (0.1M HEPES, 1.4M NaCl, 25mM CaCl2, and pH7.4). Cells were resuspended in 95µl of binding buffer and 5µl of Annexin V was added and incubated in the dark at 4℃ for 20minutes. For PI controls, Cells were washed and resuspended in 200µl of staining buffer. Just prior to acquisition on the flow cytometer, 200µl of staining buffer containing PI (0.25µg/ml) was added to the tube.

Flow Cytometry Antibodies

Table 2.7 lists the antibodies/dyes and flurochromes used in flow cytometry experiments.

Table 2. 7 Flow Cytometry antibodies

Antibody	Clone	Fluorochrome	Volume (µl)	Supplier
CD19	SJ25C1	APCCy7	5	BD
CD19	HIB19	AF488	5	Biolegend
CD62L	DREG-56	BV510	5	BD
CD38	HIT2	FITC	20	BD
CD29	MAR-4	APC	20	BD
CD11c	B-ly6	BV421	15	BD
CD31	WM59	PECy7	5	BD
CD49d	9F10	PE	20	BD
STAT3	M59-50	APC	20	BD
pSTAT3 (S727)	49/pSTAT3	AF647	20	BD
pSTAT3 (S727)	49/pSTAT3	AF488	20	BD
pSTAT3 (S727)	49/pSTAT3	BV421	20	BD
pSTAT3 (Y705)	4/p-STAT3	PE	20	BD

The lasers and detector configuration settings for the Cyan ADP are shown in table 2.8.

Table 2. 8 Laser and Detector Configuration for the Cyan ADP

Detector Name	Parameter Detected	Range
FSC	Forward scatter	
SSC	Side scatter	
FL1/FITC	FITC, GFP, AF488	510-550
FL2/PE	PE	562.5-587.5
FL3/PE-Texas Red	PI	603-623
FL4/PE-Cy5	PE-Cy5.5	665-695
FL5/PE-Cy7	PE-Cy7	750LP
FL6/Violet 1	BV421	425-475
FL7/Violet 2	BV510	510-550
FL8/APC	APC, AF647	655-675
FL9/APC-Cy7	APC-Cy7	750LP
Blue Laser	488nm Excitation	
Violet Laser	405nm Excitation	
Red Laser	635nm Excitation	

2.2.6.1 Surface molecule expression

Surface molecule expression was assessed by multicolour flow cytometry. Cells were treated as per section 2.2.3.2. Cells were transferred to 5ml flow cytometry tubes and washed twice by adding 500µl staining buffer (PBS, 1mM EDTA, 2% FBS, 0.09% Sodium Azide) and centrifuging at 300xg for 3 minutes. Cells were kept on ice from this point to prevent receptor internalisation and preserve fluorophores. Cells were incubated with 100µl panels of flow antibodies (Table 2.7) for 20 minutes at 4˚C. Cells were washed by adding 500µl staining buffer (PBS, 1mM EDTA, 2% FBS, 0.09% Sodium Azide) and centrifuging at 300xg for 3 minutes and resuspended in 200µl staining buffer for analysis on a CyAn ADP flow cytometer (Beckman Coulter CA, USA). 200µl of staining buffer containing Propidium Iodide (PI) (0.25µg/ml) was added to each tube prior to flow cytometry analysis. Data was analysed using FlowJo (V10) Software (FlowJo (OR, USA)). Cells were gated on single, CD19 positive cells, live (PI negative) populations as shown in figure 2.1.

2.2.6.2 Intracellular phosphorylated STAT3 (pSTAT3) expression

Intracellular serine and tyrosine pSTAT3 expression was assessed by flow cytometry. After treatment, cells were transferred to 5ml flow cytometry tubes and washed twice

by adding 500µl staining buffer (PBS, 1mM EDTA, 2% FBS and 0.09% Sodium Azide) and centrifuging at 300xg for 3 minutes. Cells were stained with CD19 by adding anti-CD19 antibody and incubating for ten minutes at 4°C. Cells were fixed by adding 250µl of Cytofix Buffer (BD Biosciences, Switzerland) dropwise while gently vortexing and incubated for 15 minutes at 4˚C. Cells were washed by adding 500µl staining buffer and centrifuging at 300xg for 3minutes and permeabilised using 1ml ice-cold PermBuffer III (BD Biosciences, Switzerland) for 30 minutes on ice. Cells were washed by adding 500µl staining buffer and centrifuging at 300xg for 3minutes and extra care was taken to remove all supernatant. Cells were stained for 30 minutes at room temperature by resuspending in 100µl staining solution containing 1:20 dilution of PE-tyrosine pSTAT3 and/or APC-serine pSTAT3 or APC-total STAT3 PhosFlow antibodies (BD Biosciences, Switzerland) (Table 2.8). Cells were washed by adding 500µl staining buffer and centrifuging at 300xg for 3 minutes. Cells were resuspended in 400µl staining buffer. All samples were analysed on a CyAn ADP flow cytometer. Positive populations were gated on based on unstained and Fluorescence minus one (FMO) samples. Compensation was performed using BD compensation beads. Data was analysed using FlowJo (V10) Software.

2.2.6.3 Cell cycle Analysis

Cell cycle was assessed using propidium iodide (PI) staining by flow cytometry. Propidium iodide intercalates between nucleic acid bases and the amount of fluorescence is proportional to the amount of DNA present. As a cell progresses through different stages of the cell cycle, different amounts of DNA are present, cells in the S phase will have more DNA than those in the G0/G1 phase and cells in G2 should be twice as bright as those in G0/G1. Cell cycle progression was assessed by fixing cells with 70% ethanol, added dropwise while vortexing, for 30 minutes at 4˚C before incubation with RNase and PI (50µg/ml) for 10min. Cells were washed and resuspended in 500µl buffer (PBS, 1mM EDTA, 2% FBS, 0.09% Sodium Azide) before samples were analysed on cyan ADP. Data was analysed using FlowJo (V10) Software.

2.2.6.4 Apoptosis by AV/PI staining

Apoptosis was assessed by flow cytometry. Phosphatidylserine is located on the cytosolic side of the plasma membrane in healthy cells but translocates to the extracellular side when cells begin to undergo apoptosis. Fluorescently tagged Annexin V binds to this exposed phosphatidylserine on the cell surface, in a calcium dependent

manner, indicating cells undergoing apoptosis. As mentioned above propidium iodide (PI) is a fluorescent dye that binds to DNA by intercalating between the bases. PI is excluded by viable cells with an intact membrane. Late-stage apoptosis results in the loss of membrane integrity allowing Annexin V to bind cytosolic phosphatidylserine and allowing PI to enter the cell and bind DNA. As shown in figure 2.2, the lower left quadrant (Q1), shows cells negative for both stains are the non-apoptotic cells. The lower right quadrant (Q2), shows early apoptotic cells stained for AV only. Cells in the upper right quadrant (Q3) are late apoptotic or necrotic cells positive for both AV and PI. The upper left quadrant (Q4) shows necrotic cells positive for PI only. Cells were treated, transferred to 5ml flow cytometry tubes and washed by adding 500µl Annexin V (AV) binding buffer (0.1M HEPES, 1.4M NaCl, 25mM $CaCl_2$, and pH7.4) and centrifuging at 300g for 3 minutes. Cells were then incubated with Annexin V-FITC (IQ Products) or Annexin V-PE (ImmunoTools, Friesoythe, Germany) (100µl AV binding buffer and 2µl-3µl of Annexin V stain per sample) and CD19, for 20 minutes at 4˚C. Cells from this point were kept on ice and in the dark to preserve the FITC/PE fluorochromes. Cells were washed (300xg, 3minutes) and resuspended in 200ul AV binding buffer. 200µl of staining buffer containing Propidium Iodide (PI) (1mg/ml diluted 1:2000 to a final concentration of 0.25µg/ml) was added to each tube prior to running. Cells were gated on single, CD19 + population. Cells were run on a CyAn ADP flow cytometer and data was analysed using FlowJo (V10) Software.

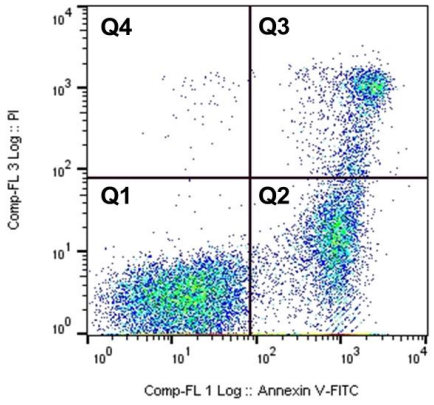

Figure 2. 2 Example of an AV/PI dotplot. Annexin V-FITC was identified by the FL1 channel and is shown on the X axis PI was identified by the FL3 channel and is shown on the Y axis. Quadrant 1 represents AV/PI negative, viable cells. Quadrant 2 represents AV positive, PI negative early apoptotic cells, Quadrant 3 represents AV/PI positive, late apoptotic cells and quadrant 4 represents PI positive, Annexin V negative, necrotic cells. Quadrants were gated using an unstained and single stain (AV only and PI only) samples.

2.2.7 MTT assay

The MTT (3-(4, 5-Dimethylthiazol-2-yl)-2, 5-diphenyltetrazolium bromide) colorimetric assay (Roche Applied Science, Switzerland) was used to assess cell viability of CLL cell lines. The MTT tetrazolium salt is cleaved by mitochondrial oxidoreductase enzymes in metabolically active cells in a reduction reaction involving NADH and NADPH. The resulting formazan crystals are solubilised by the solubilising solution to give a coloured solution that can be quantified by a spectrophotometer at a wavelength of 560nm.

$3x10^4$ I83 or $2x10^4$ HG3 cells were plated in a total of 100µl of RPMI media in a 96-well plate treated in triplicate with various concentrations of inhibitor and were incubated at 37°C in a 5% CO_2 environment. After 24 or 48 hours 10µl of MTT tetrazolium salt labelling reagent was added to each well and incubated at 37°C in a 5% CO_2 environment for 4 hours. 100µl solubilisation solution (10% SDS, 0.01M HCl) was added to each well and the plate was incubated at 37°C overnight. The absorbance was then read at 560nm using a Perkin Elmer Victor 2 Instrument or an Epoch Microplate Spectrophotometer (BioTek, USA). MTT Assay is used to determine an EC_{50} value for a drug. An EC_{50} value is the concentration of agent required to cause a response halfway between the baseline and maximum response. A dose-response curve, describing the relationship between drug concentration and effect on the cell viability, was plotted in order to ascertain an EC_{50} value for each agent. In order to calculate an EC_{50} value, a baseline and maximum response i.e. a plateau on each end of the graph, is required. In some cases, a maximum response was not reached at the highest concentration (100µM), so an estimated EC_{50} value was calculated by constraining the baseline to 0 and extrapolating an EC_{50} value.

2.2.8 Chemotaxis assay

CLL cell chemotaxis was assessed using Neuroprobe 96-well ChemoTx Plates (5µm pores, 3.2mm diameter) (Neuroprobe, USA). 10% BSA was prepared by dissolving 1g BSA in 10ml PBS and filter sterilising using a 0.22µm filter. 250µl of 10% BSA was added to 5ml unsupplemented RPMI to give 0.5% BSA. 29µl of RPMI with 0.5% BSA containing CXCL12 (100ng/ml unless otherwise stated) was added to the wells below the filter. CLL cells were centrifuged at 300xg for 3 minutes, resuspended in RPMI with 0.5% BSA and incubated with/without inhibitors for 1 hour at 37˚C. The cell suspension is required to cover the exposed filter area. Optimised coverage is based on cell size, and pore density. The plates used were $8mm^2$ with 5µm pores at a pore density of

4000/mm^2. The average diameter for a CLL B lymphocyte is 6-7µm (Kuse et al., 1985). From the graph in figure 2.3 supplied by Neuroprobe, 7µm cells require ~27,000 cells/mm^2 or approximately 2.5x10^5 cells per well. 2.5 x10^5 CLL cells in 25µl were added to the top of the filter and cells were incubated for 3 hours at 37˚C and 5% CO_2. After 3 hours cells remaining on top of the filter were gently removed and the cells which had migrated through the filter were transferred to a 96-well plate, fixed with 4% formaldehyde and stained with Hoechst (10mg/ml stock diluted 1:2000 to give 5ng/ml) nuclear staining dye overnight in the dark at room temperature. Migrated cells were imaged by capturing 20 fields per well using an Incell Analyzer 1000 or Cytell cell imaging system (GE Healthcare Life Sciences,USA) and quantified by Incell Analyzer 1000 Software (GE Healthcare Life Sciences,USA) setting cell diameter size as 10µm and adjusting sensitivity in order to count only defined CLL cells.

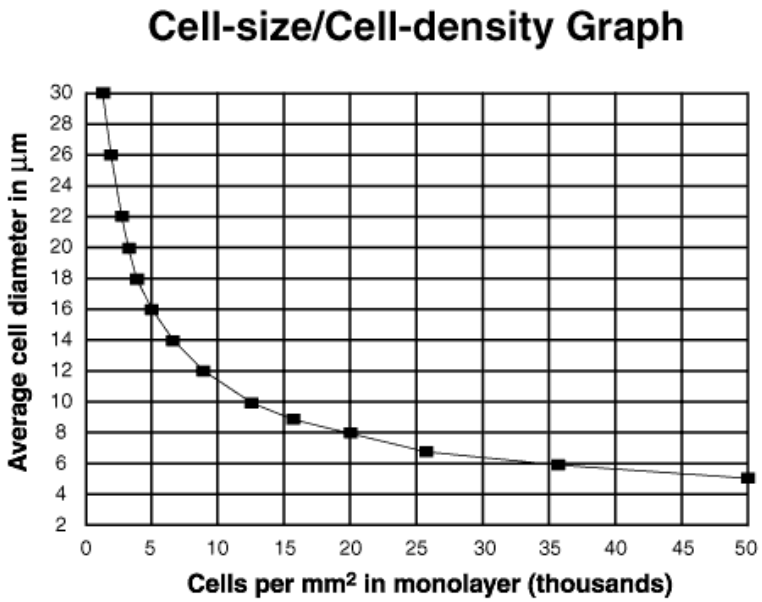

Figure 2. 3 Cell size graph supplied by Neuroprobe used to determine cell number for plating for chemotaxis. CLL cells have an average diameter of 6-7µm and the plate used had 4000 pores/mm^2 and was 8mm^2. Graph was used to determine the optimal cell number to be placed on the Neuroprobe ChTx filter for maximal chemotaxis.

2.2.9 Adhesion under shear flow

To investigate the adhesion of CLL cells under shear flow a microfluidics system utilizing a neMESYS Low Pressure syringe pump system (Cetoni GmbH,Germany) with neMESYS User Interface Software was used to introduce CLL cells into channels of Vena8Endothelial+biochips (Cellix, Ireland) under controlled shear flow rates as shown in figure 2.4. The microfluidic channel was coated with Fibronectin (100µg/ml)

overnight at 4°C. HUVEC cells were treated with TNF-α (10ng/ml) overnight to activate the HUVEC cells , washed twice with PBS and 3ml of Accutase (accutase solution in PBS containing 0.5mM EDTA) (PromoCell, Germany) was used to remove HUVECs from the flask without disrupting cell surface adhesion molecules. $5x10^4$ HUVECs were seeded per microfluidic channel and the chip was incubated for 2 hours at 37°C, allowing the cells to adhere and form a confluent monolayer. RPMI was flowed through the channels at a flow rate of 1 dyne for 2 minutes to remove any unadhered HUVECs. $4x10^5$ CLL cells were treated with Cucurbitacin or an anti-CD62L antibody for 4 or 24 hours as indicated. CLL cells were then introduced into the channel at a constant shear flow of 0.5 dynes (0.1µl/second). After 5 minutes, 2 images 30 seconds apart were captured at 3 points along the channel using a QICAM Fast 1394 Digital camera (QImaging, Canada) and Qcapture Pro Software. Total number of cells adhered was counted by stacking the two consecutive images using ImageJ (US National Institutes of Health.MA, USA; https://imagej.nih.gov/ij/) and counting cells that appeared adhered in both images.

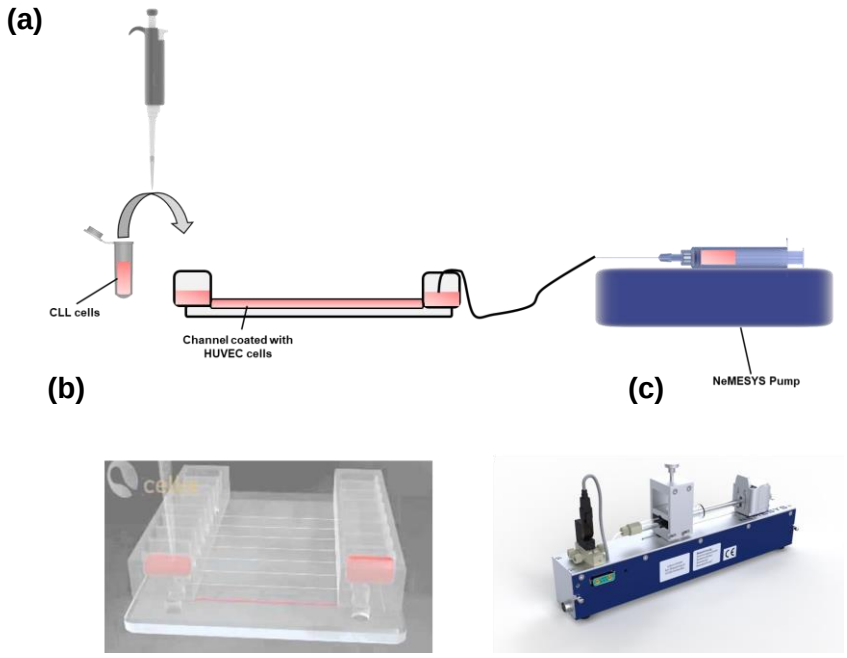

Figure 2. 4 Schematic diagram of the Shear Flow System. The Biochip (b) was coated overnight with TNFα stimulated HUVECs. The monolayer was washed to remove any loose cells and CLL cells were introduced to the channel using the NeMESYS pump system (c) and software.

2.2.10 STAT3 siRNA Knockdown

CLL cells were transfected as per Amaxa® Human B-Cell Nucleofector® Kit protocol obtained from Lonza (Basel, Switzerland). 5-6x10^6 CLL cells in RPMI containing 20% FBS were centrifuged at 300xg for 3 minutes and resuspended in 100µl of Nucleofector® solution. 500nM siRNA for STAT3 (SMARTpool®), scrambled control siRNA or pmaxGFP vector (all from Dharmacon, UK) was added to the cells and transferred to 2mm gap cuvettes. Cells were electroporated using the U-015 Nucleofector Program® as per the manufacturer's instructions. Following electroporation, the cells were removed from the cuvette using a Pasteur pipette and incubated in 2ml RPMI + 20% FBS to allow cells to recover at 37°C in a 5% CO_2 environment for 72 hours before analysis to assess knockdown, transfection efficiency and surface molecule expression by flow cytometry. Knockdown was assessed at a protein level by staining for total STAT3 by flow cytometry as per section 2.2.6.2. Transfection efficiency was assessed by the percentage of GFP positive cells by flow cytometry.

2.2.11 Protein Extraction and Western Blot

2.2.11.1 Protein Extraction and Quantification

All steps were performed on ice to prevent denaturing of proteins. After treatment, cells were washed with 500µl ice-cold PBS, and centrifuged at 4˚C at 300xg for 3 minutes. The supernatant was removed and cell pellet resuspended in 500µl ice-cold PBS and transferred to 2.5 ml Eppendorf tubes. Cells were centrifuged at 400g at 4°C for 5 minutes. The supernatant was removed, leaving no excess liquid and cells were resuspended in ice-cold radioimmunoprecipitation assay (RIPA, 25 mM Tris, 150 mM Sodium Chloride, 1% NP-40, 1% Sodium Deoxycholate, 0.1% SDS, pH 7.6) buffer containing 1mM sodium orthovanadate, 2mM phenylmethylsulfonyl fluoride and protease inhibitors (Santa Cruz Biotechnology, Germany). The cell pellets were vortexed and incubated on ice for 15 minutes followed by centrifugation at 13400xg at 4°C for 20minutes. Supernatants were harvested and protein concentration was determined by Pierce® BCA Protein Assay Kit (Thermo Fisher Scientific, Germany). The BCA Assay is a colorimetric assay that uses the reduction of Cu^{2+} to Cu^{+1} by protein in an alkaline medium to quantify the concentration of protein in a solution. BSA standards are prepared by 8 dilutions of a 2mg/ml stock of BSA to give 9 concentrations in the range of 0-2000ug/ml. The working reagent is prepared by mixing 50 parts BCA Reagent A with 1 part BCA Reagent B. 10µl of each standard in

triplicate and 10µl of each unknown sample was added to a 96-well plate and 200µl of working reagent added per well. The plate was covered and incubated at 37˚C for 30 minutes. The plate was allowed to cool and was read at 560nm on an Epoch Microplate Spectrophotometer (BioTek, VT, USA). The absorbance of the blank was subtracted from all values and a standard curve (absorbance at 560nm vs Concentration (µg/ml)) was plotted. The unknown sample values were determined from the standard curve using Prism 7 Software (Graphpad, CA, USA).

2.2.11.2 Sodium Dodecyl Sulfate Polyacrylamide Gel Electrophoresis (SDS-PAGE) and Protein Transfer

After quantification, cell lysates were boiled (95˚C) with equal volumes Laemmli sample buffer (final concentration: Tris-HCl 62.5 mM (pH 6.7), Glycerol 10% (v/v), sodium dodecyl sulfate 2% (w/v), bromophenol blue 0.002% (w/v) containing β-mercaptoethanol 143 mM) for 5 minutes. Lamelli buffer contains a bromophenol blue tracking dye to assess the separation. An equal amount of each lysate (15-20µg) was resolved by Sodium Dodecyl Sulfate Polyacrylamide Gel Electrophoresis (SDS-PAGE) in a Mini-PROTEAN Electrophoresis System (BioRad, UK). The 12% Resolving gel was prepared by combining the reagents in table 2.9. The mixture was mixed gently and sonicated to remove dissolved air. 20% Ammonium Persulfate (APS) (Thermo Fisher Scientific, Germany) was prepared fresh in H_20 and 50µl was added to the mixture with 5µl of Tetramethylethylenediamine (TEMED) (Sigma Aldrich, Switzerland). The gel solution was gently mixed and poured in between two glass plates. 100µl of cold H_20 was gently pipetted on top of the gel and the gel was allowed to set for 45 minutes. The 4% Stacking gel was prepared by combining the reagents in table 2.10. 25µl of APS and 5µl of TEMED were added and the solution was gently mixed. The H_20 was carefully removed from the resolving gel and the stacking gel was evenly poured on top. The comb was placed in the stacking gel and the gel allowed to set for 45 minutes.

Table 2. 9 Volumes of reagents required for a 12% Resolving gel.

12 % Resolving Gel	
Reagents	**Volume**
dH20	1.7ml
30% Bis-Acrylamide	2ml
1.5M Tris-HCl pH 8.8	1.25ml
10% SDS	50µl
20% APS	25µl
TEMED	5µl

Table 2. 10 Volumes of reagents required for a 4% Stacking gel.

4% Stacking Gel	
Reagents	**Volume**
dH20	1.525ml
30% Bis-Acrylamide	332.5µl
0.5M Tris-HCl pH 6.8	625µl
10% SDS	25µl
20% APS	12.5µl
TEMED	2.5µl

The comb was removed and 20µl of sample was loaded per lane. 5µl of EZ-Run Pre-Stained Protein Ladder (Thermo Fisher Scientific, Germany) was added to one lane and used as a marker to determine molecular weight of resolved proteins. 10X Running buffer was prepared by combining 30.3g Tris Base, 144g Glycine and 10g SDS with 800ml deionised H_20)and diluted to 1X by taking 100ml of 10X running buffer and adding 900ml H_20 to run the gel. The gel was run at 200V for 1 hour using a Consort Powerpack or until the dye front had almost reached the end of the gel. Transfer buffer was prepared fresh by combining 3.03g Tris Base, 14.4g Glycine, 800ml H_20 and 200ml Methanol (all Fisher Scientific, Germany). The gel, filter paper and fibre pads were left in transfer buffer for 15 minutes to equilibrate. The Polyvinylidene fluoride (PVDF) membrane was activated by immersing it in 100% Methanol for 10 seconds and washing in H_20 for 5 minutes before adding to transfer buffer to equilibrate. The fibre pads, 4 sheets of filter paper, PVDF membrane and gel were arranged in a sandwich in a Trans-Blot Cell (BioRad, UK) and ran at 100V for 1 hour. 10X Tris buffered saline (TBS) was prepared by combining 24g Tris HCl, 5.6g Tris Base, 88g NaCl and 900ml H_20. The pH of the buffer was adjusted to 7.6 and made up to 1L with H_20. 1X TBS-Tween (TBST) was prepared by adding 100ml 10X TBS to 900ml H_20 and adding 1ml Tween. The membrane was removed from the rig and washed in TBST for 5 minutes. 5% milk powder (Marvel) or 5% BSA were prepared by adding 0.5g to 10ml of TBST. The membrane was blocked in 5% milk powder at room temperature for 1 hour on a roller to prevent nonspecific binding of the primary and secondary antibodies to the membrane. The membrane was washed 3 times for 5 minutes in TBST and incubated with primary antibody overnight at 4˚C on a roller. The following dilutions of primary antibodies were used: 1:1000 for pY705 STAT3, pS727 STAT3 and Total STAT3 and 1:5000 Actin. All primary antibodies were prepared in 5% BSA. The membrane was washed 3 times in TBST for 5 minutes. The membrane was incubated in secondary antibody for one hour at room temperature. The following dilutions of

secondary antibodies were used: 1:5000 anti-rabbit and 1:5000 anti-mouse. All secondary antibodies were freshly prepared in 5% milk powder each time.

Table 2. 11 Antibodies used for Western Blotting

Antibody	Dilution	Supplier
Anti-STAT3	1:1000	Cell Signalling Technologies
Anti-STAT3 (pS727)	1:1000	Cell Signalling Technologies
Anti-STAT3 (Y705)	1:1000	Cell Signalling Technologies
Anti-Actin	1:5000	BD Biosciences
Mouse Anti-Rabbit IgG	1:5000	Santa Cruz Biotechnology
Goat Anti-Mouse IgG	1:5000	Santa Cruz Biotechnology

2.2.11.3 Immunodetection

The secondary antibodies used were conjugated to horseradish peroxidase (HRP) allowing detection of the protein of interest by chemiluminesence. After blocking, the membrane was washed 3 times in TBST for 5 minutes. Excess liquid was removed and the membrane was covered with 3ml of Pierce ECL Substrate for 5 minutes. The substrate was removed and the membrane placed in clear plastic. In a dark room, the immunoblot was exposed to RX NIF Sheet X-Ray Film (Fujifilm Corporation, Germany) and developed using an AGFA Curix CP-1000 Film Processor.

2.2.12 Proteome Profiler Array

$2.5x10^7$ cells were incubated with/without Ruxolitinib (1μM) for 1 hour and then stimulated with $F(ab)_2$ anti-human IgM fragments or left untreated for 4 hours. The Human Phospho-Kinase Array (R&D Systems, UK) was used to assess the phosphorylation of 43 kinase phosphorylation sites of 38 different kinases. The protocol was carried out as per the manufacturer's instructions. Briefly, $2.5x10^7$ per sample cells were washed in PBS and lysed in 335μl Lysis Buffer 6 and rocked gently at 4˚C for 30 minutes. The lysates were centrifuged at 14000xg for 5 minutes and protein was quantified by BCA Assay. Two membranes, (Membranes A and B which contain different sets of proteins) were blocked for 1 hour at room temperature on a shaker using 1ml of Array Buffer 1 per membrane. The lysate was made up to 2 ml in Array Buffer 1. Array Buffer 1 was removed from the membranes and 1 ml of this solution was added to each membrane for each sample. The membranes were incubated overnight on a shaker at 4˚C. The membranes were removed and washed in 20ml 1X Wash Buffer three times for 10 minutes each time. 20μl of Detection Antibodies were

reconstituted to 1ml using 1X Array Buffer for each membrane and the membrane was incubated in the 1ml for 2 hours at room temperature on a rocker.–The membranes were removed and washed in 20ml 1X Wash Buffer three times for 10 minutes each time. The membranes were removed and excess wash buffer was removed. Each membrane was placed in the plastic sheet protector and incubated with 1ml of Chemi Reagent Mix for 1 minute. The chemo reagent mix was blotted off and the membranes were exposed to X-Ray film in a dark room for 1, 5 and 10 minutes. Analysis was performed using Image J (V.1.5) with protein profiler add on software. The pixel density of each spot was calculated and background was subtracted. The relative change in signal between the different samples was calculated.

2.2.13 Gene expression analysis

2.2.13.1 RNA Extraction and quantification

CLL cells were treated and RNA was extracted using RNeasy Mini Kit obtained from Qiagen (Hilden, Germany) as per the manufacturer's instructions. Before first use, 260ml of ethanol was added to 65ml Buffer RPE. Prior to each extraction, 10µl of β-mercaptoethanol was added per 1 ml of RLT Lysis Buffer. In addition to the guanidinium isothiocyanate (GITC) in the RLT Buffer, the β-mercaptoethanol denatures RNases released after cell lysis preventing RNA degradation. CLL cells were removed from the plate and washed twice by adding 1ml ice-cold PBS and centrifuging at 400xg for 3 minutes. Cells were pelleted and supernatant was removed. The tube was flicked to loosen the cell pellet and 350µl of RLT buffer was used to lyse the cells by pipetting. The lysate was added to a QIAshredder column and centrifuged at the maximum speed for 2 minutes in order to homogenise the lysate. 350µl of 70% Ethanol was added to the flow through, to promote binding, mixed by pipetting and transferred to an RNeasy spin column. The column was centrifuged at 8200xg for 15 seconds and flow through was discarded. Nucleic acids were retained on the column. The column was washed by adding 350µl of Buffer RW1 and centrifuging at 8200xg for 15 seconds. An on-column DNA digestion was performed using RNase-Free DNase Kit (Qiagen, Germany). The DNase I stock solution was prepared by injecting 550µl RNase-free water and inverting gently. Lyophilised DNase I was aliquoted and stored at -20˚C. 10µl of DNase I stock solution was added to 70µl of Buffer RDD and mixed gently by inverting the tube. 40µl of the DNase I incubation mix was placed directly on the RNeasy column and left at room temperature for 15 minutes. The column was washed by adding 350µl Buffer RW1 and centrifuging at 8200xg for 15 seconds. The column

was washed twice with 500µl of Buffer RPE to elute contaminants. The RNeasy column was transferred to a new collection tube and centrifuged at maximum speed for 1 minute to dry the membrane. 30µl of RNase free water was added to the column and centrifuged at 8200xg for 1minute to elute the RNA. RNA quality (A260/280 >1.9, <2.1) and quantity (A230, ng/ul) was assessed by Nanodrop ND 1000 UV-Vis Spectrophotometer (Thermo Fisher Scientific (MA, USA).

2.2.13.2 cDNA preparation

500ng-1500ng of RNA was converted to cDNA. The required amount of RNA was made up to 12ul or 24ul using sterile RNase/DNase free H_20. A Mastermix of the components in table 2.11 was made and 11µl or 22µl was aliquoted, per tube. 12/24µl of the diluted RNA was added. Samples were heated to 96˚C for 2 minutes and chilled on ice for 5 minutes. Tubes were gently centrifuged and 1µl of RNase OUT (Invitrogen, UK) and 1µl of Superscript II Reverse Transcriptase (Invitrogen, UK) was added to each sample. Tubes were placed at 42˚C for 90 minutes. Samples were centrifuged and stored at -20˚C. Prior to use, samples were heated to 96˚C and chilled on ice for 5 minutes to eliminate any secondary structures that had formed.

Table 2. 12 Reagents and volumes required for cDNA mastermix

	Supplier	**Volume per sample (1X 25µl reaction)**
5X Superscript First Strand Buffer	Invitrogen	5
25mM dNTPs	Invitrogen	1
H_20	Sigma Aldrich	1.5
100mM DTT	Invitrogen	2.5
3µg/µl Random Hexamers	Promega	1

2.2.13.3 Quantitative reverse transcription PCR (RT-qPCR)

Gene expression was assessed using single-tube TaqMan Gene Expression Assays (Applied Bioystems, Netherlands) (Table 2.12). The assays consist of dual-labelled probes specific for the sequence of interest. The probes contain a FAM reporter dye at the 5´ end and a non-fluorescent quencher with a minor groove binding moiety at the 3´ end of the probe. The fluorescence emitted by the intact probe is reduced due to the close proximity of the quencher and the fluorescent probe. The probe anneals between primer sites of the target sequence and is cleaved by the 5´ nuclease activity of the DNA polymerase. This cleavage separates the dye from the quencher, leading to increased fluorescence and also releases the probe from the target strand to allow the PCR process to continue. This occurs with each cycle resulting in fluorescence intensity proportional to the amount of amplicon produced. The higher the initial copy number of the target the sooner a significant increase in fluorescence is seen.

Table 2. 13 TaqMan assays used for RT-qPCR

Gene	Type	Assay Number
CD62L	Target	Hs01046459_m1
MCL1	Target	Hs01050896_m1
BCL2	Target	Hs00608023_m1
Cyclin D1	Target	Hs00765553_m1
STAT3	Target	Hs01047580_m1
β2M	Reference	Hs00187842_m1
HPRT1	Reference	Hs02800695_m1

PCR preparation was carried out in a designated hood. The hood and all reagents were cleaned with 70% Ethanol, RNase Zap and treated with UV light for 20 minutes prior to use. PCR Mastermix was prepared by adding 1µl of TaqMan gene expression assay to 10ul TaqMan Universal PCR Mastermix per sample. 11µl was added per well of the MicroAmp Optical 96 well Reaction plate (Qiagen, Netherlands). cDNA tubes were thawed on ice, vortexed and centrifuged prior to use. cDNA was diluted to 20-50ng/9µl in NF H_20. 9µl was added to each well of the 96 well plate in duplicate. A MicroAmp Optical Adhesive Film was used to cover the plate and seal each individual well. The plate was gently vortexed and centrifuged at 100xg for 30 seconds. Amplification was run on an ABI 7500 Real Time PCR System (Applied Biosystems, Netherlands).

2.2.14 TaqMan Array

The TaqMan Human Extracellular Matrix and Adhesion Molecules 96 well Array (Applied Biosytems, Netherlands) was used to assess changes in gene expression of 86 genes involved in adhesion and migration. The plate contains 86 predefined assays and 10 endogenous controls dried-down in each well. Amplification was run on an ABI 7500 Real Time PCR System (Applied Biosystems Netherlands) under the conditions in table 2.13.

Table 2. 14 Conditions for TaqMan array amplification

Stage	Hold	Hold	PCR (40 cycles)	
			Denature	Anneal/Extend
Temperature (˚C)	50	95	95	60
Time (minutes)	02:00	10:00	00:15	01:00

Data analysis was carried out by SDS Software. An amplification plot was produced plotting ΔR_n vs cycle number. R_n is defined as the ratio of fluorescence emission intensity of the reporter dye to the passive reference dye. The baseline and threshold settings were determined by the SDS Software. The baseline was set in the initial cycles where no change in fluorescence intensity is seen and is set as background fluorescence. This baseline value is subtracted from the fluorescence emission (R_n) to give the ΔR_n. The threshold was set to be above the baseline and within the exponential growth region of the amplification curve. The Ct is the cycle at which the signal of the reporter dye crosses this threshold line.

The Comparative Ct ($2^{-\Delta\Delta Ct}$) relative quantitation method was used to quantify changes in gene expression in one sample relative to another sample (Livak and Schmittgen, 2001). The comparative Ct equation is defined as:

$2^{-\Delta\Delta Ct}$= [Ct gene of interest- Average Ct endogenous controls] Sample 1 - [Ct gene of interest- Average Ct endogenous controls] Sample 2. Two endogenous controls were used, β-2 microglobulin (B2M) and Hypoxanthine Phosphoribosyltransferase 1 (HPRT1) as these are suitable controls for CLL (Valceckiene et al., 2010).

2.2.15 Immunofluorescent Microscopy

STAT3 localisation in CLL cells was determined by immunofluorescent microscopy. Chamber slides were coated in 300µl Poly-L-Lysine and incubated at 37˚C for 20min. Excess Poly-L-Lysine was removed and 100µl of cells were transferred to the chamber slide and 100µl of RPMI was added to ensure the bottom of the slide was covered. After treatment cells were added to the chamber slide and left to bed down for 1 hour at 37˚C and 5% CO_2. The RPMI was removed and cells were then fixed in 250µl of 4%

formaldehyde for 20 minutes at room temperature. Formaldehyde was removed and cells were washed twice by adding 300µl of PBS for 5 minutes. Cells were then either stored in PBS for future staining or stained immediately. Cells were permeabilised by adding 300ul of 100%, ice-cold methanol and incubated at -20˚C for 10 minutes. Cells were washed with 300µl PBS for 5 minutes. Blocking buffer was prepared by combining 1X PBS, 5% normal goat serum and 0.3% Triton X-100 and was added for 60 minutes at room temperature. Staining buffer was prepared by combining 1X PBS, 1%BSA and 0.3% Triton X-100 and was used to dilute AF-488 STAT3 Antibody (1:400), Hoechst (10ng/ml, 1:2000 of 10mg/ml) and Rhodium Phalloidin (1:60). 250µl of staining solution was added to each sample and incubated overnight, in the dark at 4˚C. The slide was washed with PBS for 5 minutes and incubated with secondary AF488 or AF647 antibodies for 2 hours at room temperature. Slides stained with the secondary antibody only were used to control for non-specific staining. Cells were washed 3X with PBS for 5 minutes. The top section of the chamber slide was removed and 30µl of mounting media was gently placed on each sample. A rectangular coverslip was slowly placed over the samples, at an angle, avoiding the introduction of air bubbles. Nitrocellulose was placed at the corners and along the edges of the coverslip to create a seal. The slide was covered with tinfoil and allowed to dry at room temperature for at least 1 hour. Slides were stored in the dark at 4˚C until imaged. Cells were imaged using Leica SP8 Scanning Confocal (Leica Microsystems, Germany).

2.2.16 Statistical analysis

Graphs were prepared and data analysed using Prism 7 from Graphpad (CA, USA). Significance was measured using Student's *t*-test and all p-values were noted. Groups were first tested for normality using the D'Agostino-Pearson omnibus test for sample sizes of 8 or more. For sample sizes below 8, the Shapiro Wilk normality test was used. In cases where data was paired (i.e. before and after treatments in the same samples), a paired t-test was used for groups passing the normality tests or the Wilcoxon matched pairs test for non-normal data. In other cases (i.e. UM-IGVH vs M-IGVH) an unpaired t-test or Mann Whitney test was used. Error bars on graphs represent the mean $\pm$ standard error of the mean (s.e.m). The s.e.m is defined as $\sigma/\sqrt{n}$ where σ= the standard deviation of the original sample and n= the sample size. i.e. the deviation of the sample mean from the population mean. Linear regression was performed to determine if there were correlations between two variables. Variable X was plotted against Variable Y and a best fit linear regression line was fitted to the data. The regression model views the data as the sum of two components: the systematic

component i.e. the variation of the line that is predictable and the chance variation. The coefficient of determination of R^2 value is the proportion of total variation that is associated with the regression line as opposed to chance variation of points around the line. The closer the R^2 value is to 1 the better the model fits the data.

Chapter 3

The role of STAT3 in CLL cell survival

3.1 Introduction

STAT3 is a transcription factor that has a role in a number of normal cellular processes including proliferation and survival. STAT3 is constitutively active in different cancers and this activation can directly contribute to tumorigenesis. After stimulation STAT3 is phosphorylated by JAK2, dimerizes and translocates to the nucleus where it regulates the expression of a number of target genes, including anti-apoptotic genes, MCL1, BCL2 and Bcl-x_L (Iwamaru et al., 2007, Nielsen et al., 1999, Epling-Burnette et al., 2001, Alas and Bonavida, 2003), and cell cycle genes c-jun, c-fos and cyclin D1 (Carpenter and Lo, 2014). STAT3 has two phosphorylation sites, a tyrosine residue at position 705 and a serine residue at position 727, both located in the transactivation domain. The Janus Kinase (JAK) family of proteins are the main activators of STAT proteins through phosphorylation of tyrosine residues. Tyrosine phosphorylation of STAT3 occurs mainly through JAK1 and JAK2 activation. Tyrosine phosphorylation of STATs can also occur through non-JAK mediated activation such as by GPCR or non-receptor tyrosine kinases. While tyrosine phosphorylation is regarded as essential for STAT3 activation, the role of serine phosphorylation is controversial, having both up and down-regulatory effects on STAT3 activity in different cell types and under different conditions (Qin et al., 2008, Shi et al., 2006). In contrast to the constitutive activation on tyrosine seen in a number of cancers, STAT3 is constitutively activated on serine in the absence of tyrosine phosphorylation in CLL cells. It has been shown in CLL that this serine phosphorylation is mediated by the CK2-BLNK-CD5 complex (Rozovski et al., 2017). Serine phosphorylated STAT3 in CLL cells translocates to the nucleus and activates the transcription of STAT3-regulated genes; however, the biological significance of this in CLL is not fully elucidated (Hazan-Halevy et al., 2010).

Generally in cancer cells, STAT3 activation has been thought to be oncogenic: inhibiting apoptosis and promoting proliferation and oncogenic transformation. Knockdown of STAT3 has been shown to induce apoptosis and inhibit growth of ovarian cancer cells (Zhao et al., 2011) glioblastoma cells (Konnikova et al., 2003) prostate cancer cells (Han et al., 2014) and chronic myeloid leukaemia cells (Ma et al., 2010). However in contrast to this, it has also emerged that STAT3 activation has tumour suppressor functions; inducing apoptosis and slowing tumour growth in other cancers. Knockdown of STAT3 in thyroid cancer cells (Couto et al., 2012) and lung cancer cells resulted in increased tumour growth (Grabner et al., 2015)

STAT3 can also have tumour suppressive or oncogenic function in the same cell type depending on other coexisting biochemical or genetic factors. STAT3 has been shown to have oncogenic and tumour suppressive roles in glioblastoma depending on the levels of PTEN expression (de la Iglesia et al., 2008) and STAT3 oncogenic and tumour suppressive roles were described in colorectal cancer models depending on the stage of the cancer (Musteanu et al., 2010). In addition, constitutive STAT3 expression was shown to result in less tumour formation or higher tumour formation in liver carcinogenesis depending on the carcinogenic agent (Wang et al., 2011).

A dual role for STAT3 in CLL cell survival has been suggested. It has been shown that serine pSTAT3 regulates the expression of apoptotic and cell cycle genes in CLL and inhibition of STAT3 using STAT3 shRNA resulted in an increase in apoptosis, suggesting a pro-survival role for STAT3 in CLL (Hazan-Halevy et al., 2010). Liu et al. (2016) also suggested a prosurvival role for STAT3 in CLL, showing the level of spontaneous apoptosis of CLL cells is inversely correlated with constitutive serine phosphorylation of STAT3. However, the role of STAT3 in CLL survival is complex and contrary to these pro-survival roles, Rozovski et al. (2016) recently showed that high-levels of constitutively activated serine pSTAT3 correlated with high levels of background apoptosis and high lymphocyte counts, and suggested the mechanism behind the induction of apoptosis is the binding of pSTAT3 to the caspase-3 promoter. These studies suggest both pro-survival and pro-apoptotic functions for STAT3 in CLL cells.

As it appears STAT3 has role in CLL cell survival, we want to investigate the activation status of STAT3 in CLL cells and the effect of a number of putative STAT3 interacting agents, in order to better understand the role of STAT3 in CLL. Three agents, small molecule S3I-201 (S3I), naturally derived product Cucurbitacin and upstream JAK2/STAT3 inhibitor Ruxolitinib were used as tools to investigate the role of the STAT3 pathway in CLL (Figure 3.1). As discussed in the introduction, inhibitors to directly target STAT3 have been difficult to develop. High-throughput screening identified some of the first STAT3 non-peptide small molecule inhibitors that inhibited STAT3 selectively over STAT1 (Schust et al., 2006). A National Cancer Institute (NCI) chemical library screen using a computer model of the STAT3 SH2 domain bound to its phosphorylated tyrosine peptide yielded S3I-201, a chemical probe inhibitor of STAT3. It was shown to inhibit STAT3-STAT3 complex formation and transcriptional activity, repressing the expression of STAT3 regulated genes BCL-x_L, cyclin D1 and survivin. It has been shown to induce apoptosis in breast cancer cell lines at 30-100μM and inhibit

the growth of breast and lung tumour xenografts in mouse models (Chen et al., 2012, Siddiquee et al., 2007). S3I has recently been shown to act as an alkylating agent, alkylating STAT3 on 5 cysteine residues and globally alkylating a range of other intracellular proteins (Ball et al., 2016). Although not available commercially, a number of derivatives of S3I have now been developed with increased specificity and improved potencies, the most promising being S31-201.1066 and BP-1-102 (Zhang et al., 2013, Zhang et al., 2012).

A number of lead compounds have been developed from natural STAT3 inhibitors. Molecules derived from plants, for example caeffic acid, cucurmin from turmeric, capsaicin from hot pepper and resveratrol from berries have been shown to have anti-cancer activities through various mechanisms, including the inhibition of STAT3 activation (Nardini et al., 1998, Aggarwal and Shishodia, 2006). A number of Chinese medicine plants including buetin from stem bark, celastrol from Tripterygium wilfordii, honokiol from *Magnolia officinalis* and cucurbitacins have also been shown to have anti-cancer effects in part through the inhibition of STAT3 (Rajendran et al., 2011, Rajendran et al., 2012b, Rajendran et al., 2012a, Chan et al., 2010, Arora et al., 2012). Cucurbitacins are a class of tetracyclic triterpenoids isolated from a number of plant families, the most common being Cucurbitaceae. There are twelve sub-families A-T, all with a tetracyclic cucurbitane skeleton with varying degrees of oxygen substitution (Chen et al., 2005). In plants, cucurbitacins act to protect from external biological insults. Cucurbitacin I (Cucurbitacin) was discovered from a high throughput screen of the NCI Diversity Set. Cucurbitacin has been shown reduce pSTAT3 activation and induce apoptosis in colon, breast, lung and prostate cancer (Ayyad et al., 2012, Jayaprakasam et al., 2003, Blaskovich et al., 2003). Cucurbitacin also induced apoptosis in CLL cells and sensitizes the cells to treatment with cytotoxic agent Fludarabine (Ishdorj et al., 2010). Ishdorj et al. (2011) also showed that Cucurbitacin activated JNK/c-jun leading to increased VEGF expression in CLL cells, indicating the induction of a stress response; however, this was independent of its effect on STAT3 and apoptosis.

As STAT3 has proved challenging to inhibit directly, a number of upstream molecules have been targeted as an alternative mechanism for inhibiting STAT3. Ruxolitinib is a potent, selective inhibitor of JAK2 and can also inhibit JAK1 (Zhou et al., 2014). It was FDA approved for use in for high-risk myelofibrosis following the results of the COMFORT-I and –II trials (Verstovsek et al., 2012, Harrison et al., 2012, Harrison et al., 2016) and has also been approved for the treatment of Polycythaemia Vera (Vannucchi, 2015). 50% of patients with myelofibrosis and 95% of patients with

polycythaemia Vera carry mutations in JAK2 (Cross, 2011). Ruxolitinib is currently undergoing clinical trials for other haematological malignancies including CLL (Spaner et al., 2016). We used these three agents to interrogate the role of STAT3 in the survival of CLL cells.

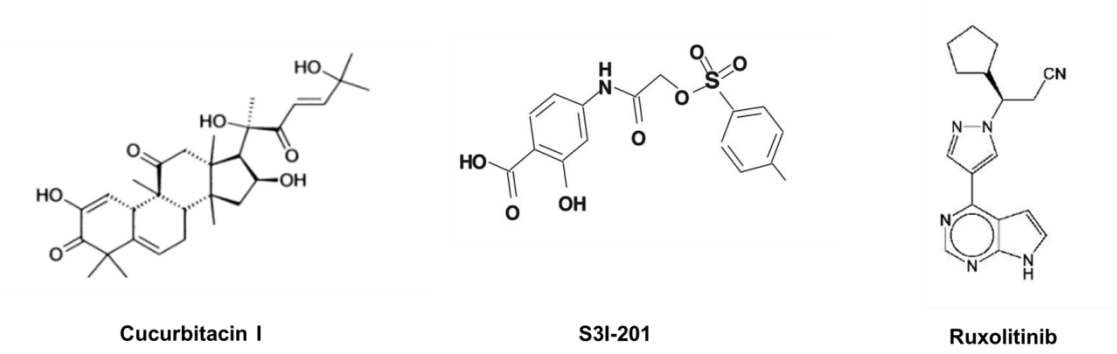

Cucurbitacin I S3I-201 Ruxolitinib

Figure 3. 1 The chemical structures of Cucurbitacin I, S3I-201 and Ruxolitinib.

3.2 Aims

The role of STAT3 in CLL pathobiology is not fully understood. The overall aim of this chapter was to investigate the role of STAT3 pathway in the survival of CLL cells using CLL cell lines and CLL patient samples which have been well characterised and annotated both clinically and molecularly. We also sought to investigate the effects of pharmacological targeting of the STAT3 pathway on STAT3 phosphorylation and localisation.

This aim will be achieved by

- Assessing the phosphorylation status of STAT3 in CLL cell lines and patient samples
- Investigate the relationship between STAT3 phosphorylation and CLL cell survival
- Investigating the effects of Cucurbitacin, S3I and Ruxolitinib on:
    - STAT3 activation and survival and
    - STAT3 localisation in CLL cells.

.

3.3 Results

3.3.1 CLL cells are constitutively phosphorylated on serine pSTAT3 and some on tyrosine pSTAT3

Frank et al. (1997) were the first to show that CLL cells were constitutively phosphorylated on serine but not tyrosine STAT3. Hazan-Halevy et al. (2010) confirmed this and showed that serine pSTAT3 is transcriptionally active in CLL cells, resulting in an upregulation of STAT3 regulated genes. Additional studies have found constitutive tyrosine phosphorylation in CLL cells isolated from some CLL patients (Steele et al., 2010).

We showed by flow cytometry that both cell lines, I83 and HG3 cells, were constitutively phosphorylated on serine residue 727 (Figure 3.2 (a)). We showed that constitutive phosphorylation of serine pSTAT3 is seen only in CLL cells and not normal B cells (Figure 3.2 (b i)) and all patient samples tested were constitutively phosphorylated on serine (n=28). Typically samples had >70% cells positive for serine pSTAT3 (Figure 3.2 b (ii)). In addition to this, 6 out of 28 patient samples in our cohort showed detectable tyrosine phosphorylation in addition to serine phosphorylation (Figure 3.2 b (ii)). In contrast to the high constitutive serine phosphorylation, the percentage of cells positive for tyrosine phosphorylation was variable, ranging from 7% to 60%. As shown in table 3.1 all patient samples with constitutive tyrosine phosphorylation had poor prognostic markers. All 6 patient samples had UM-IGVH and 5 out of 6 harboured a NOTCH1 mutation. In 5 of these samples CD38 expression was determined and 3 were CD38 positive, and CD49d expression was assessed in 3 of these samples and all were CD49d positive.

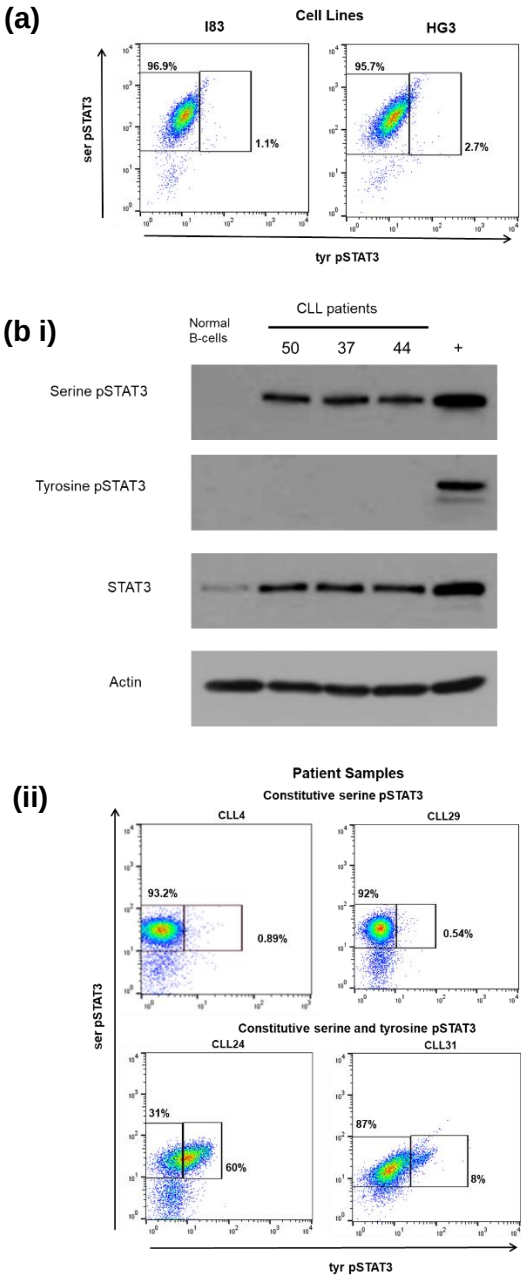

Figure 3. 2 CLL cells exhibit constitutive serine pSTAT3 and a small number exhibit both constitutive serine and tyrosine pSTAT3. (a) I83 and HG3 CLL cell lines exhibiting constitutive serine (ser) pSTAT3 (98% and 98.4% respectively) and lack of tyrosine (tyr) pSTAT3 (both <3%). **(b i)** CLL Patient samples (CLL 50, 37 and 44) show constitutive serine pSTAT3 compared to no constitutive serine pSTAT3 in normal B cells. (+ =positive control, CLL cells treated with IL-6 for 30 minutes). No constitutive tyrosine pSTAT3 was detected. Actin was used as a loading control. (ii) Patient samples (CLL4 and CLL29) exhibiting constitutive serine pSTAT3 (94.1% and 92.5% respectively and lack of tyrosine pSTAT3 (both <1%). **(ii)** Patient samples (CLL24 and CLL31) exhibiting constitutive serine pSTAT3 (91% and 95% respectively) and tyrosine phosphorylation (60% and 8% respectively). For STAT3 intracellular staining cells were gated on CD19 positive cells. Gating was determined using fluorescence minus one (FMO) and unstained controls. The percentage of serine pSTAT3 and serine + tyrosine pSTAT3 cells indicated in all dotplots.

Table 3. 1 Clinical characteristics of patient samples with constitutive tyrosine pSTAT3

CLL	% tyr pSTAT3	IGVH	NOTCH	Flow cytometry Markers	
		M/UM	M/UM	CD38	CD49d
13	16	UM	M	P	ND
23	9	UM	M	ND	ND
24	8	UM	M	N	P
31	60	UM	M	P	P
35	16	UM	UM	N	ND
50	7	UM	M	P	P

UM=unmutated; M= mutated; ND= Not defined; P= positive, defined as >30% expression for CD38 and CD49d; N= negative

3.3.2 IL-6 induces tyrosine pSTAT3 that can be abrogated by Ruxolitinib

We have shown that some patient samples have a proportion of cells which exhibit constitutive tyrosine phosphorylation; however, in CLL cells, microenvironmental stimuli can induce tyrosine pSTAT3, the most characterized of these stimuli being activation of the JAK/STAT3 signalling pathway with Interleukin 6 (IL-6) (Hazan-Halevy et al., 2010). IL-6 is a prosurvival factor that can activate a number of signalling pathways via the IL-6 surface receptor (Hibi et al., 1990), resulting in recruitment and activation of JAK molecules, followed by JAK activation of downstream MAPK/ERK pathway and of STAT1 or STAT3 hetero or homodimers. We showed that significant tyrosine phosphorylation of STAT3 can be induced using IL-6 in CLL ($p=0.0082$; Figure 3.3 (i)). The mean induction of tyrosine pSTAT3 in CLL patient samples was only 19% $\pm$ 5% compared to constitutive serine pSTAT3 which was typically >70%. The induction of tyrosine pSTAT3 was greater in CLL cell lines. Pretreatment with the JAK inhibitor Ruxolitinib at concentrations below cytotoxicity can abrogate tyrosine induced phosphorylation in both patient samples and CLL cell line (Figure 3.3 (ii & iii)). However, Cucurbitacin and S3I had no effect on IL-6 induced tyrosine pSTAT3 (Figure 3.3 (ii & iii)).

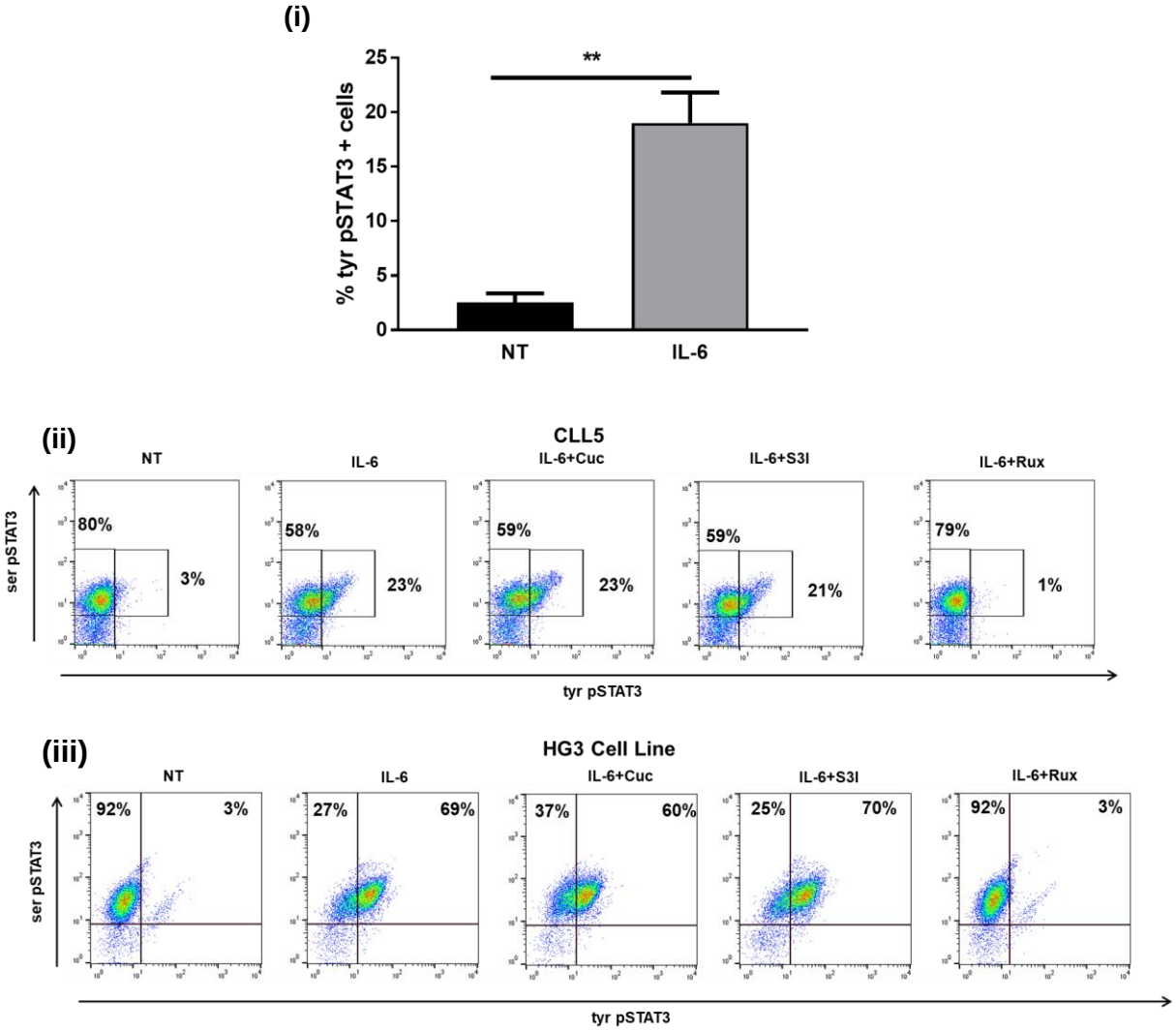

Figure 3. 3 IL-6 results in an increase in tyrosine pSTAT3 that can be abrogated by treatment with Ruxolitinib (i) Significant induction of tyrosine pSTAT3 (tyr pSTAT3) expression in CLL cells after 30 minutes treatment with IL-6 (50ng/ml). Bars represent mean (± s.e.m) of tyrosine STAT3 positive cells (** p=0.0082, n=4; No treatment (NT) *vs* IL-6). Dotplots displaying the percentage of serine pSTAT3 and serine and tyrosine pSTAT3 positive cells in **(ii)** patient derived CLL cells or **(iii)** HG3 cell line after treatment IL-6 for 30 minutes or pretreatment with 1μM Cucurbitacin (Cuc), 100μM S3I or 1μM Ruxolitinib (Rux) for one hour followed by IL-6 treatment for 30 minutes. Dotplots representative of n=3.

3.3.3 The cytotoxic effect of Cucurbitacin, S3I and Ruxolitinib on CLL cells

Having established the STAT3 phosphorylation status and showing that STAT3 is constitutively phosphorylated on serine 727 in CLL cells, we wanted to investigate the effects of three STAT3 targeting agents with distinct mechanisms of action, Cucurbitacin, S3I and Ruxolitinib. We used three methods to assess the cytotoxic effect of Cucurbitacin, S3I and Ruxolitinib in two CLL cell lines, I83 with M-IGVH and HG3 with UM-IGVH. We also assessed the cytotoxicity of two BCR pathway inhibitors, Bruton tyrosine Kinase inhibitor Ibrutinib and PI3Kδ inhibitor Idelalisib. The MTT assay assesses cell viability by measuring metabolic activity of cells which can decrease due to agents having a cytotoxic effect or having an effect on cell proliferation. S3I and Idelalisib had minimal effect on cell viability after 24 and 48 hours in both cell lines. Reduction in cell viability after 24 and 48 hours was observed with Cucurbitacin, Ibrutinib and Ruxolitinib.

In the HG3 cell lines, Cucurbitacin had an EC_{50} of 1.7μM (95% C.I. 1.4μM -2.1μM) and 3.6μM (95% C.I. 2.3μM- 6.0μM) after 24 hours and 48 hours respectively. While in I83 cells, Cucurbiticin had an EC50 of 1.3μM (95% C.I. 0.96μM-1.7μM) after 24 hours and 1μM (95% C.I. 0.75μM-1.3μM) after 48 hours (Figure 3.4 (i)). In HG3 cells Ibrutinib had an EC50 value of 27.5μM (95% C.I 20.8μM-36.6μM) after 24 hours and 32.1μM (95% C.I. 23.1μM-45.3μM) after 48 hours and in I83 an EC50 of 20μM (95% C.I.14.0μM-28.6μM) after 24 hours and 27.6μM (95% C.I, 20.1μM-38.1μM) after 48 hours (Figure 3.4 (iv)). Ruxolitinib reduced cell viability in both cell lines at concentrations greater than 10μM; however, as a maximal response plateau was not reached at 100μM, and an EC50 value was not calculated.

Reduction in cell viability seen with the MTT assay can be due to cytotoxic effects or effects on cell proliferation so, in order to investigate this further, we performed cell cycle analysis. We used Propidium Iodide, a DNA stain to assess the amount of DNA in cells as they progress through the cell cycle. We performed cell cycle analysis by flow cytometry in the I83 cell line as we saw the greatest effects with Cucurbitacin and S3I in these cells by MTT. As shown in figure 3.5, we found that Cucurbitacin induced a G2/M cell cycle arrest after 24 hours. Ruxolitinib had no effect on cell cycle progression in I83 cells. Cucurbitacin and S3I treatment induced an increase in the subG1 population which may be indicative of programmed cell death. BCR inhibitors, Ibrutinib and Idelalisib, resulted in a small increase in cells in G0/G1 phase of the cell cycle.

To further investigate the mechanism of action of these agents, we performed an annexin V/propidium iodine (AV/PI) assay by flow cytometry to assess if cytotoxicity

was due to cells undergoing apoptosis. AV/PI identifies early and late apoptotic cells as Annexin V binds to phosphatidylserine expressed on the surface of apoptotic cells and PI is only taken up by non-viable cells. Treatment with 1μM Cucurbitacin resulted in a significant increase in early and late apoptosis in both cell lines after 24 hours (I83 p=0.0335; HG3 p=0.0459) and 48 hours (I83 p=0.0133, HG3 p=0.0374). Although S3I exhibited minimal cytotoxicity by MTT assay, we did observe that 100μM S31 resulted in a significant increase in both early and late apoptosis in HG3 cells after 24 (p=0.0335) and 48 hours (p=0.0374). Treatment with 10μM BCR inhibitor Ibrutinib resulted in a significant increase in apoptosis in both cell lines after 24 hours (I83 p=0.0424, HG3 p=0.0454) and 48 hours (I83 p=0.0172, HG3 p=0.0424). I83 cells were treated with the cytotoxic agent and a current front-line therapy for CLL, Fludarabine, as a comparison and both concentrations resulted in significant increases in apoptosis up to 40% after 24 hours and 60% after 48 hours (Figure 3.6).

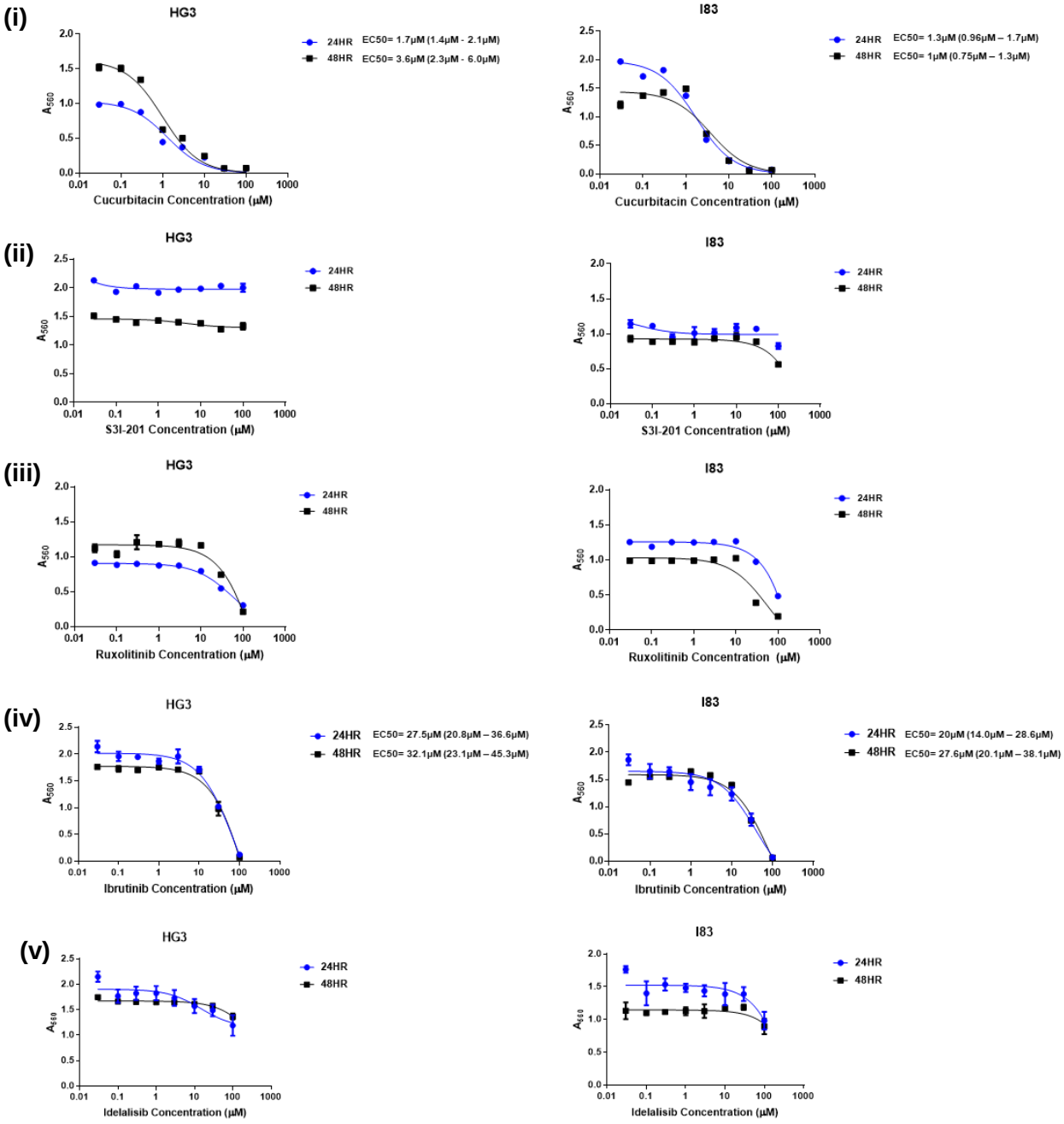

Figure 3. 4 Dose Response examining the effect of STAT3 targeting agents and BCR inhibitors on HG3 and I83 CLL cell lines The dose response effect on cell viability in I83 and HG3 cell lines after treatment with increasing (0.03-100μM) doses of the specified agent **(i)-(v)**. Concentrations are represented using a semi -logarithmic plot and dose response curves are generated following non-linear regression**.** EC_{50} values and 95% confidence intervals (C.I.) were determined and are displayed for treatment with Cucurbitacin and Ibrutinib. Bars are representative of mean absorbance (± s.d) of triplicate measurements. Graphs are representative of 3 independent experiments.

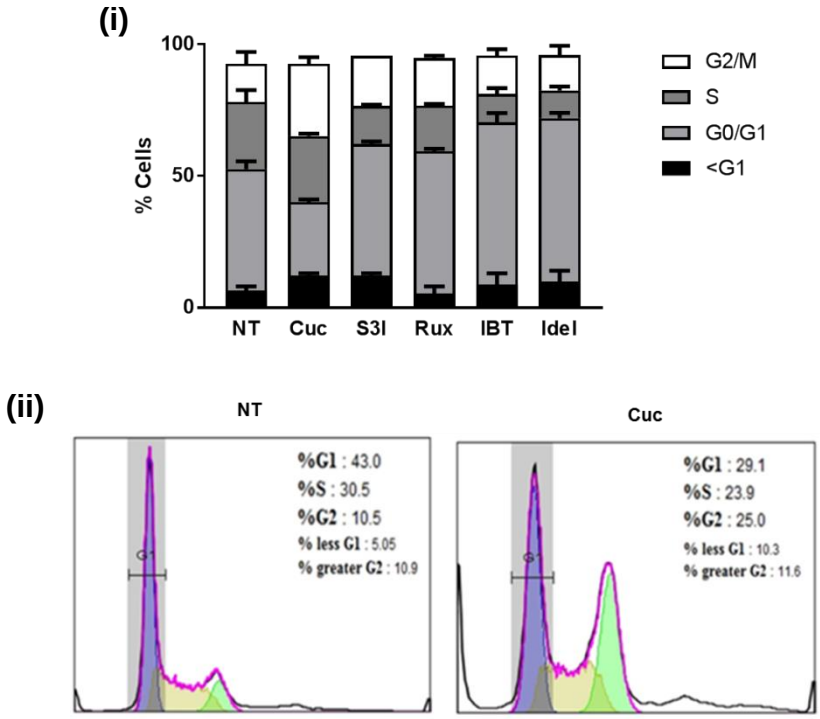

Figure 3. 5 Cucurbitacin results in cell cycle arrest in I83 cell line. (i) Percentage of cells in each stage of the cell cycle (<G1, G0/G1, S and G2/M) in I83 cells after treatment with 1μM Cucurbitacin, 100μM S3I, 1μM Ruxolitinib, 10μM Ibrutinib or 10μM Idelalisib for 24 hours. Bars represent mean (± s.e.m) of 3 independent experiments **(ii)** Representative histogram displaying the percentage of I83 cells in each stage of the cell cycle after treatment with Cucurbitacin (Cuc) for 24 hours.

.

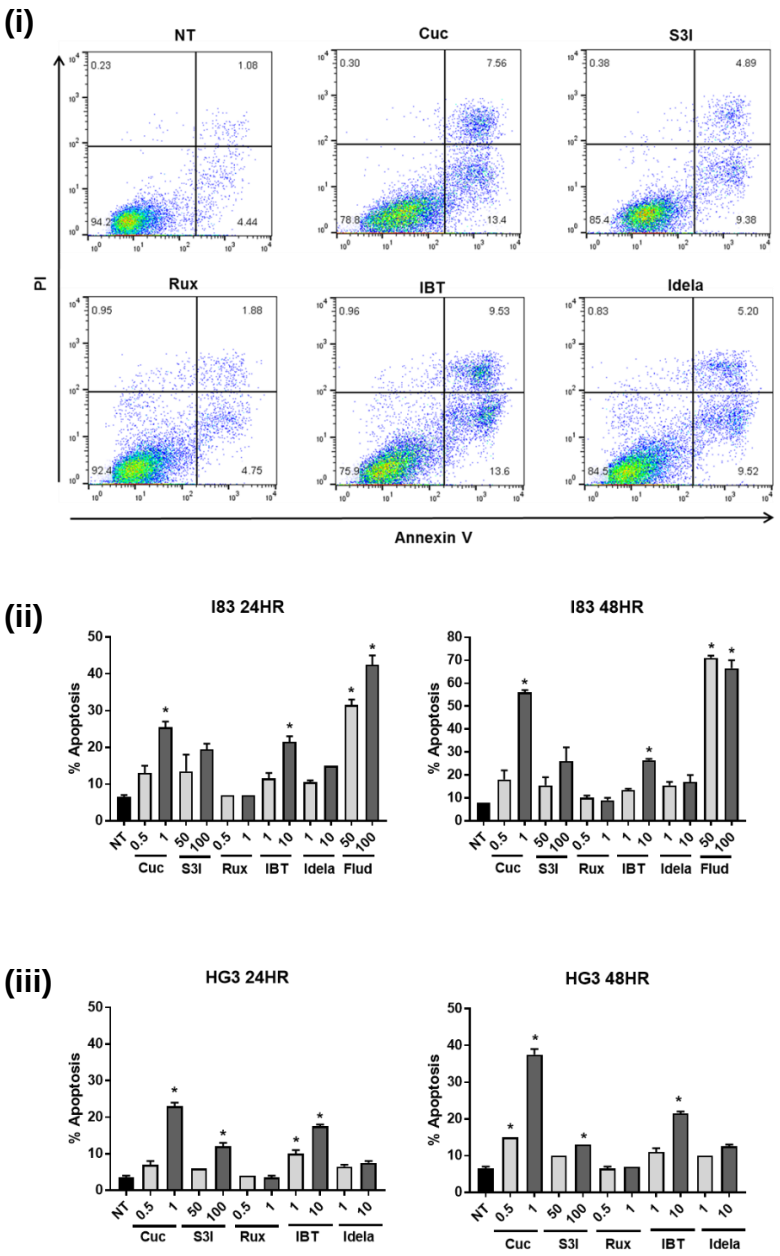

Figure 3. 6 Apoptosis in response to STAT3 targeting agents and BCR inhibitors after 24 and 48 hours in I83 and HG3 CLL cell lines. (i) Representative dotplots displaying the percentage of AV/PI positive cells after 24 hours cultured with 1μM Cucurbitacin (Cuc), 100μM S3I, 1μM Ruxolitinib (Rux), 10μM Idelalisib (Idela) and 10μM Ibrutinib (IBT). The percentage of the total early (lower right hand quadrant) and late apoptosis (upper right hand quadrant) as determined by AV/PI assay and flow cytometry in **(ii)** I83 and **(iii)** HG3 cells cultured with Cucurbitacin , S3I, Ruxolitinib , Idelalisib , Ibrutinib or Fludarabine (Flud) for 24 and 48 hours 1μM Cucurbitacin resulted in a significant increase in apoptosis in both cell lines after 24 hours (I83 * p=0.0335; HG3 *p=0.0459) and 48 hours (I83 *p=0.0133; HG3 *p=0.0374). 100μM S3I resulted in a significant increase in apoptosis in the HG3 cell line after 24 (*p=0.0335) and 48 hours (*p=0.0374). 10μM Ibrutinib resulted in a significant increase in apoptosis in both cell lines after 24 (I83 *p=0.0424; HG3 *p=0.0454) and 48 hours (I83 *p=0.0172; HG3 *p=0.0424). p values determined by t-test *vs* no treatment (NT). Bars represent mean apoptosis ± s.e.m of 3 independent experiments.

3.3.4 Serine pSTAT3 is downregulated in CLL cells where Cucurbitacin and S3I are cytotoxic but not where they are protective

Having assessed the effect Cucurbitacin, S3I and Ruxolitinib on cell survival in in two CLL cell lines, we wanted to determine the effect on patient derived CLL cells. Unlike cell lines, patient derived CLL cells can undergo spontaneous apoptosis when cultured *ex vivo* (Oliveira et al., 2001) and we saw different rates of this spontaneous apoptosis in our patient samples. Ruxolitinib had no effect on the spontaneous apoptosis of CLL cells. However, interestingly, we showed that treatment with Cucurbitacin and S3I have a variable effect on patient derived CLL cells: these agents induced apoptosis in some patient samples, and were protective and reduced the amount of spontaneous apoptosis in others (Figure 3.7 (a i)). We also show that the toxic and protective effect of Cucurbitacin is dose-responsive (Figure 3.7 (a iii)). Investigating the variable effect of Cucurbitacin further, we showed a significantly lower level of spontaneous apoptosis in cells where Cucurbitacin is toxic compared to cells where Cucurbitacin is protective ($p=0.0400$; Figure 3.7 (b)). We then categorized patient samples based on prognostic indicators: IGVH mutational status, NOTCH1 mutational status, CD38 and CD49d expression. We found a significant difference in the induction of apoptosis by Cucurbitacin between CD38 positive and CD38 negative patient samples ($p= 0.0435$; Figure 3.7 (c)) with a lower induction of apoptosis/protective effect in CD38 negative samples. There was no significant difference between NOTCH1 mutated and unmutated patient samples. Cucurbitacin showed a trend to being protective in CD49d negative patient samples although this was not significant ($p=0.1294$; Figure 3.7 (c)). While there was no significant difference between M-IGVH and UM-IGVH there was more variability in the effect of Cucurbitacin on cell survival in patient samples with UM-IGVH compared to M-IGVH.

We next investigated the role of phosphorylation of STAT3 on the variability of cytotoxic response to Cucurbitacin and S3I in CLL cells, as the levels of STAT3 phosphorylation have been implicated in CLL cell survival (Rozovski et al., 2016). In the HG3 and I83 cell lines, we show, in addition to a cytotoxic effect (Figure 3.7), treatment with Cucurbitacin and S3I also results in a decrease in serine pSTAT3 in HG3 cells, while in the I83 cells treatment with Cucurbitacin results in a decrease in serine pSTAT3 (Figure 3.8 (a)). In CLL patient samples, in addition to the variable effect of Cucurbitacin and S3I on cell survival, the agents also had a variable effect on

serine pSTAT3. In CLL cells where the agents resulted in cytotoxicity, Cucurbitacin ($p=0.0068$) and S3I ($p=0.0233$) treatment resulted in significant decreases in the serine pSTAT3; however, in CLL cells where Cucurbitacin and S3I treatment resulted in a decrease in spontaneous apoptosis, the agents had no significant effect on the levels of serine pSTAT3 (Figure 3.8 (b i)). Ruxolitinib, which had no effect on CLL cell survival also, had no effect on serine pSTAT3.

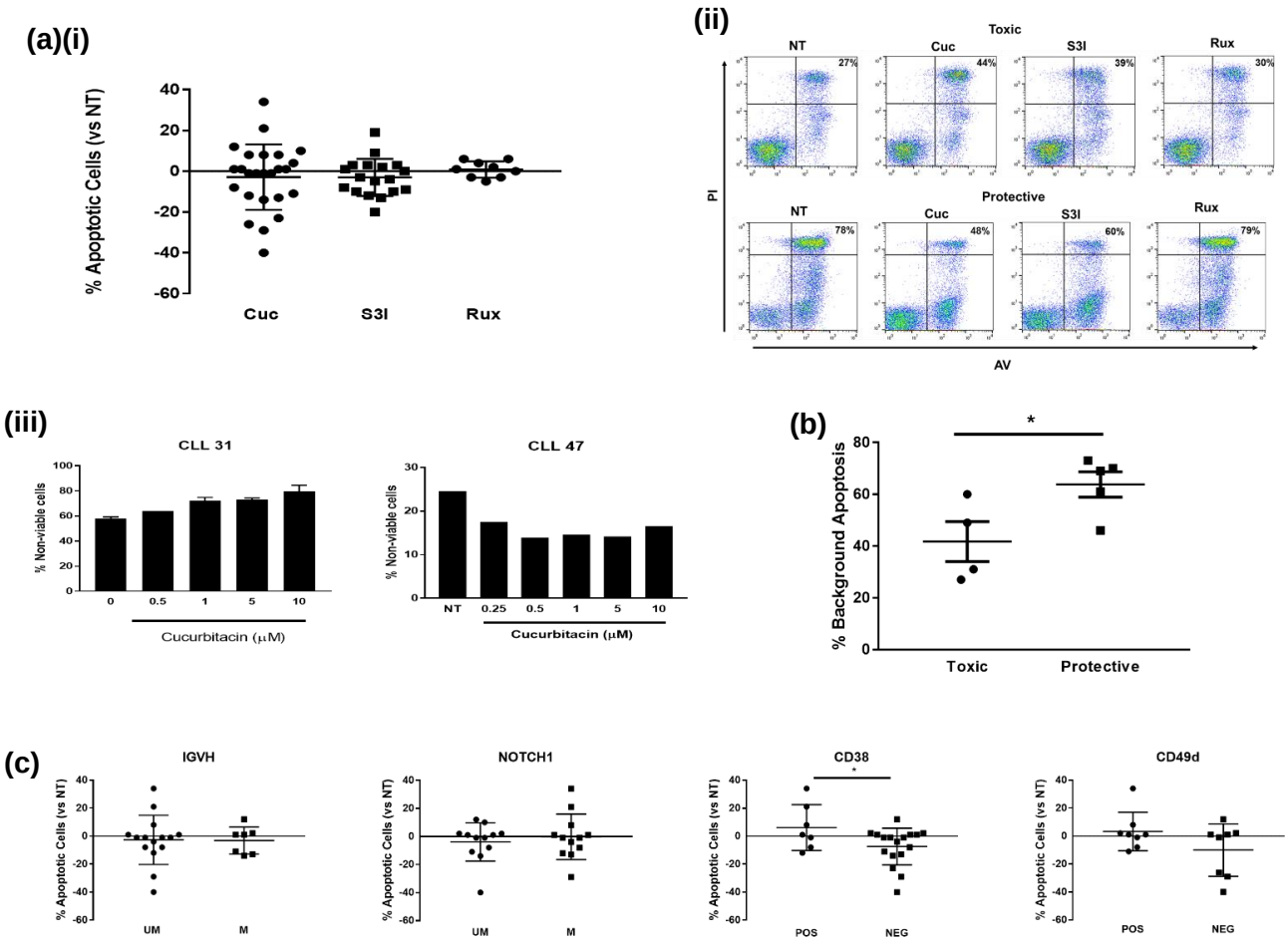

Figure 3. 7 STAT3 inhibitors have a variable effect on apoptosis in *ex vivo* CLL cells.

(a i) Patient derived CLL cells were treated with 1μM Cucurbitacin (Cuc) (n=27), 100μM S31 (n=20) or 1μM Ruxolitinib (Rux) (n=11) for 24 hours and apoptosis was quantified by AV/PI staining in CD19+ cells. Each dot represents a patient sample and bars show mean (± s.e.m). **(ii)** Representative dotplots displaying the percentage of apoptotic CLL cells after treatment with Cucurbitacin, S3I or Ruxolitinib for 24 hours. The top row shows a patient sample (CLL13) where Cucurbitacin and S3I induced an increase in apoptosis and the bottom row shows a patient sample (CLL6) where the agents were protective (i.e. reduced spontaneous apoptosis). **(iii)** Dose response effect of Cucurbitacin on the viability of CLL cells from patients (CLL 31 and CLL47) after 24 hours. Flow cytometry was used to quantify non-viable cells by PI uptake. **(b)** Cuc is protective in CLL cells exhibiting higher spontaneous apoptosis. 'Protective' are patient samples (n=5) where apoptosis decreases and 'toxic' are samples (n=4) where apoptosis increases after treatment with Cucurbitacin for 24 hours (* p=0.0400). Bars represent mean (± s.e.m). **(c)** The percentage increase in apoptotic CLL cells after treatment with Cucurbitacin for 24 hours in patient samples categorized by IGVH mutational status unmutated (UM, n=15) and mutated (M, n=7), NOTCH1 unmutated (UM, n=12) and mutated, CD38 positive (POS, n=7) and negative (NEG, n=17)(* p= 0.0435) and CD49d positive (POS, n=8) and negative (NEG, n=8).

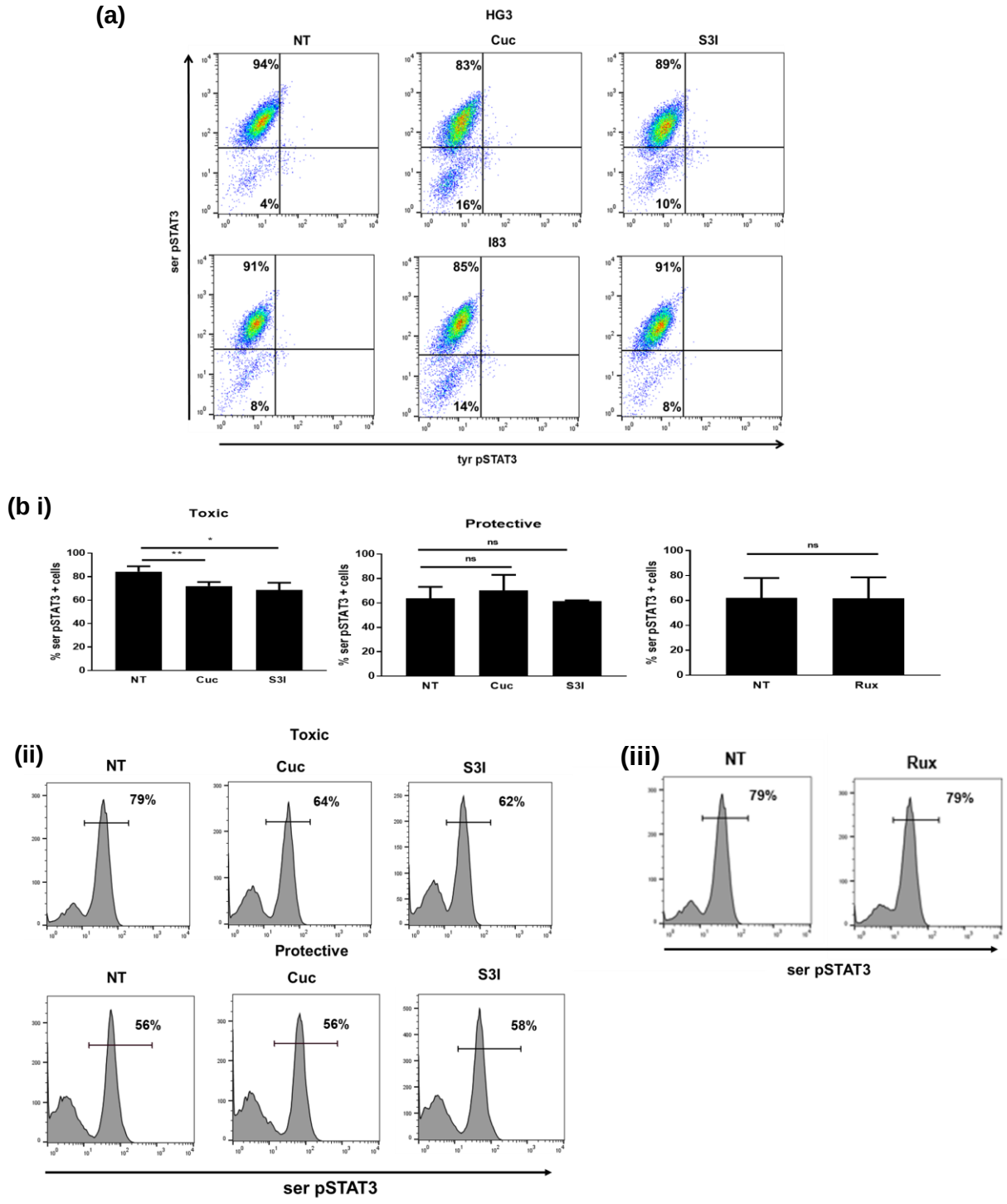

Figure 3. 8 Cucurbitacin and S3I-201 result in the downregulation of serine pSTAT3 in cells where they are toxic but not protective. (a) Serine (ser) and Tyrosine (tyr) phosphorylation of STAT3 (pSTAT3) in HG3 and I83 cells after treatment with 1μM Cucurbitacin (Cuc) or 100μM S3I for 24 hours. The percentages of serine pSTAT3 positive and negative cells are shown. Dotplots representative of 3 independent experiments (No treatment- NT) **(b i)** percentage of serine pSTAT3 in CLL cells where Cucurbitacin (Cuc) and S3I was toxic and protective after treatment with Cucurbitacin (** p=0.0068, n=4), S3I (* p= 0.0233, n=3) or Ruxolitinib (n=4) for 24 hours. Bars represent mean percentage (± s.e.m) (Not significant- ns). Representative histograms displaying percentage of serine pSTAT3 in CLL cells after treatment with **(ii)** Cucurbitacin or S3I or **(iii)** Ruxolitinib (CLL13) for 24 hours. The top panel shows a patient sample where Cucurbitacin was toxic and resulted in a decrease in serine pSTAT3 (CLL 31) and the bottom shows a patient sample where Cucurbitacin and S3I were protective and had no effect on serine pSTAT3 (CLL 6).

3.3.5 Treatment with Cucurbitacin results in the aggregation of STAT3 and F-actin in CLL patient samples

STAT3 can be regulated by other mechanisms, in addition to phosphorylation, such as being sequestered in the cytoskeleton (Verma et al., 2009, Ng et al., 2006). The mechanism of action of Cucurbitacin is not known so we wanted to investigate whether it had an effect on non-phosphorylation mechanisms of STAT3 regulation. We specifically wanted to investigate whether Cucurbitacin mediated cytoskeletal changes that could affect STAT3 cellular distribution and regulation. STAT3 in untreated CLL cells and cells treated with Ruxolitinib and S3I was mostly uniformly distributed between the cytoplasm and nucleus. Treatment with Cucurbitacin resulted in the polar localisation of F-actin and STAT3 in the cell cytoplasm (Figure 3.9).

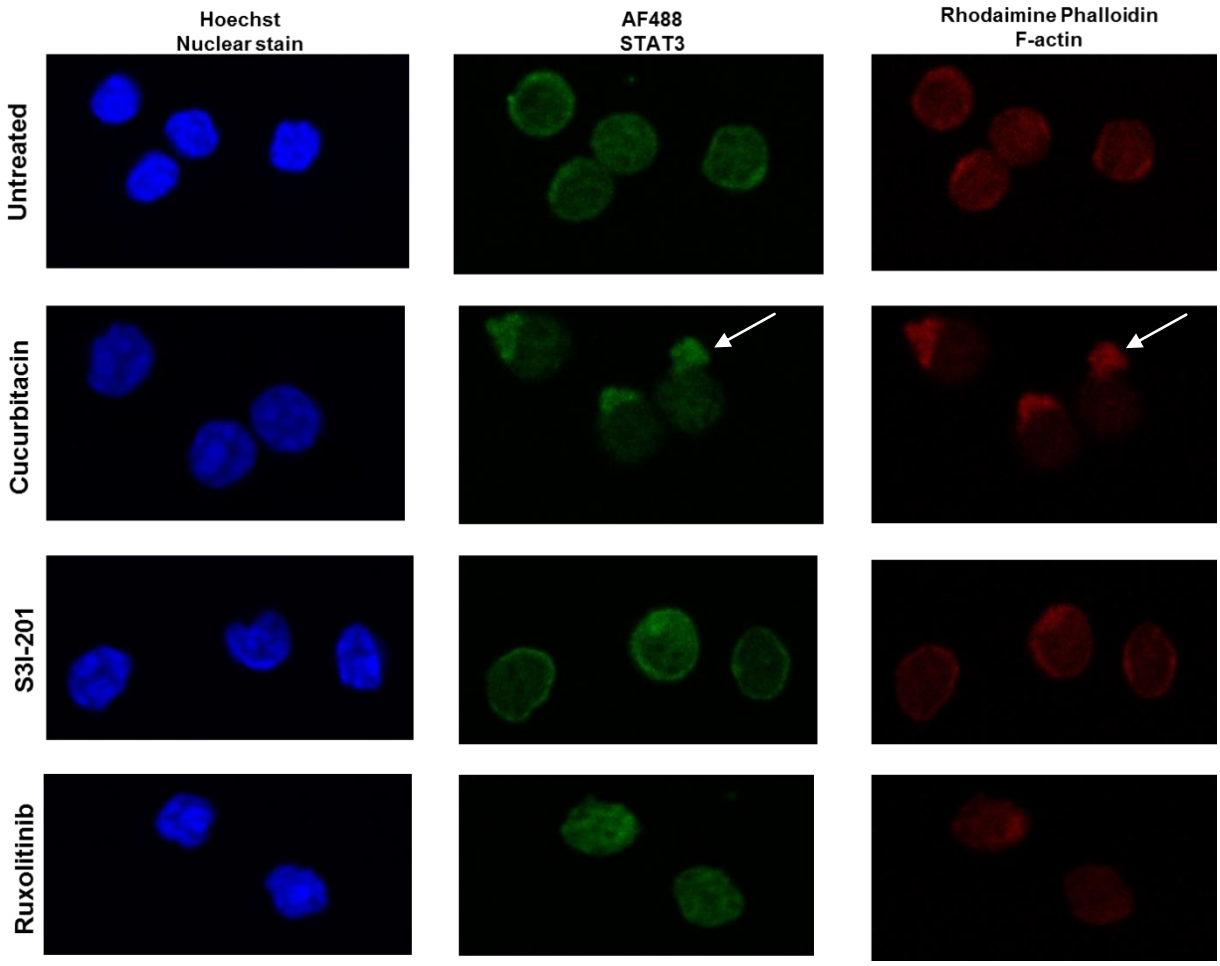

Figure 3. 9 Cucurbitacin I but not S3I or Ruxolitinib results in the aggregation of F-actin and STAT3 in CLL cells. Confocal images showing the staining of the nucleus, total STAT3 and F-actin in CLL cells treated with 1μM Cucurbitacin, 100μM S3I and 1μM Ruxolitinib for 4 hours. CLL samples used were >90% CD19/CD5+. Treatment with Cucurbitacin resulted in polarisation of STAT3 and F-action in the cytoplasm (indicated by the arrows). Images are representative of 4 independent experiments.

3.4 Discussion

STAT3 is a transcription factor that is known to have both oncogenic and tumour suppressor functions. Normally it is phosphorylated on tyrosine residue 705; however, it has an additional serine phosphorylation site at 727 which has been suggested to be required for maximal transcriptional activity (Wen et al., 1995). It has been shown that CLL cells are constitutively phosphorylated on serine STAT3 (Hazan-Halevy et al., 2010) however some studies have also shown constitutive tyrosine pSTAT3 (Steele et al., 2010). Six samples from our patient cohort showed detectable tyrosine phosphorylation in addition to constitutive serine phosphorylation and tyrosine phosphorylation was associated with poor prognostic markers. All 6 had UM-IGVH and 5 out of 6 had mutated NOTCH1. No association has previously been made in CLL between patient samples exhibiting tyrosine pSTAT3 and poor prognostic markers. However, further work is needed in a larger cohort of patients to investigate this association and whether tyrosine pSTAT3 may be a poor prognostic marker in CLL.

We assessed the effects of STAT3 targeting agents, Cucurbitacin, S3I and Ruxolitinib on the phosphorylation of STAT3 and investigated whether STAT3 had a role in CLL cell survival. Cucurbitacin and S3I resulted in a decrease in serine pSTAT3 and induced apoptosis in the HG3 cell line with UM-IGVH, a poor prognostic marker for CLL. Cucurbitacin resulted in a decrease in serine pSTAT3 and induced apoptosis in the I83 cell line with M-IGVH, a good prognostic marker for CLL. Ruxolitinib had no effect on pSTAT3 and cell death in either cell line. There are a number of mechanisms for targeting STAT3 including direct and indirect targeting. Ruxolitinib is an indirect inhibitor of STAT3, inhibiting JAK2, upstream of STAT3. The JAK/STAT3 pathway may not be activated as we see no tyrosine phosphorylation in unstimulated HG3 or I83 cells (Figure 3.2 (a)) therefore Ruxolitinib has no effect on STAT3 phosphorylation. The two cell lines, I83 and HG3 differ in their IGVH mutational status and may also differ in other biochemical and genetic factors as they are derived from separate CLL patients. The mechanism of activation of STAT3 in the HG3 and I83 cell lines is not elucidated and different mechanisms of the activation of STAT3 may explain why S3I has an effect on STAT3 phosphorylation in the HG3 cell line but not the I83 cell line. The BCR inhibitors Ibrutinib and Idelalisib were less toxic to the cell lines than Cucurbitacin. The BCR is not stimulated in the CLL cell lines and this may contribute to the lack of efficacy of the BCR inhibitors. Primary CLL cells are resistant to transformation by Epstein Barr Virus (EBV) (Walls et al., 1989) and a number of cell lines where EBV transformation is successful in CLL is normally due to successful transformation of the

normal B cell compartment from CLL patients resulting in a lack of immortalised CLL cell lines that accurately reflect the disease. In addition EBV has been shown to effect BCR activation and cross-linking (Miller et al., 1994, Miller et al., 1993). The BCR is important in the pathogenesis of CLL and ability to study its activation is key to further understanding the disease. The BCR pathway can be stimulated in patient samples, highlighting the importance of the difference between cell line models and patient samples. This difference was further highlighted by the fact that while we saw apoptosis and a decrease in pSTAT3 in our cell lines, we show variable toxicity of our STAT3 inhibitors in our patient cohort, with Cucurbitacin and S3I resulting in an increase in apoptosis in some samples and protection from spontaneous apoptosis in others.

In addition, our cohort was well-characterized clinically, allowing us to investigate the variability of Cucurbitacin on CLL cell survival. We stratified patient samples by background serine pSTAT3, levels of spontaneous apoptosis and clinical parameters. Liu et al. (2016) have shown that high levels of spontaneous apoptosis correlated with low levels of serine pSTAT3 however no study has investigated the variable susceptibility of CLL patient samples to STAT3 targeting agents. We showed that samples with higher serine pSTAT3 and lower background apoptosis were more susceptible to toxicity with STAT3 targeting agents Cucurbitacin and S3I. We also showed that patient samples positive for the poor prognostic marker CD38 were more susceptible to Cucurbitacin induced toxicity. Although the direct activation of STAT3 by CD38 has not been studied, CD38 engagement has been shown to indirectly activate the STAT3 pathway through the production of the JAK/STAT3 activator IL-6 in myeloma (Fedele et al., 2013). CD38 engagement in CLL has been shown to activate a number of signal transduction pathways including the Syk pathway (Benkisser-Petersen et al., 2016) and its engagement could potentially activate STAT3 and a link between CD38 and STAT3 may in-part explain the mechanism behind CD38 positive patient samples showing more susceptibility to toxicity using STAT3 targeting agents. Further investigations in a larger cohort to confirm this association are needed.

The variable results of STAT3 targeting agents Cucurbitacin and S3I on CLL cell death suggest a complex role for STAT3 in CLL cell survival. The oncogenic role for STAT3 in CLL has been demonstrated (Hazan-Halevy et al., 2010) but Rozovski et al. (2016) have also shown a tumour suppressor role, showing that at high levels serine pSTAT3 can induce apoptosis in CLL cells. Our data supports the idea of STAT3 having both pro-survival and toxic roles in CLL as we show a variable effect of STAT3 targeting

agents Cucurbitacin and S3I, being prosurvival in some patients and toxic in others. We also show that toxicity is associated with a concomitant downregulation in the serine phosphorylation of STAT3, suggesting a mechanism for the toxicity induced by Cucurbitacin and S3I. Ruxolitinib had no effect on STAT3 phosphorylation or CLL cell survival, suggesting the JAK activation of STAT3 is not contributing to cell survival in unstimulated CLL cells.

Ishdorj et al. (2010) also investigated the effect of Cucurbitacin on CLL patient samples and they found that Cucurbitacin resulted in a decrease in serine pSTAT3 and induced apoptosis. However, they only examined the effects of Cucurbitacin in 6 patients after 72 hours and found an increase in apoptosis in all patients but found this toxicity varied from 20% to 80%. We found the effect of Cucurbitacin after 24 hours which was sustained up to 72 hours. CLL cells undergo spontaneous apoptosis and the selection of a single timepoint at 72 hour hours may lead to *in vitro* artefacts predominating. In addition, we showed the protective and toxic effects of Cucurbitacin were dose responsive while Ishdorj et al (2010) only performed studies at one concentration (1μM) of Cucurbitacin. Ishdorj et al (2010) did not indicate the characteristics of the patient samples they tested while as discussed, we also found the effect of Cucurbitacin was associated with high CD38 expression.

We also assessed the localisation of STAT3 in response to Cucurbitacin, S3I and Ruxolitinib. We found that Cucurbitacin resulted in polarisation of F-actin and STAT3 in the cytoplasm. Cucurbitacins can affect microtubule networks and actin reorganization (Duncan et al., 1996, Graness et al., 2006, Yin et al., 2008) (Sari-Hassoun et al., 2016). We found this effect of Cucurbitacin on actin aggregation in patient samples where Cucurbitacin was both toxic and protective so this did not contribute to the variability seen in toxicity. This does, however; suggest a mechanism of the effect of Cucurbitacin on STAT3 in CLL cells by indirect sequestering of STAT3 which warrants further investigation.

We have shown that Cucurbitacin and S3I show variable toxicity to CLL cells and our results suggest a complex role for STAT3 in CLL survival, however; we have shown that CD38 positive CLL patient samples may be more susceptible to toxicity by STAT3 targeting agents. Therapeutically, in addition to cell survival, cell trafficking and microenvironmental interactions have emerged as important potential therapeutic targets for CLL. This is demonstrated by the effects of BCR inhibitors Ibrutinib and Idelalisib which are not highly toxic to CLL cells but in addition to targeting the BCR pathway, have effects on microenvironmental interactions of CLL cells (Chang et al.,

2013, Chen et al., 2016). In chapters 4 and 5 we investigate whether STAT3 is involved in cell trafficking and microenvironmental interactions and whether targeting STAT3 may be therapeutically beneficial from this angle aside from its role in cell survival in CLL.

.

Chapter 4

The role of STAT3 in the regulation of CD62L and the migration and adhesion of CLL cells

4.1 Introduction

The ability of normal B cells to recirculate between the blood and secondary lymphoid organs is critical to their development and to maintaining immune function. In order to achieve this, B cells must be able to adhere to endothelial layers, roll over the surface of these cells and transmigrate through cellular junctions. Interactions of B cells with endothelial cells and extracellular matrix components are transient and flexible. The same processes are crucial in CLL pathobiology, allowing infiltration of CLL cells to proliferation centres (PCs) in the secondary lymphoid organs, and resulting in splenomegaly and lymphadenopathy which are associated with poor prognosis (Binet et al., 1981, Schmid and Isaacson, 1994). Having investigated the role for STAT3 in CLL cell survival in chapter 3, we next wanted to investigate if STAT3 has a role in CLL cell homing and migration to PCs, and protective niches in the lymph nodes and bone marrow, as this could provide additional therapeutic potential to targeting STAT3 in CLL.

The process of migration of B cells from the high endothelial venules (HEVs) to the protective microenvironment of the lymph node is mediated by a number of sequential interactions between adhesion molecules expressed on cells and molecules on endothelial cells that line the HEVs. The initial steps of the adhesion cascade require B cells to be tethered from circulation in the blood in order to roll along the endothelium. Studies with CD62L deficient mice have identified a key role for CD62L in the tethering and rolling of B cells to the endothelial cells of the HEVs (Rosen et al., 1997) (Grailer et al., 2009, Arbones et al., 1994). Selectins are type I membrane proteins that have an extracellular domain, consisting of a calcium dependent lectin domain, an epidermal growth factor (EGF) domain, short tandem repeats and a cytoplasmic tail (Drickamer, 1988). CD62L initiates the tethering of cells by forming protein-carbohydrate bonds with glycosylated ligands such as GlyCAM-1, CD34, MadCAM and PSGL1 expressed on endothelial cells lining the HEVs (Rosen, 1993). CD62L dependent adhesion requires cells to be under minimal fluid shear conditions to stabilize the catch bonds formed between CD62L and its ligands (Lawrence et al., 1997, Dwir et al., 2003). The activation of the CD62L results in the initiation of the next step in the cascade; the activation of integrins and an increase in adhesion to endothelial cells (Giblin et al., 1997, Steeber et al., 1997). Integrins are adhesion molecules composed of α and β subunits that can be transiently activated to mediate the adhesion of cells to endothelial cells and the extracellular matrix (Hemler, 1990). Integrin αX (CD11c) forms a dimer with the β2 subunit (CD18) to form a molecule that binds fibrinogen (Postigo et al.,

1991), ICAM-1 (Blackford et al., 1996) and ICAM-4 (Ihanus et al., 2007) which are expressed on endothelial cells. Other members of this integrin family, CD11a/CD18 and CD11c/CD18, also play a key role in the migration to the lymph nodes (Berlin-Rufenach et al., 1999). High expression of CD11c has been reported in CLL patients with splenomegaly, suggesting it may have a role in migration of CLL cells to the spleen (Hanson et al., 1990). Integrin VLA4, a heterodimer of α4 (CD49d) and β1(CD29) subunits, is activated and mediates cell-cell and cell-ECM interactions through adhesion to ligand VCAM-1 expressed on endothelial cells (Elices et al., 1990) and fibronectin, a component of the ECM (Guan and Hynes, 1990) (Yago et al., 1997). CLL cells have been shown to express variable VLA4 expression that is reduced compared to normal B cells (Hartmann et al., 2009). Despite its lower expression, VLA4 on CLL cells is functional and increased expression on CLL cells is associated with enhanced migration and adhesion to endothelial cells (Brachtl et al., 2011, Till et al., 2002). VLA4 can form a complex with CD38 in CLL cells (Zucchetto et al., 2012). CD38 is a surface glycoprotein that mediates cell-cell interactions important in the transmigration of cells by engaging with CD31 (platelet endothelial cell adhesion molecule-1 (PECAM-1)) on endothelial cells (Deaglio et al., 1998). High expression of CD38 in CLL has been shown to enhance homing (Vaisitti et al., 2010). As discussed earlier, both CD49d (Bulian et al., 2014, Shanafelt et al., 2008, Zucchetto et al., 2006) and CD38 (Damle et al., 1999) are independent prognostic markers associated with a poor prognosis in CLL. Following adhesion to the endothelial cells, through interactions with integrins and chemokines, CLL cells must then undergo transmigration through cellular junctions, mediated by late adhesion molecules, such as CD31 (Dasgupta B1, 2009). CD31 expression is variable on CLL cells; however, low expression of both CD38 and CD31 was associated with longer survival in CLL patients (Ibrahim et al., 2003).

Parallel to this integrin activation and engagement, chemokine networks, including CXCL13 (Burkle et al., 2007), CCL19, CCL21 (Till et al., 2002) and, in particular, the CXCL12/CXCR4 axis also contribute to the activation and expression of integrins on CLL cells (Montresor et al., 2015). CXCL12 is constitutively produced by stromal cells in the bone marrow and lymph node microenvironments producing a gradient to home and position CLL cells. CXCL12 signals through its receptor, CXCR4, a G protein coupled receptor which is overexpressed on the surface of CLL cells (Mohle et al., 1999, Burger et al., 1999); resulting in the activation of Akt and ERK1/2 signalling, and integrin dependent arrest under shear flow conditions (Nishio et al., 2005).

In addition to impaired chemokine signalling, it is known that CLL cells have impaired transmigrational capacity compared to healthy B cells (Chen et al., 1999, Bazerbashi et al., 1978); however, the capacity of CLL cells to transmigrate varies between patients, with increased capacity to transmigrate seen in cells from patients with advanced disease and lymph node involvement (Till et al., 2002). CD62L is a key factor in controlling B cell rolling to endothelial cells in the HEVs (Arbones et al., 1994). Reports on the expression of CD62L in CLL cells, compared to non-malignant cells, have been contradictory. Spertini et al. (1991) showed that the expression of CD62L is similar, while Gu et al. (2001) found CLL cells expressed significantly less CD62L and showed impaired trans endothelial migration compared to non-malignant B cells. The expression of CD62L between patient samples is highly variable but it has been shown that CD62L expression correlates with functional capacity of the CLL cells to bind HEVs (Csanaky et al., 1994). Importantly, it has been shown that CD62L controls the trafficking of CLL cells in the HEVs of the lymph nodes in *in vivo* mouse models (Lafouresse et al., 2015), and may have a prosurvival role in CLL (Burgess et al., 2013).

Here, we examine the effect of pharmacologically targeting the BCR and STAT3 signalling pathways on a panel of CLL cell surface molecules key to separate steps of the multistep cell trafficking cascade: the selectin, CD62L; integrins CD49d, CD29 and CD11c; and adhesion molecules CD38 and CD31. In addition to their important role in the recirculation of CLL cells, the expression of adhesion molecules alone can inform on disease progression in CLL (Byrd et al., 2013, Woyach et al., 2014a). Huang et al. (2013) distinguished stable, stable-progressive and progressive CLL by differences in the expression of 27 cell surface antigens, suggesting that these molecules have a role in disease pathogenesis.

A number of downstream signalling pathways are activated after engagement of adhesion molecules (Buchner et al., 2010b, Aoudjit and Vuori, 2012). Few studies have investigated the role of STAT3 in CLL cell migration and recirculation. JAK2, the upstream activator of STAT3 has been shown to mediate CXCL12 induced expression of integrins LFA-1 and CD49d (Montresor et al., 2015). Burger et al (2005) showed that CXCL12 signalling results in an increase in serine pSTAT3 and this can be inhibited by pretreatment with peptide inhibitors of CXCR4, which also interrupt the homing of CLL cells to protective microenvironments. STAT3 has, however, been implicated in the migration of other cell types and dissemination of other cancer types. STAT3 was first implicated in the regulation of cell migration in wound healing studies, where inhibition

of STAT3 in keratinocytes resulted in disrupted migration, leading to impaired wound healing in response to external cytokines (Sano et al., 1999). In solid tumours, invasion and metastasis are complex multistep processes requiring cancer cells to detach, enter surrounding tissue and basement membrane and extravaste through the blood vessels to distant organs. Results from a number of studies have shown a role for STAT3 in this process in a number of different cancers by regulating genes that are involved in adhesion and migration. STAT3 has been shown to upregulate different matrix metalloproteinases (MMP) which can degrade the basement membrane; MMP1 in colorectal adenocarcinoma (Zugowski et al., 2011); MMP2 in melanoma cells (Xie et al., 2004) and MMP9 in breast cancer cells (Song et al., 2008) and integrins including integrin β6 promoting invasion in prostate cancer cells and integrin β4 in mammary tumorigenesis resulting in enhanced migration (Guo et al., 2006, Azare et al., 2007). In breast cancer cell lines, activation of STAT3 upregulates fascin and vimentin, proteins involved in cytoskeletal rearrangement, allowing migration to occur (Snyder et al., 2011, Wu et al., 2016). STAT3 also affects cell migration through non-transcriptional regulation of molecules involved in adhesion and migration; non-phosphorylated cytoplasmic STAT3 has been shown to interact with stathmin to regulate microtubule dynamics by inhibiting microtubule destabilization in T cells (Verma et al., 2009, Ng et al., 2006).

In addition to investigating a panel of molecules involved in the migration of CLL cells, we also wanted to investigate the effect of Cucurbitacin on the adhesion of CLL cells under shear flow. A number of studies in CLL examine adhesion under static conditions *in vitro*; however, given the importance of fluid shear flow in the tethering, rolling and subsequent adhesion, we established a model in which we expose CLL cells to controlled physiologic shear forces, by flowing CLL cells through endothelial cell coated channels in biochips to mimic the conditions CLL cells undergo in the HEVs. Elucidating further the mechanisms of CLL cell trafficking may provide new targets to interfere with the trafficking of CLL cells, preventing dissemination to the lymph node compartments and increasing efficacy of existing therapeutics (Hayden et al., 2012).

.

4.2 Aims

The overall aims of this chapter were to investigate the role of the STAT3 pathway in regulating the expression of adhesion molecules, and the chemotaxis and migration of CLL cells. This was achieved by:

- Examining the effect of pharmacologically targeting the BCR and STAT3 signalling pathways on a panel of key adhesion molecules, previously shown to have keys roles in CLL cell interaction with endothelial cells in HEV
- Investigating a role of for STAT3 in mediating CD62L expression in CLL cells
- Examining the effect of Cucurbitacin and S3I on the chemotaxis of CLL cells
- Determining the effect of Cucurbitacin on CLL cell adhesion to HUVECs under physiologically relevant fluid shear flow

4.3 Results

4.3.1 Treatment with Cucurbitacin and S3I results in the downregulation of CD62L

We investigated the effect of pharmacologically targeting the BCR and STAT3 signalling pathways on a panel of surface molecules involved in cell adhesion and migration. These molecules were chosen as they play key roles in the transmigration of CLL cells across the endothelia in HEVs, as well as, in the case of CD38 and CD49d, being unfavourable prognostic indicators. We first investigated the baseline expression of these inhibitors at time 0. We saw variable expression in CD38 (0.13%-96.3%) CD49d (0.77%-92.8%) and CD62L (14.4%-85.7%) and similar expression in CD11c, CD31 and CD29 between patient samples(Figure 4.1 (a)). Using a cut-off of 30%, five patient samples were positive for CD38 expression and four out of five of these were also positive for CD49d. CD62L expression was not associated with CD49d or CD38 expression in our cohort. There was no association between CD49d, CD38 or CD62L expression with IGVH mutational status. There was no association between CD62L, CD49d or CD38 expression and NOTCH1 mutational status. Treatment for 24 hours with the upstream JAK inhibitor Ruxolitinib and BCR inhibitors, Ibrutinib and Idelalisib had no effect on the expression of any molecules within the panel. Treatment with Cucurbitacin and S3I resulted in a significant downregulation of CD62L positive cells ($p=0.0442$, $p=0.0242$ respectively) and the MFI of the positive CD62L population. In addition to CD62L, we saw small shift in CD31 expression and no changes in the expression of the other adhesion molecules assessed with Cucurbitacin or S3I (Figure 4.1 (b i & ii))

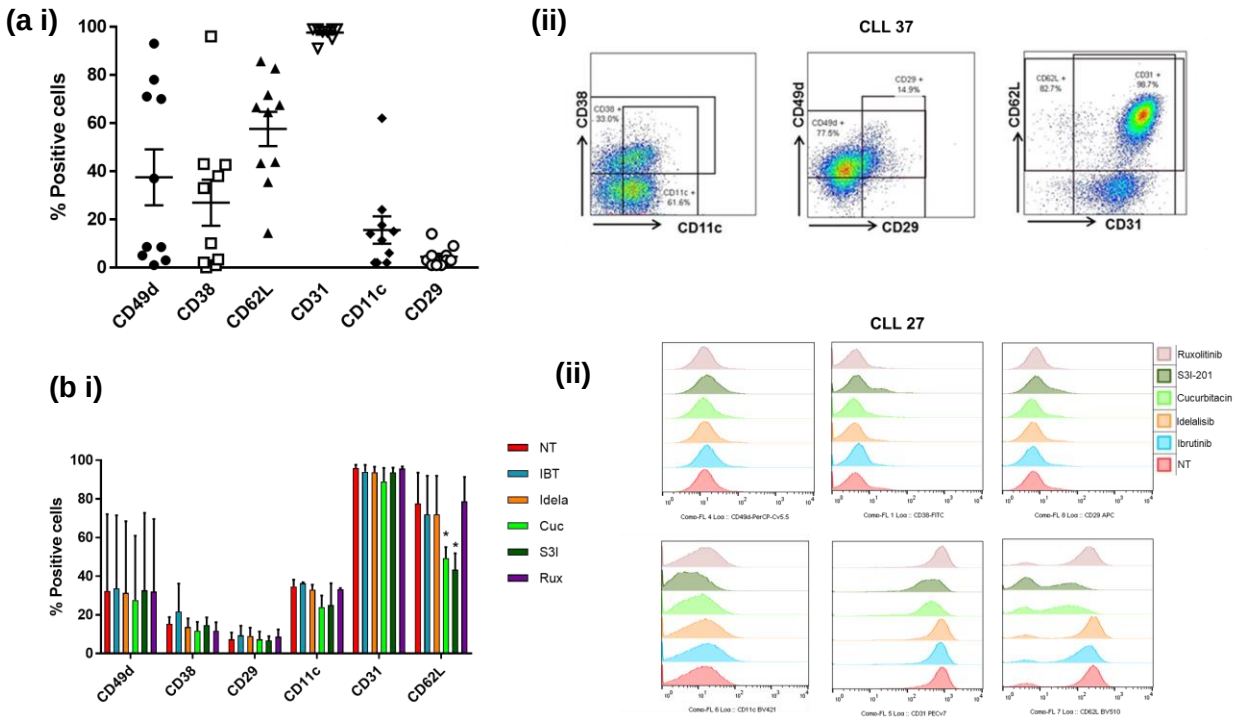

Figure 4. 1 Treatment with Cucurbitacin and S3I results in the downregulation of CD62L.

(a i) Variable expression of six adhesion markers in 10 CLL patient samples. Bars represent mean percentage of positive cells (± s.e.m). **(ii)** Representative dot plots depicting positive gates displaying percentage of positive cells in each population for each adhesion molecule. Cells were gated on single, live (PI negative), CD19 positive populations. Gating was performed using an unstained control and fluorescence minus one (FMO) where required Compensation was performed using compensation beads for each fluorophore. **(b i)** Expression of six adhesion markers in CLL cells incubated with 10μM Ibrutinib (IBT), 10μM Idelalisib (Idela), 1μM Cucurbitacin (Cuc), 100μM S3I and 1μM Ruxolitinib (Rux) for 24 hours. Significant downregulation of CD62L compared to no treatment (NT) was seen following treatment with Cucurbitacin and S31 (* p=0.0442, p=0.0242 respectively, n=3). The bars represent mean (± s.e.m) from 3 patient samples **(b ii)** Histograms depicting expression of each adhesion molecule after treatment with inhibitors in a representative patient sample (CLL27).

4.3.2 Treatment with Cucurbitacin and S3I results in a significant decrease in CD62L expression

We showed selective downregulation of CD62L expression after treatment with Cucurbitacin and S3I (Figure 4.1 (b)) and further investigated this in samples from an extended patient cohort. CLL cells were treated with 1µM Cucurbitacin, 100µM S3I or 1µM Ruxolitinib for 24 hours and CD62L expression was assessed by flow cytometry. Cucurbitacin resulted in a mean decrease of 17.1% $\pm$ 3.1% of CD62L positive cells ($p<0.0001$; Figure 4.2 (a i)) and S3I resulted in a mean decrease of 22.2% $\pm$ 2.5% CD62L positive cells ($p<0.0001$). Ruxolitinib had no significant effect on the expression of CD62L (ns, $p=0.6129$; Figure 4.2 (a i)). As we saw the greatest effect with Cucurbitacin, we also investigated whether there was an effect at the mRNA level. The downregulation of CD62L by Cucurbitacin occurred at both the protein and mRNA level (Figure 4.2 (b i & ii)). We also investigated the variability in the decrease in CD62L expression after Cucurbitacin by stratifying patient samples by clinical characteristics, IGVH mutational status, NOTCH1 mutational status, CD38 and CD49d positivity. We found a difference in the effect of Cucurbitacin on CD62L expression between CD38 positive and negative patient samples ($p=0.0060$), with CD38 positive patient samples exhibiting a greater decrease in CD62L expression following Cucurbitacin treatment (Figure 4.2 (c)). Similar to the effect of Cucurbitacin on cell viability (Figure 3.7), the effect of Cucurbitacin on the expression of CD62L showed patient variability; however, this reduction of expression of CD62L did not correlate with cell death induced by Cucurbitacin ($R^2=0.06$; Figure 4.3). Cucurbitacin resulted in a decrease in CD62L expression in CLL cells in a dose-responsive and time dependent manner (Figure 4.4 (i)). Cucurbitacin induced CD62L downregulation was seen as early as 4 hours and was sustained up to 72 hours. Interestingly, with increasing time in culture, we observed an increase in CD62L expression in untreated CLL cells (Figure 4.4 (ii)).

It has been reported that cryopreservation and thawing of lymphocytes causes a significant decrease of CD62L expression (Costantini et al., 2003). We use Ficoll density gradient isolated CLL cells which had been cryopreserved before resuscitation and we wanted to compare expression of CD62L after 24 hours in these samples compared to the expression obtained on the same samples following whole blood staining. There was no correlation between the CD62L expression in fresh whole blood samples compared to cryopreserved samples ($R^2=0.2$; Figure 4.5 (a)). In order to determine if the Cucurbitacin induced reduction in expression CD62L was due

cryopreservation and thawing, we assessed CD62L expression in CLL cells treated with Cucurbitacin pre- and post-cryopreservation. While the expression levels of CD62L varied between pre- and post-cryopreservation samples, Cucurbitacin resulted in a similar downregulation in CLL cells in both (Figure 4.5 (b i)).

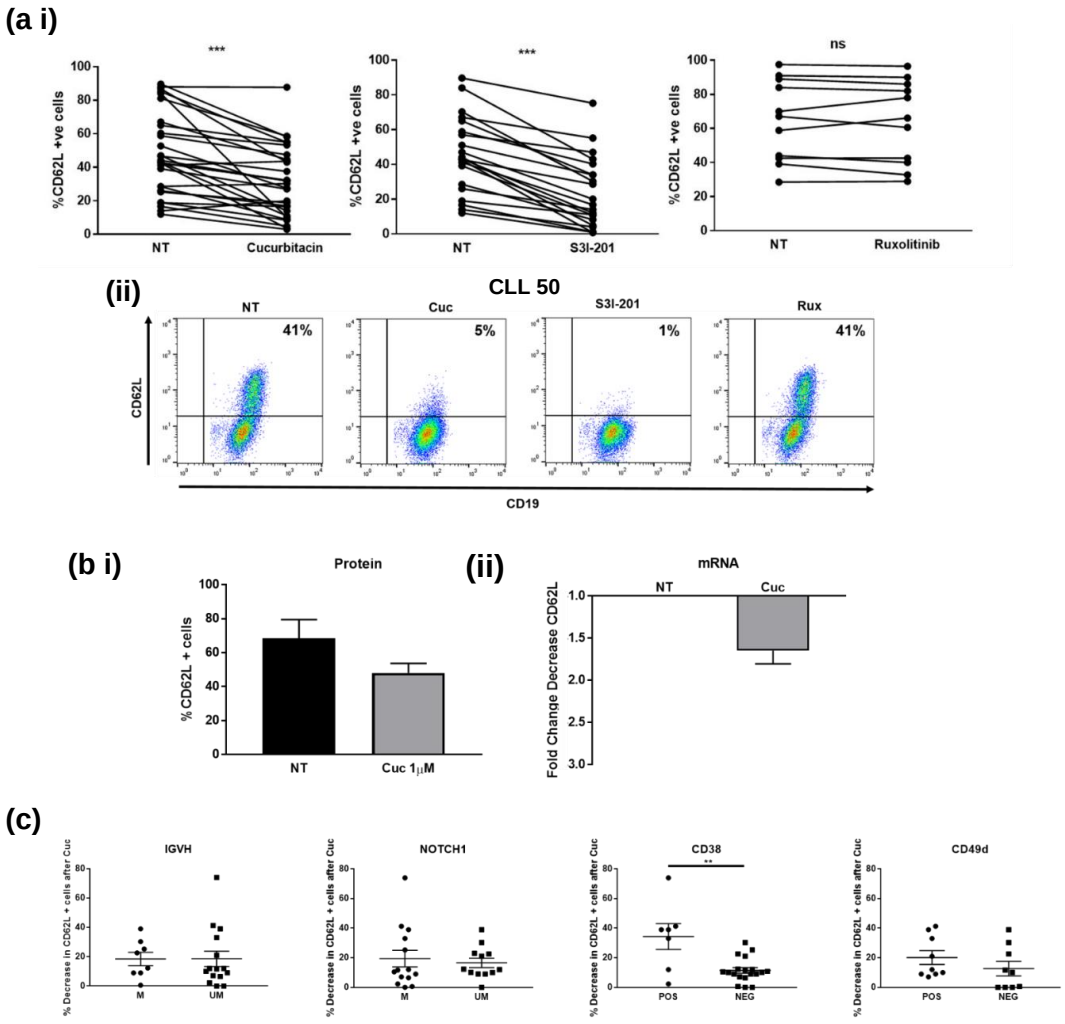

Figure 4. 2 Treatment with Cucurbitacin and S3I results in a significant decrease in the expression of CD62L while the JAK2/STAT3 inhibitor Ruxolitinib has no effect. (a i) CLL patient samples were treated with 1μM Cucurbitacin (n=29), 100μM S3I (n=21) or 1μM Ruxolitinib (n=11) for 24 hours and CD62L expression was assessed by flow cytometry. (*** p<0.001, no treatment (NT) *vs* treatment; ns – not significant) **(ii)** Representative dotplots depicting CD62L expression in CD19 positive cells after 24 hours culture with Cucurbitacin, S3I or Ruxolitinib with the percentage CD62L positive cells displayed. **(b)** CLL cells were treated with Cucurbitacin as indicated for 24 hours and CD62L cell surface protein expression was analysed by flow cytometry (i) and CD62L gene expression was analysed by RT-qPCR (ii). Bars represent mean expression/fold change (± s.e.m) (n=4). **(c)** Changes in the percentage of CD62L positive CLL cells after treatment with Cucurbitacin for 24 hours in patient samples categorized by unmutated (UM, n=15) and mutated (M, n=8) IGVH genes. NOTCH1 unmutated (UM, n=14) and mutated (M, n=12), CD38 positive (POS, n=7) and negative (NEG, n= 19) and CD49d positive (POS, n=9) and negative (NEG, n=9) (** p= 0.0060).

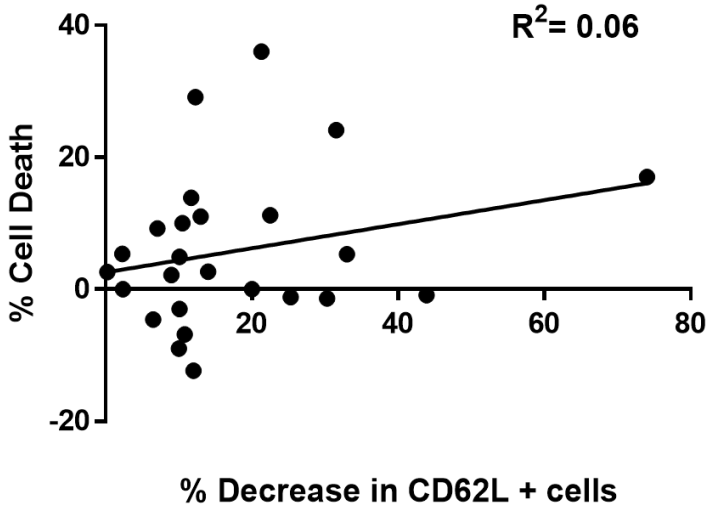

Figure 4. 3 Loss of CD62L does not correlate with cell death induced by Cucurbitacin

Correlation between cell death assesed by PI staining and CD62L expression by flow cytometry in CLL patient samples cultured with 1μM Cucurbitacin for 24 hours (R^2=0.06, n=25).

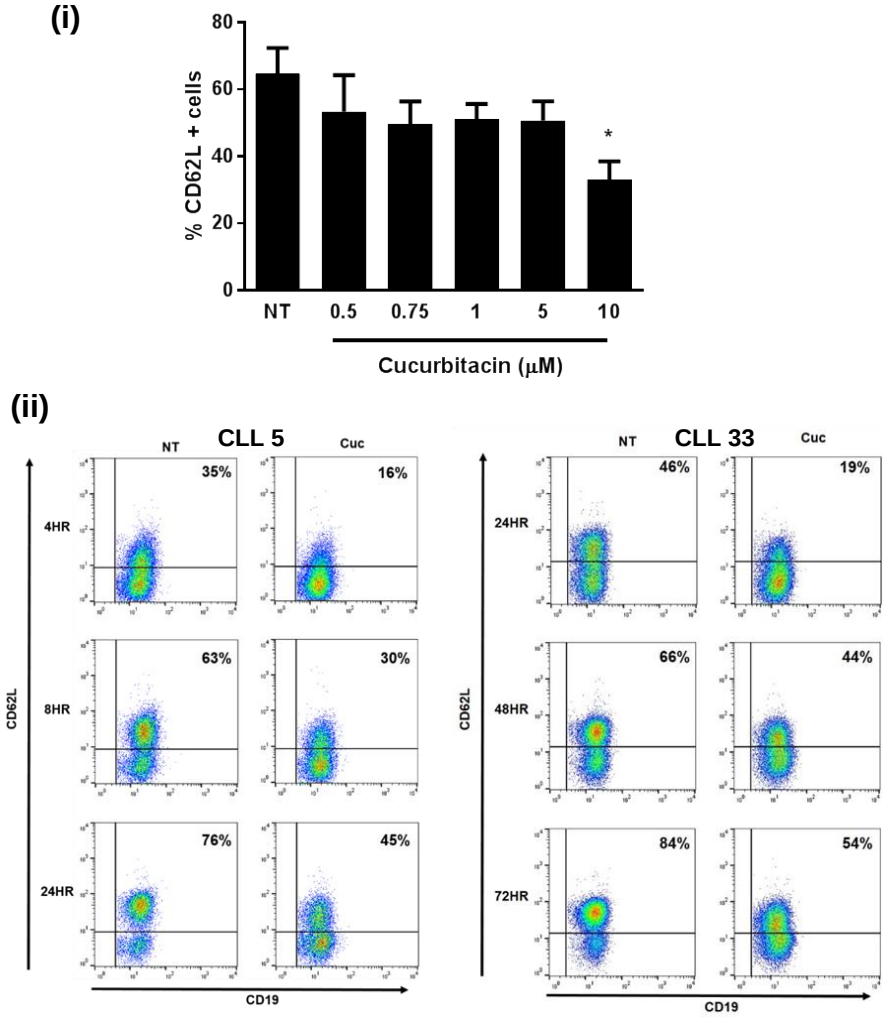

Figure 4. 4 Treatment with Cucurbitacin results in a decrease in CD62L expression in a dose-responsive manner and the effect is maintained up to 72 hours. (i) CD62L expression in CLL cells after 24 hours treatment with increasing concentrations of Cucurbitacin as indicated. Bars represent mean (± s.e.m) of CD62L positive cells (* p=0.0294**, n=3;** No treatment (NT) *vs* 10μM Cucurbitacin (Cuc)) **(ii)** Representative dotplots displaying the percentage of CD62L positive cells in CLL cells after treatment with Cucurbitacin for 4, 8, and 24 hours in CLL5 and 24, 48 and 72 hours in CLL 33.

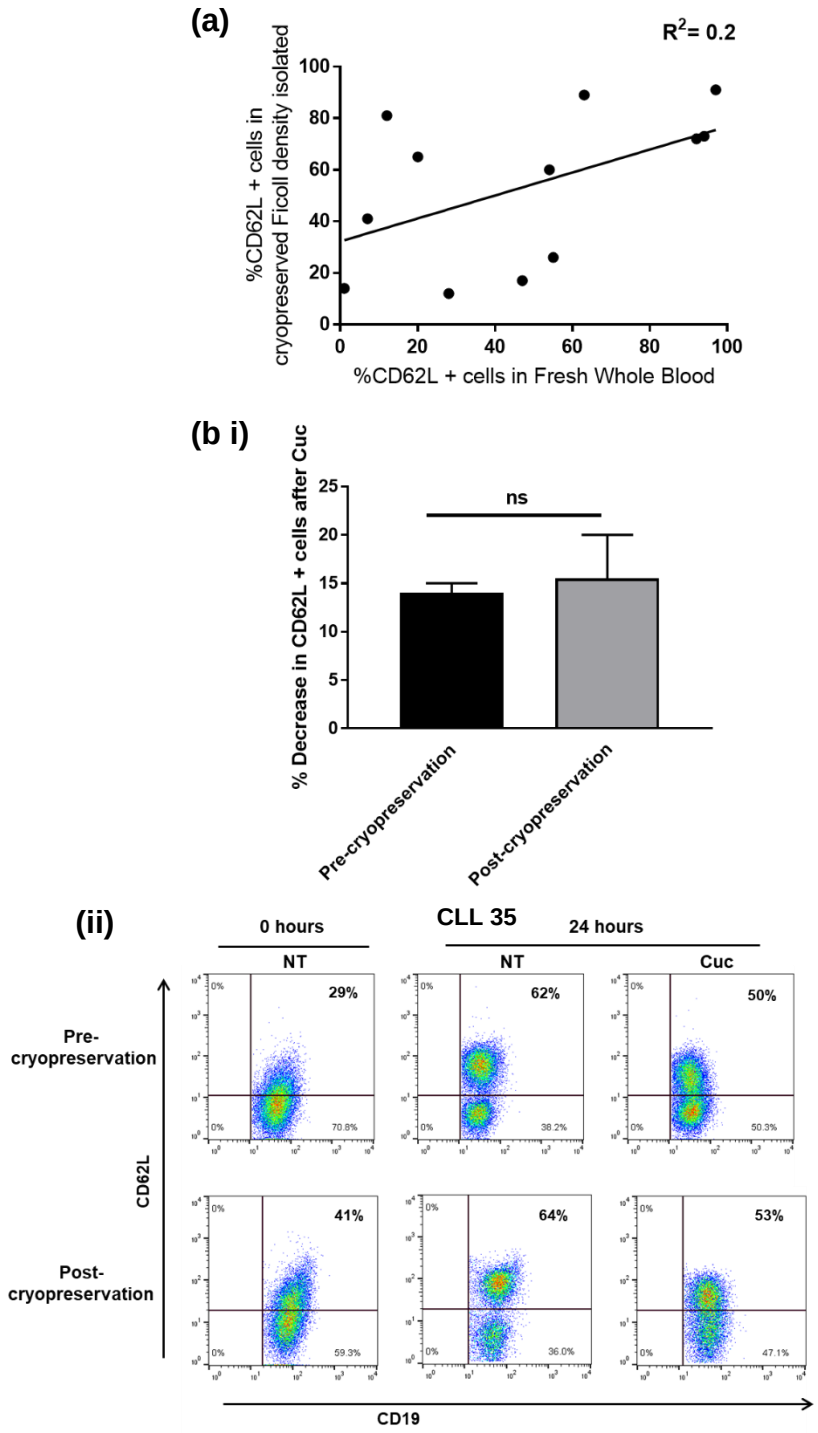

Figure 4.5 CD62L expression and the effect of Cucurbitacin on CLL cells pre- and post-cryopreservation (a) Correlation between CD62L expression by flow cytometry in fresh whole blood vs cryopreserved CLL patient samples after 24 hours (R^2=0.2, not significant (ns) n=12). **(b i)** CLL cells isolated from the same patient were treated with 1μM Cucurbitacin (Cuc) for 24 hours pre- and post-cryopreservation and thaw (Frozen). CD62L expression was assessed by flow cytometry. Bars represent mean expression (+ s.e.m)(ns-not significant p=0.7758, n=3) **(ii)** Representative dotplots displaying the percentage of CD62L positive CLL cells in pre- and post- cryopreservation and thaw after culture with Cucurbitacin for 24 hours.

4.3.3 siRNA mediated STAT3 knockdown results in a decrease in CD62L expression

STAT3 has proved to be a difficult pharmacological target and off-target effects may be significant. While Cucurbitacin and S3I have been shown to inhibit STAT3 activation and function (Ishdorj et al., 2010, Siddiquee et al., 2007), these agents also have cellular targets independent of STAT3 (Ball et al., 2016, Sari-Hassoun et al., 2016). Therefore, to confirm the role of STAT3 in the regulation of CD62L, we utilised siRNA knockdown of STAT3. STAT3 knockdown in CLL cells was performed using the Amaxa Nucleofector Kit and STAT3 expression was measure by flow cytometry. This method has been used previously to knockdown gene expression in CLL cells (Seiffert et al., 2007). GFP pMAX Vector was used to measure transfection efficiency. Although the use of GFP pMAX Vector may not directly quantify transfection efficiency of siRNA (as plasmids need to reach the nucleus to be expressed, whereas siRNA only needs to reach the cytosol, we saw similar efficiencies when optimising using increasing concentrations of fluorescent siRNA (100, 300 and 500nM) (Appendix 2). siRNA transfection of CLL cells is difficult to achieve as they are sensitive to apoptosis and are not transfected easily (Seiffert et al., 2007). Although we performed the knockdown in 10 patient samples, 8 samples either underwent significant apoptosis or showed no transfection efficiency at 72 hours post electroporation. show examples of two patient samples where transfection and partial knockdown was achieved. Transfection of pMAX GFP vector showed a transfection efficiency of 16.2% (CLL30) and 24.8% (CLL 4) (Figure 4.6 (a i) & (b i)). There was a decrease in MFI of STAT3 from 16.2 to 9.2 (CLL30) and 27.4 to 18.8 (CLL4) between cells treated with scrambled siRNA and those treated with STAT3 targeting siRNA, confirming the partial knockdown of STAT3 in both patient samples (Figure 4.6 (a ii) & (b ii)). There was a decrease of 12.4% to 8.05% (CLL30) and 47.8% to 28.9% (CLL4) CD62L positive cells in cells treated with STAT3 siRNA versus scrambled siRNA (4.6 (a iii) & (b iii)).

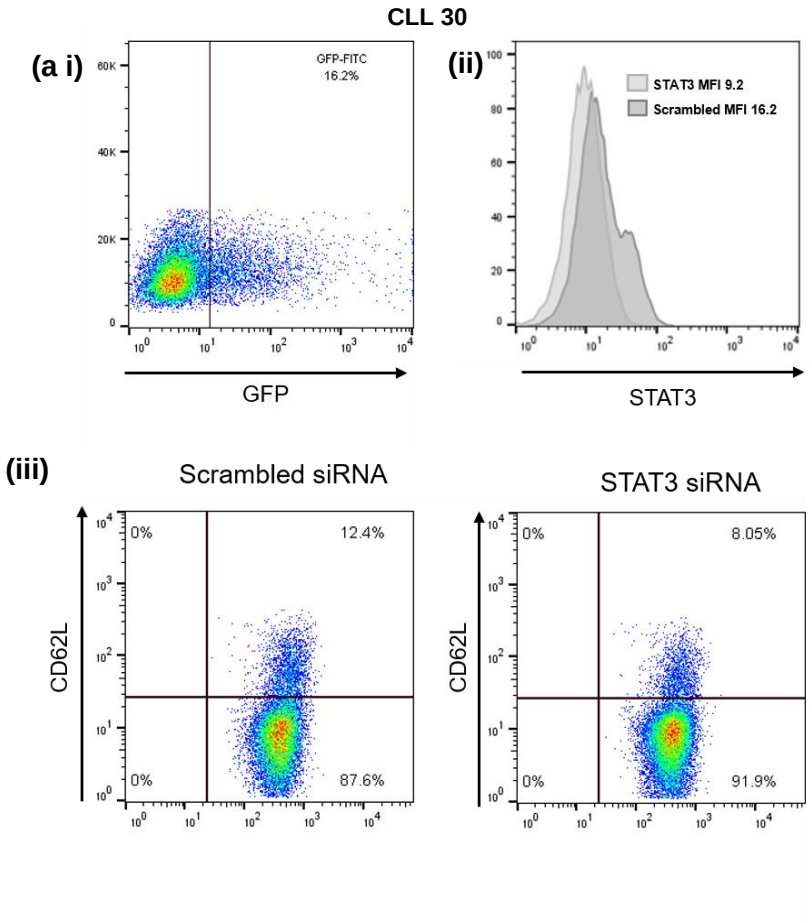
CLL 30
(a i)
GFP-FITC
16.2%
GFP
(ii)
STAT3 MFI 9.2
Scrambled MFI 16.2
STAT3
(iii)
Scrambled siRNA
STAT3 siRNA
CD62L
0%
12.4%
0%
87.6%
0%
8.05%
0%
91.9%

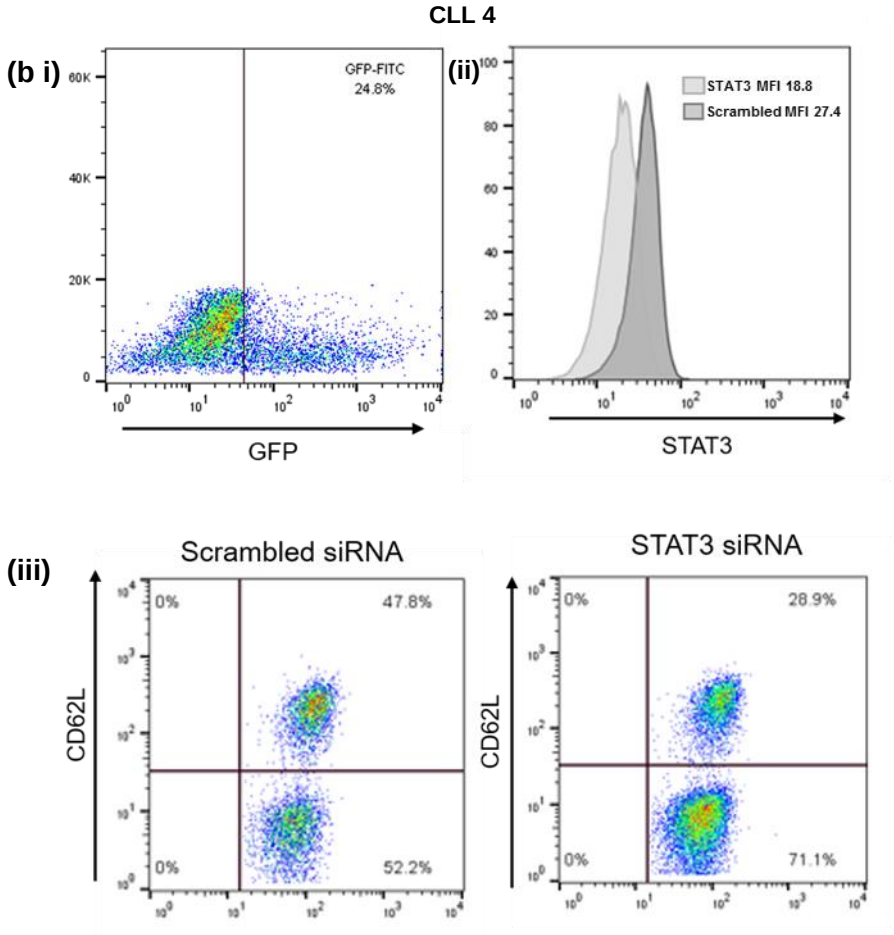

Figure 4. 6 Knockdown of STAT3 results in a decrease in the expression of CD62L. CLL cells were transfected with 2µg pMAXGFP vector, 500nM STAT3 siRNA or 500nM scrambled siRNA using the Amaxa Nucleofector protocol. Cells were incubated after transfection for 72 hours before staining for STAT3 and CD62L expression by flow cytometry. Two patient samples **(a)** CLL30 and **(b)** CLL4 are shown. Transfection efficiency was measured using pMAX GFP vector **(i)** Dotplots displaying the percentage of GFP positive cells. **(ii)** Histogram displaying the reduction of MFI of STAT3 in CLL cells after transfection with STAT3 siRNA. (iii) Dotplots displaying the decrease in the percentage of CD62L positive cells in CLL cells after transfection with STAT3 siRNA

4.3.4 Culture of CLL cells results in an induction of CD62L expression

As shown in Figure 4.4 (ii), the expression of CD62L in CLL cells increases over time *in vitro*. We confirmed this finding in a cohort of 13 patient samples incubated for 24 hours ($p=0.0002$; Figure 4.7(i)). This *in vitro* induction of CD62L expression was seen as early as 4 hours and was sustained up to 72 hours (Figure 4.7 (ii)). CD62L expression after 24 hours inversely correlated with the percentage of background apoptosis ($R^2=0.43$; Figure 4.7 (iii)) indicating it may have a pro-survival role in CLL. CD62L has previously been implicated in the survival of CLL cells and blockade of CD62L, using anti-CD62L antibodies in long-term culture, has been shown to induce CLL cell death (Burgess et al., 2013). To minimise spontaneous apoptosis, we incubated CLL at a high cell concentration (2×10^7 cells/mL) with anti-CD62L antibodies for 7 days. In 3 out of 5 patient samples, we showed blocking CD62L resulted in an increase in apoptosis (Figure 4.8). Table 4.1 shows the clinical characteristics of patient samples treated with the anti-CD62L antibody.

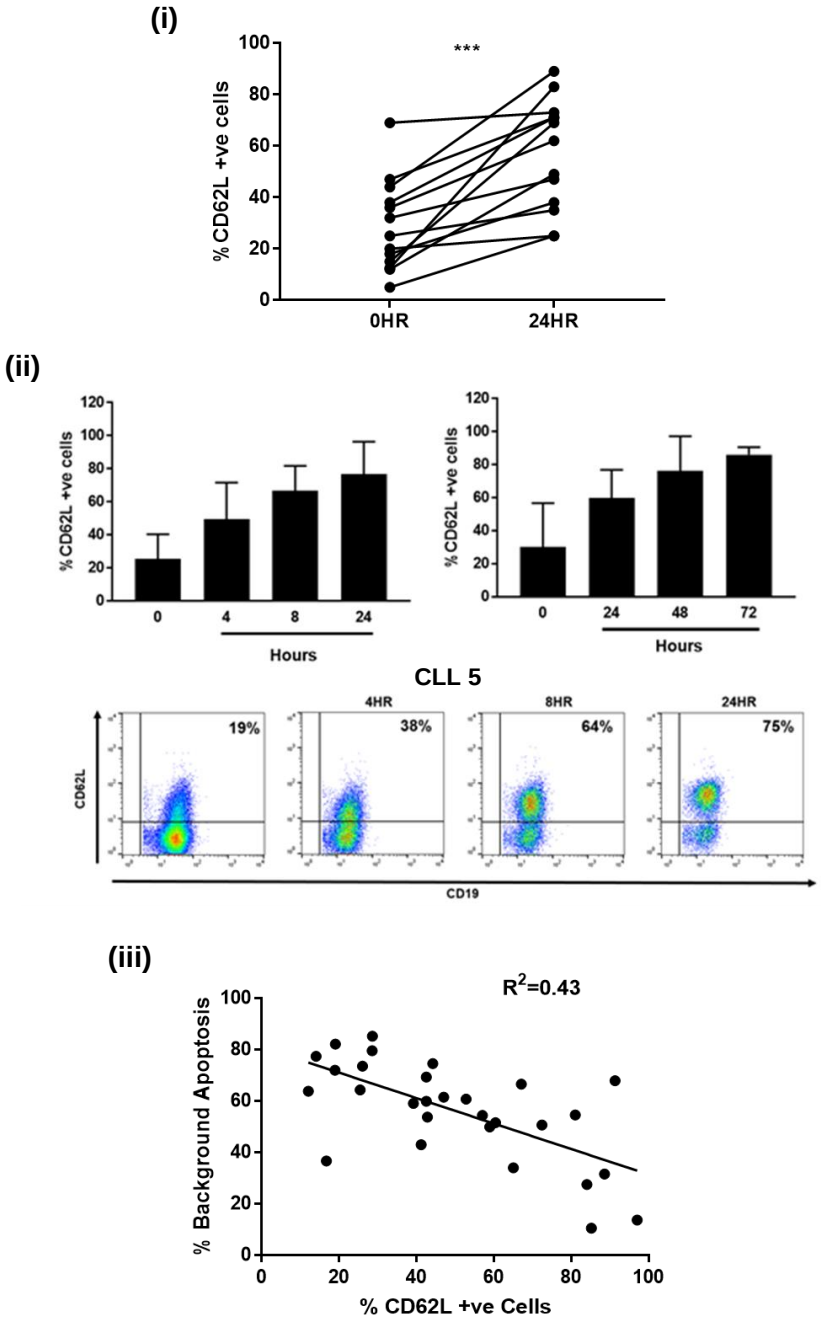

Figure 4. 7 Culture of CLL cells results in an upregulation of CD62L expression

(i) CD62L expression was determined in CLL cells before and after 24 hours culture. (0 hour *v* 24 hours; *** p=0.0002, n=13) **(ii)** CLL cells were cultured for 0, 4, 8, 24, 48 and 72 hours and CD62L expression was determined . Bars represent mean expression (+ s.e.m) (n=3). Representative dotplots displaying the percentage of CD62L positive CLL cells after culture for 4, 8 and 24 hours. **(iii)** The correlation between CD62L expression and background apoptosis assesed by AV/PI positive cells by flow cytometry in CLL cells cultured for 24 hours (R^2=0.43, n=29)

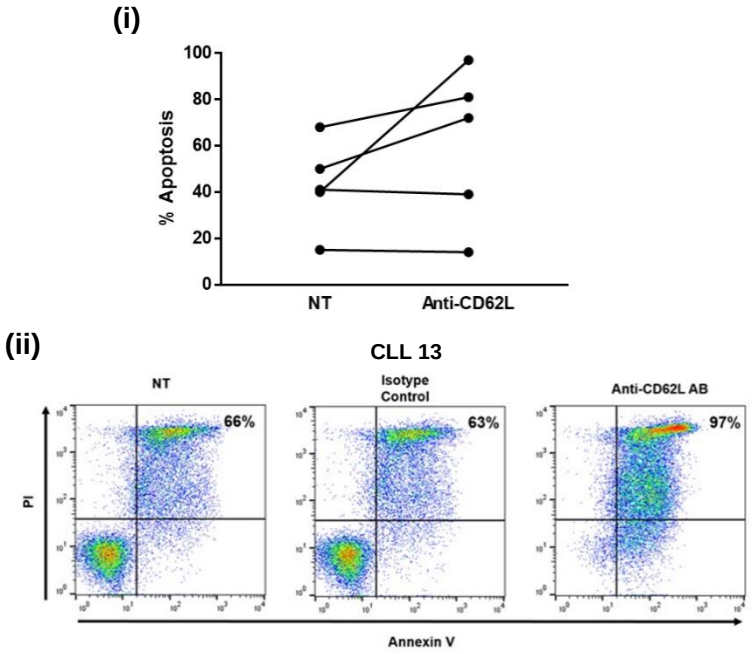

Figure 4. 8 Blockade of CD62L results in the induction of apoptosis in some patient samples (i) Induction of apoptosis, as assessed by AV/PI staining, in CLL cells cultured at $2x10^7$ cells/ml with 0.1µg/ml anti-human CD62L antibody for 7 days (No treatment- NT) **(ii)** Representative dotplot displaying the percentage of apoptosis in CLL cells cultured for 7 days with isotype control or 0.1µg/ml anti-human CD62L antibody (AB) .

Table 4. 1 Clinical characteristics of patient samples treated with anti-CD62L antibody

		IGVH	NOTCH	Flow cytometry Markers		Cytogenetics				Binet Stage	Bulky Disease
CLL	Anti CD62L Antibody	M/UM	M/UM	CD38	CD49d	Del13q	Trisomy 12	Del11q	Del17p		
21	Toxic	M	UM	N	ND	ND	ND	ND	ND	C	ND
13	Toxic	UM	M	P	ND	N	N	P	N	B	ND
6	Toxic	UM	M	N	N	N	N	N	N	A	N
48	No effect	UM	UM	N	N	N	N	N	N	C	ND
47	No effect	ND	ND	N	ND	P	N	N	N	A	N

UM=unmutated; M= Mutated; ND= Not defined; N=Negative; P= positive

4.3.5 IL-6 induced activation of the JAK/STAT3 pathway results in an increase in CD62L expression

STAT3 is constitutively phosphorylated on serine 727 in CLL cells; however, phosphorylation of tyrosine 705 is believed to be the main mechanism of STAT3 activation. Interleukin 6 (IL-6) is a prosurvival factor that activates the JAK2/STAT3 pathway inducing tyrosine phosphorylation of STAT3 in CLL cells (Hazan-Halevy et al., 2010). We also showed IL-6 can induce tyrosine pSTAT3 in CLL cells (Figure 3.3). As we showed that Cucurbitacin, S3I and siRNA knockdown of STAT3 result in a decrease in CD62L (Figures 4.2 and 4.6), we wanted to investigate if IL-6 induced activation of the STAT3 pathway had an effect on CD62L expression. Treatment with IL-6 for 24 hours results in a significant increase in CD62L expression in CLL patient samples (p=0.0139). Pre-treatment with the JAK2 inhibitor Ruxolitinib completely abrogates this CD62L up regulation (Figure 4.9 (i)). IL-6 does not prevent Cucurbitacin induced down regulation of CD62L. (Figure 4.9 (ii))

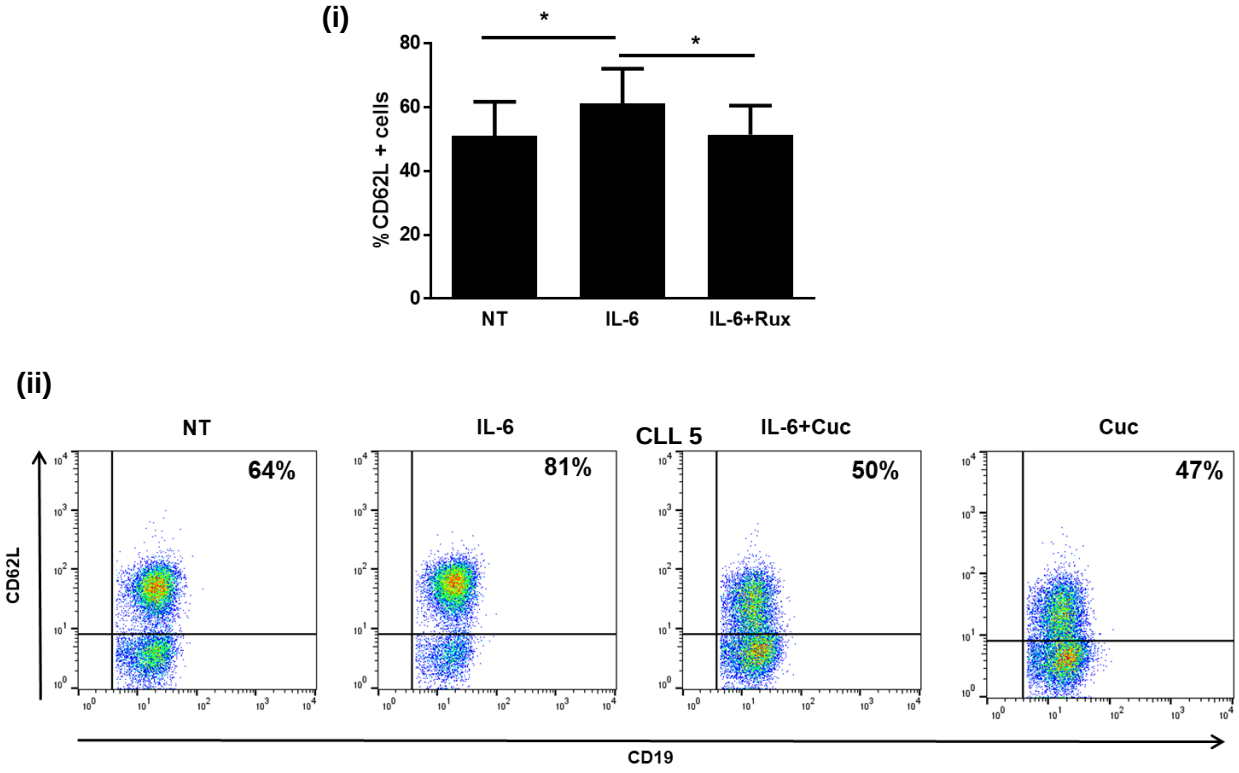

Figure 4. 9 Stimulation of the JAK/STAT3 pathway using IL-6 results in an increase in CD62L expression (i) Primary CLL cells were treated with for with IL-6 (50ng/ml) alone or in combination with 1μM Ruxolitinib (Rux). The percentage of CD62L positive CLL cells after 24 hours is shown. Bars represent mean CD62L expression (± s.e.m) (No treatment (NT) vs IL-6; * p= 0.0139, n=5)(IL-6 vs IL6+Ruxolitinib ; * p=0.0300, n=5) **(ii)** Representative result displaying the percentage CD62L positive CLL cells after preatreatment with IL-6 alone for 24 hours or in combination with 1μM Cucurbitacin (Cuc). Representative of n=3.

4.3.6 Cucurbitacin had no significant effect on the expression of CD62L in non-malignant B cells

We wanted to determine if the pro-survival increase in CD62L expression was selective to CLL cells and if Cucurbitacin had a similar effect in non-malignant B cells. B cells from normal healthy donors were cultured for up to 48 hours but, unlike CLL cells, normal B cells did not upregulate CD62L when cultured *in vitro* (Figure 4.10 (a)). Cucurbitacin had no effect on the expression of CD62L (ns p=0.5254; Figure 4.10 (b)) in normal B cells.

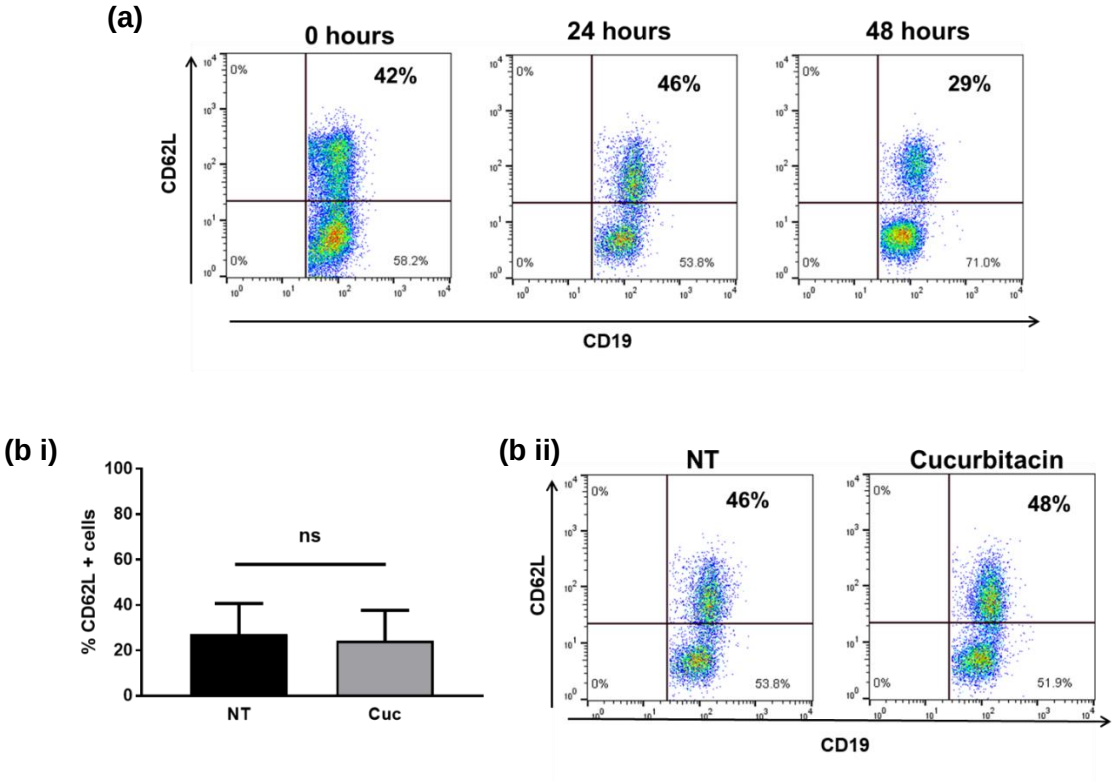

Figure 4. 10 Cucurbitacin has no effect on CD62L expression in normal B cells (a i) Dotplots displaying the percentage of CD62L positive B cells after culture for 24 and 48 hours. Representative of n=3. **(b i)** B cells were isolated from normal donor blood and treated with Cucurbitacin (Cuc) for 24 hrs before CD62L expression was determined by flow cytometry. Bars represent mean expression (± s.e.m) for 3 normal controls (No treatment (NT) vs Cucurbitacin (Cuc); not significant (ns) p=0.5254) **(ii)** Representative dotplots displaying the percentage of CD62L positive B cells after culture with 1μM Cucurbitacin for 24 hours.

4.3.7 Treatment with Cucurbitacin and S3I but not Ruxolitinib results in a downregulation in the chemotaxis of CLL cells towards CXCL12

Having shown that Cucurbitacin and S3I effect the expression of adhesion molecules in CLL cells, we next wanted to assess whether Cucurbitacin and S3I had an effect on the migration of CLL cells. We utilised a chemotaxis assay using Neuroprobe 96-well plates. Initially, to determine the optimal chemokine concentration for maximal migration, we investigated the chemotaxis of the CLL cell line I83 towards two chemokines, CXCL13 and CXCL12. We found that I83 cells showed no migration towards CXCL13 but significant migration was seen towards CXCL12 at concentrations of 100ng/ml ($p=0.0283$) and 1000ng/ml CXCL12 ($p= 0.0004$; Figure 4.11 (a)). Pretreatment with 1μM Cucurbitacin significantly blocked I83 cells migration towards 100ng/ml CXCL12 ($p=0.0334$; Figure 4.11 (b)).

Burger et al. (1999) reported that patient derived CLL cells migrate towards CXCL12 in a biphasic fashion due to receptor endocytosis with maximum migration occurring at 100ng/ml. We found chemotaxis of CLL cells increased towards 1000ng/ml CXCL12, with a maximum at 1000 ng/ml in 2 out of 4 patient samples tested and in one patient sample we found a biphasic response with a maximum migration towards 100ng/ml (Figure 4.12 (a i)). In subsequent experiments we used a concentration of 100ng/ml as biphasic responses occurred in some patient samples. 100ng/ml CXCL12 resulted in a transient increase in serine pSTAT3, reaching a maximum after 15-30 minutes and slowly resolving up to 60 minutes in CLL cells (Figure 4.12 (a ii)). No changes were seen in tyrosine pSTAT3. Pretreatment with Cucurbitacin resulted in a dose response decrease in the migration of CLL cells towards CXCL12 with 1uM Cucurbitacin significantly inhibiting CLL chemotaxis ($p=0.0020$). S3I also caused a significant decrease in the migration towards CXCL12 ($p=0.0284$); however, Ruxolitinib did not significantly affect migration towards CXCL12 ($p=0.1205$; Figure 4.12 (b)).

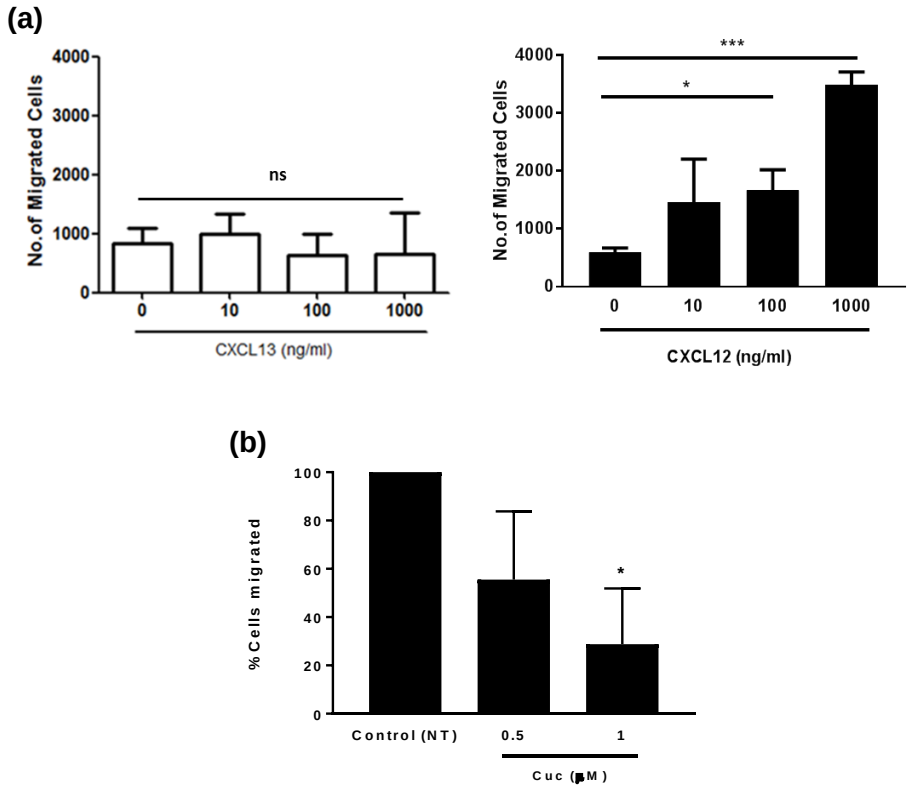

Figure 4. 11 CLL cell line I83 migrates towards CXCL12 but not CXCL13 in a dose responsive manner and this migration can be inhibited by pretreatment with Cucurbitacin (a) I83 cells migration towards increasing concentrations of CXCL13 and CXCL12 after 3 hours was assessed using Neuroprobe 96 well plate assays (n=3). Chemotaxis was assessed by staining migrated cells with nuclear Hoechst dye and counting by high content imaging (* p=0.0283, *** p= 0.0004, Not-significant –ns) **(b)** I83 cells migration in response to 100ng/ml CXCL12 was assessed after 3 hours following pretreatment with Cucurbitacin (Cuc) for 1 hour (No treatment (nt) *vs* 1μM Cucurbitacin (Cuc); * p=0.0334, n=3). Bars represent mean migration (± s.e.m) of 3 independent experiments.

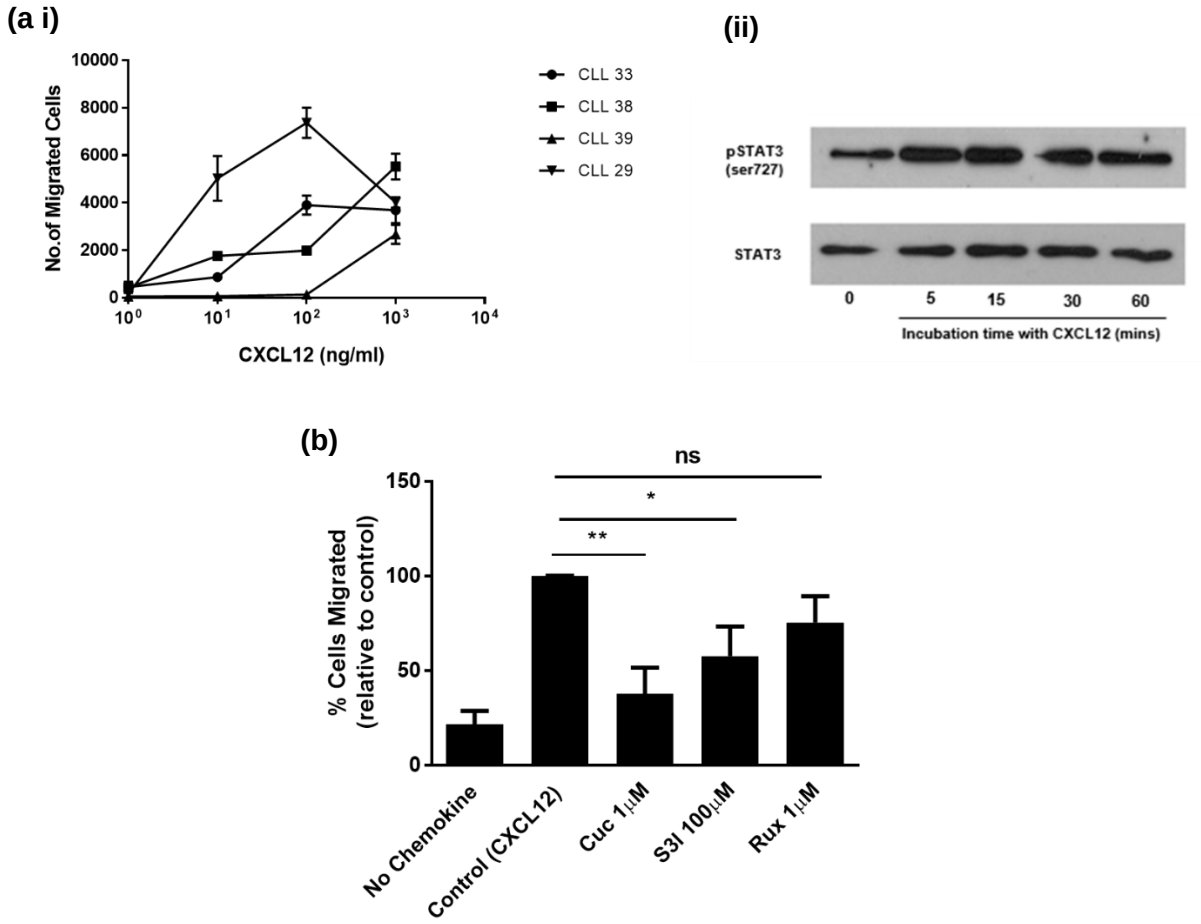

Figure 4. 12 Cucurbitacin and S3I result in a decrease in the chemotaxis of patient derived CLL cells towards CXCL12. (a i) CLL cell migration towards increasing concentrations of CXCL12 (0, 10, 100, 1000ng/ml) after 3 hours was assessed using Neuroprobe 96 well plates assays. CLL samples used were > 90% CD19/CD5+. Chemotaxis was assessed by staining migrated cells with nuclear Hoechst dye and counting by high content imaging. Each line represents an individual patient sample. **(ii)** CLL cells treated with CXCL12 for 0, 5, 15, 30 and 60 minutes in RPMI +0.5% BSA. CLL cells were lysed after each timepoint and serine pSTAT3 and total STAT3 were assessed by western blotting. **(b)** CLL cells were pretreated with 1μM Cucurbitacin (Cuc), 100μM S3I or 1μM Ruxolitinib (Rux) for 1 hour and CLL cell migration towards CXCL12 (100ng/ml) was assessed as above. Bars represent mean percentage migration (± s.e.m) (**p=0.0020, *p=0.0284, ns p=0.1205, n=5).

4.3.8 Cucurbitacin results in a decrease in the adhesion of CLL cells to HUVEC under shear flow

Adhesion of CLL cells to endothelial cells in the HEV *in vivo* occurs under conditions of fluid shear flow. The stabilisation of catch bonds formed between CD62L and its ligands requires fluid shear flow. We have shown that CD62L expression in CLL cells is regulated by treatment with Cucurbitacin and wanted to assess its effect on CLL cell adhesion to endothelial cells under fluid shear flow conditions. We also wanted to assess the effect of blocking CD62L on primary CLL cell adhesion.

We developed an in vitro assay utilising Cellix Vena8 endothelial biochips coated with a monolayer of HUVEC cells using a shear flow rate of 0.5 dynes/cm^2**.** We found that incubation with a CD62L blocking antibody resulted in a significant decrease in adhesion under shear flow (p=0.0085; Figure 4.13 (a)). We found that treatment with Cucurbitacin after 4 hours resulted in a non-significant decrease (ns p=0.1106) in cell adhesion, but treatment for 24 hours resulted in a significant decrease in the adhesion of CLL cells (p=0.0005; Figure 4.13 (a ii)). All 5 patient samples showed a decrease in CD62L expression (Figure 4.13 (a iii)) and no significant increase in apoptosis after 24 hours treatment with Cucurbitacin (Figure 4.13 (a iv)).

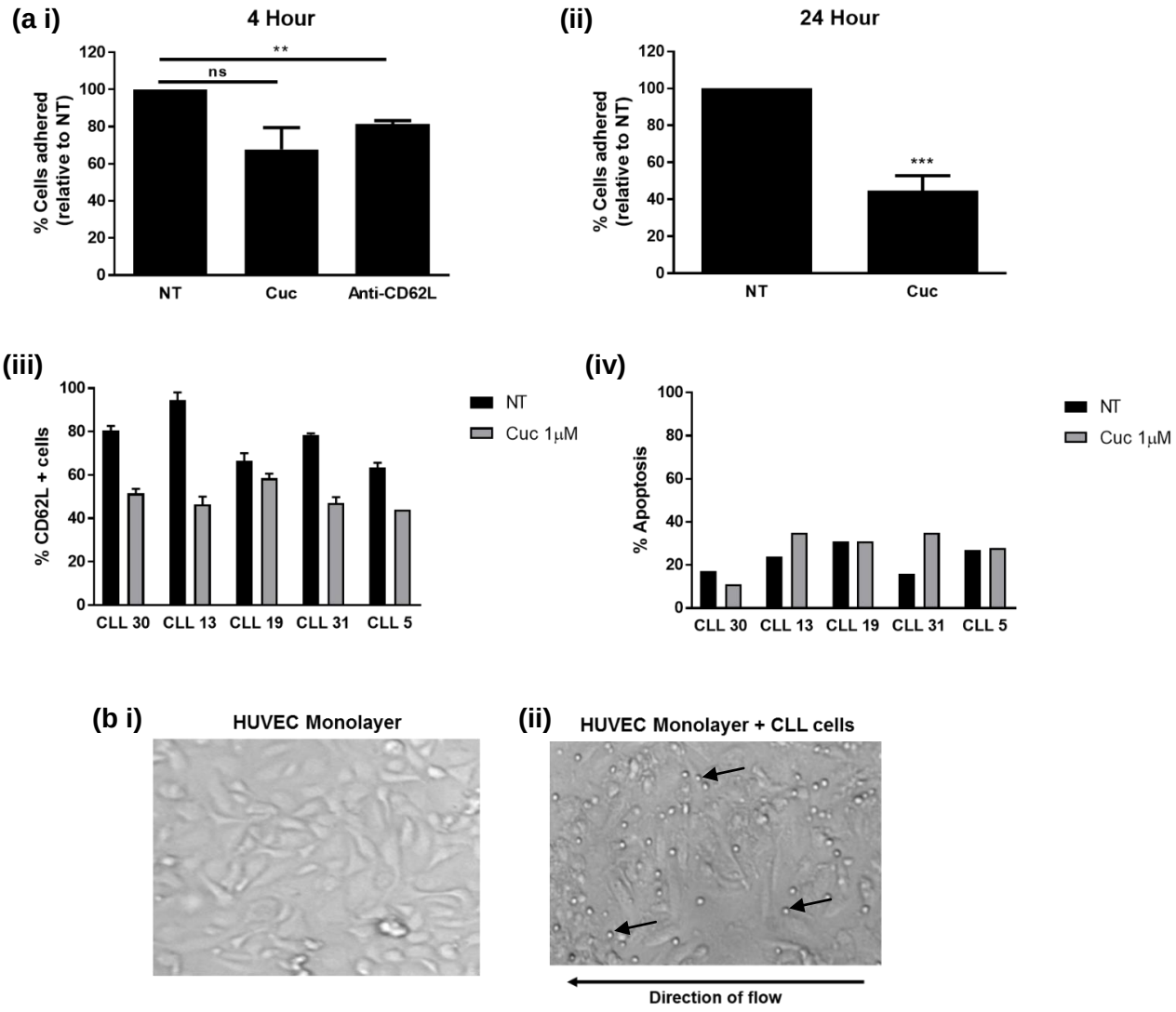

Figure 4. 13 Anti-CD62L blocking antibody and Cucurbitacin resulted in a decrease in the adhesion of CLL cells to HUVEC under fluid shear flow. A microfluidic system was used to assess adhesion of CLL cells to endothelial cells under shear flow. CLL samples used were >990% CD19/CD5+. Cells were introduced to the Cellix microfluidic chamber coated with HUVECs under a shear flow of 0.5 dynes/cm^2. After 5 minutes adhered cells were counted at 3 positions along the channel. **(a)** CLL cells were (**i)** treated with anti-CD62L (0.1μg/ml) antibody or pretreated for 4 hours with 1μM Cucurbitacin (Cuc). Bars represent mean number of cells adhered (± s.e.m) for 3 patient samples (** p=0.0085, n=3; not significant (ns)) **(ii)** pretreated for 24 hours with 1μM Cucurbitacin (Cuc) (*** p=0.0005, n=5). Bars represent mean number of cells adhered (± s.e.m) **(iii)** The percentage of CD62L positive CLL cells and **(iv)** the percentage apoptosis assessed by AV/PI flow cytometry after 24 hours treatment with 1μM Cucurbitacin. Each bar represents an individual patient sample **(b i)** An image depicting the HUVEC monolayer prior to the addition of CLL cells and **(ii)** after the addition of CLL cells to the chamber. Adhered CLL to HUVEC monolayer is indicted with arrows.

4.4 Discussion

CLL cells interaction with the lymph node and bone marrow microenvironments promotes their survival and protects from drug induced apoptosis. It is, therefore, of interest to understand the steps that mediate the mechanism of how circulating CLL cells enter these secondary lymphoid organs. The multi-step adhesion cascade that normal B lymphocytes undergo through the HEV to the lymph node has been well characterized and, while CLL cells are thought to use the same processes, this has not been fully elucidated. Initially, we chose 6 molecules known to be involved in lymphocyte migration to the lymph nodes: the selectin CD62L; integrins CD49d, CD29 and CD11c; and surface adhesion molecules CD38 and CD31. We saw variability in the expression of CD38, CD49d and CD62L. In our cohort 5/10 (50%) patient samples were >30% CD49d positive which is associated with unfavourable progression in CLL, This is in general agreement with other studies (Bulian et al., 2014). We found 5/10 (50%) of patient samples in our cohort were CD38 positive, which is also comparable to other studies (Damle et al., 1999, Ibrahim et al., 2001) with 4 of these patient samples being both CD38 and CD49d positive.

We examined the effect of treatment with STAT3 targeting agents, Cucurbitacin, S3I, the JAK inhibitor Ruxolitinib; and BCR inhibitors Ibrutinib and Idelalisib, on 6 adhesion molecules. Treatment with Cucurbitacin and S3I resulted in a decrease in the expression of CD62L in CLL cells. Cucurbitacin and S3I are two unrelated compounds which have been shown to inhibit STAT3 activity and the selective action of these agents suggests a role for the STAT3 pathway in the regulation of CD62L. Furthermore, we show that the JAK/STAT pathway activator IL-6 increases CD62L expression which is inhibited by Ruxolitinib (Figure 4.9). However, both Cucurbitacin and S3I have been shown to have effects independent of their effect on STAT3. S3I has recently been shown to act as an alkylating agent, alkylating STAT3 on 5 cysteine residues and globally alkylating a range of other intracellular proteins (Ball et al., 2016). Cucurbitacin has been shown to activate JNK/c-jun in CLL (Ishdorj et al., 2011) and we have shown that Cucurbitacin affects the actin cytoskeleton in CLL cells (Figure 3.9).
In order to confirm a role for the STAT3 pathway in the regulation of CD62L, we performed STAT3 knockdown using siRNA. CLL cells are known to be resistant to most gene transfer techniques (Seiffert et al., 2007) and, in addition to this, undergo spontaneous apoptosis after prolonged in vitro culture required for siRNA knockdown. (Seiffert et al., 2007) performed tests on transfection of CLL cells with different nucleic acid structures in different conditions to promote cell survival after electroporation.

They determined that plasmid DNA induced rapid apoptosis and mRNA and siRNA were preferential. They developed a protocol with Hs5 stromal cell coculture and conditioned media in order to increase cell survival and transfection efficiency. We also tested different concentrations of fluorescent siRNA (100nM-1000nM) to see if this had an impact on transfection efficiency; however, we found very little difference between concentrations (Appendix 2). We did not use Hs5 coculture or conditioned media, as we show that Hs5 cells and soluble factors such as IL-6 can affect the expression of CD62L (Figure 5.3) in CLL cells and did not want to introduce confounding experimental factors.

Here, we show STAT3 knockdown in CLL cells results in a decrease in STAT3 and CD62L expression, further implicating STAT3 in CD62L regulation. A role for STAT3 in the regulation of CD62L has been suggested previously in other cell types but has not previously been reported for CLL. Both (Cui et al., 2011) and (Pallandre et al., 2007) showed that CD62L was significantly downregulated in T cells from STAT3 knockout mice. The mechanism of this downregulation of CD62L in CLL cells isn't clear; however, we did see a non-significant downregulation in CD62L gene expression following treatment with Cucurbitacin. Additional mechanisms of regulation of CD62L expression may be the shedding of CD62L and a role for STAT3 in TACE/ADAM17 activity and expression should be investigated.

As mentioned previously, Lafouresse et al. (2015) have shown CD62L to be a critical determinant in controlling initial tethering interactions of CLL cells with endothelium of the HEV *in vivo*. Given this role of CD62L in facilitating CLL cell recirculation, blocking CD62L mediated adhesion may be a potential therapeutic target in CLL, preventing the dissemination of CLL cells to the protective microenvironments of the lymph node and bone marrow. We developed an assay to study the interactions of CLL cells with endothelial cells under physiologically relevant fluid shear flow to investigate a functional effect to blocking or downregulating CD62L in CLL cells. In contrast to *in vivo* models, which can be costly and difficult to perform, we developed a relatively simple model to study the interactions of CLL cells with endothelial cells under fluid shear flow. Although more difficult than static adhesion assays, it has been shown that shear forces alone can increase the expression of CD62L. In addition, while CD62L binds some glycoproteins without siayl Lewis^X modifications in the absence of shear flow (Celie et al., 2009), CD62L interactions with its main siayl Lewis^x type ligands are considered 'shear dependent' given the nature of the slip and catch bonds formed between the two under shear flow conditions (McEver and Zhu, 2010), indicating the importance of studying this molecule under fluid shear flow (Walsby et al., 2014). Shear

stress levels differ in different vessel types, shear stress in large arteries has been determined to be 10 to 70 dynes/cm^2 while veins 1 to 6 dynes/cm^2 (Papaioannou and Stefanadis, 2005). Lymphatic flow is lower again at, ~0.1-0.5 dynes/cm^2 Optimal shear stresses of 0.3-1.0 dynes/cm^2 prolong adhesion molecule bonds in particular, the stabilization of CD62L interactions with its ligands which requires minimal shear force >0.3 dynes/cm^2 (Yago et al., 2004, Lawrence et al., 1997). Our model allowed the precise control of fluid shear flow forces using NeMESYS software and pump.
Using this model we found that blocking CD62L resulted in a significant decrease in the number of CLL cells adhered to endothelial cells. We also showed that Cucurbitacin results in a non-significant decrease in the adhesion of CLL cells to endothelial cells after 4 hours pretreatment, but a significant decrease adhesion of CLL cells to endothelial cells after 24 hours pretreatment. While we saw a reduction in CD62L expression following Cucurbitacin pretreatment we saw in chapter 1 that Cucurbitacin results in the aggregation of actin in CLL cells so non-STAT3 effects of Cucurbitacin may be contributing to this reduction in adhesion and requires further investigation. In summary, we have developed a model that is useful for looking at the key process of migration in CLL biology. Our model confirms a role for CD62L in adhesion to HUVECs under fluid shear flow conditions.

Stromal cells secrete chemokines which are additional important molecules in the migration of CLL cells to the lymph nodes. We assessed migration towards CXCL12 a chemokine that is secreted by stromal and nurse-like cells of the tumour microenvironment. We showed an increase in serine pSTAT3 in response to CXCL12 in agreement with previous reports (Burger et al., 2005) and we found treatment with Cucurbitacin and S3I inhibited the migration of CLL cells towards CXCL12. Disrupting CXCL12 signalling may interrupt the migration of CLL cells to the lymph node and bone marrow microenvironment. Treatment with Ibrutinib results in a downregulation in the membrane expression of CXCR4 and this is suggested to contribute to the redistribution of CLL cells after treatment with Ibrutinib *in vivo* showing the importance of this molecule in CLL cell recirculation (Chen et al., 2016).

Burgess et al. (2013) showed that CD62L has a prosurvival role in CLL cells; and we showed that blockade of CD62L using anti-CD62L antibody, resulted in an increase in apoptosis in a subset of our CLL samples examined. (Burgess et al., 2017) have recently shown that cells derived from patients with progressive disease requiring treatment were resistant to cell death induced by anti-CD62L antibodies while those with stable disease underwent apoptosis in response to treatment with anti-CD62L

antibodies. We showed a correlation between the expression of CD62L and the amount of background apoptosis which has not been previously reported, further suggesting a prosurvival role for CD62L in CLL (Figure 4.7 (a iii)). Importantly, we saw upregulation in the expression of CD62L in CLL cells but not in normal B cells when cultured *in vitro*, suggesting a cancer specific role for CD62L

Overall this chapter suggests that disrupting the STAT3 signalling pathway may interfere with the expression of the prosurvival and adhesion molecule CD62L in CLL. Therapeutics targeting selectins have been investigated; however, difficulties in developing targeted molecules and the non-selectivity of inhibitors a large number of compounds do not make it to clinical trials. Given the importance of CD62L in the initial steps of the migration of CLL cells from the HEV to the protective microenvironment of the lymph node (Lafouresse et al., 2015), our results present additional mechanisms for potentially targeting this molecule. CLL cells undergo key interactions within the lymph node microenvironment and the BCR signalling pathway has emerged a key pathway in this crosstalk and a key pathway in understanding the biology of CLL (Herishanu et al., 2011). In the next chapter, we investigate the effects of BCR stimulation on STAT3 and CD62L expression in CLL in order to elucidate further the potential of CD62L and STAT3 as therapeutic targets for the treatment of CLL.

Chapter 5

Microenvironmental mediated regulation of STAT3 and CD62L in CLL cells

5.1 Introduction

The pathogenesis of CLL relies heavily on the interaction of the cells with their microenvironment. CLL cells recirculate between the peripheral blood, bone marrow, spleen and lymph node compartments. Key interactions occur, primarily in the bone marrow and secondary lymphoid organs, between CLL cells and surrounding cells that promote CLL cell survival. CLL cell proliferation occurs in pseudo follicular proliferation centres (PC) in the lymph nodes and bone marrow and gives rise to a daily turnover of 1% of the entire CLL clone (Messmer et al., 2005). Further analysis of the role of the microenvironment and its interactions with CLL cells are important to improve therapeutic options. Having investigated the role STAT3 plays in the trafficking of CLL cells to and from these microenvironments in the previous chapter, we wanted to further investigate the importance of STAT3 in the interactions of CLL cells with key components of the CLL microenvironment.

The bone marrow and lymphoid organs have distinct microenvironments as they support different haematopoietic processes. The generation of B cells from haematopoietic stem cells (HSC) occurs in the bone marrow, where bone marrow stromal cells (BMSC) act as important attachment sites and also provide soluble and surface-bound growth factors to generate B cells with functioning B cell receptors (BCRs). CLL cells have a high affinity for BMSC undergoing pseudoemperipolesis after a short time in culture (Burger et al., 1999). Panayiotidis et al (1996) first showed that contact with stromal cells *in vitro* protects CLL cells from spontaneous apoptosis. It was shown in further studies that BMSC also protect from drug-induced apoptosis and secretion of chemokines promote the trafficking and homing of CLL cells (Kurtova et al., 2009, Lagneaux et al., 1998). The mechanism of BMSC mediated survival and drug induced resistance of the CLL cells is cell-cell contact-dependent (Buchner et al., 2010a, Ding et al., 2009), occurring through integrins β1 and β2, and binding of CD49d to VCAM-1 or fibronectin (Maffei et al., 2012). The cross-talk between CLL cells and BMSC is bidirectional with CLL cells secreting factors such as PDGF to enhance proliferation of BMSC and their production of VEGF which in turn promotes the survival of CLL cells (Ghosh et al., 2010, Gehrke et al., 2011). Some studies have shown an effect of BMSC on STAT3; VEGF produced by stromal cells has been shown to activate STAT3 in CLL (Gehrke et al., 2011). Mature B cells then migrate from the bone marrow to the lymph node where they come into contact with CD4+ T cells and follicular dendritic cells (FDC) within germinal centres. Activated CD4+ T cells transiently express CD40L which can ligate CD40 on germinal centre B cells resulting in proliferation, expression of activation markers and differentiation with isotype

switching (Lederman et al. 1994, Saeland et al. 1993). T cells in the lymph nodes of CLL patients express CD40L (Pizzolo et al., 1983) and can induce CLL growth and survival through engagement of CD40 on the CLL cell surface by membrane bound and soluble CD40L (Bagnara et al., 2011, Granziero et al., 2001). These two cellular components, BMSC and T cells are important in supporting CLL cell growth and survival within the bone marrow and lymph nodes (Patten et al, 2008., Schmid and Isaacson, 1994).

One of the most prominent and activated signalling pathways in the cross talk between CLL cells and their microenvironment is the B-cell receptor signalling pathway (Herishanu et al., 2011). The consequences of this activation are complex and, despite being well studied, remain ill- defined. The importance of the BCR in the pathogenesis of the disease is shown by the fact that the strongest predictor of disease outcome is the mutational status of the BCR, with patients with UM-IGVH having a poor prognosis (Hamblin et al., 1999, Damle et al., 1999). Herishanu et al (2011) showed the BCR pathway to be the most activated in cells isolated form the lymph nodes of CLL patients. Studies of BCR stimulation in CLL have been conflicting, some studies have shown that there is a patient-dependent heterogeneous response that correlates with progressive disease (Deglesne et al., 2006, Guarini et al., 2008, Quiroga et al., 2009), while others showed a more homogenous response with no difference between prognostic subgroups (Pede et al., 2013, Petlickovski et al., 2005). The consensus is that CLL cells with UM-IGVH have greater poly- or self-reactivity and respond better to BCR stimulation while M-IGVH are monoreactive and less responsive to BCR stimulation (Ten Hacken et al., 2015,. The outcome of BCR stimulation is also thought to differ between the two groups, leading to responsiveness and proliferation in cells with UM-IGVH and failure to respond and anergy in CLL cells with M-IGVH (Muzio et al, 2008., Packham et al., 2014)

In the work presented in this thesis, various models have been used to mimic the effect of these microenvironmental components on CLL cells. The premise being investigated in this chapter is that these *in vitro* models can allow the study of microenvironmental mediated activation of STAT3 in CLL. In the previous chapter, we showed a role for the STAT3 pathway in the regulation of the adhesion molecule CD62L, so next we investigated how these microenvironmental stimuli impact on STAT3 activation and regulation of the expression of CD62L. BMSC coculture models have been shown in both human and murine cell lines to protect CLL cells and promote drug resistance (Trimarco et al., 2015, Kurtova et al., 2009). In this chapter, we use the Hs5 Bone

Marrow Stromal cell line which has been shown to support the proliferation of haematopoietic progenitor cells in the absence of exogenous factors (Roecklein and Torok-Storb, 1995).

Various *in vitro* models have utilised CD40L/IL4 signalling to mimic T cell activation of B cells, including the use of CD40L expressing fibroblasts, or soluble CD40L alone and in combination with soluble IL4 (Schattner et al., 1998, Bhattacharya et al., 2015, Scielzo et al., 2011, Buske et al., 1997). Here, we use soluble CD40L in combination with IL4 to investigate the effect of T cell signals on STAT3 activation in CLL cells, mimicking CLL cells interactions with T cells within the lymph node microenvironment (Hamilton et al., 2012). As discussed above, the BCR signalling pathway is crucial in the pathobiology of CLL. However, there is no standardized method for BCR stimulation and many studies have shown conflicting results depending on the method and duration of stimulation. We used soluble and immobilised forms of goat $F(ab)_2$ anti-human IgM fragments to stimulate the BCR in order to comprehensively study this pathway and its role on STAT3 activation and CD62L expression in CLL. In addition to this we use BCR inhibitors to see how they may modulate these effects. For this chapter we used the FDA-approved JAK/STAT3 inhibitor Ruxolitinib in combination with these inhibitors.

5.2 Aims and Objectives

The aims of this chapter were to investigate the effect of microenvironmental stimuli on the activation of STAT3 and the expression of CD62L and other adhesion molecules in CLL cells. This was achieved by:

- Co-culturing CLL cells on Hs5 BMSC;
- Investigating the effect of CD40L/IL4 stimulation;
- Stimulating the BCR with $F(ab')_2$ anti-IgM fragments;
- Investigating the response to BCR stimulation in CLL cells isolated from the peripheral blood and lymph node compartments in the same patient;
- Investigating the effect of BCR and JAK/STAT pathway inhibitors

5.3 Results

5.3.1 Hs5 BMSC coculture is prosurvival and results in an increase in pSTAT3 and CD62L in CLL cells

A heterogeneous cell population comprises the bone marrow stroma, including mesenchymal stem cells (MSC) which are stem-like and can differentiate into cartilage, bone, adipocytes and haematopoietic supporting tissues (Krebsbach et al., 1999, Whitfield et al., 2013). CLL cells interact with this network of different stromal cells within the tumour microenvironment and rely on paracrine signals and cell-cell contact with these stromal cells to enhance survival and promote drug-resistance. It has been shown that CLL cells cocultured with BMSC results in a decrease in spontaneous apoptosis *in vitro* (Kurtova et al., 2009, Panayiotidis et al., 1996, Lagneaux et al., 1998). It has also previously been shown that prosurvival microenvironmental signals such as IL-4 and interferons can enhance CD62L expression in CLL (Jewell and Yong, 1997, Purroy et al., 2015). In the previous chapter, we showed Cucurbitacin and S3I could downregulate CD62L in CLL cells (Figure 4.2). Here, we investigated whether coculture with stromal cells could upregulate CD62L expression and protect CLL cells from Cucurbitacin and S3I induced downregulation of CD62L.

We initially investigated whether coculture with the BMSC line, Hs5, had an effect on the CLL cell survival in samples from our patient cohort. We observed a wide variability in spontaneous apoptosis after 24 hours in CLL cells between patient samples (10%-86%, n=8) and, in agreement with previous studies (Kurtova et al., 2009) (Trimarco et al., 2015), coculture with Hs5 cells resulted in a significant decrease in spontaneous apoptosis ($p=0.0032$; Figure 5.1 (a i)). As shown in figure 5.1 (a ii) this protection from apoptosis in CLL cells is contact mediated as Hs5 conditioned media had no effect on spontaneous apoptosis. The JAK/STAT3 inhibitor, Ruxolitinib, and the BCR signalling pathway inhibitor, Ibrutinib, partially abrogated this prosurvival effect (Figure 5.1 (b)).

We next quantified serine and tyrosine pSTAT3 in CLL cells after 4 hours in Hs5 coculture. As shown in figure 5.2 (a i & ii), Hs5 coculture resulted in an increase in tyrosine pSTAT3 ($p=0.0094$). STAT3 in CLL cells is constitutively phosphorylated on serine 727 (ser pSTAT3); however, we did observe an increase in serine pSTAT3 in CLL cells in co-culture with Hs5 cells (Figure 5.2 (a iii)). Pre-treatment with Ruxolitinib reduced Hs5 induced tyrosine pSTAT3, while Ibrutinib had no effect (Figure 5.2 (b)).

In addition to an increase in pSTAT3, Hs5 coculture resulted in an increase in CD62L expression in CLL cells (p=0.0001; Figure 5.3 (a i)), which was dependent on CLL-stromal cell contact (Figure 5.3 (a ii)). Hs5 Co-culture had no effect on the other adhesion molecules shown in figure 5.3 (a iii) expressed on CLL cells. Cucurbitacin and S3I significantly downregulated CD62L expression in CLL cells in coculture with Hs5 stromal cells (p=0.0401and p=0.0198 respectively; Figure 5.3 (b i)). Hs5 coculture did not protect CLL cells from Cucurbitacin induced CD62L downregulation (ns, p=0.0500; Figure 5.3(b i)). Treatment with both Ruxolitinib and Ibrutinib partially downregulated Hs5 induced CD62L expression in CLL cells (Figure 5.3 (b ii)). Co-culture with patient derived bone marrow stromal cells (PD-BMSC) and HUVEC also significantly upregulated CD62L expression (Figure 5.3 (c i)).Cucurbitacin also results in a downregulation of CD62L expression in CLL cells in coculture with PD-BMSC and HUVEC coculture (Figure 5.3 (c ii)).

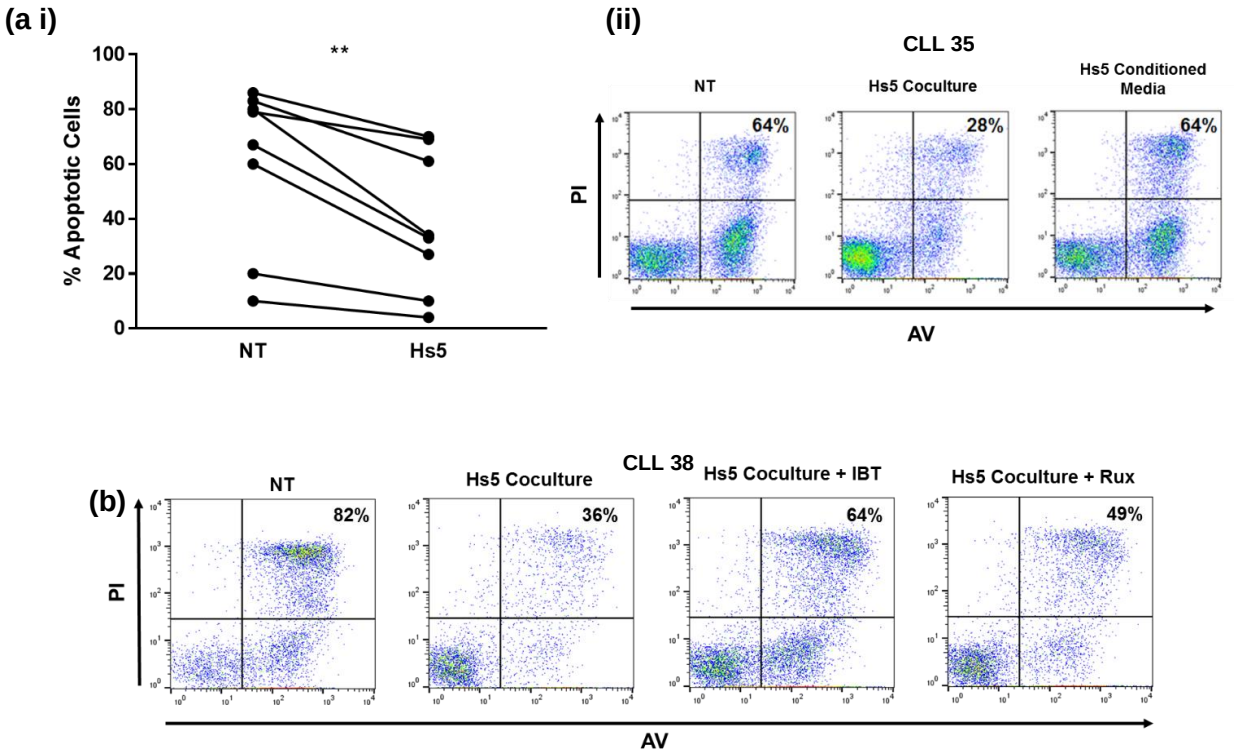

Figure 5. 1 Hs5 Coculture protects against spontaneous apoptosis of CLL cells (a i) Spontaneous apoptosis in CLL cells alone (NT) and cultured on Hs5 cells for 24 hours was assessed by AV/PI flow cytometry (** p=0.0032, n=8). **(a ii)** Dotplots displaying the percentage of AV/PI positive CLL cells after 24 hours cultured with Hs5 cells or in Hs5 conditioned media. Representative of n=3 **(b)** Dotplots displaying the percentage of AV/PI positive CLL cells after 24 hours cultured with Hs5 cells and 10μM Ibrutinib (IBT) or 1μM Ruxolitinib (Rux). Representative of n=3.

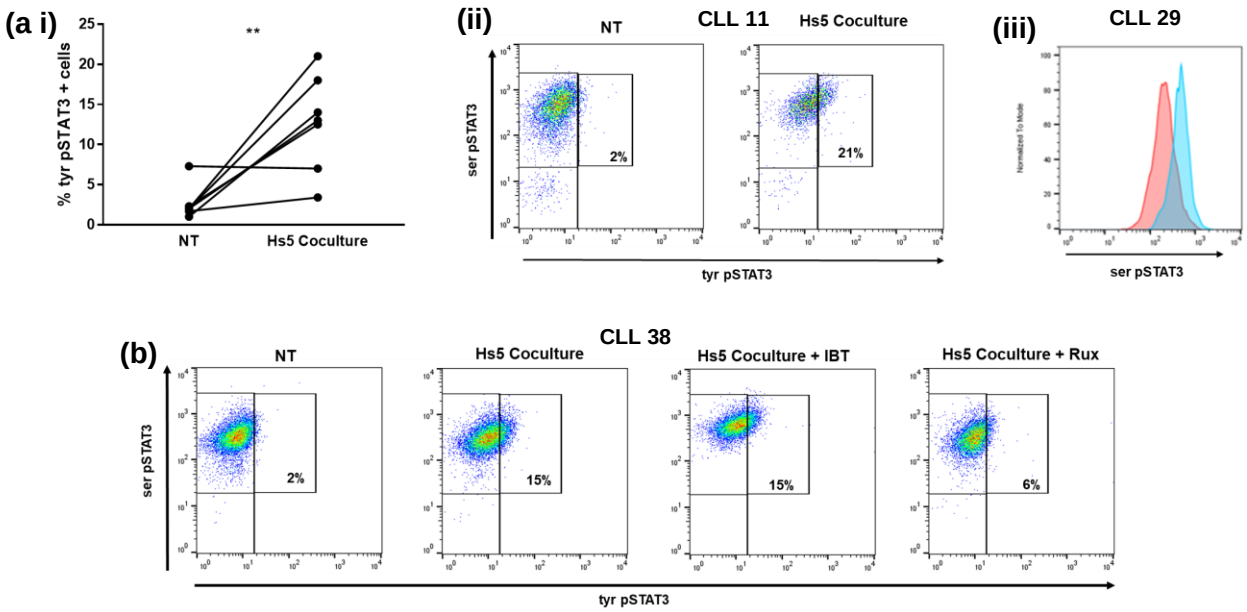

Figure 5. 2 Hs5 Coculture induces phosphorylation of STAT3 in CLL cells. (a i) CLL samples were cultured alone (NT) or with Hs5 cells for 24 hours and tyrosine phosphorylated STAT3 (tyr pSTAT3) was assessed by flow cytometry (** p=0.0094, n=7) **(ii)** Representative dotplots displaying the percentage of tyrosine pSTAT3 and (iii) a representative histogram showing the shift in serine pSTAT3 in CLL cells cultured with Hs5 for 24 hours. **(b)** Dotplots displaying the percentage of tyrosine pSTAT3 in CLL cells cultured for 24 hours after pretreatment with 10μM Ibrutinib (IBT) or 1μM Ruxolitinib (Rux). Representative of n=3.

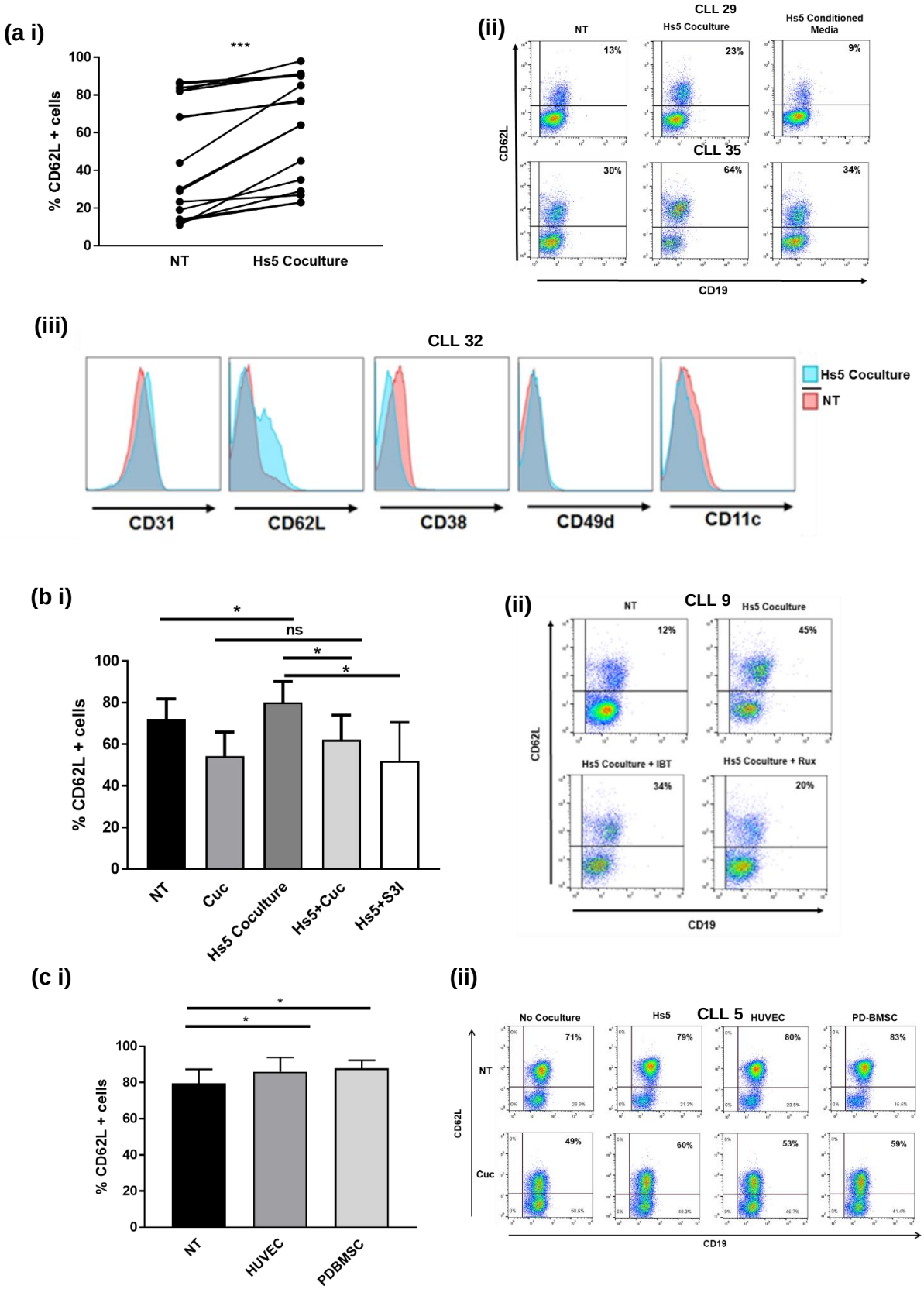
(a i)
***
% CD62L + cells
100
80
60
40
20
0
NT
Hs5 Coculture
(ii)
CLL 29
NT
Hs5 Coculture
Hs5 Conditioned Media
13%
23%
9%
CLL 35
30%
64%
34%
CD62L
CD19
(iii)
CLL 32
Hs5 Coculture
NT
CD31
CD62L
CD38
CD49d
CD11c
(b i)
*
ns
*
*
% CD62L + cells
100
80
60
40
20
0
NT
Cuc
Hs5 Coculture
Hs5+Cuc
Hs5+S3I
(ii)
CLL 9
NT
Hs5 Coculture
12%
45%
Hs5 Coculture + IBT
Hs5 Coculture + Rux
34%
20%
CD62L
CD19
(c i)
*
*
% CD62L + cells
100
80
60
40
20
0
NT
HUVEC
PDBMSC
(ii)
CLL 5
No Coculture
Hs5
HUVEC
PD-BMSC
71%
79%
80%
83%
NT
49%
60%
53%
59%
Cuc
CD62L
CD19

Figure 5. 3 Hs5 Coculture results in an increase in the expression of CD62L in CLL cells in a contact-dependant manner that can be decreased by pre-treatment with BCR and STAT3 targeting agents. (a i) CLL cells were cultured alone (NT) or in co-culture with Hs5 cells for 24 hrs. Percentage of CD62L positive CLL cells was assessed by flow cytometry. (*** p=0.0001, n=16). **(ii)** Dotplots of a $CD62L^{+}$ sample (CLL29) and a $CD62L^{-}$ sample (CLL35) displaying the percentage CD62L positive CLL cells cultured for 24 hours with Hs5 cells or Hs5 conditioned media. Representative of n=3. (iii) Histograms showing the expression of 5 adhesion markers in CLL cells after 24 hours culture with Hs5 cells. Representative of n=3. **(b i)** CLL were treated as shown and CD62L expression was assessed by flow cytometry after 1 hour pretreatment with 1μM Cucurbitacin (Hs5 coculture vs Hs5+Cucurbitacin (Cuc); *p=0.0401, n=6) or 100μM S3I (Hs5 coculture *vs* Hs5+S3I; *p=0.0198) **(ii)** Dotplots displaying the percentage of CD62L positive CLL cells cultured with Hs5 cells for 24 hours after pretreatment for 1 hour with 10μM Ibrutinib (IBT) or 1μM Ruxolitinib (Rux). Representative of n=3. **(c)** 24 hour culture with Human Umbilical vein endothelial cells (HUVEC) or patient derived bone marrow stromal cells (PDBMSC). Bars represent mean expression (± s.e.m) (No treatment (NT) *vs* Hs5 Coculture; **p= 0.024, n=4) (NT vs HUVEC coculture; * p=0.0202, n=4) (NT *vs* PDBMSC coculture; * p=0.0142, n=4) **(ii)** Representative dotplots displaying the percentage of CD62L positive CLL cells after 24 hour cocultures with or without Cucurbitacin.

.

5.3.2 BCR stimulation has a prosurvival effect in CLL cells and pre-treatment with Ibrutinib or Ruxolitinib abrogates this prosurvival signal

The importance of BCR stimulation in CLL is underlined by the clinical efficacy of BCR pathway inhibitors, Ibrutinib and Idelalisib (Byrd et al., 2014, Brown et al., 2014) and the prognostic significance of the mutational status of the immunoglobulin genes (Hamblin et al., 1999) . Simulation of the BCR by cross linking using anti-IgM results in prosurvival signalling that can prevent CLL cells undergoing spontaneous apoptosis (Quiroga et al., 2009). We used $F(ab')_2$ anti-IgM fragments to stimulate the BCR and investigate its effect of the survival of CLL cells using Annexin V (AV)/ Propidium Iodide (PI) staining by flow cytometry. BCR stimulation had a patient variable effect on survival but, overall, significantly reduced spontaneous apoptosis after 24 hours by 11% ($p<0.001$, Figure 5.4 (a i)). Greater than a 5% reduction in spontaneous apoptosis was seen in in 18/23 patient samples. Patient samples were then grouped by mutational status of their IGVH genes (13 UM-IGVH, 7 M-IGVH). Although a greater decrease in apoptosis was seen in samples with UM-IGVH genes, there was no significant difference between the prosurvival effect of BCR stimulation in samples with UM- or M-IGVH genes ($p=0.6010$; Figure 5.4 (a ii)). The BCR pathway inhibitor, Ibrutinib, ($p=0.0341$) and the JAK/STAT3 pathway inhibitor, Ruxolitinib ($p=0.0102$) both abrogated the pro-survival effect of BCR stimulation in CLL cells (Figure 5.4 b).

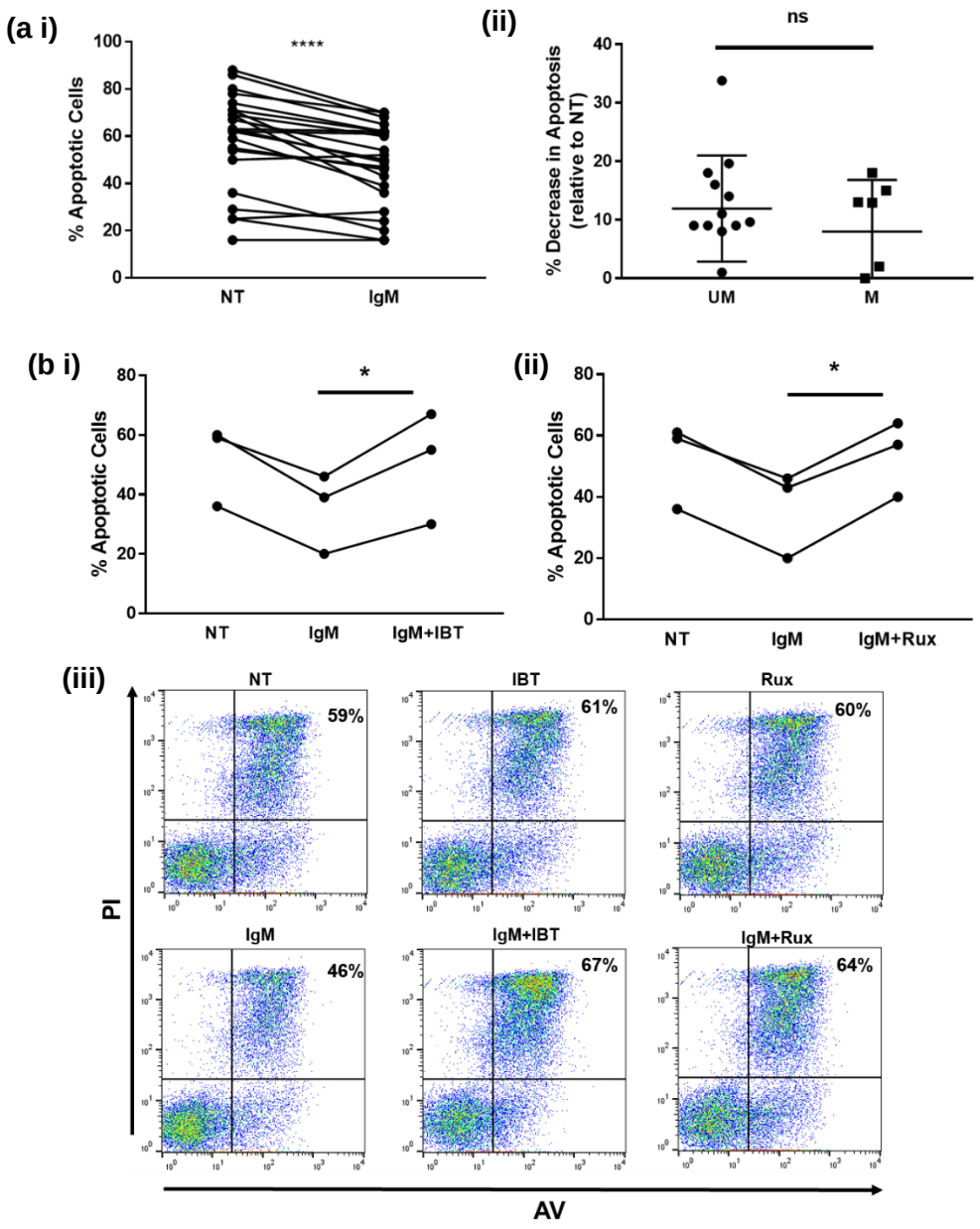

Figure 5. 4 Stimulation of the BCR using F(ab´)$_2$ anti-IgM fragments has a prosurvival effect in CLL cells with both UM- and M- IGVH genes. BCR stimulation was performed by incubating CLL cells with 10µg/ml F(ab)$_2$ anti-IgM fragments **(a i)** Following BCR stimulation for 18 hours percentage of apoptosis was assessed by AV/PI assay and flow cytometry (No treatment (NT) v IgM stimulation,**** p<0.0001, n=23) **(ii)** The percentage decrease in apoptosis in CLL cells with UM-IGVH and M-IGVH after 18 hours BCR stimulation. Bars represent the mean decrease (± s.e.m) for 13 UM-IGVH and 7 M-IGVH patient samples (ns, p=0.6010). **(b)** CLL cells were pre-treated with either **(i)** 10µM Ibrutinib (IBT) (IgM v IgM+IBT, *p=0.0341, n=3) or **(ii)** 1µM Ruxolitinib (Rux) (IgM v IgM+Rux, *p=0.0102 n=3) for 1 hour before BCR stimulation as above for 18 hours **(iii)** Representative dotplots (CLL8) displaying the percentage of AV/PI positive CLL cells pre-treated with either Ibrutinib or Ruxolitinib for 1 hour before BCR stimulation (IgM) for 18 hours.

5.3.3 BCR stimulation results in an increased phosphorylation of STAT3 in CLL cells with UM-IGVH genes

In the previous section, we have shown that the JAK2 inhibitor, Ruxolitinib, abrogates the BCR stimulation induced prosurvival effect in CLL (Figure 5.4 (b i)). BCR stimulation has been shown to activate the STAT3 pathway through phosphorylation of tyrosine in CLL via the activation of JAK2 (Rozovski et al., 2014). We confirmed that BCR stimulation resulted in phosphorylation of STAT3 in CLL cells (Figure 5.5 (a i) after 4 hrs and this was sustained up to 18hrs (Figure 5.5 (a ii). In addition, we found that BCR stimulation resulted in a significant increase in tyrosine pSTAT3 ($p=0.0080$, 16 UM-IGVH, 10M-IGVH; Figure 5.5 (a iii)) and, also, serine pSTAT3 ($p=0.0199$, 16 UM-IGVH, 10 M-IGVH) in CLL cells with UM-IGVH compared to M-IGVH. The induction of tyrosine pSTAT3 was variable with an average induction of 17.9% $\pm$ 3.1% for UM-IGVH and 6.4% $\pm$ 1.2% for M-IGVH. The increase in serine pSTAT3 was 8% $\pm$ 2.5% for UM-IGVH and 0% $\pm$ 1.2% for M-IGVH.

We saw variable responses in tyrosine STAT3 phosphorylation in patent samples with UM-IGVH after BCR stimulation so we investigated if NOTCH1, CD38 expression or CD49d expression had any impact on the level of activation. NOTCH1 activity has been shown in normal B cells to synergize with BCR signalling to enhance activation of the MAPK pathway (Thomas et al., 2007) and stimulation of NOTCH1 synergised with BCR signalling resulting in enhanced proliferation in B cell lymphoma (He et al., 2009). Of the 24 UM-IGVH patient samples investigated here, 15 were positive for NOTCH1 mutation; however, we saw no difference in amount of tyrosine pSTAT3 induction after BCR stimulation between UM-IGVH patient samples with mutated and unmutated NOTCH1 (Fig 5.5 (a v)). As shown in figure 5.5 (a v) there was no difference in the amount of tyrosine pSTAT3 induction after BCR stimulation between UM-IGVH patient samples with , positive or negative CD38 or CD49d. We also saw variable increases in serine pSTAT3 in UM-IGVH patient samples (Figure 5.5 (b i) with significantly increased serine pSTAT3 seen in patient samples with <80% baseline serine pSTAT3 compared to those with >80% positive serine pSTAT3 ($p=0.0003$; Figure 5.5 (b iii).

In order to assess the phosphorylation of STAT3 relative to other downstream targets of BCR signalling, we utilised the Proteome Profiler Phospho-Kinase Array to assess changes in phosphorylation status of 43 different kinases (full list in appendix 3). CLL cells from a patient sample with UM-IGVH (CLL30) incubated with $F(ab')_2$ anti-IgM fragments for 15 minutes and 4 hours. As shown in figure 5.6 (a i), after 15 mins stimulation we found greater than a two-fold increase in phosphorylation of

downstream effectors of BCR signalling, AKT 1/2/3 (4.2 fold) and ERK1/2 (3.6 fold), as well as p70 S6 Kinase (2.4 fold). Smaller changes less than two fold in the phosphorylation are shown on the blot and listed in Appendix 3. After 4 hours stimulation, these increases had resolved but we saw large fold increases in tyrosine pSTAT3 (15.3 fold) and serine pSTAT3 (27 fold), as well as greater than 2 fold increase in phosphorylation of p53 (2.4 fold) and p70 S6 kinase (3.3 fold). Smaller increases of less than 2 fold in phosphorylation after 4 hours are listed in Appendix 3. Treatment with Ruxolitinib prior to BCR stimulation for 4 hours completely abrogated both tyrosine pSTAT3 and serine pSTAT3 (Appendix 3). .

Given that BCR stimulation occurs mainly in the bone marrow and lymph node microenvironments, the response of cells from these compartments to BCR stimulation may be more relevant. Here, we utilised two matched samples, one with M-IGVH and one with UM-IGVH, with CLL cells isolated from the bone marrow and the peripheral blood. As shown in figure 5.7 there was no difference in tyrosine pSTAT3 induction between cells from the peripheral blood and cells from the bone marrow in the sample with M-IGVH. Interestingly, in the patient sample with UM-IGVH, there was less tyrosine pSTAT3 activation in cells from the bone marrow compared to peripheral blood (18% vs 11% respectively).

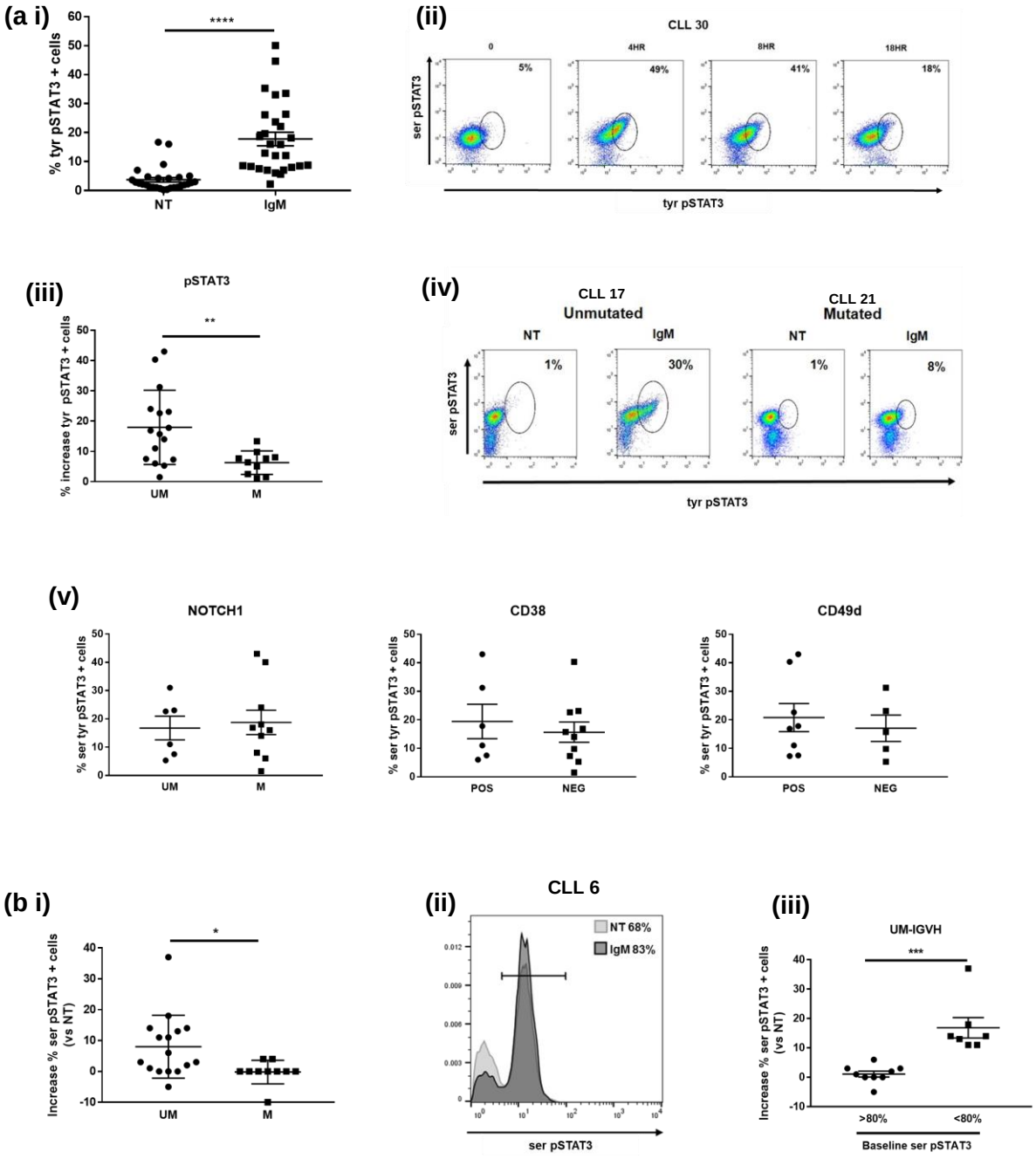

Figure 5. 5 BCR stimulation results in STAT3 activation in CLL cells with UM-IGVH. BCR stimulation was performed by incubating CLL cells with 10µg/ml $F(ab)_2$ anti-IgM fragments **(a i)** CLL cells were stimulated as above for 4 hours. The percentage of serine (ser) and tyrosine (tyr) positive pSTAT3 CLL cells in unstimulated (NT) and BCR stimulated (IgM) CLL cells. Bars represent mean increase (± s.e.m) (**** p<0.0001, n=28) **(ii)** Dotplots displaying the percentage of serine and tyrosine pSTAT3 positive CLL cells after 4, 8 and 18 hours BCR stimulation in a UM-IGVH patient sample. Representative of n=3. CLL cells were stimulated as above for 4 hours. **(iii)** The percentage increase in serine and tyrosine pSTAT3 positive CLL cells with UM-IGVH and M-IGVH. Bars represent mean increase (± s.e.m) for 16 UM-IGVH and 10 M-IGVH patient samples (** p=0.0080) **(iv)** Representative dotplots displaying the percentage of serine and tyrosine pSTAT3 positive CLL cells after 4 hours BCR stimulation in one UM-IGVH (CLL17)

and one M-IGVH (CLL21) patient sample. **(v)** The percentage increase in tyrosine pSTAT3 in NOTCH1 mutated (M, n=10) and unmutated (UM, n=6), CD38 positive (POS, n=6) and negative (NEG, n=10) and CD49d positive (POS, n=8) and negative (NEG, n=5) IGVH-UM CLL patient samples after 4 hours BCR stimulation. Bars represent mean increase (± s.e.m). **(b i)** Graph showing the percentage increase in serine pSTAT3 positive CLL cells with UM-IGVH and M-IGVH after 4 hours BCR stimulation. Bars represent mean increase (± s.e.m) for 16 UM-IGVH and 10 M-IGVH patient samples (* p=0.0199). **(ii)** Representative histogram displaying the percentage of serine pSTAT3 positive CLL cells after 4 hours BCR stimulation **(iii)** Graph showing the percentage increase in serine pSTAT3 positive CLL cells with >80% and <80% baseline serine pSTAT3 positive CLL cells after 4 hours BCR stimulation. Bars represent mean increase (± s.e.m) (*** p=0.0003, n=16).

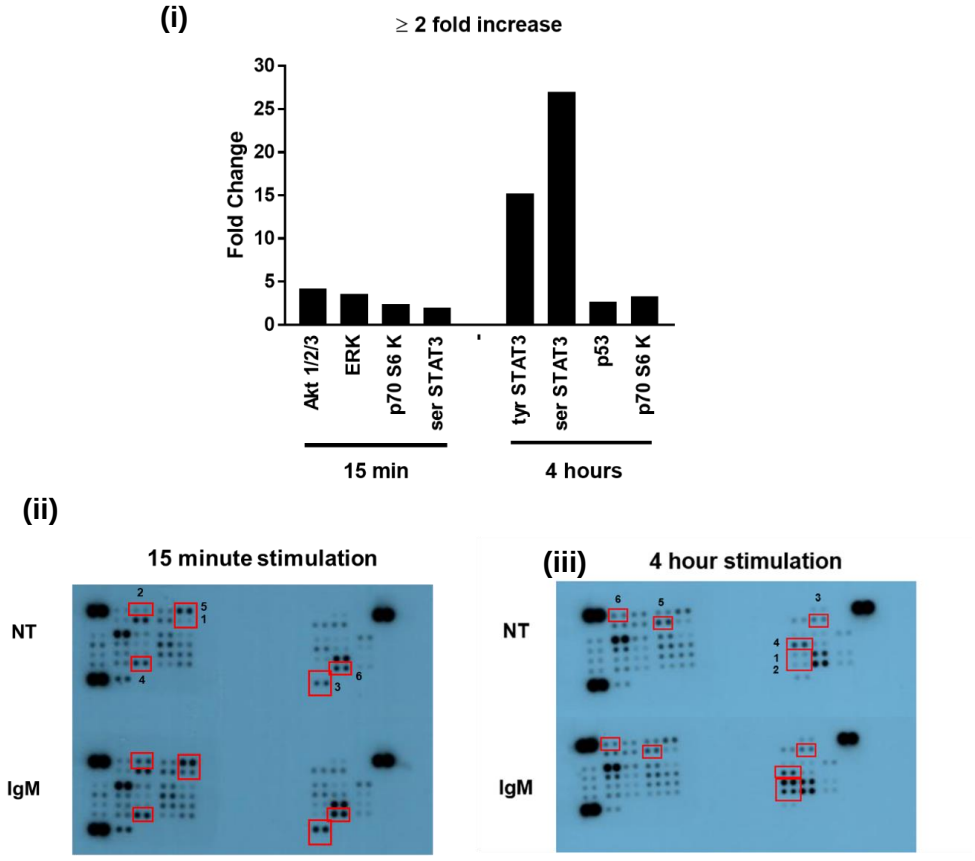

Figure 5. 6 Protein kinase phosphorylation following BCR stimulation. BCR stimulation was performed by incubating CLL cells (CLL30, >90% CD19/CD5+) with 10µg/ml $F(ab)_2$ IgM fragments and protein was extracted. Lysates were immunoblotted according to the Proteome Profiler Phospho-kinase Array protocol. Dot intensities were quantified using Image J with Protein Profiler add-on software **(i)** Graph showing >2 Fold change in the phosphorylation of proteins in CLL cells after 15 minutes and 4 hours of BCR stimulation **(ii)** Immunoblots showing the kinases with an increase in phosphorylation of >5000 mean intensity units in CLL cells after 15 minutes (1=Akt 1/2/3, 2=ERK, 3=Hsp60, 4=FAK, 5=GSK3, 6=WNK1.) or **(iii)** 4 hours (1= tyr STAT3, 2=ser STAT3, 3= AMPK1, 4=CREB, 5=p53, 6=p70 S6 Kinase) BCR stimulation.

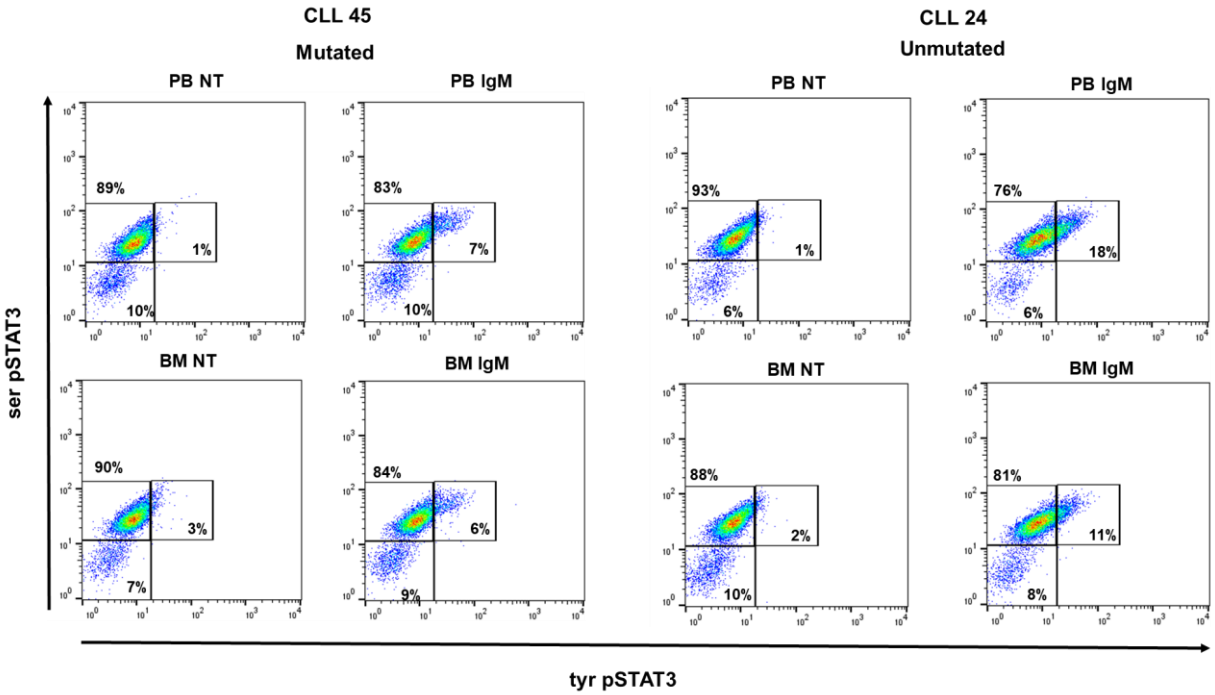

Figure 5. 7 The activation of STAT3 is similar CLL cells from the PB or BM compartments after BCR stimulation. CLL cells isolated from different tissue compartments from the same patient were incubated with 10µg/ml $F(ab)_2$ anti-IgM fragments to stimulate the BCR. Dotplots display the percentage of tyrosine and serine pSTAT3 positive CLL cells after 4 hours BCR stimulation in 1 M-IGVH (CLL 45) and one UM-IGVH (CLL 24).

5.3.4 CD40L and IL4 stimulation downregulates BCR induced STAT3 activation in CLL cells

In addition to stromal cells, T cells provide important prosurvival signals to CLL cells. The T cell population is abnormal in CLL but a significant number of T cells in the lymph nodes of CLL patients express CD40L (Pizzolo et al., 1983), which signals through CD40 on the CLL cell surface (Bagnara et al., 2011, Granziero et al., 2001). Interleukin 4 (IL4) is another important prosurvival signal T cells provide CLL cells in the lymph node microenvironment. CLL cells express higher levels of IL4 receptor than non-malignant B cells (Douglas et al., 1997) and higher levels of T cells expressing IL4 is associated with aggressive disease (Rossmann et al., 2002). IL4 enhances the proliferation and survival of CLL cells in vitro (Steele et al., 2010, Fluckiger et al., 1992).CD40L and IL4 have been shown to influence BCR signalling: IL4 has been shown to repair and reprogramme sIgM expression to enhance B cell activation (Aguilar-Hernandez et al., 2016); and CD40 enhances ERK activation induced by IgM engagement (Mizuno and Rothstein, 2005).

We found that IL4 alone ($p=0.0329$) and in combination with CD40L (* $p=0.0491$) was pro-survival, resulting in a significant decrease in apoptosis (Figure 5.8 (i)). BCR stimulation protected CLL cells from spontaneous apoptosis; however, BCR stimulation had no effect on the prosurvival effect of treatment with CD40L and IL4 (Figure 5.8 (i)). Interestingly, CD40L and IL4 treatment significantly decreased BCR stimulation-induced phosphorylation of STAT3 ($p= 0.0447$; Figure 5.8 (ii)). CD40L and IL4 alone or in combination had no effect on the phosphorylation of STAT3 (Figure 5.4 (ii)).

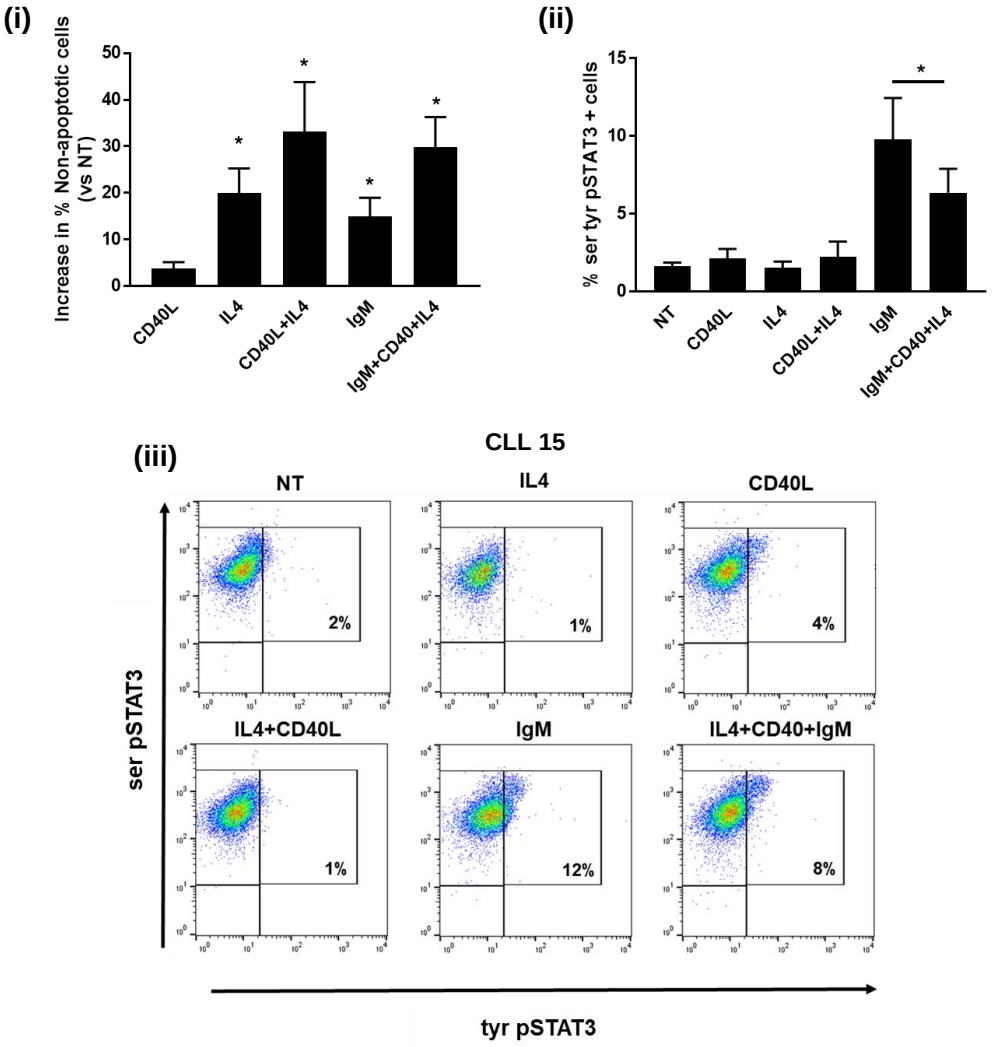

Figure 5. 8 Treatment with IL4 and CD40L results in a decrease in BCR stimulation- induced tyrosine pSTAT3. BCR stimulation was performed by incubating CLL cells with 10μg/ml $F(ab')_2$ anti-IgM fragments alone or in combination with 10ng/ml IL4 and 1μg/ml CD40L. **(i)** CLL cells were treated as shown and apoptosis was assessed by AV/PI assay. Bar chart displays the mean increase (± s.e.m) in non- apoptotic CLL cells compared to control (NT) after 4 hours (IL-4 *vs* NT, p=0.0329; CD40L+IL4 *vs* NT, p= 0.0323; BCR stimulation (IgM) *vs* NT, p= 0.0491; IgM+CD40+IL4 *vs* NT, p=00194, n=4) **(ii)** Bar chart displays the mean increase (± s.e.m) in serine and tyrosine pSTAT3 double positive cells in CLL cells after incubation for 4 hours with CD40L, IL4 and IgM (BCR stimulation) alone and in combination (* p=0.0447, n=5). **(iii)** Representative dotplots displaying the percentage of tyrosine positive cells in CLL cells after incubation for 4 hours with CD40L, IL4 and IgM alone and in combination in one patient sample.

5.3.5 BCR stimulation results in an increase in CD62L expression in CLL cells with UM-IGVH genes

In the previous chapter, we demonstrated a role for STAT3 in the regulation of CD62L expression and, given that have now demonstrated that BCR stimulation activates STAT3, we also investigated the effect of BCR stimulation on CD62L.

We found that BCR stimulation had no effect on CD62L after 4 or 8 hours but significantly up regulated CD62L expression in CLL patient samples after 18 hours (Figure 5.9 (a & b i)). BCR stimulation resulted in an increase in CD62L expression after 18 hours in CLL cells with UM-IGVH compared to M-IGVH ($p=0.0313$, 15 UM-IGVH, 8 M-IGVH). The increase in CD62L was variable with an average induction of 12.8% $\pm$ 2.5% for UM-IGVH and 4.1% $\pm$ 1.8% for M-IGVH. We saw no difference in the induction of CD62L expression after BCR stimulation in UM-IGVH patient samples between NOTCH1 mutated or unmutated, CD38 or CD49d positive or negative (Figure 5.9 (c)). BCR stimulation had no effect on the expression of other adhesion markers shown in figure 5.9 (d).

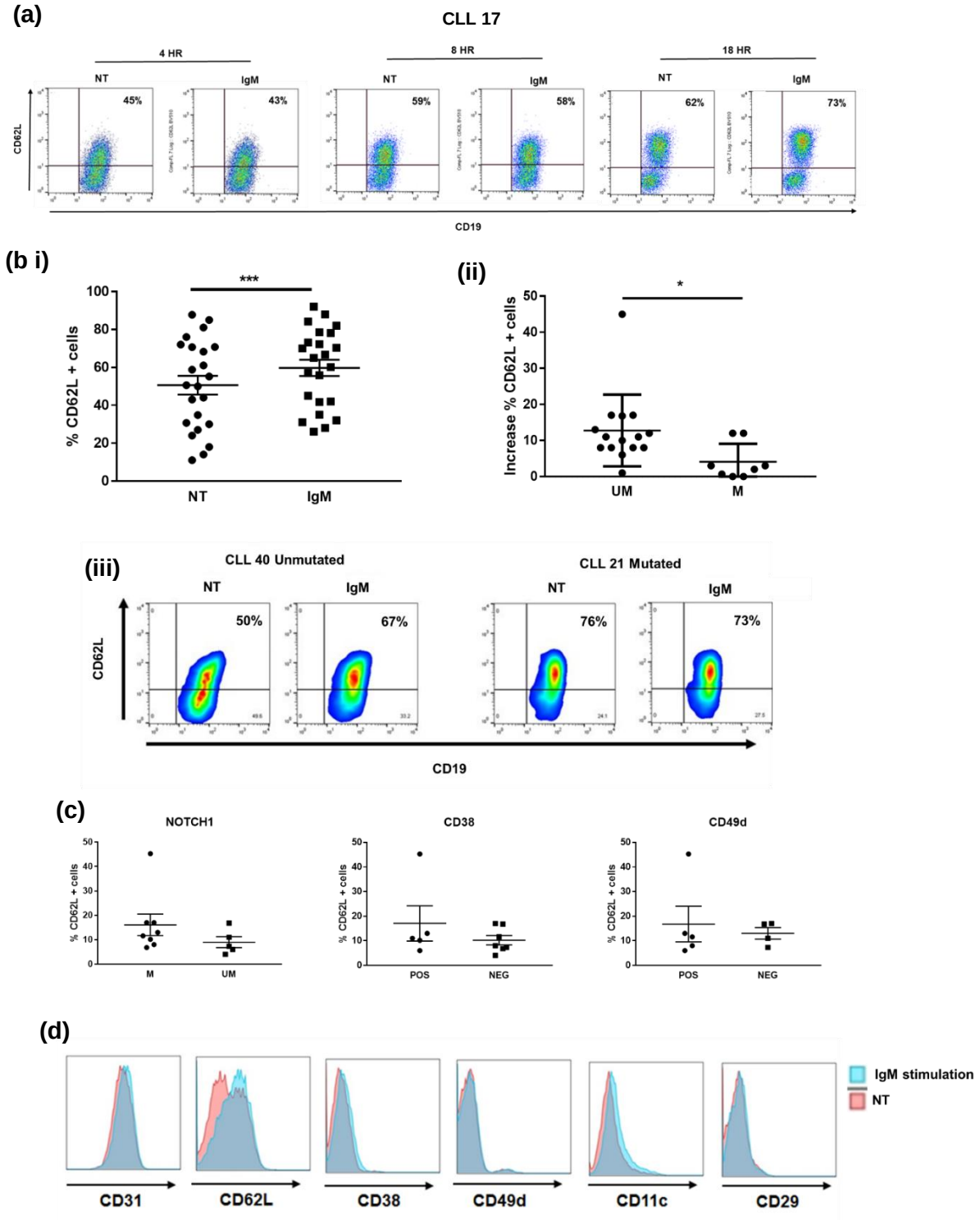

Figure 5. 9 BCR stimulation results in an increase in CD62L expression in CLL cells with UM-IGVH. BCR stimulation was performed by incubating CLL cells with 10µg/ml $F(ab)_2$ anti-IgM fragments and CD62L expressed was quantitated by flow cytometry **(a)** BCR stimulation was performed as described and untreated (NT) and stimulated CLL cells were stained for CD62L after 4, 8 and 18 hours. Representative of n=3. **(b i)** The percentage increase in CD62L positive in untreated (NT) CLL cells or after 18 hours BCR stimulation (*** p=0.0002, n=23). **(b ii)** The percentage increase in CD62L positive CLL cells after 18 hours BCR stimulation. Bars represent mean increase (± s.e.m) in 15 UM-IGVH (UM) and 8 M-IGVH (M) patient samples (* p=0.0313). **(iii)** Representative dotplots displaying the percentage CD62L positive CLL cells after 18 hours BCR stimulation (IgM) in one UM-IGVH (unmutated) (CLL40) and one M-IGVH (mutated) (CLL 21) patient sample. NT- no stimulation **(c)** The percentage increase in CD62L expression in NOTCH1

mutated (n=8) and unmutated (n=5), CD38 positive (n=5) and negative (n=7) and CD49d positive (n=5) and negative (n=4) IGVH-UM CLL patient samples after 4 hours BCR stimulation. Bars represent mean increase (± s.e.m). **(d)** Histograms showing the expression of 6 adhesion markers in CLL cells after 18 hours BCR stimulation (IgM stimulation). Representative of n=3.

5.3.6 BCR stimulation results in an increase in the expression of CD62L gene expression in CLL cells with UM-IGVH

STAT3 is a transcription factor that regulates the expression of genes that are involved in a number of different processes including survival and proliferation. When phosphorylated STAT3 dimerizes and translocates to the nucleus to control the expression of these genes. We have shown that BCR stimulation results in the activation of STAT3 and wanted to investigate its effect on the STAT3 regulated genes, MCL1, BCL2, CCND1 (Cyclin D1) and STAT3 itself. We also investigated whether the expression of CD62L was regulated at the mRNA level. We used two validated housekeeping genes B2M and HPRT1 for normalisation (Valceckiene et al., 2010). In CLL cells with UM-IGVH, CD62L had > 2 fold increase in gene expression. STAT3, MCL1 and BCL2, while upregulated in patient samples with UM-IGVH, did not increase >2 fold and were not considered statistically significant (Figure 5.10). No significant increases in gene expression were seen in CLL cells with M-IGVH genes.

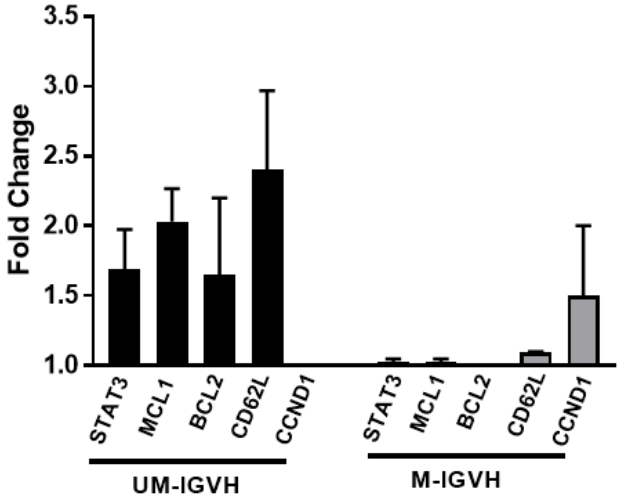

Figure 5. 10 BCR stimulation results in an increase in the expression of CD62L gene expression in CLL cells with UM-IGVH genes. BCR stimulation was performed by incubating CLL cells with $F(ab')_2$ IgM fragments (10µg/ml) and RT-qPCR was performed using TaqMan Assays. Graph shows the fold change in STAT3, MCL1, BCL2, CD62L and CCND1 gene expression in CLL cells after for 8 hours BCR stimulation. Bars represent mean change (± s.e.m) in 3 UM-IGVH and 3 M-IGVH patient samples.

5.3.7 BCR stimulation modulates the expression of genes involved in the adhesion and migration of CLL cells

Having seen an effect of BCR stimulation on the gene and protein expression of CD62L, we next wanted to investigate other genes that may be involved in the adhesion and migration of CLL cells. BCR signalling has been shown to enhance CLL cell migration (Quiroga et al., 2009), and we showed a trend towards increased chemotaxis after IgM stimulation (Figure 5.11 (a)). Stimulation of the BCR is thought to help retain CLL cells within their protective microenvironments and we wanted to investigate which adhesion molecules may be important in this process and if any are regulated through JAK2/STAT3 signalling.

We initially used the TaqMan Extracellular Matrix and Adhesion Molecule Array to assess gene expression following BCR stimulation for 4 hours in one patient sample with UM-IGVH (CLL30), with and without pre-treatment with Ruxolitinib for one hour. BCR induced STAT3 phosphorylation after 4 hours is shown in (Figure 5.11 (b)). Results of the TaqMan Array gene changes are detailed in Appendix 4. Genes that underwent >2 Fold change in expression are shown in Table 5.1.

We chose three genes with the highest fold changes and < 30 CT: Collagen type IV alpha 2 chain (COL4A2) (↑ 4.03), Thrombospondin1 (THBS1), (↓ 4.09) and Versican (VCAN) (↓ 31.7). CT values above 30 imply low target values that are sensitive to large changes (Bustin et al., 2009). We assessed the expression of these genes using individual Taqman assays in a further 10 patients, 8 UM-IGVH and 2 M-IGVH and found variable responses that were independent of mutational status. COL4A2 increased greater than 2 fold in 7/10 patients. THBS1 decreased greater than 2 fold in 4/10 patients and VCAN decreased by greater than 2 fold in 7/10 patients (Figure 5.11 (c)). Pre-treatment with Ruxolitinib reduced COL4A2 expression in 2/4 patients, reduced the downregulation of THBS1 in 2/4 patients and reduced the downregulation of VCAN in 2/4 patients (Figure 5.11 (d)).

Table 5. 1 Genes with >2 fold change after BCR stimulation or pretreatment with Ruxolitinib followed by BCR stimulation

Gene	CT	Fold Change after BCR stimulation (vs NT)	Fold Change after BCR stimulation+ Rux (vs NT)
↑ Upregulated			
CTNNA1	24	2.09	2.09
SPP1	24	2.06	1.00
COL4A2	29	4.03	1.50
ICAM1	30	3.95	4.02
ITGA3	30	2.02	2.00
COL7A1	34	2.02	4.00
ITGA1	35	2.02	2.00
TNC	40	7.22	7.70
↓ Downregulated			
THBS1	23	4.09	2.10
TGFBI	25	4.09	2.00
VCAN	27	31.7	31.00
MMP11	31	3.99	3.97
ECM1	34	2.03	1.00
ITGA5	34	2.04	2.01
FN1	35	2.16	2.08
MMP2	36	6.56	6.50
ITGB5	37	3.99	7.87
KAL1	37	6.94	1.00
MMP1	37	6.23	1.00
COL5A1	37	7.28	1.00

CT= cycle threshold, the cycle at which the signal of the reporter dye crosses this threshold line. It is a relative measurement of the concentration of target in the reaction. NT- No treatment.

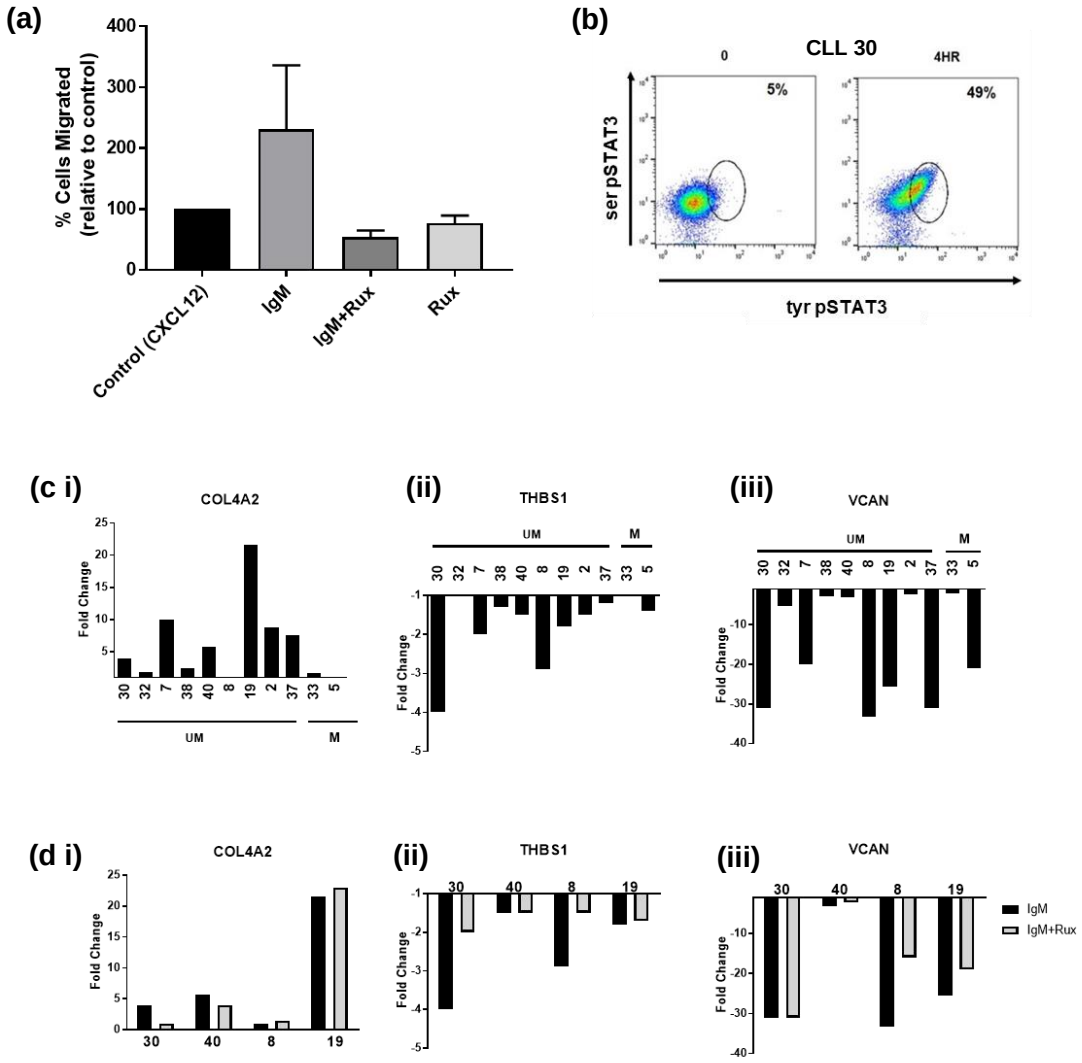

Figure 5. 11 BCR stimulation results in changes in the expression of genes involved in migration and adhesion, COL4A2, THBS1 and VCAN. (a) BCR stimulation was performed by incubating CLL cells with 10µg/ml $F(ab')_2$ IgM fragments or CLL cells were incubated with 1µM Ruxolitinib for 1 hour before stimulation for 3 hours and migration towards CXCL12 was assessed. There was trend towards an increase in chemotaxis after BCR stimulation (p=0.341, n=3) and Ruxolitinib resulted in a non-significant downregulated the effect of BCR stimulation chemotaxis of CLL cells (p=0.225, n=3). **(b)** BCR stimulation was performed as described and CLL cells were stained for tyrosine (tyr) STAT3 by flow cytometry. BCR stimulation was performed as described for 4 hours and RT-qPCR was performed using TaqMan assays. Graphs show the fold change in **(i)** COL4A2 **(ii)** THBS1 and **(iii)** VCAM in CLL cells after **(c)** 4 hour BCR stimulation in 9 UM-IGVH and 2 M-IGVH patient samples and **(d)** pretreatment with 1µM Ruxolitinib (Rux) for 1 hour followed by BCR stimulation in 4 UM-IGVH patient samples.

5.3.8 Soluble and immobilised IgM result in the phosphorylation of STAT3 and upregulation of CD62L expression

A number of *in vitro* studies on the effect of BCR stimulation in CLL cells have had contradicting results, in particular regarding the responses seen with M-IGVH compared to UM-IGVH (Deglesne et al., 2006) (Guarini et al., 2008). This is thought to be due to a lack of a standardised protocol and the use of soluble or immobilised IgM to stimulate the BCR. Studies have examined the effects of immobilised versus soluble IgM from different suppliers on the outcome of various parameters after stimulation of the BCR (Rombout et al., 2016). Although we achieved robust BCR signalling pathway activation (Figure 5.6) and an increase in CLL cell survival (Figure 5.4 (a)) using soluble goat $F(ab')_2$ anti-IgM fragments, we wanted to investigate if immobilised IgM resulted in the same effect on the phosphorylation of STAT3 and the expression of CD62L. STAT3 activation by BCR signalling has been shown using the same soluble goat $F(ab')_2$ anti-IgM (Rozovski et al., 2013) and the effect of immobilised IgM has not been reported. We found that both immobilised and soluble IgM had a prosurvival effect with no significant difference between soluble and immobilized forms of IgM (ns, p=0.8380; Fig 5.12 (i)). We saw no significant difference in the activation of STAT3 between soluble and immobilised IgM (ns, p=0.5811; Figure 5.13 (ii)), and we found IgM resulted in an increase in the expression of CD62L, with no difference between soluble or immobilised IgM (ns, p=0.5766; Fig 5.13 (iii)).

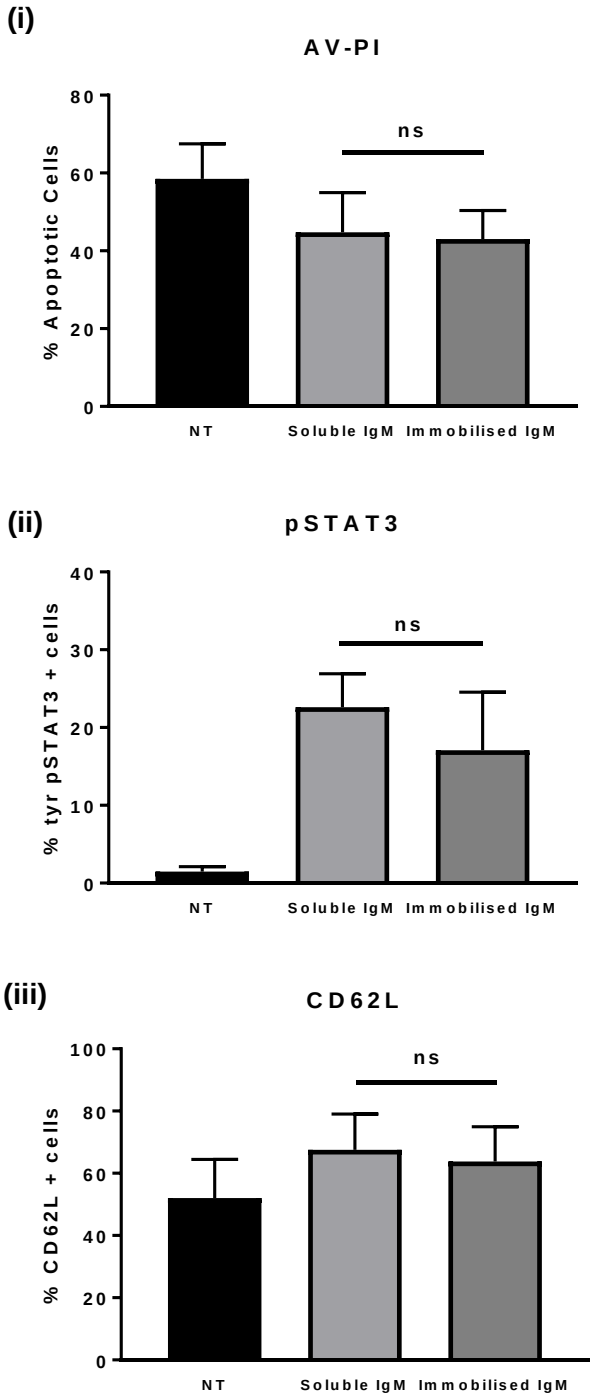

Figure 5. 12 Soluble and immobilised IgM result in STAT3 activation and CD62L upregulation in CLL cells. BCR stimulation was performed by incubating CLL cells with 10µg/ml $F(ab)_2$ IgM fragments or cultured in a plate that had been coated with 10µg/ml $F(ab)_2$ anti- IgM. Graphs showing **(i)** the percentage of apoptotic cells after 24 hrs (ns, p=0.8380, n=4); **(ii)** the percentage of serine and tyrosine pSTAT3 positive cells after 4 hours BCR stimulation (ns, p=0.5811, n=4) and **(iii)** the percentage of CD62L positive cells after 18 hours BCR stimulation (ns, p=0.5766, n=4) with soluble or immobilised IgM. Bars represent mean changes (± s.e.m).

5.3.9 Ruxolitinib and Ibrutinib inhibit BCR-induced expression of pSTAT3 and CD62L in CLL cells

We found that CLL cells upregulated tyrosine pSTAT3 and CD62L in response to BCR stimulation in patients with UM-IGVH (Figures 5.5 and 5.9). To determine whether this upregulation can be modulated using therapeutically relevant BCR signalling and JAK/STAT pathway inhibitors, we treated CLL cells with UM-IGVH with either Ibrutinib or Ruxolitinib for 1 hour prior to BCR stimulation. The upregulation of pSTAT3 can be completely abrogated by pre-treatment with Ruxolitinib ($p=0.0386$; Figure 5.13 (a)) and to a lesser but significant extent by Ibrutinib ($p=0.0251$; Figure 5.13 (b)). Increase in CD62L expression was also abrogated by pre-treatment with Ruxolitinib ($p=0.0031$; Figure 5.14 (a)) and Ibrutinib ($p=0.0141$; Figure 5.14 (b)).

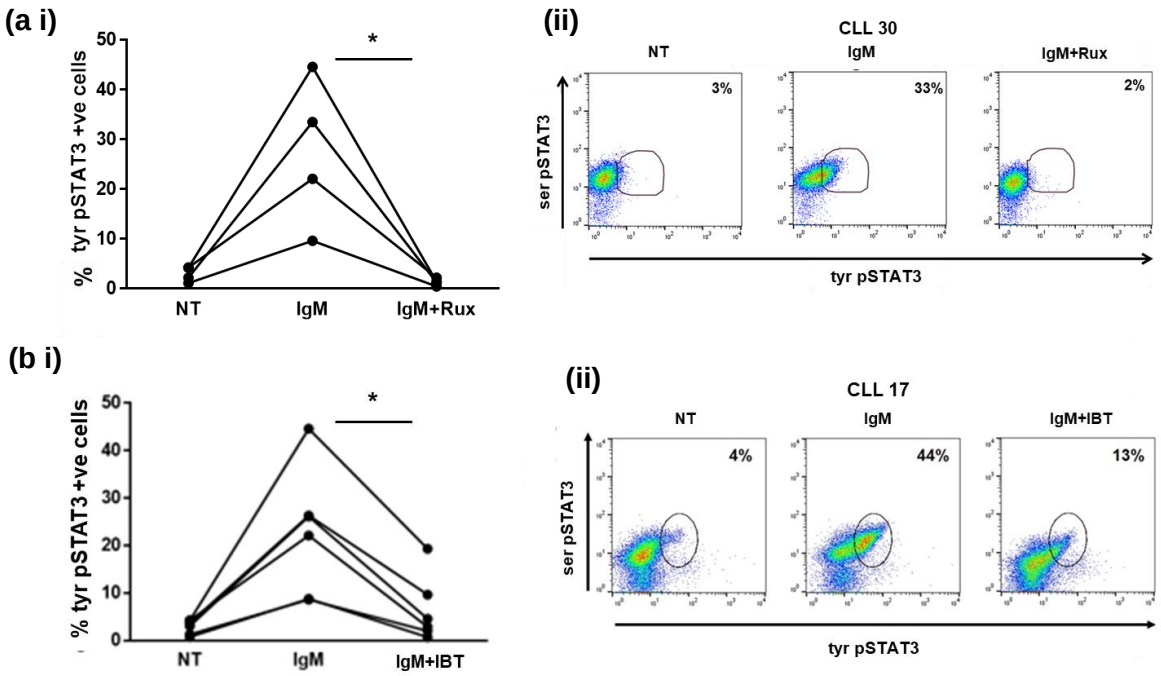

Figure 5. 13 Pre-treatment with Ruxolitinib and Ibrutinib downregulates BCR induced pSTAT3 expression. BCR stimulation was performed by incubating CLL cells with 10µg/ml $F(ab)_2$ anti-IgM fragments for 4 hours. **(a i)** the percentage of tyrosine (tyr) pSTAT3 positive CLL cells following BCR stimulation (IgM) and BCR stimulation following pre-treatment with 1µM Ruxolitinib (IgM +Rux) for 1 hours (IgM *vs* IgM+Rux, (* p=0.0386, n=4). **(ii)** Representative dotplots displaying the percentage of tyr pSTAT3 positive CLL cells following BCR stimulation (IgM) and BCR stimulation following pre-treatment with 1µM Ruxolitinib for 1 hour **(b i)** the percentage of tyrosine (tyr) pSTAT3 positive CLL cells following BCR stimulation (IgM) and BCR stimulation following pre-treatment with 10µM Ibrutinib (IgM +IBT) for 1 hours (IgM *vs* IgM+IBT; * p=0.0251, n=6) **(ii)** Representative dotplots displaying the percentage of tyr pSTAT3 positive CLL cells following BCR stimulation (IgM) and BCR stimulation following pre-treatment with 1µM Ibrutinib for 1 hour

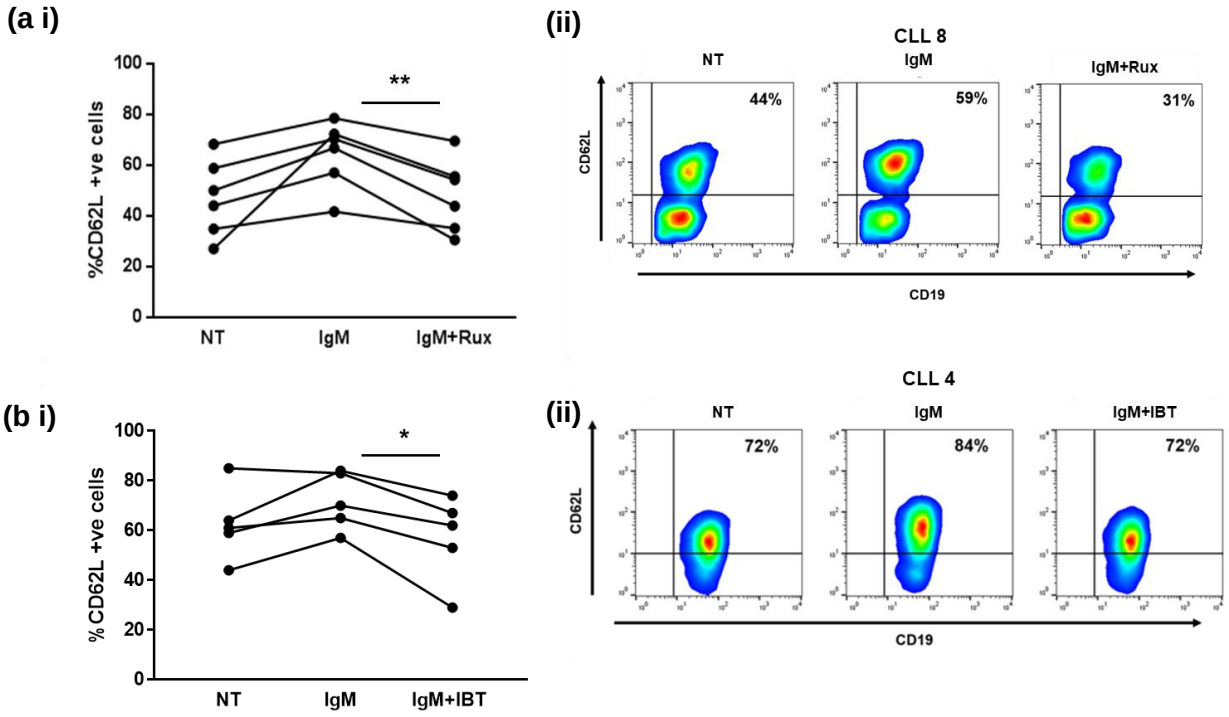

Figure 5. 14 Pre-treatment with Ruxolitinib and Ibrutinib downregulates BCR induced CD62L expression. BCR stimulation was performed by incubating CLL cells with 10µg/ml $F(ab)_2$ anti-IgM fragments for 18 hours. **(a i)** the percentage of CD62L positive CLL cells following BCR stimulation (IgM) and BCR stimulation following pre-treatment with 1µM Ruxolitinib (IgM+Rux) (IgM *vs* IgM+Rux, ** p=0.0031, n=6). **(ii)** Representative dotplots displaying the percentage of CD62L positive CLL cells following BCR stimulation (IgM) and BCR stimulation following pre-treatment with 1µM Ruxolitinib for 1 hour **(b i)** the percentage of CD62L positive CLL cells following BCR stimulation (IgM) and BCR stimulation following pre-treatment with 10µM Ibrutinib (IgM + IBT) (IgM *vs* IgM+IBT, (* p=0.0141; n=5) **(ii)** Representative dotplots displaying the percentage of CD62L positive cells CLL cells following pre-treatment with 10µM Ibrutinib for 1 hour

5.4 Discussion

It is clear the interactions of the CLL cell with the tumour microenvironment are key for CLL cell survival and proliferation, in particular within pseudo follicular proliferation centres in the lymph nodes and bone marrow. Understanding the signals involved in this microenvironmental cross talk will add to our knowledge of the pathogenesis and pathology of CLL. The aim of this chapter is to investigate the microenvironmental regulation of STAT3 activation and subsequent adhesion marker expression, in particular CD62L expression, in CLL.

Firstly, we studied the effect of two important interactions that occur in the protective microenvironments; contact of CLL cells with BMSC and signals received from accessory T cells. We found, that coculture on Hs5 BMSC resulted in induced tyrosine pSTAT3 and a contact-dependent, prosurvival effect in CLL cells. These observations are in agreement with previous studies (Lagneaux et al., 1998, Kurtova et al., 2009, Panayiotidis et al., 1996, Lu et al., 2015). We found that Ruxolitinib decreases both the prosurvival effect and tyrosine induced pSTAT3, suggesting that the activation of STAT3 is occurring through JAK. Ibrutinib, while inhibiting the prosurvival effect of Hs5 coculture, had no effect on pSTAT3, suggesting additional prosurvival pathways independent of STAT3 are activated by Hs5 BMSC. We found that Hs5 coculture resulted in an increase in CD62L. CD62L increase has been shown in cocultures with Hs5 BMSC, CD40L and CpG oligodeoxynucleotides (Purroy et al., 2015) but not Hs5 cells alone as we have shown. In chapter 4, we showed that STAT3 has a role in regulating CD62L and that CD62L may have a prosurvival role in CLL; therefore, these results may partially explain the prosurvival effect of HS5 coculture on CLL cells. We used CD40L and IL4 to mimic T cell signals in the lymph node microenvironment. We found both CD40L and IL4 were prosurvival which is in agreement with other studies (Bhattacharya et al., 2015, Grdisa, 2003). CD40L and IL-4 have been shown to induce proliferation in CLL cells (Plander et al., 2009)and IL4 is known to signal through JAK3-STAT6 (Steele et al., 2010, Bhattacharya et al., 2015), However, we found that CD40L and IL4 alone and in combination had no effect on the phosphorylation of STAT3 (Figure 5.8). Ahearne et al. (2013) showed tyrosine pSTAT3 induction after CD40L or IL4 with the addition of IL21 had a strong effect on STAT3 activation. They found that CD40L and IL4 primed CLL cells for IL21 induced proliferation and this was driven through STAT3. Interestingly, we found that CD40L and IL-4 reduced BCR stimulation-induced phosphorylation of STAT3 (Fig 5.8) which has not been shown previously, suggesting a complex interplay of prosurvival signalling pathways in CLL.

Herishanu et al. (2011) performed gene expression studies on CLL cells isolated from the lymph nodes and found the most upregulated genes in comparison to peripheral blood were gene signatures of the BCR signalling pathway. They also found BCR target gene expression was greater in CLL cells with UM-IGVH indicating the importance the BCR signalling pathway plays in microenvironmental cross-talk and disease progression. We found that BCR stimulation had a prosurvival effect that was independent of IGVH mutational status (Figure 5.4). In agreement with our results, Hoellenriegel et al (2011) and Bernal et al. (2001) show BCR stimulation results in a decrease in apoptosis but do not stratify patients based on IGVH mutational status. In contrast, Guarini et al (2008) found BCR stimulation resulted in protection from apoptosis in UM-IGVH patients and induction of apoptosis in M-IGVH patients, and Petlickovski et al (2005) found BCR stimulation induced apoptosis in both UM-IGVH and M-IGVH patients. Deglesne et al (2006) found that the type of IgM used dictated the response with soluble IgM resulting in an increase in apoptosis and immobilised IgM resulting in protection from spontaneous apoptosis. Discrepancies between studies have been postulated to be due to the type and source of IgM used and the time points chosen (Quiroga and Burger, 2010, Rombout et al., 2016). We showed that both soluble and immobilised IgM result in protection from spontaneous apoptosis in both UM- and M-IGVH subsets suggesting our model is not sensitive to the type of IgM used. We also show that the protection from apoptosis can be abrogated by pretreatment with both Ruxolitinib and Ibrutinib, suggesting multiple signalling pathways downstream of the BCR contribute to the prosurvival effect of BCR signalling. Our findings support the role of BCR stimulation in CLL cells as an important mediator of prosurvival signalling.

In this chapter, we demonstrated that BCR stimulation resulted in significantly increased activation of STAT3 through both serine and tyrosine phosphorylation in CLL cells with UM-IGVH compared to cells with M-IGVH. We also observed a non-significant upregulation of STAT3 regulated genes STAT3, BCL2 and MCL1 in CLL cells with UM-IGVH.

Our results indicate that pSTAT3 activation may play an important role in downstream effects of BCR stimulation as we showed BCR stimulation results in sustained activation of STAT3 for up to 18 hours. In a recent report, Rozovski et al. (2017b) have suggested this delayed and sustained activation of STAT3 is due to the requirement of NFkB to be transcriptionally activated. BCR stimulation activates NFkB, which upregulates the expression of IL6 and subsequent activation of the JAK2/STAT3 pathway.

We investigated the phosphorylation status of 43 kinases using the Proteome Profiler Phospho-Kinase Array (Figure 5.6) in a UM-IGVH CLL sample and saw greater than 2 fold increase in phosphorylation in known downstream effectors ERK and AKT after 15 minutes BCR stimulation. However, after 4 hours BCR stimulation, the most pronounced phosphorylation events were 15 fold and 27 fold increases in both serine and tyrosine pSTAT3 respectively, when the activation of ERK and AKT had returned to pre-stimulation levels. Interestingly, the phosphorylation of other STAT family proteins (STAT2, STAT5a/b and STAT6) was not upregulated after BCR stimulation. Rozovski et al (2013) have shown, using IgM washout experiments, that BCR stimulation induced tyrosine pSTAT3 resolves after 2 hours. They suggest this may explain why little tyrosine pSTAT3 is observed in circulating CLL cells from the peripheral blood, as these cells have been exposed to BCR stimulation in the lymph nodes and have recirculated to the peripheral blood where stimulation is no longer occurring. And, indeed, we showed in Chapter 3 (Figure 3.2) that only 6 out of 28 CLL patient samples exhibit detectable tyrosine phosphorylation of STAT3. Our results highlight the activation of STAT3, a known oncogene, as an important mediator of prolonged BCR activation in CLL. Interestingly, no mutations have been found in STAT3 in CLL (Couronne et al., 2013, Ohgami et al., 2014), which may be explained by lack of evolutionary pressure because of the prolonged activation of STAT3 by BCR stimulation in proliferation centres.

While BCR stimulation was shown by Rozovski et al (2014) to be mediated through JAK2, they did not investigate the IGVH mutational status of the CLL cells, nor did they investigate in detail the phosphorylation of serine pSTAT3. Here, we have shown that serine pSTAT3 is induced by BCR stimulation in patient samples with background serine pSTAT3 positive cells of <80%. Importantly, we show a much stronger induction of both tyrosine pSTAT3 and serine pSTAT3 in patients with UM-IGVH. We have also shown that JAK2 inhibitor, Ruxolitinib, completely abrogates BCR stimulation induced tyrosine pSTAT3 and that the BCR signalling pathway inhibitor, Ibrutinib, partially downregulates this BCR induced tyrosine pSTAT3.

Our findings agree with, and add to, multiple studies showing greater activation of the BCR signalling pathway following BCR stimulation in patient samples with UM-IGVH. Lanham et al. (2003) found that 80% of UM-IGVH CLL showed global increased tyrosine phosphorylation after BCR stimulation while only 20% of M-IGVH CLL responded. Herishanu et al (2011) showed a stronger upregulation of BCR target genes in UM-IGVH CLL compared to M-IGVH CLL. It has been shown that BCR stimulation induced gene expression changes in UM-IGVH CLL only (Guarini et al.,

2008) and Deglesne et al. (2006) showed that the survival response to BCR stimulation occurred in UM-IGVH ZAP 70 + cells.

However, some studies have reported little difference between BCR stimulation in patient samples with M-IGVH compared to those with UM-IGVH (Pede et al., 2013, Petlickovski et al., 2005). These contradicting results have been suggested to be due, in part, to differences in using soluble and immobilised forms of IgM. Immobilised IgM is thought to provide a sustained signal compared to the use of soluble IgM which can be internalised by the cells being stimulated (Rombout et al., 2016). Previous studies showing greater responses with immobilised IgM include Petlickovski et al (2005), who found that soluble IgM resulted in incomplete responses compared to immobilised IgM in both M-IGVH and UM-IGVH CLL. Rombout et al (2016) found no difference in the responsiveness of M-IGVH compared to U-IGVH CLL using either form of IgM; however, they found that immobilised IgM resulted in more robust, clearer changes in gene and protein expression compared to soluble anti-IgM. However, a number of studies, including some mentioned above, have shown strong induction of BCR stimulation using soluble IgM (Herishanu et al., 2011, Bernal et al., 2001, Quiroga et al., 2009). Because of these discrepancies in the literature, we compared BCR stimulation with immobilised and soluble IgM in our patient samples. We showed no significant difference in the effect of both types of IgM on cell survival, STAT3 activation or expression of CD62L. The response to BCR stimulation is not dependent on the type of IgM used, suggesting that our experimental model reflects physiologically relevant downstream BCR signalling events.

BCR stimulation resulted in variable induction of STAT3 activation within our cohort with UM-IGVH. It has been shown that CLL cell surface IgM (sIgM) expression and function is heterogeneous between patient samples and this can effect BCR stimulation. sIgM expression and function is higher in UM-IGVH CLL compared to M-IGVH CLL but has also been shown to be associated with NOTCH1 mutations in CLL (Mockridge et al., 2007). Two previous studies, one in normal B cells (Thomas et al., 2007) and one in Raji cells, a B cell lymphoma cell line (He et al., 2009), showed that NOTCH1 can synergistically enhance BCR signalling. We investigated whether NOTCH1 mutational status may further stratify UM-IGVH CLL; however, we saw no difference in BCR stimulation induced activation of STAT3 between NOTCH1 mutated and NOTCH1 wild type patient samples with UM-IGVH. Although CLL cells in the peripheral blood and tissue compartments receive different microenvironmental cues, we found no difference in STAT3 activation after BCR stimulation in matched samples

from the peripheral blood and bone marrow of the same patient. However, we found that BCR stimulation induced STAT3 phosphorylation was modulated by treatment with IL4 and CD40L, mimicking T cell signalling. It has been shown that IL4 can restore the expression of IgM on the CLL cell surface (Guo et al., 2016) so this finding is worth further investigation.

Our data and others suggest CD62L expression is dynamic and is influenced by microenvironmental signals and this may have implications in the trafficking of CLL cells. We showed that BMSC coculture can increase CD62L expression and it has been shown that fluid shear force (Walsby et al., 2014) and cytokine treatment (IL-4, IFN-α and IFN-γ) can increase the expression of CD62L (Jewell and Yong, 1997). Here, we showed that BCR stimulation increases CD62L expression in CLL cells which is in agreement with (Quiroga et al., 2009). In addition, we found a significantly greater increase in CD62L expression occurred in patient samples with UM-IGVH compared to M-IGVH. In contrast, it has also been reported that CD62L is down-regulated by B-cell receptor stimulation and that this downregulation is associated with progressive disease (Vlad et al., 2009). Their results showed concomitant down regulation of CXCR4, and a reduction in the CLL cell migration to CXCL12 and adhesion to endothelial cells. However, another study by Quiroga et al (2009) showed BCR stimulation resulted in an increased adhesive phenotype and migration towards CXL12 (Quiroga et al., 2009, Quiroga and Burger, 2010). Differing protocols including length of stimulation (48 hours) and type of IgM (Immobilised) was postulated to partially account for the differing results (Quiroga and Burger, 2010). While Vlad et al. showed that soluble IgM had no effect on CXCR4; they showed no data for the effect of soluble IgM on CD62L expression. We investigated both soluble and immobilised IgM to investigate if this contributed to the discrepancies in results and found both types increased CD62L expression. In addition, we found that BCR stimulation increased phosphorylation of STAT3 and subsequent upregulation of CD62L expression and these effects were significantly greater in patient samples with UM-IGVH compared to samples with M-IGVH. In chapter 4 we demonstrated a mechanism for the regulation of CD62L expression through STAT3, and here, for the first time, we suggest a mechanism for BCR stimulation-mediated upregulation of CD62L via phosphorylation and activation of STAT3. Burgess et al (2013) found a significantly higher level of CD62L expression on CD20 positive cells in both the lymph node and bone marrow niches from CLL patients. They also compared CD62L expression on cells from the peripheral blood and bone marrow and found cells from the bone marrow expressed higher levels of CD62L (Burgess et al., 2013). Purroy et al. (2015) showed an upregulation in CD62L

expression on proliferating CLL cells in a system mimicking the proliferative centres of the microenvironment using BMSC, CD40 ligand and CpG oligodeoxynucleotides. In addition to this Lafouresse et al showed that cells from patients with bulky lymph nodes had a higher expression of CD62L (Lafouresse et al., 2015). Given the high expression of CD62L in the lymph node and bone marrow of CLL patients compared to samples with no lymph node involvement (Burgess et al., 2013), this suggests CD62L may have an important role in these niches and interfering with its expression may be beneficial therapeutically. Our results show that treatment with Ruxolitinib and Ibrutinib downregulate BCR stimulation induced CD62L expression and this may contribute, in part, to the mechanism of lymphocytosis seen in patients treated with these inhibitors. Further investigation in a larger patient cohort is required to determine whether interfering with this STAT3 mediated upregulation of CD62L may be more beneficial in patients with UM-IGVH.

We performed a preliminary study to investigate BCR stimulation on 92 genes involved in adhesion and migration using a TaqMan Extracellular matrix and adhesion molecule array in CLL cells from one patient with UM-IGVH. We then pre-treated with Ruxolitinib to determine if any on these induced changes occurred through the JAK2/STAT3 pathway. The array revealed >2 fold up or downregulation in 19 genes after BCR stimulation, 3 of which we investigated further in a cohort of 10 patient samples: COL4A2, THBS1 and VCAN. We found variable responses; however, COL4A2 increased greater than 2 fold in 7/10 patients. THBS1 decreased greater than 2 fold in 4/10 patients and VCAN decreased by greater than 2 fold in 7/10 patients. COL4A2 encodes the α2 subunit of type IV collagen and forms part of the basement membrane. COL4A2 downregulation has been shown to be associated with disease progression in CLL (Fernandez et al., 2008).

Downregulation of COL4A2 in breast cancer cells promoted the invasion and migration of MCF7 cells (Wang et al., 2012). THBS1 is an adhesive glycoprotein that facilitates cell-cell and cell-matrix interactions (Liao et al., 2015). Its expression is upregulated in CLL compared to normal B cells and contact of CLL cells with stromal cells resulted in an upregulation of THBS1 in CLL cells (Maffei et al., 2012). THBS1 expression promoted the migration and invasion of oral squamous cell carcinoma cells (Pal et al., 2016). Versican is able to regulate apoptosis, adhesion, migration and invasion via the highly negatively-charged chondroitin/dermatan sulfate side chains and by interactions of the G1 and G3 domains with other proteins. Overexpression of VCAN in CLL has been associated with good prognosis (Shukla A, 2013). Overexpression of VCAN in lymphoid cell lines was shown to increase their capacity to migrate and also increased

their sensitivity to treatment with gemcitabine and doxorubicin (Fujii et al., 2015) . Further investigations are required to assess the expression of these genes at a protein level and the role they have in BCR stimulation in CLL. As BCR stimulation activates a number of transcription factors, we used pretreatment with Ruxolitinib to determine if any changes in gene expression may be regulated through the JAK2/STAT3 pathway. Ruxolitinib pretreatment reduced these BCR induced changes in THBS1 and VCAN, suggesting a role for JAK2/STAT3 pathway in their regulation; however, this requires further investigation.

In conclusion, our results indicate that STAT3 phosphorylation on both serine and tyrosine residues is an important mediator of BCR stimulation in CLL cells. We found increased phosphorylation of STAT3 in poor prognostic UM-IGVH when compared to M-IGVH CLL cells. In addition to this BCR stimulation resulted in an upregulation of CD62L gene and protein expression in CLL cells. Our results from chapter 4 suggested a role for STAT3 in the regulation of CD62L and, here, we suggest a mechanism of CD62L upregulation following an increase in STAT3 phosphorylation after BCR stimulation, particularly so in CLL cells with UM-IGVH. Pretreatment with Ruxolitinib and to some extent Ibrutinib abrogates both BCR induced pSTAT3 and CD62L expression in CLL cells, suggesting novel therapeutic options to target the tumour microenvironment in CLL.

Chapter 6

General Discussion

The treatment options for chronic lymphocytic leukaemia patients with relapsed or unfavourable prognostic markers have greatly improved over the past few years. The introduction of two novel targeted therapeutics, the kinase inhibitors, Ibrutinib and Idelalisib, targeting the BCR signalling pathway has transformed treatment of patients with relapsed CLL. Prior to the development of these targeted agents, patients with relapsed disease, following chemoimmunotherapy or single agent immunotherapy, had a very poor prognosis and outcome. Despite the efficacy of these novel therapies, some patients fail to respond and others have inferior responses due to aggressive disease as a result of presence of poor prognostic indicators such as TP53 abnormalities (Farooqui et al. (2015), and others do not tolerate these treatments. In addition, resistance to Ibrutinib is already emerging leading to relapse (Woyach et al., 2017, Ahn et al., 2017). Resistance to Idelalisib in CLL has not yet been described in patients, although resistance in B-cell lymphoma cell lines has been shown (Iyengar et al., 2013, Yahiaoui et al., 2017). These inhibitors also carry a high economic burden in cost alone and amplified by the fact they are not a cure and most patients require the inhibitors over long periods. Therefore it is important to find alternative therapies for poor prognostic patient groups and non-responders that in addition may reduce the economic burden associated with these treatments.

This thesis aimed to investigate the role of STAT3 in the pathobiology of CLL and determine potential new therapeutic avenues for investigation in CLL. STAT3 is a transcription factor that is activated in response to cytokines, forms hetero and homo-dimers and regulates the transcription of genes involved in cell cycle, apoptosis, migration and angiogenesis. STAT3 expression levels and activation varies in non-malignant cell and tissue types, but is constitutively activated in a number of cancers and contributes to oncogenesis (Alas and Bonavida, 2003, Garcia et al., 1997). In addition, STAT3 can also have tumour suppressor effects depending on cell type and conditions (Couto et al., 2012). Interestingly, we found treatments with two unrelated STAT3 targeting agents, Cucurbitacin and S3I, have a divergent effect on CLL cells, with a toxic effect in some patient samples and a protective effect is others. A dual role for STAT3 as an oncogene and tumour suppressor has been suggested in CLL (Rozovski et al., 2016) and our results support STAT3 having both pro-survival and tumour suppressor roles in CLL. It has also been postulated by Sellier et al. (2013) that different post-translational modifications of STAT3 may alter its oncogenic or tumour suppressor functions. We found that in CLL cells where Cucurbitacin and S3I treatment resulted in toxicity, we also saw a decrease in serine pSTAT3. We also found

Cucurbitacin was more toxic in CD38 positive patient samples, a poor prognostic factor for CLL. Although Cucurbitacin and S3I have been shown to inhibit STAT3 activity, their mechanisms of action are not clear and they may have off-target effects. Indeed, we have shown that treatment with Cucurbitacin results in aggregation of STAT3 and actin in CLL cells. However, given the divergent effects of these agents in CLL patient samples, the potential of STAT3 as a target to induce cytotoxicity in CLL cells is unclear.

The microenvironment has emerged as a therapeutic target in CLL. In this thesis, we identified STAT3 as a mediator of a number of important microenvironmental signals in CLL cells, such as interaction with BMSCs and BCR stimulation. CD62L has been shown to be a key molecule in the initial step of the migration of CLL cells to the lymph nodes via the HEVs (Lafouresse et al., 2015). Here, for the first time, we describe STAT3 mediated regulation of CD62L expression in CLL cells. We showed that targeting STAT3 pharmacologically and by siRNA knockdown results in downregulation of CD62L.

We showed that targeting CD62L with a blocking antibody and treatment with Cucurbitacin resulted in a decrease in the adhesion of CLL cells to endothelial cells under fluid shear flow conditions. Blocking these interactions between CD62L and its ligands may represent a therapeutic strategy for the redistribution of CLL cells from the protective environment of the lymph nodes to the peripheral blood. Lafouresse et al (2015) showed a CD62L blocking antibody stopped the dissemination of human CLL cells in mice through reduced the rolling and adhesion in the HEVs.

In the lymph node and bone marrow microenvironments, the BCR signalling pathway is one of the most prominently activated pathways in CLL cross talk with their microenvironment (Herishanu et al., 2011). We found that STAT3 appears to be an important downstream mediator of BCR signalling in CLL cells, particularly in UM-IGVH CLL patient samples. Activating STAT3 mutations occur at a low frequency, if at all, in CLL; however we show STAT3 activation is prolonged and sustained by BCR signalling. Our data suggests CD62L is regulated through STAT3 and in addition, BCR stimulation results in both the activation of STAT3 and the upregulation of CD62L cell surface expression. We also found that BCR stimulation resulted in the upregulation of CD62L gene expression in CLL cells with UM-IGVH. There are 5 putative STAT3 binding sites in the CD62L promoter and this suggests a mechanism of STAT3 in regulating CD62L expression may be transcriptional. Genes that we saw upregulated

after BCR signalling such as Mcl-1 and Bcl-2 are also potential NFκB targets so, further ChiPSeq experiments are needed to determine if STAT3 is binding directly to the CD62L promoter. In addition to the upregulation of CD62L gene expression, we also identified changes in a number of other genes, 8 genes were significantly upregulated and 11 genes significantly downregulated after BCR stimulation. These genes are involved in adhesion and migration of cells and present opportunities for further investigation of the trafficking of CLL cells.

The role of STAT3 in regulation CD62L expression suggests therapeutic potential for CLL. *In vivo* inhibition of STAT3 in mice and humans results in moderate side effects in non-malignant differentiated tissues, suggesting potential of this approach (Park et al., 2014, Sen et al., 2012). However, the development of inhibitors to directly target STAT3 has proved challenging. In addition, STAT3 is involved in important regular processes, such as prevention of obesity (Ma et al., 2014, Buettner et al., 2006) and protecting against cardiac (Jacoby et al., 2003) and liver damage (Taub, 2003). An alternative method for targeting STAT3 is inhibition of upstream JAK2 using the inhibitor Ruxolitinib. We showed that Ruxolitinib has no effect on the viability of CLL cells, unlike Cucurbitacin and S3I which had either cytotoxic or pro-survival activity. However, we show Ruxolitinib potently inhibits microenvironmental mediated STAT3 activation. In addition, we showed that the BCR signalling inhibitor
Ibrutinib targeted BCR induced activation of STAT3 and found that both Ruxolitinib and Ibrutinib could decrease BCR induced CD62L expression. Lafouresse et al (2015) found that CLL cells from patients treated with the BCR inhibitor, Idelalisib had a reduction in the expression of CD62L. Ruxolitinib has been shown to control CLL symptoms, reducing fatigue and other disease-related symptoms (Jain et al., 2017). This study also reported an increase, followed by a decrease below the baseline in WBC numbers, suggesting a decrease in tumour burden. Ruxolitinib has been recently investigated in a clinical trial for CLL (Spaner et al., 2016). Interestingly, a profound and prolonged lymphocytosis was seen with decreased lymphadenopathy in patients, as well a decrease in the expression of tyrosine pSTAT3 and pSTAT5. Although, CD62L was not examined, it supports our findings of a key role for STAT3 activation regulating trafficking of CLL cells following BCR stimulation.

Our study suggests CD62L may be a potential therapeutic target for CLL due to its roles in CLL cell survival and trafficking. Therapeutics targeting the selectin family, including CD62L have been investigated in a number of immune disorders including psoriasis (Bock et al., 2006, Friedrich et al., 2006), asthma (Romano, 2005), and

arthritis (Sfikakis and Mavrikakis, 1999). Although selectins are involved in the trafficking of normal immune cells , pan-selectin and targeted L-, P- and E- selectin inhibitors have all shown to be well tolerated in clinical trials (Schmitt et al., 2015) (Telen et al., 2015). A monoclonal anti-L-selectin antibody, aselizumab has been used in humans and showed no cytotoxicity (Seekamp et al., 2004).

We found BCR stimulation resulted in a robust statistically significant increase in pSTAT3 and CD62L We also found that inhibiting STAT3 had a functional effect on chemotaxis and adhesion under shear flow. For these functional assays however a smaller sample size was a limitation for the conclusions that can be drawn from this data. Additional experiments to increase sample size would allow us to elucidate clearly, the effect of STAT3 inhibition on these processes.

Our results may have implications in extending the reach of BCR signalling inhibitors using Ruxolitinib, monoclonal antibodies targeting CD62L or pan selectin inhibitors, and an area of future study is to identify potential synergies between BCR inhibitors and these agents. Due to the emergence of clonal evolution and resistance, new avenues for further treatment options are needed and a number of combination studies using BCR inhibitors, Ibrutinib and Idelalisib, in combinations with BCL-2 inhibitor Venetoclax (Aw and Brown, 2017), and immunomodulatory drug Lenalidomide (Pollyea, 2014) and Rituximab (Burger et al., 2014) (Furman et al., 2014) are currently ongoing in an attempt to prevent resistance emerging and target poor prognostic subsets, such as patients harbouring TP53 deletion/mutations. Further investigation is required to assess if Ruxolitinib may be useful in poorer prognostic patients to combat resistance and prevent relapse. A clinical trial with Ruxolitinib in combination with Ibrutinib is currently ongoing and results are due in 2018 (NCT02912754). Future studies to investigate a pan-selectin inhibitor in combination with BCR inhibitors would also be of interest in CLL.

This work highlights the importance of a well annotated bioresource of patient samples. We collaborated with St James's Hospital clinical services to detail a range of prognostic markers in the patient cohort. The identification of markers to stratify patients who may have a greater response to certain treatments, and treatments to improve outcomes of poorer prognostic patients are required. In particular, in this thesis we assessed NOTCH1 mutations in the patient sample cohort. This further characterises our patient samples and makes them valuable for future translational studies.

In conclusion this thesis suggests a novel mechanism for the regulation of key adhesion molecule CD62L in CLL cells (Figure 6.1). Pharmacological targeting of STAT3 and siRNA knockdown downregulated CD62L expression. CD62L is critical for CLL cell migration to the lymph node and blocking CD62L decreased the adhesion of CLL cells to HUVECs under shear flow. We propose a mechanism for the upregulation of CD62L in response to BCR signalling through the phosphorylation and activation of STAT3. This may represent a prosurvival mechanism in CLL cells as well as facilitating continuing CLL cell trafficking. BCR inhibitor Ibrutinib and JAK2/STAT3 inhibitor Ruxolitinib abrogated the upregulation of CD62L expression and these results open future avenues for therapeutic intervention in CLL using combinations of BCR inhibitors, Ibrutinib and Idelalisib in combination with Ruxolitinib or selectin inhibitors.

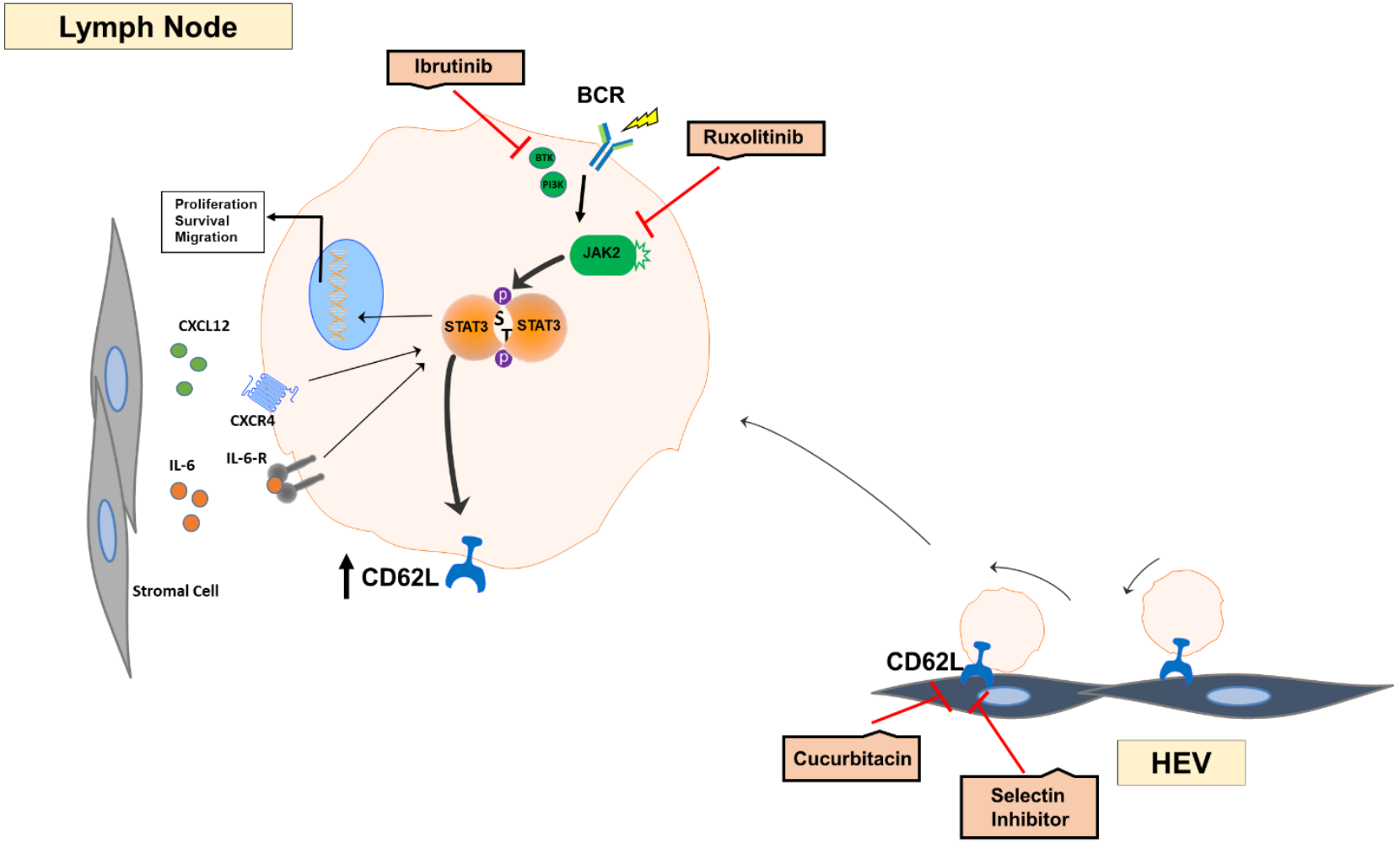

Figure 6. 1 Proposed mechanism of CD62L regulation by STAT3 in CLL cells. BCR stimulation results in the activation of JAK2 which increases bith serine and tyrosine phosphorylation of STAT3. Activation of STAT3 results in the upregulation of CD62L, a molecule used by CLL cells to migrate to the protective microenvironment of the lymph node through the High endothelial venules (HEV). Mechanisms for interfering with the expression of CD62L are shown in red boxes. BCR inhibitor, Ibrutinib and JAK2/STAT3 inhibitor Ruxolitinib inhibited BCR mediated STAT3 phosphorylation and CD62L expression. Selectin inhibitors, such as an anti-CD62L antibody may be used to inhibit the rolling and adhesion of CLL cells to the HEV, preventing dissemination of the disease.

References

AGATHANGELIDIS, A., DARZENTAS, N., HADZIDIMITRIOU, A., BROCHET, X., MURRAY, F., YAN, X. J., DAVIS, Z., VAN GASTEL-MOL, E. J., TRESOLDI, C., CHU, C. C., CAHILL, N., GIUDICELLI, V., TICHY, B., PEDERSEN, L. B., FORONI, L., BONELLO, L., JANUS, A., SMEDBY, K., ANAGNOSTOPOULOS, A., MERLE-BERAL, H., LAOUTARIS, N., JULIUSSON, G., DI CELLE, P. F., POSPISILOVA, S., JURLANDER, J., GEISLER, C., TSAFTARIS, A., LEFRANC, M. P., LANGERAK, A. W., OSCIER, D. G., CHIORAZZI, N., BELESSI, C., DAVI, F., ROSENQUIST, R., GHIA, P. & STAMATOPOULOS, K. 2012. Stereotyped B-cell receptors in one-third of chronic lymphocytic leukemia: a molecular classification with implications for targeted therapies. *Blood,* 119**,** 4467-75.

AGGARWAL, B. B. & SHISHODIA, S. 2006. Molecular targets of dietary agents for prevention and therapy of cancer. *Biochem Pharmacol,* 71**,** 1397-421.

AGUILAR-HERNANDEZ, M. M., BLUNT, M. D., DOBSON, R., YEOMANS, A., THIRDBOROUGH, S., LARRAYOZ, M., SMITH, L. D., LINLEY, A., STREFFORD, J. C., DAVIES, A., JOHNSON, P. M., SAVELYEVA, N., CRAGG, M. S., FORCONI, F., PACKHAM, G., STEVENSON, F. K. & STEELE, A. J. 2016. IL-4 enhances expression and function of surface IgM in CLL cells. *Blood,* 127**,** 3015-25.

AHEARNE, M. J., WILLIMOTT, S., PINON, L., KENNEDY, D. B., MIALL, F., DYER, M. J. & WAGNER, S. D. 2013. Enhancement of CD154/IL4 proliferation by the T follicular helper (Tfh) cytokine, IL21 and increased numbers of circulating cells resembling Tfh cells in chronic lymphocytic leukaemia. *Br J Haematol,* 162**,** 360-70.

AHN, I. E., UNDERBAYEV, C., ALBITAR, A., HERMAN, S. E., TIAN, X., MARIC, I., ARTHUR, D. C., WAKE, L., PITTALUGA, S., YUAN, C. M., STETLER-STEVENSON, M., SOTO, S., VALDEZ, J., NIERMAN, P., LOTTER, J., XI, L., RAFFELD, M., FAROOQUI, M., ALBITAR, M. & WIESTNER, A. 2017. Clonal evolution leading to ibrutinib resistance in chronic lymphocytic leukemia. *Blood,* 129**,** 1469-1479.

AKIRA, S., NISHIO, Y., INOUE, M., WANG, X. J., WEI, S., MATSUSAKA, T., YOSHIDA, K., SUDO, T., NARUTO, M. & KISHIMOTO, T. 1994. Molecular cloning of APRF, a novel IFN-stimulated gene factor 3 p91-related transcription factor involved in the gp130-mediated signaling pathway. *Cell,* 77**,** 63-71.

ALAPAT, D., COVIELLO-MALLE, J., OWENS, R., QU, P., BARLOGIE, B., SHAUGHNESSY, J. D. & LORSBACH, R. B. 2012. Diagnostic usefulness and prognostic impact of CD200 expression in lymphoid malignancies and plasma cell myeloma. *Am J Clin Pathol,* 137**,** 93-100.

ALAS, S. & BONAVIDA, B. 2003. Inhibition of constitutive STAT3 activity sensitizes resistant non-Hodgkin's lymphoma and multiple myeloma to chemotherapeutic drug-mediated apoptosis. *Clin Cancer Res,* 9**,** 316-26.

ALLEN, C. D., ANSEL, K. M., LOW, C., LESLEY, R., TAMAMURA, H., FUJII, N. & CYSTER, J. G. 2004. Germinal center dark and light zone organization is mediated by CXCR4 and CXCR5. *Nat Immunol,* 5**,** 943-52.

ALLEN, J. C., TALAB, F., ZUZEL, M., LIN, K. & SLUPSKY, J. R. 2011. c-Abl regulates Mcl-1 gene expression in chronic lymphocytic leukemia cells. *Blood,* 117**,** 2414-22.

AMREIN, P. C., ATTAR, E. C., TAKVORIAN, T., HOCHBERG, E. P., BALLEN, K. K., LEAHY, K. M., FISHER, D. C., LACASCE, A. S., JACOBSEN, E. D., ARMAND, P., HASSERJIAN, R. P., WERNER, L., NEUBERG, D. & BROWN, J. R. 2011. Phase II study of dasatinib in relapsed or refractory chronic lymphocytic leukemia. *Clin Cancer Res,* 17**,** 2977-86.

ANTONY, P., PETRO, J. B., CARLESSO, G., SHINNERS, N. P., LOWE, J. & KHAN, W. N. 2003. B cell receptor directs the activation of NFAT and NF-kappaB via distinct molecular mechanisms. *Exp Cell Res,* 291**,** 11-24.

AOUDJIT, F. & VUORI, K. 2012. Integrin signaling in cancer cell survival and chemoresistance. *Chemother Res Pract,* 2012**,** 283181.

ARBER, D. A., ORAZI, A., HASSERJIAN, R., THIELE, J., BOROWITZ, M. J., LE BEAU, M. M., BLOOMFIELD, C. D., CAZZOLA, M. & VARDIMAN, J. W. 2016. The 2016 revision to the World Health Organization classification of myeloid neoplasms and acute leukemia. *Blood,* 127**,** 2391-405.

ARBONES, M. L., ORD, D. C., LEY, K., RATECH, H., MAYNARD-CURRY, C., OTTEN, G., CAPON, D. J. & TEDDER, T. F. 1994. Lymphocyte homing and leukocyte rolling and migration are impaired in L-selectin-deficient mice. *Immunity,* 1**,** 247-60.

ARORA, S., SINGH, S., PIAZZA, G. A., CONTRERAS, C. M., PANYAM, J. & SINGH, A. P. 2012. Honokiol: a novel natural agent for cancer prevention and therapy. *Curr Mol Med,* 12**,** 1244-52.

AUDRITO, V., VAISITTI, T., SERRA, S., BOLOGNA, C., BRUSA, D., MALAVASI, F. & DEAGLIO, S. 2013. Targeting the microenvironment in chronic lymphocytic leukemia offers novel therapeutic options. *Cancer Lett,* 328**,** 27-35.

AW, A. & BROWN, J. R. 2017. The potential combination of BCL-2 inhibitors and ibrutinib as frontline therapy in chronic lymphocytic leukemia. *Leuk Lymphoma***,** 1-11.

AYYAD, S. E., ABDEL-LATEFF, A., ALARIF, W. M., PATACCHIOLI, F. R., BADRIA, F. A. & EZMIRLY, S. T. 2012. In vitro and in vivo study of cucurbitacins-type triterpene glucoside from Citrullus colocynthis growing in Saudi Arabia against hepatocellular carcinoma. *Environ Toxicol Pharmacol,* 33**,** 245-51.

AZARE, J., LESLIE, K., AL-AHMADIE, H., GERALD, W., WEINREB, P. H., VIOLETTE, S. M. & BROMBERG, J. 2007. Constitutively activated Stat3 induces tumorigenesis and enhances cell motility of prostate epithelial cells through integrin beta 6. *Mol Cell Biol,* 27**,** 4444-53.

BAAN, R., GROSSE, Y., STRAIF, K., SECRETAN, B., EL GHISSASSI, F., BOUVARD, V., BENBRAHIM-TALLAA, L., GUHA, N., FREEMAN, C., GALICHET, L., COGLIANO, V. & GROUP, W. H. O. I. A. F. R. O. C. M. W. 2009. A review of human carcinogens--Part F: chemical agents and related occupations. *Lancet Oncol,* 10**,** 1143-4.

BADOUX, X., BUESO-RAMOS, C., HARRIS, D., LI, P., LIU, Z., BURGER, J., O'BRIEN, S., FERRAJOLI, A., KEATING, M. J. & ESTROV, Z. 2011. Cross-talk between chronic lymphocytic leukemia cells and bone marrow endothelial cells: role of signal transducer and activator of transcription 3. *Hum Pathol,* 42**,** 1989-2000.

BAERISWYL, V. & CHRISTOFORI, G. 2009. The angiogenic switch in carcinogenesis. *Semin Cancer Biol,* 19**,** 329-37.

BAGNARA, D., KAUFMAN, M. S., CALISSANO, C., MARSILIO, S., PATTEN, P. E., SIMONE, R., CHUM, P., YAN, X. J., ALLEN, S. L., KOLITZ, J. E., BASKAR, S., RADER, C., MELLSTEDT, H., RABBANI, H., LEE, A., GREGERSEN, P. K., RAI, K. R. & CHIORAZZI, N. 2011. A novel adoptive transfer model of chronic lymphocytic leukemia suggests a key role for T lymphocytes in the disease. *Blood,* 117**,** 5463-72.

BAJENOFF, M., EGEN, J. G., KOO, L. Y., LAUGIER, J. P., BRAU, F., GLAICHENHAUS, N. & GERMAIN, R. N. 2006. Stromal cell networks regulate lymphocyte entry, migration, and territoriality in lymph nodes. *Immunity,* 25**,** 989-1001.

BALIAKAS, P., AGATHANGELIDIS, A., HADZIDIMITRIOU, A., SUTTON, L. A., MINGA, E., TSANOUSA, A., SCARFO, L., DAVIS, Z., YAN, X. J., SHANAFELT, T., PLEVOVA, K., SANDBERG, Y., VOJDEMAN, F. J., BOUDJOGRA, M.,

TZENOU, T., CHATZOULI, M., CHU, C. C., VERONESE, S., GARDINER, A., MANSOURI, L., SMEDBY, K. E., PEDERSEN, L. B., MORENO, D., VAN LOM, K., GIUDICELLI, V., FRANCOVA, H. S., NGUYEN-KHAC, F., PANAGIOTIDIS, P., JULIUSSON, G., ANGELIS, L., ANAGNOSTOPOULOS, A., LEFRANC, M. P., FACCO, M., TRENTIN, L., CATHERWOOD, M., MONTILLO, M., GEISLER, C. H., LANGERAK, A. W., POSPISILOVA, S., CHIORAZZI, N., OSCIER, D., JELINEK, D. F., DARZENTAS, N., BELESSI, C., DAVI, F., GHIA, P., ROSENQUIST, R. & STAMATOPOULOS, K. 2015a. Not all IGHV3-21 chronic lymphocytic leukemias are equal: prognostic considerations. *Blood,* 125**,** 856-9.

BALIAKAS, P., HADZIDIMITRIOU, A., SUTTON, L. A., ROSSI, D., MINGA, E., VILLAMOR, N., LARRAYOZ, M., KMINKOVA, J., AGATHANGELIDIS, A., DAVIS, Z., TAUSCH, E., STALIKA, E., KANTOROVA, B., MANSOURI, L., SCARFO, L., CORTESE, D., NAVRKALOVA, V., ROSE-ZERILLI, M. J., SMEDBY, K. E., JULIUSSON, G., ANAGNOSTOPOULOS, A., MAKRIS, A. M., NAVARRO, A., DELGADO, J., OSCIER, D., BELESSI, C., STILGENBAUER, S., GHIA, P., POSPISILOVA, S., GAIDANO, G., CAMPO, E., STREFFORD, J. C., STAMATOPOULOS, K., ROSENQUIST, R. & EUROPEAN RESEARCH INITIATIVE ON, C. L. L. 2015b. Recurrent mutations refine prognosis in chronic lymphocytic leukemia. *Leukemia,* 29**,** 329-36.

BALL, D. P., LEWIS, A. M., WILLIAMS, D., RESETCA, D., WILSON, D. J. & GUNNING, P. T. 2016. Signal transducer and activator of transcription 3 (STAT3) inhibitor, S3I-201, acts as a potent and non-selective alkylating agent. *Oncotarget,* 7**,** 20669-79.

BAR-NATAN, M., NELSON, E. A., XIANG, M. & FRANK, D. A. 2012. STAT signaling in the pathogenesis and treatment of myeloid malignancies. *JAKSTAT,* 1**,** 55-64.

BAUDOT, A. D., JEANDEL, P. Y., MOUSKA, X., MAURER, U., TARTARE-DECKERT, S., RAYNAUD, S. D., CASSUTO, J. P., TICCHIONI, M. & DECKERT, M. 2009. The tyrosine kinase Syk regulates the survival of chronic lymphocytic leukemia B cells through PKCdelta and proteasome-dependent regulation of Mcl-1 expression. *Oncogene,* 28**,** 3261-73.

BAUMHETER, S., SINGER, M. S., HENZEL, W., HEMMERICH, S., RENZ, M., ROSEN, S. D. & LASKY, L. A. 1993. Binding of L-selectin to the vascular sialomucin CD34. *Science,* 262**,** 436-8.

BAZERBASHI, M. B., REEVE, J. & CHANARIN, I. 1978. Studies in chronic lymphocytic leukaemia. The kinetics of 51Cr-labelled lymphocytes. *Scand J Haematol,* 20**,** 37-51.

BENEKLI, M., XIA, Z., DONOHUE, K. A., FORD, L. A., PIXLEY, L. A., BAER, M. R., BAUMANN, H. & WETZLER, M. 2002. Constitutive activity of signal transducer and activator of transcription 3 protein in acute myeloid leukemia blasts is associated with short disease-free survival. *Blood,* 99**,** 252-257.

BENKISSER-PETERSEN, M., BUCHNER, M., DORFFEL, A., DUHREN-VON-MINDEN, M., CLAUS, R., KLASENER, K., LEBERECHT, K., BURGER, M., DIERKS, C., JUMAA, H., MALAVASI, F., RETH, M., VEELKEN, H., DUYSTER, J. & ZIRLIK, K. 2016. Spleen Tyrosine Kinase Is Involved in the CD38 Signal Transduction Pathway in Chronic Lymphocytic Leukemia. *PLoS One,* 11**,** e0169159.

BERG, E. L., MCEVOY, L. M., BERLIN, C., BARGATZE, R. F. & BUTCHER, E. C. 1993. L-selectin-mediated lymphocyte rolling on MAdCAM-1. *Nature,* 366**,** 695-8.

BERGLOF, A., HAMASY, A., MEINKE, S., PALMA, M., KRSTIC, A., MANSSON, R., KIMBY, E., OSTERBORG, A. & SMITH, C. I. 2015. Targets for Ibrutinib Beyond B Cell Malignancies. *Scand J Immunol,* 82**,** 208-17.

BERLIN-RUFENACH, C., OTTO, F., MATHIES, M., WESTERMANN, J., OWEN, M. J., HAMANN, A. & HOGG, N. 1999. Lymphocyte migration in lymphocyte function-associated antigen (LFA)-1-deficient mice. *J Exp Med,* 189**,** 1467-78.

BERNAL, A., PASTORE, R. D., ASGARY, Z., KELLER, S. A., CESARMAN, E., LIOU, H. C. & SCHATTNER, E. J. 2001. Survival of leukemic B cells promoted by engagement of the antigen receptor. *Blood,* 98**,** 3050-7.

BEYER, M., KOCHANEK, M., DARABI, K., POPOV, A., JENSEN, M., ENDL, E., KNOLLE, P. A., THOMAS, R. K., VON BERGWELT-BAILDON, M., DEBEY, S., HALLEK, M. & SCHULTZE, J. L. 2005. Reduced frequencies and suppressive function of CD4+CD25hi regulatory T cells in patients with chronic lymphocytic leukemia after therapy with fludarabine. *Blood,* 106**,** 2018-25.

BHATTACHARYA, N., REICHENZELLER, M., CAUDRON-HERGER, M., HAEBE, S., BRADY, N., DIENER, S., NOTHING, M., DOHNER, H., STILGENBAUER, S., RIPPE, K. & MERTENS, D. 2015. Loss of cooperativity of secreted CD40L and increased dose-response to IL4 on CLL cell viability correlates with enhanced activation of NF-kB and STAT6. *Int J Cancer,* 136**,** 65-73.

BILLADEAU, D. D. & LEIBSON, P. J. 2002. ITAMs versus ITIMs: striking a balance during cell regulation. *J Clin Invest,* 109**,** 161-8.

BINDER, M., MULLER, F., FRICK, M., WEHR, C., SIMON, F., LEISTLER, B., VEELKEN, H., MERTELSMANN, R. & TREPEL, M. 2013. CLL B-cell receptors can recognize themselves: alternative epitopes and structural clues for autostimulatory mechanisms in CLL. *Blood,* 121**,** 239-41.

BINET, J. L., AUQUIER, A., DIGHIERO, G., CHASTANG, C., PIGUET, H., GOASGUEN, J., VAUGIER, G., POTRON, G., COLONA, P., OBERLING, F., THOMAS, M., TCHERNIA, G., JACQUILLAT, C., BOIVIN, P., LESTY, C., DUAULT, M. T., MONCONDUIT, M., BELABBES, S. & GREMY, F. 1981. A new prognostic classification of chronic lymphocytic leukemia derived from a multivariate survival analysis. *Cancer,* 48**,** 198-206.

BINET, J. L., LEPORRIER, M., DIGHIERO, G., CHARRON, D., D'ATHIS, P., VAUGIER, G., BERAL, H. M., NATALI, J. C., RAPHAEL, M., NIZET, B. & FOLLEZOU, J. Y. 1977. A clinical staging system for chronic lymphocytic leukemia: prognostic significance. *Cancer,* 40**,** 855-64.

BJORNSON, A. B. & DETMERS, P. A. 1995. The pentameric structure of IgM is necessary to enhance opsonization of Bacteroides thetaiotaomicron and Bacteroides fragilis via the alternative complement pathway. *Microb Pathog,* 19**,** 117-28.

BLACKFORD, J., REID, H. W., PAPPIN, D. J., BOWERS, F. S. & WILKINSON, J. M. 1996. A monoclonal antibody, 3/22, to rabbit CD11c which induces homotypic T cell aggregation: evidence that ICAM-1 is a ligand for CD11c/CD18. *Eur J Immunol,* 26**,** 525-31.

BLASKOVICH, M. A., SUN, J., CANTOR, A., TURKSON, J., JOVE, R. & SEBTI, S. M. 2003. Discovery of JSI-124 (cucurbitacin I), a selective Janus kinase/signal transducer and activator of transcription 3 signaling pathway inhibitor with potent antitumor activity against human and murine cancer cells in mice. *Cancer Res,* 63**,** 1270-9.

BLEUL, C. C., FUHLBRIGGE, R. C., CASASNOVAS, J. M., AIUTI, A. & SPRINGER, T. A. 1996. A highly efficacious lymphocyte chemoattractant, stromal cell-derived factor 1 (SDF-1). *J Exp Med,* 184**,** 1101-9.

BOCK, D., PHILIPP, S. & WOLFF, G. 2006. Therapeutic potential of selectin antagonists in psoriasis. *Expert Opin Investig Drugs,* 15**,** 963-79.

BRACHTL, G., SAHAKYAN, K., DENK, U., GIRBL, T., ALINGER, B., HOFBAUER, S. W., NEUREITER, D., HOFBAUER, J. P., EGLE, A., GREIL, R. & HARTMANN, T. N. 2011. Differential bone marrow homing capacity of VLA-4 and CD38 high expressing chronic lymphocytic leukemia cells. *PLoS One,* 6**,** e23758.

BROMBERG, J. & DARNELL, J. E., JR. 2000. The role of STATs in transcriptional control and their impact on cellular function. *Oncogene,* 19**,** 2468-73.

BROWN, J. R., BYRD, J. C., COUTRE, S. E., BENSON, D. M., FLINN, I. W., WAGNER-JOHNSTON, N. D., SPURGEON, S. E., KAHL, B. S., BELLO, C.,

WEBB, H. K., JOHNSON, D. M., PETERMAN, S., LI, D., JAHN, T. M., LANNUTTI, B. J., ULRICH, R. G., YU, A. S., MILLER, L. L. & FURMAN, R. R. 2014. Idelalisib, an inhibitor of phosphatidylinositol 3-kinase p110delta, for relapsed/refractory chronic lymphocytic leukemia. *Blood,* 123**,** 3390-7.

BUCHNER, M., BAER, C., PRINZ, G., DIERKS, C., BURGER, M., ZENZ, T., STILGENBAUER, S., JUMAA, H., VEELKEN, H. & ZIRLIK, K. 2010a. Spleen tyrosine kinase inhibition prevents chemokine- and integrin-mediated stromal protective effects in chronic lymphocytic leukemia. *Blood,* 115**,** 4497-4506.

BUCHNER, M., BAER, C., PRINZ, G., DIERKS, C., BURGER, M., ZENZ, T., STILGENBAUER, S., JUMAA, H., VEELKEN, H. & ZIRLIK, K. 2010b. Spleen tyrosine kinase inhibition prevents chemokine- and integrin-mediated stromal protective effects in chronic lymphocytic leukemia. *Blood,* 115**,** 4497-506.

BUETTNER, C., POCAI, A., MUSE, E. D., ETGEN, A. M., MYERS, M. G., JR. & ROSSETTI, L. 2006. Critical role of STAT3 in leptin's metabolic actions. *Cell Metab,* 4**,** 49-60.

BULIAN, P., SHANAFELT, T. D., FEGAN, C., ZUCCHETTO, A., CRO, L., NUCKEL, H., BALDINI, L., KURTOVA, A. V., FERRAJOLI, A., BURGER, J. A., GAIDANO, G., DEL POETA, G., PEPPER, C., ROSSI, D. & GATTEI, V. 2014. CD49d is the strongest flow cytometry-based predictor of overall survival in chronic lymphocytic leukemia. *J Clin Oncol,* 32**,** 897-904.

BURGER, J. A. 2011. Nurture versus nature: the microenvironment in chronic lymphocytic leukemia. *Hematology Am Soc Hematol Educ Program,* 2011**,** 96-103.

BURGER, J. A., BURGER, M. & KIPPS, T. J. 1999. Chronic lymphocytic leukemia B cells express functional CXCR4 chemokine receptors that mediate spontaneous migration beneath bone marrow stromal cells. *Blood,* 94**,** 3658-67.

BURGER, J. A. & CHIORAZZI, N. 2013. B cell receptor signaling in chronic lymphocytic leukemia. *Trends Immunol,* 34**,** 592-601.

BURGER, J. A., GHIA, P., ROSENWALD, A. & CALIGARIS-CAPPIO, F. 2009. The microenvironment in mature B-cell malignancies: a target for new treatment strategies. *Blood,* 114**,** 3367-75.

BURGER, J. A. & GRIBBEN, J. G. 2014. The microenvironment in chronic lymphocytic leukemia (CLL) and other B cell malignancies: insight into disease biology and new targeted therapies. *Semin Cancer Biol,* 24**,** 71-81.

BURGER, J. A., KEATING, M. J., WIERDA, W. G., HARTMANN, E., HOELLENRIEGEL, J., ROSIN, N. Y., DE WEERDT, I., JEYAKUMAR, G., FERRAJOLI, A., CARDENAS-TURANZAS, M., LERNER, S., JORGENSEN, J. L., NOGUERAS-GONZALEZ, G. M., ZACHARIAN, G., HUANG, X., KANTARJIAN, H., GARG, N., ROSENWALD, A. & O'BRIEN, S. 2014. Safety and activity of ibrutinib plus rituximab for patients with high-risk chronic lymphocytic leukaemia: a single-arm, phase 2 study. *Lancet Oncol,* 15**,** 1090-9.

BURGER, J. A., TEDESCHI, A., BARR, P. M., ROBAK, T., OWEN, C., GHIA, P., BAIREY, O., HILLMEN, P., BARTLETT, N. L., LI, J., SIMPSON, D., GROSICKI, S., DEVEREUX, S., MCCARTHY, H., COUTRE, S., QUACH, H., GAIDANO, G., MASLYAK, Z., STEVENS, D. A., JANSSENS, A., OFFNER, F., MAYER, J., O'DWYER, M., HELLMANN, A., SCHUH, A., SIDDIQI, T., POLLIACK, A., TAM, C. S., SURI, D., CHENG, M., CLOW, F., STYLES, L., JAMES, D. F., KIPPS, T. J. & INVESTIGATORS, R.-. 2015. Ibrutinib as Initial Therapy for Patients with Chronic Lymphocytic Leukemia. *N Engl J Med,* 373**,** 2425-37.

BURGER, J. A., TSUKADA, N., BURGER, M., ZVAIFLER, N. J., DELL'AQUILA, M. & KIPPS, T. J. 2000. Blood-derived nurse-like cells protect chronic lymphocytic leukemia B cells from spontaneous apoptosis through stromal cell-derived factor-1. *Blood,* 96**,** 2655-63.

BURGER, J. A., ZVAIFLER, N. J., TSUKADA, N., FIRESTEIN, G. S. & KIPPS, T. J. 2001. Fibroblast-like synoviocytes support B-cell pseudoemperipolesis via a

stromal cell-derived factor-1- and CD106 (VCAM-1)-dependent mechanism. *J Clin Invest,* 107**,** 305-15.

BURGER, M., HARTMANN, T., KROME, M., RAWLUK, J., TAMAMURA, H., FUJII, N., KIPPS, T. J. & BURGER, J. A. 2005. Small peptide inhibitors of the CXCR4 chemokine receptor (CD184) antagonize the activation, migration, and antiapoptotic responses of CXCL12 in chronic lymphocytic leukemia B cells. *Blood,* 106**,** 1824-30.

BURGESS, M., GILL, D., SINGHANIA, R., CHEUNG, C., CHAMBERS, L., RENYOLDS, B. A., SMITH, L., MOLLEE, P., SAUNDERS, N. & MCMILLAN, N. A. 2013. CD62L as a therapeutic target in chronic lymphocytic leukemia. *Clin Cancer Res,* 19**,** 5675-85.

BURGESS, M., MAPP, S., MAZZIERI, R., CHEUNG, C., CHAMBERS, L., MATTAROLLO, S. R., MOLLEE, P., GILL, D. & SAUNDERS, N. A. 2017. Increased FcgammaRIIB dominance contributes to the emergence of resistance to therapeutic antibodies in chronic lymphocytic leukaemia patients. *Oncogene,* 36**,** 2366-2376.

BURKLE, A., NIEDERMEIER, M., SCHMITT-GRAFF, A., WIERDA, W. G., KEATING, M. J. & BURGER, J. A. 2007. Overexpression of the CXCR5 chemokine receptor, and its ligand, CXCL13 in B-cell chronic lymphocytic leukemia. *Blood,* 110**,** 3316-25.

BUSKE, C., GOGOWSKI, G., SCHREIBER, K., RAVE-FRANK, M., HIDDEMANN, W. & WORMANN, B. 1997. Stimulation of B-chronic lymphocytic leukemia cells by murine fibroblasts, IL-4, anti-CD40 antibodies, and the soluble CD40 ligand. *Exp Hematol,* 25**,** 329-37.

BUSTIN, S. A., BENES, V., GARSON, J. A., HELLEMANS, J., HUGGETT, J., KUBISTA, M., MUELLER, R., NOLAN, T., PFAFFL, M. W., SHIPLEY, G. L., VANDESOMPELE, J. & WITTWER, C. T. 2009. The MIQE guidelines: minimum information for publication of quantitative real-time PCR experiments. *Clin Chem,* 55**,** 611-22.

BYRD, J. C., BROWN, J. R., O'BRIEN, S., BARRIENTOS, J. C., KAY, N. E., REDDY, N. M., COUTRE, S., TAM, C. S., MULLIGAN, S. P., JAEGER, U., DEVEREUX, S., BARR, P. M., FURMAN, R. R., KIPPS, T. J., CYMBALISTA, F., POCOCK, C., THORNTON, P., CALIGARIS-CAPPIO, F., ROBAK, T., DELGADO, J., SCHUSTER, S. J., MONTILLO, M., SCHUH, A., DE VOS, S., GILL, D., BLOOR, A., DEARDEN, C., MORENO, C., JONES, J. J., CHU, A. D., FARDIS, M., MCGREIVY, J., CLOW, F., JAMES, D. F., HILLMEN, P. & INVESTIGATORS, R. 2014. Ibrutinib versus ofatumumab in previously treated chronic lymphoid leukemia. *N Engl J Med,* 371**,** 213-23.

BYRD, J. C., FURMAN, R. R., COUTRE, S. E., FLINN, I. W., BURGER, J. A., BLUM, K. A., GRANT, B., SHARMAN, J. P., COLEMAN, M., WIERDA, W. G., JONES, J. A., ZHAO, W., HEEREMA, N. A., JOHNSON, A. J., SUKBUNTHERNG, J., CHANG, B. Y., CLOW, F., HEDRICK, E., BUGGY, J. J., JAMES, D. F. & O'BRIEN, S. 2013. Targeting BTK with ibrutinib in relapsed chronic lymphocytic leukemia. *N Engl J Med,* 369**,** 32-42.

BYRD, J. C., HARRINGTON, B., O'BRIEN, S., JONES, J. A., SCHUH, A., DEVEREUX, S., CHAVES, J., WIERDA, W. G., AWAN, F. T., BROWN, J. R., HILLMEN, P., STEPHENS, D. M., GHIA, P., BARRIENTOS, J. C., PAGEL, J. M., WOYACH, J., JOHNSON, D., HUANG, J., WANG, X., KAPTEIN, A., LANNUTTI, B. J., COVEY, T., FARDIS, M., MCGREIVY, J., HAMDY, A., ROTHBAUM, W., IZUMI, R., DIACOVO, T. G., JOHNSON, A. J. & FURMAN, R. R. 2016. Acalabrutinib (ACP-196) in Relapsed Chronic Lymphocytic Leukemia. *N Engl J Med,* 374**,** 323-32.

CALISSANO, C., DAMLE, RN., MARSILIO, S., YAN XJ, YANCOPOULOUS S, HAYES G, EMSON C, MURPHY EJ, HELLERSTEIN MK, SISON C, KAUFMAN MS, KOLITZ JE, ALLEN SL, RAI KR, IVANOVIC I, DOZMOROV IM, ROA S,

SCHARFF MD, LI W, CHIORAZZI N. 2011 Intraclonal complexity in chronic lymphocytic leukemia: fractions enriched in recently born/divided and older/quiescent cells. *Mol Med.* 17 1374-82

CAMPANA, D., JANOSSY, G., BOFILL, M., TREJDOSIEWICZ, L. K., MA, D., HOFFBRAND, A. V., MASON, D. Y., LEBACQ, A. M. & FORSTER, H. K. 1985. Human B cell development. I. Phenotypic differences of B lymphocytes in the bone marrow and peripheral lymphoid tissue. *J Immunol,* 134**,** 1524-30.

CARPENTER, R. L. & LO, H. W. 2014. STAT3 Target Genes Relevant to Human Cancers. *Cancers (Basel),* 6**,** 897-925.

CATERA, R., SILVERMAN, G. J., HATZI, K., SEILER, T., DIDIER, S., ZHANG, L., HERVE, M., MEFFRE, E., OSCIER, D. G., VLASSARA, H., SCOFIELD, R. H., CHEN, Y., ALLEN, S. L., KOLITZ, J., RAI, K. R., CHU, C. C. & CHIORAZZI, N. 2008. Chronic lymphocytic leukemia cells recognize conserved epitopes associated with apoptosis and oxidation. *Mol Med,* 14**,** 665-74.

CATTANEO, E., MAGRASSI, L., DE-FRAJA, C., CONTI, L., DI GENNARO, I., BUTTI, G. & GOVONI, S. 1998. Variations in the levels of the JAK/STAT and ShcA proteins in human brain tumors. *Anticancer Res,* 18**,** 2381-7.

CELIE, J. W., BEELEN, R. H. & VAN DEN BORN, J. 2009. Heparan sulfate proteoglycans in extravasation: assisting leukocyte guidance. *Front Biosci (Landmark Ed),* 14**,** 4932-49.

CHAKRABORTY, A. & TWEARDY, D. J. 1998. Granulocyte colony-stimulating factor activates a 72-kDa isoform of STAT3 in human neutrophils. *J Leukoc Biol,* 64**,** 675-80.

CHAN, K. T., LI, K., LIU, S. L., CHU, K. H., TOH, M. & XIE, W. D. 2010. Cucurbitacin B inhibits STAT3 and the Raf/MEK/ERK pathway in leukemia cell line K562. *Cancer Lett,* 289**,** 46-52.

CHANAN-KHAN, A., CRAMER, P., DEMIRKAN, F., FRASER, G., SILVA, R. S., GROSICKI, S., PRISTUPA, A., JANSSENS, A., MAYER, J., BARTLETT, N. L., DILHUYDY, M. S., PYLYPENKO, H., LOSCERTALES, J., AVIGDOR, A., RULE, S., VILLA, D., SAMOILOVA, O., PANAGIOTIDIS, P., GOY, A., MATO, A., PAVLOVSKY, M. A., KARLSSON, C., MAHLER, M., SALMAN, M., SUN, S., PHELPS, C., BALASUBRAMANIAN, S., HOWES, A., HALLEK, M. & INVESTIGATORS, H. 2016. Ibrutinib combined with bendamustine and rituximab compared with placebo, bendamustine, and rituximab for previously treated chronic lymphocytic leukaemia or small lymphocytic lymphoma (HELIOS): a randomised, double-blind, phase 3 study. *Lancet Oncol,* 17**,** 200-11.

CHANG, B. Y., FRANCESCO, M., DE ROOIJ, M. F., MAGADALA, P., STEGGERDA, S. M., HUANG, M. M., KUIL, A., HERMAN, S. E., CHANG, S., PALS, S. T., WILSON, W., WIESTNER, A., SPAARGAREN, M., BUGGY, J. J. & ELIAS, L. 2013. Egress of CD19(+)CD5(+) cells into peripheral blood following treatment with the Bruton tyrosine kinase inhibitor ibrutinib in mantle cell lymphoma patients. *Blood,* 122**,** 2412-24.

CHEN, J. C., CHIU, M. H., NIE, R. L., CORDELL, G. A. & QIU, S. X. 2005. Cucurbitacins and cucurbitane glycosides: structures and biological activities. *Nat Prod Rep,* 22**,** 386-99.

CHEN, J. R., GU, B. J., DAO, L. P., BRADLEY, C. J., MULLIGAN, S. P. & WILEY, J. S. 1999. Transendothelial migration of lymphocytes in chronic lymphocytic leukaemia is impaired and involved down-regulation of both L-selectin and CD23. *Br J Haematol,* 105**,** 181-9.

CHEN Q., JAIN N., AYER T., WIERDA, WG., FLOWERS CR., O'BRIEN SM., KEATING MJ, KANTARJIN HM., CHHATWAL J. 2017. Economic Burden of Chronic Lymphocytic Leukemia in the Era of Oral Targeted Therapies in the United States. *J Clin Oncol.* 35, 166-174

CHEN, S. S., CHANG, B. Y., CHANG, S., TONG, T., HAM, S., SHERRY, B., BURGER, J. A., RAI, K. R. & CHIORAZZI, N. 2016. BTK inhibition results in impaired CXCR4 chemokine receptor surface expression, signaling and function in chronic lymphocytic leukemia. *Leukemia,* 30**,** 833-43.

CHEN, W., SHEN, X., XIA, X., XU, G., MA, T., BAI, X. & LIANG, T. 2012. NSC 74859-mediated inhibition of STAT3 enhances the anti-proliferative activity of cetuximab in hepatocellular carcinoma. *Liver Int,* 32**,** 70-7.

CHIM, C. S., WONG, K. Y., LOONG, F. & SRIVASTAVA, G. 2004. SOCS1 and SHP1 hypermethylation in mantle cell lymphoma and follicular lymphoma: implications for epigenetic activation of the Jak/STAT pathway. *Leukemia,* 18**,** 356-8.

CHIORAZZI, N. & FERRARINI, M. 2011. Cellular origin(s) of chronic lymphocytic leukemia: cautionary notes and additional considerations and possibilities. *Blood,* 117**,** 1781-91.

CHU, C. C., CATERA, R., ZHANG, L., DIDIER, S., AGAGNINA, B. M., DAMLE, R. N., KAUFMAN, M. S., KOLITZ, J. E., ALLEN, S. L., RAI, K. R. & CHIORAZZI, N. 2010. Many chronic lymphocytic leukemia antibodies recognize apoptotic cells with exposed nonmuscle myosin heavy chain IIA: implications for patient outcome and cell of origin. *Blood,* 115**,** 3907-15.

CHUNG, C. D., LIAO, J., LIU, B., RAO, X., JAY, P., BERTA, P. & SHUAI, K. 1997. Specific inhibition of Stat3 signal transduction by PIAS3. *Science,* 278**,** 1803-5.

CHUNSONG, H., YULING, H., LI, W., JIE, X., GANG, Z., QIUPING, Z., QINGPING, G., KEJIAN, Z., LI, Q., CHANG, A. E., YOUXIN, J. & JINQUAN, T. 2006. CXC chemokine ligand 13 and CC chemokine ligand 19 cooperatively render resistance to apoptosis in B cell lineage acute and chronic lymphocytic leukemia CD23+CD5+ B cells. *J Immunol,* 177**,** 6713-22.

CIMMINO, A., CALIN, G. A., FABBRI, M., IORIO, M. V., FERRACIN, M., SHIMIZU, M., WOJCIK, S. E., AQEILAN, R. I., ZUPO, S., DONO, M., RASSENTI, L., ALDER, H., VOLINIA, S., LIU, C. G., KIPPS, T. J., NEGRINI, M. & CROCE, C. M. 2005. miR-15 and miR-16 induce apoptosis by targeting BCL2. *Proc Natl Acad Sci U S A,* 102**,** 13944-9.

CLLTRIALISTS'COLLABORATIVEGROUP 1999. Chemotherapeutic options in chronic lymphocytic leukemia: a meta-analysis of the randomized trials. CLL Trialists' Collaborative Group

J Natl Cancer Inst, 91**,** 861-8.

COLLINS, R. J., VERSCHUER, L. A., HARMON, B. V., PRENTICE, R. L., POPE, J. H. & KERR, J. F. 1989. Spontaneous programmed death (apoptosis) of B-chronic lymphocytic leukaemia cells following their culture in vitro. *Br J Haematol,* 71**,** 343-50.

COLS, M., BARRA, C. M., HE, B., PUGA, I., XU, W., CHIU, A., TAM, W., KNOWLES, D. M., DILLON, S. R., LEONARD, J. P., FURMAN, R. R., CHEN, K. & CERUTTI, A. 2012. Stromal endothelial cells establish a bidirectional crosstalk with chronic lymphocytic leukemia cells through the TNF-related factors BAFF, APRIL, and CD40L. *J Immunol,* 188**,** 6071-83.

CONZE, D. B., ZHAO, Y. & ASHWELL, J. D. 2010. Non-canonical NF-kappaB activation and abnormal B cell accumulation in mice expressing ubiquitin protein ligase-inactive c-IAP2. *PLoS Biol,* 8**,** e1000518.

CORTESE, D., SUTTON, L. A., CAHILL, N., SMEDBY, K. E., GEISLER, C., GUNNARSSON, R., JULIUSSON, G., MANSOURI, L. & ROSENQUIST, R. 2014. On the way towards a 'CLL prognostic index': focus on TP53, BIRC3, SF3B1, NOTCH1 and MYD88 in a population-based cohort. *Leukemia,* 28**,** 710-3.

COSTANTINI, A., MANCINI, S., GIULIODORO, S., BUTINI, L., REGNERY, C. M., SILVESTRI, G. & MONTRONI, M. 2003. Effects of cryopreservation on lymphocyte immunophenotype and function. *J Immunol Methods,* 278**,** 145-55.

COURONNE, L., SCOURZIC, L., PILATI, C., DELLA VALLE, V., DUFFOURD, Y., SOLARY, E., VAINCHENKER, W., MERLIO, J. P., BEYLOT-BARRY, M., DAMM, F., STERN, M. H., GAULARD, P., LAMANT, L., DELABESSE, E., MERLE-BERAL, H., NGUYEN-KHAC, F., FONTENAY, M., TILLY, H., BASTARD, C., ZUCMAN-ROSSI, J., BERNARD, O. A. & MERCHER, T. 2013. STAT3 mutations identified in human hematologic neoplasms induce myeloid malignancies in a mouse bone marrow transplantation model. *Haematologica,* 98**,** 1748-52.

COUTO, J. P., DALY, L., ALMEIDA, A., KNAUF, J. A., FAGIN, J. A., SOBRINHO-SIMOES, M., LIMA, J., MAXIMO, V., SOARES, P., LYDEN, D. & BROMBERG, J. F. 2012. STAT3 negatively regulates thyroid tumorigenesis. *Proc Natl Acad Sci U S A,* 109**,** E2361-70.

CROKER, B. A., KIU, H. & NICHOLSON, S. E. 2008. SOCS regulation of the JAK/STAT signalling pathway. *Semin Cell Dev Biol,* 19**,** 414-22.

CROSS, N. C. 2011. Genetic and epigenetic complexity in myeloproliferative neoplasms. *Hematology Am Soc Hematol Educ Program,* 2011**,** 208-14.

CSANAKY, G., VASS, J. A., MILOSEVITS, J., OCSOVSZKI, I., SZOMOR, A. & SCHMELCZER, M. 1994. Expression and function of L-selectin molecules (LECAM-1) in B-cell chronic lymphocytic leukemia. *Haematologica,* 79**,** 132-6.

CUI, W., LIU, Y., WEINSTEIN, J. S., CRAFT, J. & KAECH, S. M. 2011. An interleukin-21-interleukin-10-STAT3 pathway is critical for functional maturation of memory CD8+ T cells. *Immunity,* 35**,** 792-805.

CUNI, S., PEREZ-ACIEGO, P., PEREZ-CHACON, G., VARGAS, J. A., SANCHEZ, A., MARTIN-SAAVEDRA, F. M., BALLESTER, S., GARCIA-MARCO, J., JORDA, J. & DURANTEZ, A. 2004. A sustained activation of PI3K/NF-kappaB pathway is critical for the survival of chronic lymphocytic leukemia B cells. *Leukemia,* 18**,** 1391-400.

DAMLE, R. N., WASIL, T., FAIS, F., GHIOTTO, F., VALETTO, A., ALLEN, S. L., BUCHBINDER, A., BUDMAN, D., DITTMAR, K., KOLITZ, J., LICHTMAN, S. M., SCHULMAN, P., VINCIGUERRA, V. P., RAI, K. R., FERRARINI, M. & CHIORAZZI, N. 1999. Ig V gene mutation status and CD38 expression as novel prognostic indicators in chronic lymphocytic leukemia. *Blood,* 94**,** 1840-7.

DASGUPTA B1, D. E., MAMDOUH Z, MULLER WA. 2009. A novel and critical role for tyrosine 663 in platelet endothelial cell adhesion molecule-1 trafficking and transendothelial migration. *Journal of Immunology,* 15;182(8):5041-51.

DAVIDS, M. S. & BURGER, J. A. 2012. Cell Trafficking in Chronic Lymphocytic Leukemia. *Open J Hematol,* 3.

DE ANGELIS, R., MINICOZZI, P., SANT, M., DAL MASO, L., BREWSTER, D. H., OSCA-GELIS, G., VISSER, O., MAYNADIE, M., MARCOS-GRAGERA, R., TROUSSARD, X., AGIUS, D., ROAZZI, P., MENEGHINI, E., MONNEREAU, A. & GROUP, E.-W. 2015. Survival variations by country and age for lymphoid and myeloid malignancies in Europe 2000-2007: Results of EUROCARE-5 population-based study. *Eur J Cancer,* 51**,** 2254-2268.

DE GORTER, D. J., BEULING, E. A., KERSSEBOOM, R., MIDDENDORP, S., VAN GILS, J. M., HENDRIKS, R. W., PALS, S. T. & SPAARGAREN, M. 2007. Bruton's tyrosine kinase and phospholipase Cgamma2 mediate chemokine-controlled B cell migration and homing. *Immunity,* 26**,** 93-104.

DE LA IGLESIA, N., KONOPKA, G., PURAM, S. V., CHAN, J. A., BACHOO, R. M., YOU, M. J., LEVY, D. E., DEPINHO, R. A. & BONNI, A. 2008. Identification of a PTEN-regulated STAT3 brain tumor suppressor pathway. *Genes Dev,* 22**,** 449-62.

DE ROOIJ, M. F., KUIL, A., GEEST, C. R., ELDERING, E., CHANG, B. Y., BUGGY, J. J., PALS, S. T. & SPAARGAREN, M. 2012. The clinically active BTK inhibitor PCI-32765 targets B-cell receptor- and chemokine-controlled adhesion and migration in chronic lymphocytic leukemia. *Blood,* 119**,** 2590-4.

DEAGLIO, S., MORRA, M., MALLONE, R., AUSIELLO, C. M., PRAGER, E., GARBARINO, G., DIANZANI, U., STOCKINGER, H. & MALAVASI, F. 1998. Human CD38 (ADP-ribosyl cyclase) is a counter-receptor of CD31, an Ig superfamily member. *J Immunol,* 160**,** 395-402.

DECKER, T. & KOVARIK, P. 2000. Serine phosphorylation of STATs. *Oncogene,* 19**,** 2628-37.

DEGLESNE, P. A., CHEVALLIER, N., LETESTU, R., BARAN-MARSZAK, F., BEITAR, T., SALANOUBAT, C., SANHES, L., NATAF, J., ROGER, C., VARIN-BLANK, N. & AJCHENBAUM-CYMBALISTA, F. 2006. Survival response to B-cell receptor ligation is restricted to progressive chronic lymphocytic leukemia cells irrespective of Zap70 expression. *Cancer Res,* 66**,** 7158-66.

DEMARIA, M., GIORGI, C., LEBIEDZINSKA, M., ESPOSITO, G., D'ANGELI, L., BARTOLI, A., GOUGH, D. J., TURKSON, J., LEVY, D. E., WATSON, C. J., WIECKOWSKI, M. R., PROVERO, P., PINTON, P. & POLI, V. 2010. A STAT3-mediated metabolic switch is involved in tumour transformation and STAT3 addiction. *Aging (Albany NY),* 2**,** 823-42.

DENG, J., ISIK, E., FERNANDES, S. M., BROWN, J. R., LETAI, A. & DAVIDS, M. S. 2017. Bruton's tyrosine kinase inhibition increases BCL-2 dependence and enhances sensitivity to venetoclax in chronic lymphocytic leukemia. *Leukemia*.

DETTLAFF-POKORA, K. 2010. Signal transducer and activator of transcription 3β in pancreatic cancer. *Central European Journal of Biology,* 5**,** 435-438.

DING, W., KNOX, T. R., TSCHUMPER, R. C., WU, W., SCHWAGER, S. M., BOYSEN, J. C., JELINEK, D. F. & KAY, N. E. 2010. Platelet-derived growth factor (PDGF)-PDGF receptor interaction activates bone marrow-derived mesenchymal stromal cells derived from chronic lymphocytic leukemia: implications for an angiogenic switch. *Blood,* 116**,** 2984-93.

DING, W., NOWAKOWSKI, G. S., KNOX, T. R., BOYSEN, J. C., MAAS, M. L., SCHWAGER, S. M., WU, W. T., WELLIK, L. E., DIETZ, A. B., GHOSH, A. K., SECRETO, C. R., MEDINA, K. L., SHANAFELT, T. D., ZENT, C. S., CALL, T. G. & KAY, N. E. 2009. Bi-directional activation between mesenchymal stem cells and CLL B-cells: implication for CLL disease progression. *British Journal of Haematology,* 147**,** 471-483.

DOHNER, H., FISCHER, K., BENTZ, M., HANSEN, K., BENNER, A., CABOT, G., DIEHL, D., SCHLENK, R., COY, J., STILGENBAUER, S. & ET AL. 1995. p53 gene deletion predicts for poor survival and non-response to therapy with purine analogs in chronic B-cell leukemias. *Blood,* 85**,** 1580-9.

DOHNER, H., STILGENBAUER, S., BENNER, A., LEUPOLT, E., KROBER, A., BULLINGER, L., DOHNER, K., BENTZ, M. & LICHTER, P. 2000. Genomic aberrations and survival in chronic lymphocytic leukemia. *N Engl J Med,* 343**,** 1910-6.

DOHNER, H., STILGENBAUER, S., JAMES, M. R., BENNER, A., WEILGUNI, T., BENTZ, M., FISCHER, K., HUNSTEIN, W. & LICHTER, P. 1997. 11q deletions identify a new subset of B-cell chronic lymphocytic leukemia characterized by extensive nodal involvement and inferior prognosis. *Blood,* 89**,** 2516-22.

DOUGLAS, R. S., CAPOCASALE, R. J., LAMB, R. J., NOWELL, P. C. & MOORE, J. S. 1997. Chronic lymphocytic leukemia B cells are resistant to the apoptotic effects of transforming growth factor-beta. *Blood,* 89**,** 941-7.

DREGER, P., CORRADINI, P., KIMBY, E., MICHALLET, M., MILLIGAN, D., SCHETELIG, J., WIKTOR-JEDRZEJCZAK, W., NIEDERWIESER, D., HALLEK, M., MONTSERRAT, E. & CHRONIC LEUKEMIA WORKING PARTY OF THE, E. 2007. Indications for allogeneic stem cell transplantation in chronic lymphocytic leukemia: the EBMT transplant consensus. *Leukemia,* 21**,** 12-7.

DRICKAMER, K. 1988. Two distinct classes of carbohydrate-recognition domains in animal lectins. *J Biol Chem,* 263**,** 9557-60.

DUBOVSKY, J. A., BECKWITH, K. A., NATARAJAN, G., WOYACH, J. A., JAGLOWSKI, S., ZHONG, Y., HESSLER, J. D., LIU, T. M., CHANG, B. Y., LARKIN, K. M., STEFANOVSKI, M. R., CHAPPELL, D. L., FRISSORA, F. W., SMITH, L. L., SMUCKER, K. A., FLYNN, J. M., JONES, J. A., ANDRITSOS, L. A., MADDOCKS, K., LEHMAN, A. M., FURMAN, R., SHARMAN, J., MISHRA, A., CALIGIURI, M. A., SATOSKAR, A. R., BUGGY, J. J., MUTHUSAMY, N., JOHNSON, A. J. & BYRD, J. C. 2013. Ibrutinib is an irreversible molecular inhibitor of ITK driving a Th1-selective pressure in T lymphocytes. *Blood,* 122**,** 2539-49.

DUHREN-VON MINDEN, M., UBELHART, R., SCHNEIDER, D., WOSSNING, T., BACH, M. P., BUCHNER, M., HOFMANN, D., SUROVA, E., FOLLO, M., KOHLER, F., WARDEMANN, H., ZIRLIK, K., VEELKEN, H. & JUMAA, H. 2012. Chronic lymphocytic leukaemia is driven by antigen-independent cell-autonomous signalling. *Nature,* 489**,** 309-12.

DUNCAN, K. L., DUNCAN, M. D., ALLEY, M. C. & SAUSVILLE, E. A. 1996. Cucurbitacin E-induced disruption of the actin and vimentin cytoskeleton in prostate carcinoma cells. *Biochem Pharmacol,* 52**,** 1553-60.

DWIR, O., SOLOMON, A., MANGAN, S., KANSAS, G. S., SCHWARZ, U. S. & ALON, R. 2003. Avidity enhancement of L-selectin bonds by flow: shear-promoted rotation of leukocytes turn labile bonds into functional tethers. *J Cell Biol,* 163**,** 649-59.

DYLKE, J., LOPES, J., DANG-LAWSON, M., MACHTALER, S. & MATSUUCHI, L. 2007. Role of the extracellular and transmembrane domain of Ig-alpha/beta in assembly of the B cell antigen receptor (BCR). *Immunol Lett,* 112**,** 47-57.

EDELMANN, J., KLEIN-HITPASS, L., CARPINTEIRO, A., FUHRER, A., SELLMANN, L., STILGENBAUER, S., DUHRSEN, U. & DURIG, J. 2008. Bone marrow fibroblasts induce expression of PI3K/NF-kappaB pathway genes and a pro-angiogenic phenotype in CLL cells. *Leuk Res,* 32**,** 1565-72.

EICHHORST, B., ROBAK, T., MONTSERRAT, E., GHIA, P., HILLMEN, P., HALLEK, M., BUSKE, C. & COMMITTEE, E. G. 2015. Chronic lymphocytic leukaemia: ESMO Clinical Practice Guidelines for diagnosis, treatment and follow-up. *Ann Oncol,* 26 Suppl 5**,** v78-84.

ELICES, M. J., OSBORN, L., TAKADA, Y., CROUSE, C., LUHOWSKYJ, S., HEMLER, M. E. & LOBB, R. R. 1990. VCAM-1 on activated endothelium interacts with the leukocyte integrin VLA-4 at a site distinct from the VLA-4/fibronectin binding site. *Cell,* 60**,** 577-84.

EPLING-BURNETTE, P. K., LIU, J. H., CATLETT-FALCONE, R., TURKSON, J., OSHIRO, M., KOTHAPALLI, R., LI, Y., WANG, J. M., YANG-YEN, H. F., KARRAS, J., JOVE, R. & LOUGHRAN, T. P., JR. 2001. Inhibition of STAT3 signaling leads to apoptosis of leukemic large granular lymphocytes and decreased Mcl-1 expression. *J Clin Invest,* 107**,** 351-62.

FALISI, E., NOVELLA, E., VISCO, C., GUERCINI, N., MAURA, F., GIARETTA, I., POMPONI, F., NICHELE, I., FINOTTO, S., MONTALDI, A., NERI, A. & RODEGHIERO, F. 2014. B-cell receptor configuration and mutational analysis of patients with chronic lymphocytic leukaemia and trisomy 12 reveal recurrent molecular abnormalities. *Hematol Oncol,* 32**,** 22-30.

FAROOQUI, M. Z., VALDEZ, J., MARTYR, S., AUE, G., SABA, N., NIEMANN, C. U., HERMAN, S. E., TIAN, X., MARTI, G., SOTO, S., HUGHES, T. E., JONES, J., LIPSKY, A., PITTALUGA, S., STETLER-STEVENSON, M., YUAN, C., LEE, Y. S., PEDERSEN, L. B., GEISLER, C. H., CALVO, K. R., ARTHUR, D. C., MARIC, I., CHILDS, R., YOUNG, N. S. & WIESTNER, A. 2015. Ibrutinib for previously untreated and relapsed or refractory chronic lymphocytic leukaemia with TP53 aberrations: a phase 2, single-arm trial. *Lancet Oncol,* 16**,** 169-76.

FEDELE, G., DI GIROLAMO, M., RECINE, U., PALAZZO, R., URBANI, F., HORENSTEIN, A. L., MALAVASI, F. & AUSIELLO, C. M. 2013. CD38 ligation in

peripheral blood mononuclear cells of myeloma patients induces release of protumorigenic IL-6 and impaired secretion of IFNgamma cytokines and proliferation. *Mediators Inflamm,* 2013**,** 564687.

FERLAY, J., PARKIN, D. M. & STELIAROVA-FOUCHER, E. 2010. Estimates of cancer incidence and mortality in Europe in 2008. *Eur J Cancer,* 46**,** 765-81.

FERNANDEZ, V., JARES, P., SALAVERRIA, I., GINE, E., BEA, S., AYMERICH, M., COLOMER, D., VILLAMOR, N., BOSCH, F., MONTSERRAT, E. & CAMPO, E. 2008. Gene expression profile and genomic changes in disease progression of early-stage chronic lymphocytic leukemia. *Haematologica,* 93**,** 132-6.

FISCHER, K., BAHLO, J., FINK, A. M., GOEDE, V., HERLING, C. D., CRAMER, P., LANGERBEINS, P., VON TRESCKOW, J., ENGELKE, A., MAURER, C., KOVACS, G., HERLING, M., TAUSCH, E., KREUZER, K. A., EICHHORST, B., BOTTCHER, S., SEYMOUR, J. F., GHIA, P., MARLTON, P., KNEBA, M., WENDTNER, C. M., DOHNER, H., STILGENBAUER, S. & HALLEK, M. 2016. Long-term remissions after FCR chemoimmunotherapy in previously untreated patients with CLL: updated results of the CLL8 trial. *Blood,* 127**,** 208-15.

FLINN IW, B. M., CHOI MY, DYER MJS, GRIBBEN JG, HILLMEN P, ET AL. 2015. Safety and efficacy of a combination of venetoclax (GDC-0199/ABT-199) and obinutuzumab in patients with relapsed/refractory or previously untreated

chronic lymphocytic leukemia - Results from a phase 1b study (GP28331). *Blood (ASH Annual Meeting Abstracts),* 126: Abstract 494.

FLUCKIGER, A. C., ROSSI, J. F., BUSSEL, A., BRYON, P., BANCHEREAU, J. & DEFRANCE, T. 1992. Responsiveness of chronic lymphocytic leukemia B cells activated via surface Igs or CD40 to B-cell tropic factors. *Blood,* 80**,** 3173-81.

FONTAINE, F., OVERMAN, J. & FRANCOIS, M. 2015. Pharmacological manipulation of transcription factor protein-protein interactions: opportunities and obstacles. *Cell Regen (Lond),* 4**,** 2.

FRANK, D. A. 2007. STAT3 as a central mediator of neoplastic cellular transformation. *Cancer Lett,* 251**,** 199-210.

FRANK, D. A., MAHAJAN, S. & RITZ, J. 1997. B lymphocytes from patients with chronic lymphocytic leukemia contain signal transducer and activator of transcription (STAT) 1 and STAT3 constitutively phosphorylated on serine residues. *J Clin Invest,* 100**,** 3140-8.

FRIEDRICH, M., BOCK, D., PHILIPP, S., LUDWIG, N., SABAT, R., WOLK, K., SCHROETER-MAAS, S., AYDT, E., KANG, S., DAM, T. N., ZAHLTEN, R., STERRY, W. & WOLFF, G. 2006. Pan-selectin antagonism improves psoriasis manifestation in mice and man. *Arch Dermatol Res,* 297**,** 345-51.

FRUSTACI, A. M., TEDESCHI, A., PICARDI, P., MAZZUCCHELLI, M., CAIROLI, R. & MONTILLO, M. 2016. Ofatumumab plus chlorambucil as a first-line therapy in less fit patients with chronic lymphocytic leukemia: analysis of COMPLEMENT1 and other monoclonal antibodies association data. *Ther Adv Hematol,* 7**,** 222-30.

FUJII, K., KARPOVA, M. B., ASAGOE, K., GEORGIEV, O., DUMMER, R. & UROSEVIC-MAIWALD, M. 2015. Versican upregulation in Sezary cells alters growth, motility and resistance to chemotherapy. *Leukemia,* 29**,** 2024-32.

FUJIMOTO, M., POE, J. C., HASEGAWA, M. & TEDDER, T. F. 2000. CD19 regulates intrinsic B lymphocyte signal transduction and activation through a novel mechanism of processive amplification. *Immunol Res,* 22**,** 281-98.

FURMAN, R. R., ASGARY, Z., MASCARENHAS, J. O., LIOU, H. C. & SCHATTNER, E. J. 2000. Modulation of NF-kappa B activity and apoptosis in chronic lymphocytic leukemia B cells. *J Immunol,* 164**,** 2200-6.

FURMAN, R. R., SHARMAN, J. P., COUTRE, S. E., CHESON, B. D., PAGEL, J. M., HILLMEN, P., BARRIENTOS, J. C., ZELENETZ, A. D., KIPPS, T. J., FLINN, I., GHIA, P., ERADAT, H., ERVIN, T., LAMANNA, N., COIFFIER, B., PETTITT, A. R., MA, S., STILGENBAUER, S., CRAMER, P., AIELLO, M., JOHNSON, D. M.,

MILLER, L. L., LI, D., JAHN, T. M., DANSEY, R. D., HALLEK, M. & O'BRIEN, S. M. 2014. Idelalisib and rituximab in relapsed chronic lymphocytic leukemia. *N Engl J Med,* 370**,** 997-1007.

GAO, W., WANG, M., WANG, L., LU, H., WU, S., DAI, B., OU, Z., ZHANG, L., HEYMACH, J. V., GOLD, K. A., MINNA, J., ROTH, J. A., HOFSTETTER, W. L., SWISHER, S. G. & FANG, B. 2014. Selective antitumor activity of ibrutinib in EGFR-mutant non-small cell lung cancer cells. *J Natl Cancer Inst,* 106.

GARCIA, R., YU, C. L., HUDNALL, A., CATLETT, R., NELSON, K. L., SMITHGALL, T., FUJITA, D. J., ETHIER, S. P. & JOVE, R. 1997. Constitutive activation of Stat3 in fibroblasts transformed by diverse oncoproteins and in breast carcinoma cells. *Cell Growth Differ,* 8**,** 1267-76.

GATTEI, V., BULIAN, P., DEL PRINCIPE, M. I., ZUCCHETTO, A., MAURILLO, L., BUCCISANO, F., BOMBEN, R., DAL-BO, M., LUCIANO, F., ROSSI, F. M., DEGAN, M., AMADORI, S. & DEL POETA, G. 2008. Relevance of CD49d protein expression as overall survival and progressive disease prognosticator in chronic lymphocytic leukemia. *Blood,* 111**,** 865-73.

GEHRKE, I., GANDHIRAJAN, R. K., POLL-WOLBECK, S. J., HALLEK, M. & KREUZER, K. A. 2011. Bone marrow stromal cell-derived vascular endothelial growth factor (VEGF) rather than chronic lymphocytic leukemia (CLL) cell-derived VEGF is essential for the apoptotic resistance of cultured CLL cells. *Mol Med,* 17**,** 619-27.

GENEVIER, H. C., HINSHELWOOD, S., GASPAR, H. B., RIGLEY, K. P., BROWN, D., SAELAND, S., ROUSSET, F., LEVINSKY, R. J., CALLARD, R. E., KINNON, C. & ET AL. 1994. Expression of Bruton's tyrosine kinase protein within the B cell lineage. *Eur J Immunol,* 24**,** 3100-5.

GHIA, P. & CALIGARIS-CAPPIO, F. 2006. The origin of B-cell chronic lymphocytic leukemia. *Semin Oncol,* 33**,** 150-6.

GHIA, P., STAMATOPOULOS, K., BELESSI, C., MORENO, C., STILGENBAUER, S., STEVENSON, F., DAVI, F., ROSENQUIST, R. & EUROPEAN RESEARCH INITIATIVE ON, C. L. L. 2007. ERIC recommendations on IGHV gene mutational status analysis in chronic lymphocytic leukemia. *Leukemia,* 21**,** 1-3.

GHOBRIAL, I. M., BONE, N. D., STENSON, M. J., NOVAK, A., HEDIN, K. E., KAY, N. E. & ANSELL, S. M. 2004. Expression of the chemokine receptors CXCR4 and CCR7 and disease progression in B-cell chronic lymphocytic leukemia/ small lymphocytic lymphoma. *Mayo Clin Proc,* 79**,** 318-25.

GHOSH, A. K., SECRETO, C. R., KNOX, T. R., DING, W., MUKHOPADHYAY, D. & KAY, N. E. 2010. Circulating microvesicles in B-cell chronic lymphocytic leukemia can stimulate marrow stromal cells: implications for disease progression. *Blood,* 115**,** 1755-64.

GIBLIN, P. A., HWANG, S. T., KATSUMOTO, T. R. & ROSEN, S. D. 1997. Ligation of L-selectin on T lymphocytes activates beta1 integrins and promotes adhesion to fibronectin. *J Immunol,* 159**,** 3498-507.

GOEDE, V., FISCHER, K., BUSCH, R., ENGELKE, A., EICHHORST, B., WENDTNER, C. M., CHAGOROVA, T., DE LA SERNA, J., DILHUYDY, M. S., ILLMER, T., OPAT, S., OWEN, C. J., SAMOYLOVA, O., KREUZER, K. A., STILGENBAUER, S., DOHNER, H., LANGERAK, A. W., RITGEN, M., KNEBA, M., ASIKANIUS, E., HUMPHREY, K., WENGER, M. & HALLEK, M. 2014. Obinutuzumab plus chlorambucil in patients with CLL and coexisting conditions. *N Engl J Med,* 370**,** 1101-10.

GONZALEZ-RODRIGUEZ, A. P., CONTESTI, J., HUERGO-ZAPICO, L., LOPEZ-SOTO, A., FERNANDEZ-GUIZAN, A., ACEBES-HUERTA, A., GONZALEZ-HUERTA, A. J., GONZALEZ, E., FERNANDEZ-ALVAREZ, C. & GONZALEZ, S. 2010. Prognostic significance of CD8 and CD4 T cells in chronic lymphocytic leukemia. *Leuk Lymphoma,* 51**,** 1829-36.

GOUILLEUX-GRUART, V., GOUILLEUX, F., DESAINT, C., CLAISSE, J. F., CAPIOD, J. C., DELOBEL, J., WEBER-NORDT, R., DUSANTER-FOURT, I., DREYFUS, F., GRONER, B. & PRIN, L. 1996. STAT-related transcription factors are constitutively activated in peripheral blood cells from acute leukemia patients. *Blood,* 87**,** 1692-7.

GOWANS, J. L. & KNIGHT, E. J. 1964. The Route of Re-Circulation of Lymphocytes in the Rat. *Proc R Soc Lond B Biol Sci,* 159**,** 257-82.

GRABNER, B., SCHRAMEK, D., MUELLER, K. M., MOLL, H. P., SVINKA, J., HOFFMANN, T., BAUER, E., BLAAS, L., HRUSCHKA, N., ZBORAY, K., STIEDL, P., NIVARTHI, H., BOGNER, E., GRUBER, W., MOHR, T., ZWICK, R. H., KENNER, L., POLI, V., ABERGER, F., STOIBER, D., EGGER, G., ESTERBAUER, H., ZUBER, J., MORIGGL, R., EFERL, R., GYORFFY, B., PENNINGER, J. M., POPPER, H. & CASANOVA, E. 2015. Disruption of STAT3 signalling promotes KRAS-induced lung tumorigenesis. *Nat Commun,* 6**,** 6285.

GRAILER, J. J., KODERA, M. & STEEBER, D. A. 2009. L-selectin: role in regulating homeostasis and cutaneous inflammation. *J Dermatol Sci,* 56**,** 141-7.

GRANESS, A., POLI, V. & GOPPELT-STRUEBE, M. 2006. STAT3-independent inhibition of lysophosphatidic acid-mediated upregulation of connective tissue growth factor (CTGF) by cucurbitacin I. *Biochem Pharmacol,* 72**,** 32-41.

GRANZIERO, L., GHIA, P., CIRCOSTA, P., GOTTARDI, D., STROLA, G., GEUNA, M., MONTAGNA, L., PICCOLI, P., CHILOSI, M. & CALIGARIS-CAPPIO, F. 2001. Survivin is expressed on CD40 stimulation and interfaces proliferation and apoptosis in B-cell chronic lymphocytic leukemia. *Blood,* 97**,** 2777-83.

GRDISA, M. 2003. Influence of CD40 ligation on survival and apoptosis of B-CLL cells in vitro. *Leuk Res,* 27**,** 951-6.

GU, B., DAO, L. P. & WILEY, J. 2001. Impaired transendothelial migration of B-CLL lymphocytes: a defect linked to low L-selectin expression. *Leuk Lymphoma,* 42**,** 5-12.

GUAN, J. L. & HYNES, R. O. 1990. Lymphoid cells recognize an alternatively spliced segment of fibronectin via the integrin receptor alpha 4 beta 1. *Cell,* 60**,** 53-61.

GUARINI, A., CHIARETTI, S., TAVOLARO, S., MAGGIO, R., PERAGINE, N., CITARELLA, F., RICCIARDI, M. R., SANTANGELO, S., MARINELLI, M., DE PROPRIS, M. S., MESSINA, M., MAURO, F. R., DEL GIUDICE, I. & FOA, R. 2008. BCR ligation induced by IgM stimulation results in gene expression and functional changes only in IgV H unmutated chronic lymphocytic leukemia (CLL) cells. *Blood,* 112**,** 782-92.

GUIEZE, R., ROBBE, P., CLIFFORD, R., DE GUIBERT, S., PEREIRA, B., TIMBS, A., DILHUYDY, M. S., CABES, M., YSEBAERT, L., BURNS, A., NGUYEN-KHAC, F., DAVI, F., VERONESE, L., COMBES, P., LE GARFF-TAVERNIER, M., LEBLOND, V., MERLE-BERAL, H., ALSOLAMI, R., HAMBLIN, A., MASON, J., PETTITT, A., HILLMEN, P., TAYLOR, J., KNIGHT, S. J., TOURNILHAC, O. & SCHUH, A. 2015. Presence of multiple recurrent mutations confers poor trial outcome of relapsed/refractory CLL. *Blood,* 126**,** 2110-7.

GUNNARSSON, R., MANSOURI, L., ISAKSSON, A., GORANSSON, H., CAHILL, N., JANSSON, M., RASMUSSEN, M., LUNDIN, J., NORIN, S., BUHL, A. M., SMEDBY, K. E., HJALGRIM, H., KARLSSON, K., JURLANDER, J., GEISLER, C., JULIUSSON, G. & ROSENQUIST, R. 2011. Array-based genomic screening at diagnosis and during follow-up in chronic lymphocytic leukemia. *Haematologica,* 96**,** 1161-9.

GUO, B., ZHANG, L., CHIORAZZI, N. & ROTHSTEIN, T. L. 2016. IL-4 rescues surface IgM expression in chronic lymphocytic leukemia. *Blood,* 128**,** 553-62.

GUO, W., PYLAYEVA, Y., PEPE, A., YOSHIOKA, T., MULLER, W. J., INGHIRAMI, G. & GIANCOTTI, F. G. 2006. Beta 4 integrin amplifies ErbB2 signaling to promote mammary tumorigenesis. *Cell,* 126**,** 489-502.

HALLEK, M. 2017. Chronic lymphocytic leukemia: 2017 update on diagnosis, risk stratification, and treatment. *Am J Hematol,* 92**,** 946-965.

HALLEK, M., CHESON, B. D., CATOVSKY, D., CALIGARIS-CAPPIO, F., DIGHIERO, G., DOHNER, H., HILLMEN, P., KEATING, M. J., MONTSERRAT, E., RAI, K. R., KIPPS, T. J. & INTERNATIONAL WORKSHOP ON CHRONIC LYMPHOCYTIC, L. 2008. Guidelines for the diagnosis and treatment of chronic lymphocytic leukemia: a report from the International Workshop on Chronic Lymphocytic Leukemia updating the National Cancer Institute-Working Group 1996 guidelines. *Blood,* 111**,** 5446-56.

HALLEK, M., FISCHER, K., FINGERLE-ROWSON, G., FINK, A. M., BUSCH, R., MAYER, J., HENSEL, M., HOPFINGER, G., HESS, G., VON GRUNHAGEN, U., BERGMANN, M., CATALANO, J., ZINZANI, P. L., CALIGARIS-CAPPIO, F., SEYMOUR, J. F., BERREBI, A., JAGER, U., CAZIN, B., TRNENY, M., WESTERMANN, A., WENDTNER, C. M., EICHHORST, B. F., STAIB, P., BUHLER, A., WINKLER, D., ZENZ, T., BOTTCHER, S., RITGEN, M., MENDILA, M., KNEBA, M., DOHNER, H., STILGENBAUER, S., INTERNATIONAL GROUP OF, I. & GERMAN CHRONIC LYMPHOCYTIC LEUKAEMIA STUDY, G. 2010. Addition of rituximab to fludarabine and cyclophosphamide in patients with chronic lymphocytic leukaemia: a randomised, open-label, phase 3 trial. *Lancet,* 376**,** 1164-74.

HAMBLIN, T. J., DAVIS, Z., GARDINER, A., OSCIER, D. G. & STEVENSON, F. K. 1999. Unmutated Ig V(H) genes are associated with a more aggressive form of chronic lymphocytic leukemia. *Blood,* 94**,** 1848-54.

HAMBLIN, T. J., ORCHARD, J. A., GARDINER, A., OSCIER, D. G., DAVIS, Z. & STEVENSON, F. K. 2000. Immunoglobulin V genes and CD38 expression in CLL. *Blood,* 95**,** 2455-7.

HAMILTON, E., PEARCE, L., MORGAN, L., ROBINSON, S., WARE, V., BRENNAN, P., THOMAS, N. S., YALLOP, D., DEVEREUX, S., FEGAN, C., BUGGINS, A. G. & PEPPER, C. 2012. Mimicking the tumour microenvironment: three different co-culture systems induce a similar phenotype but distinct proliferative signals in primary chronic lymphocytic leukaemia cells. *Br J Haematol,* 158**,** 589-99.

HAN, Z., WANG, X., MA, L., CHEN, L., XIAO, M., HUANG, L., CAO, Y., BAI, J., MA, D., ZHOU, J. & HONG, Z. 2014. Inhibition of STAT3 signaling targets both tumor-initiating and differentiated cell populations in prostate cancer. *Oncotarget,* 5**,** 8416-28.

HANAHAN, D. & WEINBERG, R. A. 2011. Hallmarks of cancer: the next generation. *Cell,* 144**,** 646-74.

HANSEL, T. T., KROPSHOFER, H., SINGER, T., MITCHELL, J. A. & GEORGE, A. J. 2010. The safety and side effects of monoclonal antibodies. *Nat Rev Drug Discov,* 9**,** 325-38.

HANSON, C. A., GRIBBIN, T. E., SCHNITZER, B., SCHLEGELMILCH, J. A., MITCHELL, B. S. & STOOLMAN, L. M. 1990. CD11c (LEU-M5) expression characterizes a B-cell chronic lymphoproliferative disorder with features of both chronic lymphocytic leukemia and hairy cell leukemia. *Blood,* 76**,** 2360-7.

HARRISON, C., KILADJIAN, J. J., AL-ALI, H. K., GISSLINGER, H., WALTZMAN, R., STALBOVSKAYA, V., MCQUITTY, M., HUNTER, D. S., LEVY, R., KNOOPS, L., CERVANTES, F., VANNUCCHI, A. M., BARBUI, T. & BAROSI, G. 2012. JAK inhibition with ruxolitinib versus best available therapy for myelofibrosis. *N Engl J Med,* 366**,** 787-98.

HARRISON, C. N., VANNUCCHI, A. M., KILADJIAN, J. J., AL-ALI, H. K., GISSLINGER, H., KNOOPS, L., CERVANTES, F., JONES, M. M., SUN, K., MCQUITTY, M., STALBOVSKAYA, V., GOPALAKRISHNA, P. & BARBUI, T. 2016. Long-term findings from COMFORT-II, a phase 3 study of ruxolitinib vs best available therapy for myelofibrosis. *Leukemia,* 30**,** 1701-7.

HARTMANN, T. N., GRABOVSKY, V., WANG, W., DESCH, P., RUBENZER, G., WOLLNER, S., BINSKY, I., VALLON-EBERHARD, A., SAPOZNIKOV, A., BURGER, M., SHACHAR, I., HARAN, M., HONCZARENKO, M., GREIL, R. & ALON, R. 2009. Circulating B-cell chronic lymphocytic leukemia cells display impaired migration to lymph nodes and bone marrow. *Cancer Res,* 69**,** 3121-30.

HAYDEN, R. E., PRATT, G., ROBERTS, C., DRAYSON, M. T. & BUNCE, C. M. 2012. Treatment of chronic lymphocytic leukemia requires targeting of the protective lymph node environment with novel therapeutic approaches. *Leuk Lymphoma,* 53**,** 537-49.

HAZAN-HALEVY, I., HARRIS, D., LIU, Z., LIU, J., LI, P., CHEN, X., SHANKER, S., FERRAJOLI, A., KEATING, M. J. & ESTROV, Z. 2010. STAT3 is constitutively phosphorylated on serine 727 residues, binds DNA, and activates transcription in CLL cells. *Blood,* 115**,** 2852-63.

HE, F., WANG, L., HU, X. B., YIN, D. D., ZHANG, P., LI, G. H., WANG, Y. C., HUANG, S. Y., LIANG, Y. M. & HAN, H. 2009. Notch and BCR signaling synergistically promote the proliferation of Raji B-lymphoma cells. *Leuk Res,* 33**,** 798-802.

HEMLER, M. E. 1990. VLA proteins in the integrin family: structures, functions, and their role on leukocytes. *Annu Rev Immunol,* 8**,** 365-400.

HENDRIKS, R. W., YUVARAJ, S. & KIL, L. P. 2014. Targeting Bruton's tyrosine kinase in B cell malignancies. *Nat Rev Cancer,* 14**,** 219-32.

HERISHANU, Y., PEREZ-GALAN, P., LIU, D., BIANCOTTO, A., PITTALUGA, S., VIRE, B., GIBELLINI, F., NJUGUNA, N., LEE, E., STENNETT, L., RAGHAVACHARI, N., LIU, P., MCCOY, J. P., RAFFELD, M., STETLER-STEVENSON, M., YUAN, C., SHERRY, R., ARTHUR, D. C., MARIC, I., WHITE, T., MARTI, G. E., MUNSON, P., WILSON, W. H. & WIESTNER, A. 2011. The lymph node microenvironment promotes B-cell receptor signaling, NF-kappaB activation, and tumor proliferation in chronic lymphocytic leukemia. *Blood,* 117**,** 563-74.

HERMAN, S. E., BARR, P. M., MCAULEY, E. M., LIU, D., WIESTNER, A. & FRIEDBERG, J. W. 2013. Fostamatinib inhibits B-cell receptor signaling, cellular activation and tumor proliferation in patients with relapsed and refractory chronic lymphocytic leukemia. *Leukemia,* 27**,** 1769-73.

HERMAN, S. E., GORDON, A. L., HERTLEIN, E., RAMANUNNI, A., ZHANG, X., JAGLOWSKI, S., FLYNN, J., JONES, J., BLUM, K. A., BUGGY, J. J., HAMDY, A., JOHNSON, A. J. & BYRD, J. C. 2011. Bruton tyrosine kinase represents a promising therapeutic target for treatment of chronic lymphocytic leukemia and is effectively targeted by PCI-32765. *Blood,* 117**,** 6287-96.

HERMAN, S. E. & JOHNSON, A. J. 2012. Molecular pathways: targeting phosphoinositide 3-kinase p110-delta in chronic lymphocytic leukemia. *Clin Cancer Res,* 18**,** 4013-8.

HERRMANN, A., VOGT, M., MONNIGMANN, M., CLAHSEN, T., SOMMER, U., HAAN, S., POLI, V., HEINRICH, P. C. & MULLER-NEWEN, G. 2007. Nucleocytoplasmic shuttling of persistently activated STAT3. *J Cell Sci,* 120**,** 3249-61.

HERVE, M., XU, K., NG, Y. S., WARDEMANN, H., ALBESIANO, E., MESSMER, B. T., CHIORAZZI, N. & MEFFRE, E. 2005. Unmutated and mutated chronic lymphocytic leukemias derive from self-reactive B cell precursors despite expressing different antibody reactivity. *J Clin Invest,* 115**,** 1636-43.

HIBI, M., MURAKAMI, M., SAITO, M., HIRANO, T., TAGA, T. & KISHIMOTO, T. 1990. Molecular cloning and expression of an IL-6 signal transducer, gp130. *Cell,* 63**,** 1149-57.

HILLMEN, P., ROBAK, T., JANSSENS, A., BABU, K. G., KLOCZKO, J., GROSICKI, S., DOUBEK, M., PANAGIOTIDIS, P., KIMBY, E., SCHUH, A., PETTITT, A. R., BOYD, T., MONTILLO, M., GUPTA, I. V., WRIGHT, O., DIXON, I., CAREY, J. L., CHANG, C. N., LISBY, S., MCKEOWN, A., OFFNER, F. &

INVESTIGATORS, C. S. 2015. Chlorambucil plus ofatumumab versus chlorambucil alone in previously untreated patients with chronic lymphocytic leukaemia (COMPLEMENT 1): a randomised, multicentre, open-label phase 3 trial. *Lancet,* 385**,** 1873-83.

HODGE, J. A., KAWABATA, T. T., KRISHNASWAMI, S., CLARK, J. D., TELLIEZ, J. B., DOWTY, M. E., MENON, S., LAMBA, M. & ZWILLICH, S. 2016. The mechanism of action of tofacitinib - an oral Janus kinase inhibitor for the treatment of rheumatoid arthritis. *Clin Exp Rheumatol,* 34**,** 318-28.

HOELLENRIEGEL, J., MEADOWS, S. A., SIVINA, M., WIERDA, W. G., KANTARJIAN, H., KEATING, M. J., GIESE, N., O'BRIEN, S., YU, A., MILLER, L. L., LANNUTTI, B. J. & BURGER, J. A. 2011. The phosphoinositide 3'-kinase delta inhibitor, CAL-101, inhibits B-cell receptor signaling and chemokine networks in chronic lymphocytic leukemia. *Blood,* 118**,** 3603-12.

HONG, D., KURZROCK, R., KIM, Y., WOESSNER, R., YOUNES, A., NEMUNAITIS, J., FOWLER, N., ZHOU, T., SCHMIDT, J., JO, M., LEE, S. J., YAMASHITA, M., HUGHES, S. G., FAYAD, L., PIHA-PAUL, S., NADELLA, M. V., MOHSENI, M., LAWSON, D., REIMER, C., BLAKEY, D. C., XIAO, X., HSU, J., REVENKO, A., MONIA, B. P. & MACLEOD, A. R. 2015. AZD9150, a next-generation antisense oligonucleotide inhibitor of STAT3 with early evidence of clinical activity in lymphoma and lung cancer. *Sci Transl Med,* 7**,** 314ra185.

HONJO, T., KINOSHITA, K. & MURAMATSU, M. 2002. Molecular mechanism of class switch recombination: linkage with somatic hypermutation. *Annu Rev Immunol,* 20**,** 165-96.

HOOGEBOOM, R., VAN KESSEL, K. P., HOCHSTENBACH, F., WORMHOUDT, T. A., REINTEN, R. J., WAGNER, K., KATER, A. P., GUIKEMA, J. E., BENDE, R. J. & VAN NOESEL, C. J. 2013. A mutated B cell chronic lymphocytic leukemia subset that recognizes and responds to fungi. *J Exp Med,* 210**,** 59-70.

HOWLADER, Y., S.M., LI, J., GALE. R. P., & HUANG. X. J. 2013. *SEER Cancer Statistics Review 1975-2010* [Online]. http://seer.cancer.gov/csr/1975_2010/.

HU, G., WITZIG, T. E. & GUPTA, M. 2013. A novel missense (M206K) STAT3 mutation in diffuse large B cell lymphoma deregulates STAT3 signaling. *PLoS One,* 8**,** e67851.

HUANG, J., LI, C. Y., MESA, R. A., WU, W., HANSON, C. A., PARDANANI, A. & TEFFERI, A. 2008. Risk factors for leukemic transformation in patients with primary myelofibrosis. *Cancer,* 112**,** 2726-32.

HUANG, P. Y., KOHNKE, P., BELOV, L., BEST, O. G., MULLIGAN, S. P. & CHRISTOPHERSON, R. I. 2013. Profiles of surface mosaics on chronic lymphocytic leukemias distinguish stable and progressive subtypes. *J Pharm Pharm Sci,* 16**,** 231-7.

HUANG, Y., QIU, J., DONG, S., REDELL, M. S., POLI, V., MANCINI, M. A. & TWEARDY, D. J. 2007. Stat3 isoforms, alpha and beta, demonstrate distinct intracellular dynamics with prolonged nuclear retention of Stat3beta mapping to its unique C-terminal end. *J Biol Chem,* 282**,** 34958-67.

IACOBUCCI, I., PAPAYANNIDIS, C., LONETTI, A., FERRARI, A., BACCARANI, M. & MARTINELLI, G. 2012. Cytogenetic and molecular predictors of outcome in acute lymphocytic leukemia: recent developments. *Curr Hematol Malig Rep,* 7**,** 133-43.

IACOVELLI, S., HUG, E., BENNARDO, S., DUEHREN-VON MINDEN, M., GOBESSI, S., RINALDI, A., SULJAGIC, M., BILBAO, D., BOLASCO, G., ECKL-DORNA, J., NIEDERBERGER, V., AUTORE, F., SICA, S., LAURENTI, L., WANG, H., CORNALL, R. J., CLARKE, S. H., CROCE, C. M., BERTONI, F., JUMAA, H. & EFREMOV, D. G. 2015. Two types of BCR interactions are positively selected during leukemia development in the Emu-TCL1 transgenic mouse model of CLL. *Blood,* 125**,** 1578-88.

IBRAHIM, S., JILANI, I., O'BRIEN, S., ROGERS, A., MANSHOURI, T., GILES, F., FADERL, S., THOMAS, D., KANTARJIAN, H., KEATING, M. & ALBITAR, M. 2003. Clinical relevance of the expression of the CD31 ligand for CD38 in patients with B-cell chronic lymphocytic leukemia. *Cancer,* 97**,** 1914-9.

IBRAHIM, S., KEATING, M., DO, K. A., O'BRIEN, S., HUH, Y. O., JILANI, I., LERNER, S., KANTARJIAN, H. M. & ALBITAR, M. 2001. CD38 expression as an important prognostic factor in B-cell chronic lymphocytic leukemia. *Blood,* 98**,** 181-6.

IHANUS, E., UOTILA, L. M., TOIVANEN, A., VARIS, M. & GAHMBERG, C. G. 2007. Red-cell ICAM-4 is a ligand for the monocyte/macrophage integrin CD11c/CD18: characterization of the binding sites on ICAM-4. *Blood,* 109**,** 802-10.

ISHDORJ, G., JOHNSTON, J. B. & GIBSON, S. B. 2010. Inhibition of constitutive activation of STAT3 by curcurbitacin-I (JSI-124) sensitized human B-leukemia cells to apoptosis. *Mol Cancer Ther,* 9**,** 3302-14.

ISHDORJ, G., JOHNSTON, J. B. & GIBSON, S. B. 2011. Cucurbitacin-I (JSI-124) activates the JNK/c-Jun signaling pathway independent of apoptosis and cell cycle arrest in B leukemic cells. *BMC Cancer,* 11**,** 268.

IWAMARU, A., SZYMANSKI, S., IWADO, E., AOKI, H., YOKOYAMA, T., FOKT, I., HESS, K., CONRAD, C., MADDEN, T., SAWAYA, R., KONDO, S., PRIEBE, W. & KONDO, Y. 2007. A novel inhibitor of the STAT3 pathway induces apoptosis in malignant glioma cells both in vitro and in vivo. *Oncogene,* 26**,** 2435-44.

IYENGAR, S., CLEAR, A., BODOR, C., MAHARAJ, L., LEE, A., CALAMINICI, M., MATTHEWS, J., IQBAL, S., AUER, R., GRIBBEN, J. & JOEL, S. 2013. P110alpha-mediated constitutive PI3K signaling limits the efficacy of p110delta-selective inhibition in mantle cell lymphoma, particularly with multiple relapse. *Blood,* 121**,** 2274-84.

JACOBY, J. J., KALINOWSKI, A., LIU, M. G., ZHANG, S. S., GAO, Q., CHAI, G. X., JI, L., IWAMOTO, Y., LI, E., SCHNEIDER, M., RUSSELL, K. S. & FU, X. Y. 2003. Cardiomyocyte-restricted knockout of STAT3 results in higher sensitivity to inflammation, cardiac fibrosis, and heart failure with advanced age. *Proc Natl Acad Sci U S A,* 100**,** 12929-34.

JAIN, P., KEATING, M., RENNER, S., CLEELAND, C., XUELIN, H., GONZALEZ, G. N., HARRIS, D., LI, P., LIU, Z., VELETIC, I., ROZOVSKI, U., JAIN, N., THOMPSON, P., BOSE, P., DINARDO, C., FERRAJOLI, A., O'BRIEN, S., BURGER, J., WIERDA, W., VERSTOVSEK, S., KANTARJIAN, H. & ESTROV, Z. 2017. Ruxolitinib for symptom control in patients with chronic lymphocytic leukaemia: a single-group, phase 2 trial. *Lancet Haematol,* 4**,** e67-e74.

JAMROZIAK, K., TADMOR, T., ROBAK, T. & POLLIACK, A. 2015. Richter syndrome in chronic lymphocytic leukemia: updates on biology, clinical features and therapy. *Leuk Lymphoma,* 56**,** 1949-58.

JAYAPRAKASAM, B., SEERAM, N. P. & NAIR, M. G. 2003. Anticancer and antiinflammatory activities of cucurbitacins from Cucurbita andreana. *Cancer Lett,* 189**,** 11-6.

JEROMIN, S., WEISSMANN, S., HAFERLACH, C., DICKER, F., BAYER, K., GROSSMANN, V., ALPERMANN, T., ROLLER, A., KOHLMANN, A., HAFERLACH, T., KERN, W. & SCHNITTGER, S. 2014. SF3B1 mutations correlated to cytogenetics and mutations in NOTCH1, FBXW7, MYD88, XPO1 and TP53 in 1160 untreated CLL patients. *Leukemia,* 28**,** 108-17.

JEWELL, A. P. & YONG, K. L. 1997. Regulation and function of adhesion molecules in B-cell chronic lymphocytic leukaemia. *Acta Haematol,* 97**,** 67-72.

JIANG, R., JIN, Z., LIU, Z., SUN, L., WANG, L. & LI, K. 2011. Correlation of activated STAT3 expression with clinicopathologic features in lung adenocarcinoma and squamous cell carcinoma. *Mol Diagn Ther,* 15**,** 347-52.

JOHNSON, G. L. & LAPADAT, R. 2002. Mitogen-activated protein kinase pathways mediated by ERK, JNK, and p38 protein kinases. *Science,* 298**,** 1911-2.

JOU, S. T., CARPINO, N., TAKAHASHI, Y., PIEKORZ, R., CHAO, J. R., CARPINO, N., WANG, D. & IHLE, J. N. 2002. Essential, nonredundant role for the phosphoinositide 3-kinase p110delta in signaling by the B-cell receptor complex. *Mol Cell Biol,* 22**,** 8580-91.

K. SCHLESSINGER, D. E. L. 2005. Malignant transformation but not normal cell growth depends on signal transducer and activator of transcription 3. *Cancer Research,* 65**,** 5828-5834.

KAMEL, S., HORTON, L., YSEBAERT, L., LEVADE, M., BURBURY, K., TAN, S., COLE-SINCLAIR, M., REYNOLDS, J., FILSHIE, R., SCHISCHKA, S., KHOT, A., SANDHU, S., KEATING, M. J., NANDURKAR, H. & TAM, C. S. 2015. Ibrutinib inhibits collagen-mediated but not ADP-mediated platelet aggregation. *Leukemia,* 29**,** 783-7.

KANSAS, G. S. 1992. Structure and function of L-selectin. *APMIS,* 100**,** 287-93.

KAY, N. E. & ZARLING, J. 1987. Restoration of impaired natural killer cell activity of B-chronic lymphocytic leukemia patients by recombinant interleukin-2. *Am J Hematol,* 24**,** 161-7.

KINASHI, T. 2005. Intracellular signalling controlling integrin activation in lymphocytes. *Nat Rev Immunol,* 5**,** 546-59.

KLEIN, U. & DALLA-FAVERA, R. 2008. Germinal centres: role in B-cell physiology and malignancy. *Nat Rev Immunol,* 8**,** 22-33.

KONNIKOVA, L., KOTECKI, M., KRUGER, M. M. & COCHRAN, B. H. 2003. Knockdown of STAT3 expression by RNAi induces apoptosis in astrocytoma cells. *BMC Cancer,* 3**,** 23.

KOSKELA, H. L., ELDFORS, S., ELLONEN, P., VAN ADRICHEM, A. J., KUUSANMAKI, H., ANDERSSON, E. I., LAGSTROM, S., CLEMENTE, M. J., OLSON, T., JALKANEN, S. E., MAJUMDER, M. M., ALMUSA, H., EDGREN, H., LEPISTO, M., MATTILA, P., GUINTA, K., KOISTINEN, P., KUITTINEN, T., PENTTINEN, K., PARSONS, A., KNOWLES, J., SAARELA, J., WENNERBERG, K., KALLIONIEMI, O., PORKKA, K., LOUGHRAN, T. P., JR., HECKMAN, C. A., MACIEJEWSKI, J. P. & MUSTJOKI, S. 2012. Somatic STAT3 mutations in large granular lymphocytic leukemia. *N Engl J Med,* 366**,** 1905-13.

KOSTARELI, E., GOUNARI, M., JANUS, A., MURRAY, F., BROCHET, X., GIUDICELLI, V., POSPISILOVA, S., OSCIER, D., FORONI, L., DI CELLE, P. F., TICHY, B., PEDERSEN, L. B., JURLANDER, J., PONZONI, M., KOUVATSI, A., ANAGNOSTOPOULOS, A., THOMPSON, K., DARZENTAS, N., LEFRANC, M. P., BELESSI, C., ROSENQUIST, R., DAVI, F., GHIA, P. & STAMATOPOULOS, K. 2012. Antigen receptor stereotypy across B-cell lymphoproliferations: the case of IGHV4-59/IGKV3-20 receptors with rheumatoid factor activity. *Leukemia,* 26**,** 1127-31.

KOSTARELI, E., HADZIDIMITRIOU, A., STAVROYIANNI, N., DARZENTAS, N., ATHANASIADOU, A., GOUNARI, M., BIKOS, V., AGATHAGELIDIS, A., TOULOUMENIDOU, T., ZORBAS, I., KOUVATSI, A., LAOUTARIS, N., FASSAS, A., ANAGNOSTOPOULOS, A., BELESSI, C. & STAMATOPOULOS, K. 2009. Molecular evidence for EBV and CMV persistence in a subset of patients with chronic lymphocytic leukemia expressing stereotyped IGHV4-34 B-cell receptors. *Leukemia,* 23**,** 919-24.

KREBSBACH, P. H., KUZNETSOV, S. A., BIANCO, P. & ROBEY, P. G. 1999. Bone marrow stromal cells: characterization and clinical application. *Crit Rev Oral Biol Med,* 10**,** 165-81.

KUMAR, C. C. 1998. Signaling by integrin receptors. *Oncogene,* 17**,** 1365-73.

KUNKEL, E. J. & LEY, K. 1996. Distinct phenotype of E-selectin-deficient mice. E-selectin is required for slow leukocyte rolling in vivo. *Circ Res,* 79**,** 1196-204.

KUPPERS, R. 2005. Mechanisms of B-cell lymphoma pathogenesis. *Nat Rev Cancer,* 5**,** 251-62.

KUROSAKI, T. 1999. Genetic analysis of B cell antigen receptor signaling. *Annu Rev Immunol,* 17**,** 555-92.

KURTOVA, A. V., BALAKRISHNAN, K., CHEN, R., DING, W., SCHNABL, S., QUIROGA, M. P., SIVINA, M., WIERDA, W. G., ESTROV, Z., KEATING, M. J., SHEHATA, M., JAGER, U., GANDHI, V., KAY, N. E., PLUNKETT, W. & BURGER, J. A. 2009. Diverse marrow stromal cells protect CLL cells from spontaneous and drug-induced apoptosis: development of a reliable and reproducible system to assess stromal cell adhesion-mediated drug resistance. *Blood,* 114**,** 4441-50.

KUSE, R., SCHUSTER, S., SCHUBBE, H., DIX, S. & HAUSMANN, K. 1985. Blood lymphocyte volumes and diameters in patients with chronic lymphocytic leukemia and normal controls. *Blut,* 50**,** 243-8.

LAFOURESSE, F., BELLARD, E., LAURENT, C., MOUSSION, C., FOURNIE, J. J., YSEBAERT, L. & GIRARD, J. P. 2015. L-selectin controls trafficking of chronic lymphocytic leukemia cells in lymph node high endothelial venules in vivo. *Blood*.

LAGNEAUX, L., DELFORGE, A., BRON, D., DE BRUYN, C. & STRYCKMANS, P. 1998. Chronic lymphocytic leukemic B cells but not normal B cells are rescued from apoptosis by contact with normal bone marrow stromal cells. *Blood,* 91**,** 2387-96.

LANDAU, D. A., CARTER, S. L., STOJANOV, P., MCKENNA, A., STEVENSON, K., LAWRENCE, M. S., SOUGNEZ, C., STEWART, C., SIVACHENKO, A., WANG, L., WAN, Y., ZHANG, W., SHUKLA, S. A., VARTANOV, A., FERNANDES, S. M., SAKSENA, G., CIBULSKIS, K., TESAR, B., GABRIEL, S., HACOHEN, N., MEYERSON, M., LANDER, E. S., NEUBERG, D., BROWN, J. R., GETZ, G. & WU, C. J. 2013. Evolution and impact of subclonal mutations in chronic lymphocytic leukemia. *Cell,* 152**,** 714-26.

LANDAU, D. A. & WU, C. J. 2013. Chronic lymphocytic leukemia: molecular heterogeneity revealed by high-throughput genomics. *Genome Med,* 5**,** 47.

LANEMO MYHRINDER, A., HELLQVIST, E., SIDOROVA, E., SODERBERG, A., BAXENDALE, H., DAHLE, C., WILLANDER, K., TOBIN, G., BACKMAN, E., SODERBERG, O., ROSENQUIST, R., HORKKO, S. & ROSEN, A. 2008. A new perspective: molecular motifs on oxidized LDL, apoptotic cells, and bacteria are targets for chronic lymphocytic leukemia antibodies. *Blood,* 111**,** 3838-48.

LANHAM, S., HAMBLIN, T., OSCIER, D., IBBOTSON, R., STEVENSON, F. & PACKHAM, G. 2003. Differential signaling via surface IgM is associated with VH gene mutational status and CD38 expression in chronic lymphocytic leukemia. *Blood,* 101**,** 1087-93.

LARRAYOZ, M., ROSE-ZERILLI, M. J., KADALAYIL, L., PARKER, H., BLAKEMORE, S., FORSTER, J., DAVIS, Z., STEELE, A. J., COLLINS, A., ELSE, M., CATOVSKY, D., OSCIER, D. G. & STREFFORD, J. C. 2017. Non-coding NOTCH1 mutations in chronic lymphocytic leukemia; their clinical impact in the UK CLL4 trial. *Leukemia,* 31**,** 510-514.

LAWRENCE, M. B., KANSAS, G. S., KUNKEL, E. J. & LEY, K. 1997. Threshold levels of fluid shear promote leukocyte adhesion through selectins (CD62L,P,E). *J Cell Biol,* 136**,** 717-27.

LAWRENCE, M. B. & SPRINGER, T. A. 1991. Leukocytes roll on a selectin at physiologic flow rates: distinction from and prerequisite for adhesion through integrins. *Cell,* 65**,** 859-73.

LEDERMAN, S., YELLIN, M. J., CLEARY, A. M., PERNIS, A., INGHIRAMI, G., COHN, L. E., COVEY, L. R., LEE, J. J., ROTHMAN, P. & CHESS, L. 1994. T-BAM/CD40-L on helper T lymphocytes augments lymphokine-induced B cell Ig

isotype switch recombination and rescues B cells from programmed cell death. *J Immunol,* 152**,** 2163-71.

LEE, Y. K., SHANAFELT, T. D., BONE, N. D., STREGE, A. K., JELINEK, D. F. & KAY, N. E. 2005. VEGF receptors on chronic lymphocytic leukemia (CLL) B cells interact with STAT 1 and 3: implication for apoptosis resistance. *Leukemia,* 19**,** 513-23.

LEVADE, M., DAVID, E., GARCIA, C., LAURENT, P. A., CADOT, S., MICHALLET, A. S., BORDET, J. C., TAM, C., SIE, P., YSEBAERT, L. & PAYRASTRE, B. 2014. Ibrutinib treatment affects collagen and von Willebrand factor-dependent platelet functions. *Blood,* 124**,** 3991-5.

LEVY, D. E. & LEE, C. K. 2002. What does Stat3 do? *J Clin Invest,* 109**,** 1143-8.

LI, H., LIU, A., ZHAO, Z., XU, Y., LIN, J., JOU, D. & LI, C. 2011. Fragment-based drug design and drug repositioning using multiple ligand simultaneous docking (MLSD): identifying celecoxib and template compounds as novel inhibitors of signal transducer and activator of transcription 3 (STAT3). *J Med Chem,* 54**,** 5592-6.

LIAO, W., JORDAAN, G., NHAM, P., PHAN, R. T., PELEGRINI, M. & SHARMA, S. 2015. Gene expression and splicing alterations analyzed by high throughput RNA sequencing of chronic lymphocytic leukemia specimens. *BMC Cancer,* 15**,** 714.

LICHTMAN, M. A. 2008. Battling the hematological malignancies: the 200 years' war. *Oncologist,* 13**,** 126-38.

LIU, F. T., JIA, L., WANG, P., WANG, H., FARREN, T. W. & AGRAWAL, S. G. 2016. STAT3 and NF-kappaB cooperatively control in vitro spontaneous apoptosis and poor chemo-responsiveness in patients with chronic lymphocytic leukemia. *Oncotarget,* 7**,** 32031-45.

LIU, W., MECKEL, T., TOLAR, P., SOHN, H. W. & PIERCE, S. K. 2010. Intrinsic properties of immunoglobulin IgG1 isotype-switched B cell receptors promote microclustering and the initiation of signaling. *Immunity,* 32**,** 778-89.

LIU, Y. J., JOSHUA, D. E., WILLIAMS, G. T., SMITH, C. A., GORDON, J. & MACLENNAN, I. C. 1989. Mechanism of antigen-driven selection in germinal centres. *Nature,* 342**,** 929-31.

LIU, Z., HAZAN-HALEVY, I., HARRIS, D. M., LI, P., FERRAJOLI, A., FADERL, S., KEATING, M. J. & ESTROV, Z. 2011. STAT-3 activates NF-kappaB in chronic lymphocytic leukemia cells. *Mol Cancer Res,* 9**,** 507-15.

LIVAK, K. J. & SCHMITTGEN, T. D. 2001. Analysis of relative gene expression data using real-time quantitative PCR and the 2(-Delta Delta C(T)) Method. *Methods,* 25**,** 402-8.

LOHR, J. G., STOJANOV, P., LAWRENCE, M. S., AUCLAIR, D., CHAPUY, B., SOUGNEZ, C., CRUZ-GORDILLO, P., KNOECHEL, B., ASMANN, Y. W., SLAGER, S. L., NOVAK, A. J., DOGAN, A., ANSELL, S. M., LINK, B. K., ZOU, L., GOULD, J., SAKSENA, G., STRANSKY, N., RANGEL-ESCARENO, C., FERNANDEZ-LOPEZ, J. C., HIDALGO-MIRANDA, A., MELENDEZ-ZAJGLA, J., HERNANDEZ-LEMUS, E., SCHWARZ-CRUZ Y CELIS, A., IMAZ-ROSSHANDLER, I., OJESINA, A. I., JUNG, J., PEDAMALLU, C. S., LANDER, E. S., HABERMANN, T. M., CERHAN, J. R., SHIPP, M. A., GETZ, G. & GOLUB, T. R. 2012. Discovery and prioritization of somatic mutations in diffuse large B-cell lymphoma (DLBCL) by whole-exome sequencing. *Proc Natl Acad Sci U S A,* 109**,** 3879-84.

LONG, E. T., BAKER, S., OLIVEIRA, V., SAWITZKI, B. & WOOD, K. J. 2010. Alpha-1,2-mannosidase and hence N-glycosylation are required for regulatory T cell migration and allograft tolerance in mice. *PLoS One,* 5**,** e8894.

LOU, W., NI, Z., DYER, K., TWEARDY, D. J. & GAO, A. C. 2000. Interleukin-6 induces prostate cancer cell growth accompanied by activation of stat3 signaling pathway. *Prostate,* 42**,** 239-42.

LU, K., FANG, X. S., FENG, L. L., JIANG, Y. J., ZHOU, X. X., LIU, X., LI, P. P., CHEN, N., DING, M., WANG, N., ZHANG, J. & WANG, X. 2015. The STAT3 inhibitor WP1066 reverses the resistance of chronic lymphocytic leukemia cells to histone deacetylase inhibitors induced by interleukin-6. *Cancer Lett,* 359**,** 250-8.

LUNDIN, J., KIMBY, E., BERGMANN, L., KARAKAS, T., MELLSTEDT, H. & OSTERBORG, A. 2001. Interleukin 4 therapy for patients with chronic lymphocytic leukaemia: a phase I/II study. *Br J Haematol,* 112**,** 155-60.

LUTZNY, G., KOCHER, T., SCHMIDT-SUPPRIAN, M., RUDELIUS, M., KLEIN-HITPASS, L., FINCH, A. J., DURIG, J., WAGNER, M., HAFERLACH, C., KOHLMANN, A., SCHNITTGER, S., SEIFERT, M., WANNINGER, S., ZABORSKY, N., OOSTENDORP, R., RULAND, J., LEITGES, M., KUHNT, T., SCHAFER, Y., LAMPL, B., PESCHEL, C., EGLE, A. & RINGSHAUSEN, I. 2013. Protein kinase c-beta-dependent activation of NF-kappaB in stromal cells is indispensable for the survival of chronic lymphocytic leukemia B cells in vivo. *Cancer Cell,* 23**,** 77-92.

MA, L. D., ZHOU, M., WEN, S. H., NI, C., JIANG, L. J., FAN, J. & XIA, L. 2010. Effects of STAT3 silencing on fate of chronic myelogenous leukemia K562 cells. *Leuk Lymphoma,* 51**,** 1326-36.

MA, Z., WANG, G., CHEN, X., OU, Z. & ZOU, F. 2014. Association of STAT3 common variations with obesity and hypertriglyceridemia: protective and contributive effects. *Int J Mol Sci,* 15**,** 12258-69.

MAFFEI, R., FIORCARI, S., BULGARELLI, J., MARTINELLI, S., CASTELLI, I., DEAGLIO, S., DEBBIA, G., FONTANA, M., COLUCCIO, V., BONACORSI, G., ZUCCHINI, P., NARNI, F., TORELLI, G., LUPPI, M. & MARASCA, R. 2012. Physical contact with endothelial cells through beta1- and beta2- integrins rescues chronic lymphocytic leukemia cells from spontaneous and drug-induced apoptosis and induces a peculiar gene expression profile in leukemic cells. *Haematologica,* 97**,** 952-60.

MAINOU-FOWLER, T., PROCTOR, S. J., MILLER, S. & DICKINSON, A. M. 2001. Expression and production of interleukin 4 in B-cell chronic lymphocytic leukaemia. *Leuk Lymphoma,* 42**,** 689-98.

MAKI, G., HAYES, G. M., NAJI, A., TYLER, T., CAROSELLA, E. D., ROUAS-FREISS, N. & GREGORY, S. A. 2008. NK resistance of tumor cells from multiple myeloma and chronic lymphocytic leukemia patients: implication of HLA-G. *Leukemia,* 22**,** 998-1006.

MANGOLINI, M., DE BOER, J., WALF-VORDERWULBECKE, V., PIETERS, R., DEN BOER, M. L. & WILLIAMS, O. 2013. STAT3 mediates oncogenic addiction to TEL-AML1 in t(12;21) acute lymphoblastic leukemia. *Blood,* 122**,** 542-9.

MARCHESI, V. T. & GOWANS, J. L. 1964. The Migration of Lymphocytes through the Endothelium of Venules in Lymph Nodes: An Electron Microscope Study. *Proc R Soc Lond B Biol Sci,* 159**,** 283-90.

MARITANO, D., SUGRUE, M. L., TININI, S., DEWILDE, S., STROBL, B., FU, X., MURRAY-TAIT, V., CHIARLE, R. & POLI, V. 2004. The STAT3 isoforms alpha and beta have unique and specific functions. *Nat Immunol,* 5**,** 401-9.

MARTI, G. E., RAWSTRON, A. C., GHIA, P., HILLMEN, P., HOULSTON, R. S., KAY, N., SCHLEINITZ, T. A., CAPORASO, N. & INTERNATIONAL FAMILIAL, C. L. L. C. 2005. Diagnostic criteria for monoclonal B-cell lymphocytosis. *Br J Haematol,* 130**,** 325-32.

MARTINET, L., GARRIDO, I., FILLERON, T., LE GUELLEC, S., BELLARD, E., FOURNIE, J. J., ROCHAIX, P. & GIRARD, J. P. 2011. Human solid tumors contain high endothelial venules: association with T- and B-lymphocyte infiltration and favorable prognosis in breast cancer. *Cancer Res,* 71**,** 5678-87.

MARTINEZ-TRILLOS, A., PINYOL, M., NAVARRO, A., AYMERICH, M., JARES, P., JUAN, M., ROZMAN, M., COLOMER, D., DELGADO, J., GINE, E., GONZALEZ-DIAZ, M., HERNANDEZ-RIVAS, J. M., COLADO, E., RAYON, C.,

PAYER, A. R., TEROL, M. J., NAVARRO, B., QUESADA, V., PUENTE, X. S., ROZMAN, C., LOPEZ-OTIN, C., CAMPO, E., LOPEZ-GUILLERMO, A. & VILLAMOR, N. 2014. Mutations in TLR/MYD88 pathway identify a subset of young chronic lymphocytic leukemia patients with favorable outcome. *Blood,* 123**,** 3790-6.

MASCARENHAS, J. & HOFFMAN, R. 2012. Ruxolitinib: the first FDA approved therapy for the treatment of myelofibrosis. *Clin Cancer Res,* 18**,** 3008-14.

MATRAI, Z. 2005. CD38 as a prognostic marker in CLL. *Hematology,* 10**,** 39-46.

MATUTES, E., OSCIER, D., GARCIA-MARCO, J., ELLIS, J., COPPLESTONE, A., GILLINGHAM, R., HAMBLIN, T., LENS, D., SWANSBURY, G. J. & CATOVSKY, D. 1996. Trisomy 12 defines a group of CLL with atypical morphology: correlation between cytogenetic, clinical and laboratory features in 544 patients. *Br J Haematol,* 92**,** 382-8.

MCCLANAHAN, F., HANNA, B., MILLER, S., CLEAR, A. J., LICHTER, P., GRIBBEN, J. G. & SEIFFERT, M. 2015. PD-L1 checkpoint blockade prevents immune dysfunction and leukemia development in a mouse model of chronic lymphocytic leukemia. *Blood,* 126**,** 203-11.

MCEVER, R. P. & ZHU, C. 2010. Rolling cell adhesion. *Annu Rev Cell Dev Biol,* 26**,** 363-96.

MEADS, M. B., GATENBY, R. A. & DALTON, W. S. 2009. Environment-mediated drug resistance: a major contributor to minimal residual disease. *Nat Rev Cancer,* 9**,** 665-74.

MEBIUS, R. E., DOWBENKO, D., WILLIAMS, A., FENNIE, C., LASKY, L. A. & WATSON, S. R. 1993. Expression of GlyCAM-1, an endothelial ligand for L-selectin, is affected by afferent lymphatic flow. *J Immunol,* 151**,** 6769-76.

MELO, J. V., CATOVSKY, D. & GALTON, D. A. 1986. The relationship between chronic lymphocytic leukaemia and prolymphocytic leukaemia. II. Patterns of evolution of 'prolymphocytoid' transformation. *Br J Haematol,* 64**,** 77-86.

MESSMER, B. T., ALBESIANO, E., EFREMOV, D. G., GHIOTTO, F., ALLEN, S. L., KOLITZ, J., FOA, R., DAMLE, R. N., FAIS, F., MESSMER, D., RAI, K. R., FERRARINI, M. & CHIORAZZI, N. 2004. Multiple distinct sets of stereotyped antigen receptors indicate a role for antigen in promoting chronic lymphocytic leukemia. *J Exp Med,* 200**,** 519-25.

MESSMER, B. T., MESSMER, D., ALLEN, S. L., KOLITZ, J. E., KUDALKAR, P., CESAR, D., MURPHY, E. J., KODURU, P., FERRARINI, M., ZUPO, S., CUTRONA, G., DAMLE, R. N., WASIL, T., RAI, K. R., HELLERSTEIN, M. K. & CHIORAZZI, N. 2005. In vivo measurements document the dynamic cellular kinetics of chronic lymphocytic leukemia B cells. *J Clin Invest,* 115**,** 755-64.

MILLER, C. J., KASSEM, H. S., PEPPER, S. D., HEY, Y., WARD, T. H. & MARGISON, G. P. 2003. Mycoplasma infection significantly alters microarray gene expression profiles. *Biotechniques,* 35**,** 812-4.

MILLER, C. L., LEE, J. H., KIEFF, E. & LONGNECKER, R. 1994. An integral membrane protein (LMP2) blocks reactivation of Epstein-Barr virus from latency following surface immunoglobulin crosslinking. *Proc Natl Acad Sci U S A,* 91**,** 772-6.

MILLER, C. L., LONGNECKER, R. & KIEFF, E. 1993. Epstein-Barr virus latent membrane protein 2A blocks calcium mobilization in B lymphocytes. *J Virol,* 67**,** 3087-94.

MIYASAKA, M. & TANAKA, T. 2004. Lymphocyte trafficking across high endothelial venules: dogmas and enigmas. *Nat Rev Immunol,* 4**,** 360-70.

MIZUNO, T. & ROTHSTEIN, T. L. 2005. B cell receptor (BCR) cross-talk: CD40 engagement enhances BCR-induced ERK activation. *J Immunol,* 174**,** 3369-76.

MOCKRIDGE, C. I., POTTER, K. N., WHEATLEY, I., NEVILLE, L. A., PACKHAM, G. & STEVENSON, F. K. 2007. Reversible anergy of sIgM-mediated signaling in the two subsets of CLL defined by VH-gene mutational status. *Blood,* 109**,** 4424-31.

MOHLE, R., FAILENSCHMID, C., BAUTZ, F. & KANZ, L. 1999. Overexpression of the chemokine receptor CXCR4 in B cell chronic lymphocytic leukemia is associated with increased functional response to stromal cell-derived factor-1 (SDF-1). *Leukemia,* 13**,** 1954-9.

MONTRESOR, A., TOFFALI, L., MIRENDA, M., RIGO, A., VINANTE, F. & LAUDANNA, C. 2015. JAK2 tyrosine kinase mediates integrin activation induced by CXCL12 in B-cell chronic lymphocytic leukemia. *Oncotarget,* 6**,** 34245-57.

MOUSSION, C. & GIRARD, J. P. 2011. Dendritic cells control lymphocyte entry to lymph nodes through high endothelial venules. *Nature,* 479**,** 542-6.

MUELLER, S. N. & GERMAIN, R. N. 2009. Stromal cell contributions to the homeostasis and functionality of the immune system. *Nat Rev Immunol,* 9**,** 618-29.

MURPHY, P. M., BAGGIOLINI, M., CHARO, I. F., HEBERT, C. A., HORUK, R., MATSUSHIMA, K., MILLER, L. H., OPPENHEIM, J. J. & POWER, C. A. 2000. International union of pharmacology. XXII. Nomenclature for chemokine receptors. *Pharmacol Rev,* 52**,** 145-76.

MUSTEANU, M., BLAAS, L., MAIR, M., SCHLEDERER, M., BILBAN, M., TAUBER, S., ESTERBAUER, H., MUELLER, M., CASANOVA, E., KENNER, L., POLI, V. & EFERL, R. 2010. Stat3 is a negative regulator of intestinal tumor progression in Apc(Min) mice. *Gastroenterology,* 138**,** 1003-11 e1-5.

MUZIO, M., APPOLLONIO, B., SCIELZO, C., FRENQUELLI, M., VANDONI, I., BOUSSIOTIS, V. 2008. Constitutive activation of distinct BCR---signaling pathways in a subset of CLL patients: a molecular signature of anergy. Blood, 112, 188–195.

NABHAN, C., ASCHEBROOK-KILFOY, B., CHIU, B. C., SMITH, S. M., SHANAFELT, T. D., EVENS, A. M. & KAY, N. E. 2014. The impact of race, ethnicity, age and sex on clinical outcome in chronic lymphocytic leukemia: a comprehensive Surveillance, Epidemiology, and End Results analysis in the modern era. *Leuk Lymphoma,* 55**,** 2778-84.

NARDINI, M., PISU, P., GENTILI, V., NATELLA, F., DI FELICE, M., PICCOLELLA, E. & SCACCINI, C. 1998. Effect of caffeic acid on tert-butyl hydroperoxide-induced oxidative stress in U937. *Free Radic Biol Med,* 25**,** 1098-105.

NCT02912754, C. G. ClinicalTrials.gov [Internet]. Bethesda (MD): National Library of Medicine

(US). 2000 Feb 29 - . NCT02912754 Ruxolitinib Combined With Ibrutinib in Chronic Lymphocytic Leukemia Patients September 19, 2016 [cited June 23, 2017] [1 page]https://clinicaltrials.gov/ct2/show/NCT02912754.

NG, D. C., LIN, B. H., LIM, C. P., HUANG, G., ZHANG, T., POLI, V. & CAO, X. 2006. Stat3 regulates microtubules by antagonizing the depolymerization activity of stathmin. *J Cell Biol,* 172**,** 245-57.

NG, I. H., BOGOYEVITCH, M. A. & JANS, D. A. 2014. Cytokine-induced slowing of STAT3 nuclear import; faster basal trafficking of the STAT3beta isoform. *Traffic,* 15**,** 946-60.

NG, I. H., NG, D. C., JANS, D. A. & BOGOYEVITCH, M. A. 2012. Selective STAT3-alpha or -beta expression reveals spliceform-specific phosphorylation kinetics, nuclear retention and distinct gene expression outcomes. *Biochem J,* 447**,** 125-36.

NICHOLSON, M. W., BARCLAY, A. N., SINGER, M. S., ROSEN, S. D. & VAN DER MERWE, P. A. 1998. Affinity and kinetic analysis of L-selectin (CD62L) binding to glycosylation-dependent cell-adhesion molecule-1. *J Biol Chem,* 273**,** 763-70.

NIELSEN, M., KAESTEL, C. G., ERIKSEN, K. W., WOETMANN, A., STOKKEDAL, T., KALTOFT, K., GEISLER, C., ROPKE, C. & ODUM, N. 1999. Inhibition of constitutively activated Stat3 correlates with altered Bcl-2/Bax expression and induction of apoptosis in mycosis fungoides tumor cells. *Leukemia,* 13**,** 735-8.

NISHIO, M., ENDO, T., TSUKADA, N., OHATA, J., KITADA, S., REED, J. C., ZVAIFLER, N. J. & KIPPS, T. J. 2005. Nurselike cells express BAFF and APRIL, which can promote survival of chronic lymphocytic leukemia cells via a paracrine pathway distinct from that of SDF-1alpha. *Blood,* 106**,** 1012-20.

O'BRIEN, M. P., BRAD S. KAHL, STEVEN M. HORWITZ, FRANCINE M. FOSS, PIERLUIGI PORCU, JENNIFER SWEENEY, KERSTIN ALLEN, KERRIE FAIA, HOWARD M. STERN, PATRICK KELLY AND IAN FLINN 2014. Duvelisib (IPI-145), a PI3K-δ,γ Inhibitor, Is Clinically Active in Patients with Relapsed/Refractory Chronic Lymphocytic Leukemia. *Blood* 124:3334.

O'BRIEN, S. M., LAMANNA, N., KIPPS, T. J., FLINN, I., ZELENETZ, A. D., BURGER, J. A., KEATING, M., MITRA, S., HOLES, L., YU, A. S., JOHNSON, D. M., MILLER, L. L., KIM, Y., DANSEY, R. D., DUBOWY, R. L. & COUTRE, S. E. 2015. A phase 2 study of idelalisib plus rituximab in treatment-naive older patients with chronic lymphocytic leukemia. *Blood,* 126**,** 2686-94.

OETTINGER, M. A., SCHATZ, D. G., GORKA, C. & BALTIMORE, D. 1990. RAG-1 and RAG-2, adjacent genes that synergistically activate V(D)J recombination. *Science,* 248**,** 1517-23.

OH, D. Y., LEE, S. H., HAN, S. W., KIM, M. J., KIM, T. M., KIM, T. Y., HEO, D. S., YUASA, M., YANAGIHARA, Y. & BANG, Y. J. 2015. Phase I Study of OPB-31121, an Oral STAT3 Inhibitor, in Patients with Advanced Solid Tumors. *Cancer Res Treat,* 47**,** 607-15.

OHGAMI, R. S., MA, L., MONABATI, A., ZEHNDER, J. L. & ARBER, D. A. 2014. STAT3 mutations are present in aggressive B-cell lymphomas including a subset of diffuse large B-cell lymphomas with CD30 expression. *Haematologica,* 99**,** e105-7.

OJHA, J., AYRES, J., SECRETO, C., TSCHUMPER, R., RABE, K., VAN DYKE, D., SLAGER, S., SHANAFELT, T., FONSECA, R., KAY, N. E. & BRAGGIO, E. 2015. Deep sequencing identifies genetic heterogeneity and recurrent convergent evolution in chronic lymphocytic leukemia. *Blood,* 125**,** 492-8.

OLIVEIRA, G. B., PEREIRA, F. G., METZE, K. & LORAND-METZE, I. 2001. Spontaneous apoptosis in chronic lymphocytic leukemia and its relationship to clinical and cell kinetic parameters. *Cytometry,* 46**,** 329-35.

OSCIER, D. G., GARDINER, A. C., MOULD, S. J., GLIDE, S., DAVIS, Z. A., IBBOTSON, R. E., CORCORAN, M. M., CHAPMAN, R. M., THOMAS, P. W., COPPLESTONE, J. A., ORCHARD, J. A. & HAMBLIN, T. J. 2002. Multivariate analysis of prognostic factors in CLL: clinical stage, IGVH gene mutational status, and loss or mutation of the p53 gene are independent prognostic factors. *Blood,* 100**,** 1177-84.

OSCIER, D. G., ROSE-ZERILLI, M. J., WINKELMANN, N., GONZALEZ DE CASTRO, D., GOMEZ, B., FORSTER, J., PARKER, H., PARKER, A., GARDINER, A., COLLINS, A., ELSE, M., CROSS, N. C., CATOVSKY, D. & STREFFORD, J. C. 2013. The clinical significance of NOTCH1 and SF3B1 mutations in the UK LRF CLL4 trial. *Blood,* 121**,** 468-75.

OSCIER, D. G., STEVENS, J., HAMBLIN, T. J., PICKERING, R. M., LAMBERT, R. & FITCHETT, M. 1990. Correlation of chromosome abnormalities with laboratory features and clinical course in B-cell chronic lymphocytic leukaemia. *Br J Haematol,* 76**,** 352-8.

OSMOND, D. G. 1990. B cell development in the bone marrow. *Semin Immunol,* 2**,** 173-80.

OUILLETTE, P., SAIYA-CORK, K., SEYMOUR, E., LI, C., SHEDDEN, K. & MALEK, S. N. 2013. Clonal evolution, genomic drivers, and effects of therapy in chronic lymphocytic leukemia. *Clin Cancer Res,* 19**,** 2893-904.

PACKHAM, G., KRYSOV, S., ALLEN, A., SAVELYEVA, N., STEELE, A. J., FORCONI, F. & STEVENSON, F. K. 2014. The outcome of B-cell receptor signaling in

chronic lymphocytic leukemia: proliferation or anergy. *Haematologica,* 99**,** 1138-48.

PAGGETTI, J., HADERK, F., SEIFFERT, M., JANJI, B., DISTLER, U., AMMERLAAN, W., KIM, Y. J., ADAM, J., LICHTER, P., SOLARY, E., BERCHEM, G. & MOUSSAY, E. 2015. Exosomes released by chronic lymphocytic leukemia cells induce the transition of stromal cells into cancer-associated fibroblasts. *Blood,* 126**,** 1106-17.

PAL, S. K., NGUYEN, C. T., MORITA, K. I., MIKI, Y., KAYAMORI, K., YAMAGUCHI, A. & SAKAMOTO, K. 2016. THBS1 is induced by TGFB1 in the cancer stroma and promotes invasion of oral squamous cell carcinoma. *J Oral Pathol Med,* 45**,** 730-739.

PALLANDRE, J. R., BRILLARD, E., CREHANGE, G., RADLOVIC, A., REMY-MARTIN, J. P., SAAS, P., ROHRLICH, P. S., PIVOT, X., LING, X., TIBERGHIEN, P. & BORG, C. 2007. Role of STAT3 in CD4+CD25+FOXP3+ regulatory lymphocyte generation: implications in graft-versus-host disease and antitumor immunity. *J Immunol,* 179**,** 7593-604.

PANAYIOTIDIS, P., JONES, D., GANESHAGURU, K., FORONI, L. & HOFFBRAND, A. V. 1996. Human bone marrow stromal cells prevent apoptosis and support the survival of chronic lymphocytic leukaemia cells in vitro. *Br J Haematol,* 92**,** 97-103.

PANSKY, A., HILDEBRAND, P., FASLER-KAN, E., BASELGIA, L., KETTERER, S., BEGLINGER, C. & HEIM, M. H. 2000. Defective Jak-STAT signal transduction pathway in melanoma cells resistant to growth inhibition by interferon-alpha. *Int J Cancer,* 85**,** 720-5.

PAPAIOANNOU, T. G. & STEFANADIS, C. 2005. Vascular wall shear stress: basic principles and methods. *Hellenic J Cardiol,* 46**,** 9-15.

PARK, J. S., KWOK, S. K., LIM, M. A., KIM, E. K., RYU, J. G., KIM, S. M., OH, H. J., JU, J. H., PARK, S. H., KIM, H. Y. & CHO, M. L. 2014. STA-21, a promising STAT-3 inhibitor that reciprocally regulates Th17 and Treg cells, inhibits osteoclastogenesis in mice and humans and alleviates autoimmune inflammation in an experimental model of rheumatoid arthritis. *Arthritis Rheumatol,* 66**,** 918-29.

PASIKOWSKA M, WALSBY E, APOLLONIO B, CUTHILL K, PHILLIPS E, COULTER E, LONGHI MS, MA Y, YALLOP D, BARBER LD, PATTEN P, FEGAN C, RAMSAY AG, PEPPER C, DEVEREUX S, BUGGINS AG. 2016. Phenotype and immune function of lymph node and peripheral blood CLL cells are linked to transendothelial migration. *Blood* 128, 563-73.

PATTEN, P. E., BUGGINS, A. G., RICHARDS, J., WOTHERSPOON, A., SALISBURY, J., MUFTI, G. J., HAMBLIN, T. J. & DEVEREUX, S. 2008. CD38 expression in chronic lymphocytic leukemia is regulated by the tumor microenvironment. *Blood,* 111**,** 5173-81.

PAYELLE-BROGARD, B., MAGNAC, C., ALCOVER, A., ROUX, P. & DIGHIERO, G. 2002. Defective assembly of the B-cell receptor chains accounts for its low expression in B-chronic lymphocytic leukaemia. *Br J Haematol,* 118**,** 976-85.

PEDE, V., ROMBOUT, A., VERMEIRE, J., NAESSENS, E., MESTDAGH, P., ROBBERECHT, N., VANDERSTRAETEN, H., VAN ROY, N., VANDESOMPELE, J., SPELEMAN, F., PHILIPPE, J. & VERHASSELT, B. 2013. CLL cells respond to B-Cell receptor stimulation with a microRNA/mRNA signature associated with MYC activation and cell cycle progression. *PLoS One,* 8**,** e60275.

PEDERSEN, I. M., KITADA, S., LEONI, L. M., ZAPATA, J. M., KARRAS, J. G., TSUKADA, N., KIPPS, T. J., CHOI, Y. S., BENNETT, F. & REED, J. C. 2002. Protection of CLL B cells by a follicular dendritic cell line is dependent on induction of Mcl-1. *Blood,* 100**,** 1795-801.

PETLICKOVSKI, A., LAURENTI, L., LI, X., MARIETTI, S., CHIUSOLO, P., SICA, S., LEONE, G. & EFREMOV, D. G. 2005. Sustained signaling through the B-cell receptor induces Mcl-1 and promotes survival of chronic lymphocytic leukemia B cells. *Blood,* 105**,** 4820-7.

PETRO, J. B., RAHMAN, S. M., BALLARD, D. W. & KHAN, W. N. 2000. Bruton's tyrosine kinase is required for activation of IkappaB kinase and nuclear factor kappaB in response to B cell receptor engagement. *J Exp Med,* 191**,** 1745-54.

PIZZOLO, G., CHILOSI, M., AMBROSETTI, A., SEMENZATO, G., FIORE-DONATI, L. & PERONA, G. 1983. Immunohistologic study of bone marrow involvement in B-chronic lymphocytic leukemia. *Blood,* 62**,** 1289-96.

PLANDER, M., SEEGERS, S., UGOCSAI, P., DIERMEIER-DAUCHER, S., IVANYI, J., SCHMITZ, G., HOFSTADTER, F., SCHWARZ, S., ORSO, E., KNUCHEL, R. & BROCKHOFF, G. 2009. Different proliferative and survival capacity of CLL-cells in a newly established in vitro model for pseudofollicles. *Leukemia,* 23**,** 2118-28.

POLLYEA, S. C., LIA GORE, NICHOLE ADLER, PAMELA HARRIS, MITCH A. PHELPS, AMY J. JOHNSON, YONGHUA LING, HAO LI, JONATHAN A GUTMAN AND JOHN C. BYRD 2014. A Dose Escalation Study of Ibrutinib with Lenalidomide for Relapsed and Refractory Chronic Lymphocytic Leukemia/Small Lymphocytic Lymphoma. *Blood (ASH Annual Meeting Abstracts)*.

PONADER, S., CHEN, S. S., BUGGY, J. J., BALAKRISHNAN, K., GANDHI, V., WIERDA, W. G., KEATING, M. J., O'BRIEN, S., CHIORAZZI, N. & BURGER, J. A. 2012. The Bruton tyrosine kinase inhibitor PCI-32765 thwarts chronic lymphocytic leukemia cell survival and tissue homing in vitro and in vivo. *Blood,* 119**,** 1182-9.

PONTIKOGLOU, C., KASTRINAKI, M. C., KLAUS, M., KALPADAKIS, C., KATONIS, P., ALPANTAKI, K., PANGALIS, G. A. & PAPADAKI, H. A. 2013. Study of the quantitative, functional, cytogenetic, and immunoregulatory properties of bone marrow mesenchymal stem cells in patients with B-cell chronic lymphocytic leukemia. *Stem Cells Dev,* 22**,** 1329-41.

POSTIGO, A. A., CORBI, A. L., SANCHEZ-MADRID, F. & DE LANDAZURI, M. O. 1991. Regulated expression and function of CD11c/CD18 integrin on human B lymphocytes. Relation between attachment to fibrinogen and triggering of proliferation through CD11c/CD18. *J Exp Med,* 174**,** 1313-22.

PRYSTAS, E. M., PARKER, C. J., HOLGUIN, M. H. & BOHNSACK, J. F. 1993. Aberrant glycosylation of L-selectin on the lymphocytes of chronic lymphocytic leukemia. *Leukemia,* 7**,** 1355-62.

PUENTE, X. S., PINYOL, M., QUESADA, V., CONDE, L., ORDONEZ, G. R., VILLAMOR, N., ESCARAMIS, G., JARES, P., BEA, S., GONZALEZ-DIAZ, M., BASSAGANYAS, L., BAUMANN, T., JUAN, M., LOPEZ-GUERRA, M., COLOMER, D., TUBIO, J. M., LOPEZ, C., NAVARRO, A., TORNADOR, C., AYMERICH, M., ROZMAN, M., HERNANDEZ, J. M., PUENTE, D. A., FREIJE, J. M., VELASCO, G., GUTIERREZ-FERNANDEZ, A., COSTA, D., CARRIO, A., GUIJARRO, S., ENJUANES, A., HERNANDEZ, L., YAGUE, J., NICOLAS, P., ROMEO-CASABONA, C. M., HIMMELBAUER, H., CASTILLO, E., DOHM, J. C., DE SANJOSE, S., PIRIS, M. A., DE ALAVA, E., SAN MIGUEL, J., ROYO, R., GELPI, J. L., TORRENTS, D., OROZCO, M., PISANO, D. G., VALENCIA, A., GUIGO, R., BAYES, M., HEATH, S., GUT, M., KLATT, P., MARSHALL, J., RAINE, K., STEBBINGS, L. A., FUTREAL, P. A., STRATTON, M. R., CAMPBELL, P. J., GUT, I., LOPEZ-GUILLERMO, A., ESTIVILL, X., MONTSERRAT, E., LOPEZ-OTIN, C. & CAMPO, E. 2011. Whole-genome sequencing identifies recurrent mutations in chronic lymphocytic leukaemia. *Nature,* 475**,** 101-5.

PULTE, D., REDANIEL, M. T., BIRD, J. & JEFFREYS, M. 2015. Survival for patients with chronic leukemias in the US and Britain: Age-related disparities and changes in the early 21st century. *Eur J Haematol,* 94**,** 540-5.

PURROY, N., ABRISQUETA, P., CARABIA, J., CARPIO, C., PALACIO, C., BOSCH, F. & CRESPO, M. 2015. Co-culture of primary CLL cells with bone marrow mesenchymal cells, CD40 ligand and CpG ODN promotes proliferation of chemoresistant CLL cells phenotypically comparable to those proliferating in vivo. *Oncotarget,* 6**,** 7632-7643.

QIN, H. R., KIM, H. J., KIM, J. Y., HURT, E. M., KLARMANN, G. J., KAWASAKI, B. T., DUHAGON SERRAT, M. A. & FARRAR, W. L. 2008. Activation of signal transducer and activator of transcription 3 through a phosphomimetic serine 727 promotes prostate tumorigenesis independent of tyrosine 705 phosphorylation. *Cancer Res,* 68**,** 7736-41.

QUESADA, V., CONDE, L., VILLAMOR, N., ORDONEZ, G. R., JARES, P., BASSAGANYAS, L., RAMSAY, A. J., BEA, S., PINYOL, M., MARTINEZ-TRILLOS, A., LOPEZ-GUERRA, M., COLOMER, D., NAVARRO, A., BAUMANN, T., AYMERICH, M., ROZMAN, M., DELGADO, J., GINE, E., HERNANDEZ, J. M., GONZALEZ-DIAZ, M., PUENTE, D. A., VELASCO, G., FREIJE, J. M., TUBIO, J. M., ROYO, R., GELPI, J. L., OROZCO, M., PISANO, D. G., ZAMORA, J., VAZQUEZ, M., VALENCIA, A., HIMMELBAUER, H., BAYES, M., HEATH, S., GUT, M., GUT, I., ESTIVILL, X., LOPEZ-GUILLERMO, A., PUENTE, X. S., CAMPO, E. & LOPEZ-OTIN, C. 2012. Exome sequencing identifies recurrent mutations of the splicing factor SF3B1 gene in chronic lymphocytic leukemia. *Nat Genet,* 44**,** 47-52.

QUIROGA, M. P., BALAKRISHNAN, K., KURTOVA, A. V., SIVINA, M., KEATING, M. J., WIERDA, W. G., GANDHI, V. & BURGER, J. A. 2009. B-cell antigen receptor signaling enhances chronic lymphocytic leukemia cell migration and survival: specific targeting with a novel spleen tyrosine kinase inhibitor, R406. *Blood,* 114**,** 1029-37.

QUIROGA, M. P. & BURGER, J. A. 2010. BCR-mediated decrease of CXCR4 and CD62L in CLL. *Cancer Res,* 70**,** 5194; author reply 5195.

RAI, K. R., SAWITSKY, A., CRONKITE, E. P., CHANANA, A. D., LEVY, R. N. & PASTERNACK, B. S. 1975. Clinical staging of chronic lymphocytic leukemia. *Blood,* 46**,** 219-34.

RAJENDRAN, P., LI, F., SHANMUGAM, M. K., KANNAIYAN, R., GOH, J. N., WONG, K. F., WANG, W., KHIN, E., TERGAONKAR, V., KUMAR, A. P., LUK, J. M. & SETHI, G. 2012a. Celastrol suppresses growth and induces apoptosis of human hepatocellular carcinoma through the modulation of STAT3/JAK2 signaling cascade in vitro and in vivo. *Cancer Prev Res (Phila),* 5**,** 631-43.

RAJENDRAN, P., LI, F., SHANMUGAM, M. K., VALI, S., ABBASI, T., KAPOOR, S., AHN, K. S., KUMAR, A. P. & SETHI, G. 2012b. Honokiol inhibits signal transducer and activator of transcription-3 signaling, proliferation, and survival of hepatocellular carcinoma cells via the protein tyrosine phosphatase SHP-1. *J Cell Physiol,* 227**,** 2184-95.

RAJENDRAN, P., ONG, T. H., CHEN, L., LI, F., SHANMUGAM, M. K., VALI, S., ABBASI, T., KAPOOR, S., SHARMA, A., KUMAR, A. P., HUI, K. M. & SETHI, G. 2011. Suppression of signal transducer and activator of transcription 3 activation by butein inhibits growth of human hepatocellular carcinoma in vivo. *Clin Cancer Res,* 17**,** 1425-39.

RAMSAY, A. G., JOHNSON, A. J., LEE, A. M., GORGUN, G., LE DIEU, R., BLUM, W., BYRD, J. C. & GRIBBEN, J. G. 2008. Chronic lymphocytic leukemia T cells show impaired immunological synapse formation that can be reversed with an immunomodulating drug. *J Clin Invest,* 118**,** 2427-37.

RATECH, H., SHEIBANI, K., NATHWANI, B. N. & RAPPAPORT, H. 1988. Immunoarchitecture of the "pseudofollicles" of well-differentiated (small) lymphocytic lymphoma: a comparison with true follicles. *Hum Pathol,* 19**,** 89-94.

RAWSTRON, A. C., BENNETT, F. L., O'CONNOR, S. J., KWOK, M., FENTON, J. A., PLUMMER, M., DE TUTE, R., OWEN, R. G., RICHARDS, S. J., JACK, A. S. & HILLMEN, P. 2008. Monoclonal B-cell lymphocytosis and chronic lymphocytic leukemia. *N Engl J Med,* 359**,** 575-83.

RAZ, R., DURBIN, J. E. & LEVY, D. E. 1994. Acute phase response factor and additional members of the interferon-stimulated gene factor 3 family integrate diverse signals from cytokines, interferons, and growth factors. *J Biol Chem,* 269**,** 24391-5.

REDELL, M. S., RUIZ, M. J., ALONZO, T. A., GERBING, R. B. & TWEARDY, D. J. 2011. Stat3 signaling in acute myeloid leukemia: ligand-dependent and -independent activation and induction of apoptosis by a novel small-molecule Stat3 inhibitor. *Blood,* 117**,** 5701-9.

REINART, N., NGUYEN, P. H., BOUCAS, J., ROSEN, N., KVASNICKA, H. M., HEUKAMP, L., RUDOLPH, C., RISTOVSKA, V., VELMANS, T., MUELLER, C., REINERS, K. S., VON STRANDMANN, E. P., KRAUSE, G., MONTESINOS-RONGEN, M., SCHLEGELBERGER, B., HERLING, M., HALLEK, M. & FINGERLE-ROWSON, G. 2013. Delayed development of chronic lymphocytic leukemia in the absence of macrophage migration inhibitory factor. *Blood,* 121**,** 812-21.

REINERS, K. S., TOPOLAR, D., HENKE, A., SIMHADRI, V. R., KESSLER, J., SAUER, M., BESSLER, M., HANSEN, H. P., TAWADROS, S., HERLING, M., KRONKE, M., HALLEK, M. & POGGE VON STRANDMANN, E. 2013. Soluble ligands for NK cell receptors promote evasion of chronic lymphocytic leukemia cells from NK cell anti-tumor activity. *Blood,* 121**,** 3658-65.

RICHES, J. C., DAVIES, J. K., MCCLANAHAN, F., FATAH, R., IQBAL, S., AGRAWAL, S., RAMSAY, A. G. & GRIBBEN, J. G. 2013. T cells from CLL patients exhibit features of T-cell exhaustion but retain capacity for cytokine production. *Blood,* 121**,** 1612-21.

RICHES, J. C., RAMSAY, A. G. & GRIBBEN, J. G. 2011. Chronic lymphocytic leukemia: an update on biology and treatment. *Curr Oncol Rep,* 13**,** 379-85.

RINGSHAUSEN, I., SCHNELLER, F., BOGNER, C., HIPP, S., DUYSTER, J., PESCHEL, C. & DECKER, T. 2002. Constitutively activated phosphatidylinositol-3 kinase (PI-3K) is involved in the defect of apoptosis in B-CLL: association with protein kinase Cdelta. *Blood,* 100**,** 3741-8.

ROBERTS, A. W., DAVIDS, M. S., PAGEL, J. M., KAHL, B. S., PUVVADA, S. D., GERECITANO, J. F., KIPPS, T. J., ANDERSON, M. A., BROWN, J. R., GRESSICK, L., WONG, S., DUNBAR, M., ZHU, M., DESAI, M. B., CERRI, E., HEITNER ENSCHEDE, S., HUMERICKHOUSE, R. A., WIERDA, W. G. & SEYMOUR, J. F. 2016. Targeting BCL2 with Venetoclax in Relapsed Chronic Lymphocytic Leukemia. *N Engl J Med,* 374**,** 311-22.

ROBERTS, A. W., STILGENBAUER, S., SEYMOUR, J. F. & HUANG, D. C. 2017. Venetoclax in patients with previously treated chronic lymphocytic leukemia. *Clin Cancer Res*.

ROECKLEIN, B. A. & TOROK-STORB, B. 1995. Functionally distinct human marrow stromal cell lines immortalized by transduction with the human papilloma virus E6/E7 genes. *Blood,* 85**,** 997-1005.

ROMANO, S. J. 2005. Selectin antagonists : therapeutic potential in asthma and COPD. *Treat Respir Med,* 4**,** 85-94.

ROMBOUT, A., LUST, S., OFFNER, F., NAESSENS, E., VERHASSELT, B. & PHILIPPE, J. 2016. Mimicking the tumour microenvironment of chronic lymphocytic leukaemia in vitro critically depends on the type of B-cell receptor stimulation. *Br J Cancer,* 114**,** 704-12.

ROOZENDAAL, R., MEMPEL, T. R., PITCHER, L. A., GONZALEZ, S. F., VERSCHOOR, A., MEBIUS, R. E., VON ANDRIAN, U. H. & CARROLL, M. C. 2009. Conduits mediate transport of low-molecular-weight antigen to lymph node follicles. *Immunity,* 30**,** 264-76.

ROSEN, S. D. 1993. Cell surface lectins in the immune system. *Semin Immunol,* 5**,** 237-47.

ROSEN, S. D. 2004. Ligands for L-selectin: homing, inflammation, and beyond. *Annu Rev Immunol,* 22**,** 129-56.

ROSEN, S. D., HWANG, S. T., GIBLIN, P. A. & SINGER, M. S. 1997. High-endothelial-venule ligands for L-selectin: identification and functions. *Biochem Soc Trans,* 25**,** 428-33.

ROSSI, D., CERRI, M., DEAMBROGI, C., SOZZI, E., CRESTA, S., RASI, S., DE PAOLI, L., SPINA, V., GATTEI, V., CAPELLO, D., FORCONI, F., LAURIA, F. & GAIDANO, G. 2009. The prognostic value of TP53 mutations in chronic lymphocytic leukemia is independent of Del17p13: implications for overall survival and chemorefractoriness. *Clin Cancer Res,* 15**,** 995-1004.

ROSSI, D., CIARDULLO, C. & GAIDANO, G. 2013a. Genetic aberrations of signaling pathways in lymphomagenesis: revelations from next generation sequencing studies. *Semin Cancer Biol,* 23**,** 422-30.

ROSSI, D., FANGAZIO, M., RASI, S., VAISITTI, T., MONTI, S., CRESTA, S., CHIARETTI, S., DEL GIUDICE, I., FABBRI, G., BRUSCAGGIN, A., SPINA, V., DEAMBROGI, C., MARINELLI, M., FAMA, R., GRECO, M., DANIELE, G., FORCONI, F., GATTEI, V., BERTONI, F., DEAGLIO, S., PASQUALUCCI, L., GUARINI, A., DALLA-FAVERA, R., FOA, R. & GAIDANO, G. 2012. Disruption of BIRC3 associates with fludarabine chemorefractoriness in TP53 wild-type chronic lymphocytic leukemia. *Blood,* 119**,** 2854-62.

ROSSI, D., RASI, S., SPINA, V., BRUSCAGGIN, A., MONTI, S., CIARDULLO, C., DEAMBROGI, C., KHIABANIAN, H., SERRA, R., BERTONI, F., FORCONI, F., LAURENTI, L., MARASCA, R., DAL-BO, M., ROSSI, F. M., BULIAN, P., NOMDEDEU, J., DEL POETA, G., GATTEI, V., PASQUALUCCI, L., RABADAN, R., FOA, R., DALLA-FAVERA, R. & GAIDANO, G. 2013b. Integrated mutational and cytogenetic analysis identifies new prognostic subgroups in chronic lymphocytic leukemia. *Blood,* 121**,** 1403-12.

ROSSI, D., SPINA, V., BOMBEN, R., RASI, S., DAL-BO, M., BRUSCAGGIN, A., ROSSI, F. M., MONTI, S., DEGAN, M., CIARDULLO, C., SERRA, R., ZUCCHETTO, A., NOMDEDEU, J., BULIAN, P., GROSSI, A., ZAJA, F., POZZATO, G., LAURENTI, L., EFREMOV, D. G., DI-RAIMONDO, F., MARASCA, R., FORCONI, F., DEL POETA, G., GAIDANO, G. & GATTEI, V. 2013c. Association between molecular lesions and specific B-cell receptor subsets in chronic lymphocytic leukemia. *Blood,* 121**,** 4902-5.

ROSSMANN, E. D., LEWIN, N., JEDDI-TEHRANI, M., OSTERBORG, A. & MELLSTEDT, H. 2002. Intracellular T cell cytokines in patients with B cell chronic lymphocytic leukaemia (B-CLL). *Eur J Haematol,* 68**,** 299-306.

ROWLEY, R. B., BURKHARDT, A. L., CHAO, H. G., MATSUEDA, G. R. & BOLEN, J. B. 1995. Syk protein-tyrosine kinase is regulated by tyrosine-phosphorylated Ig alpha/Ig beta immunoreceptor tyrosine activation motif binding and autophosphorylation. *J Biol Chem,* 270**,** 11590-4.

ROZOVSKI, U., CALIN, G. A., SETOYAMA, T., D'ABUNDO, L., HARRIS, D. M., LI, P., LIU, Z., GRGUREVIC, S., FERRAJOLI, A., FADERL, S., BURGER, J. A., O'BRIEN, S., WIERDA, W. G., KEATING, M. J. & ESTROV, Z. 2013. Signal transducer and activator of transcription (STAT)-3 regulates microRNA gene expression in chronic lymphocytic leukemia cells. *Mol Cancer,* 12**,** 50.

ROZOVSKI, U., HARRIS, D. M., LI, P., LIU, Z., JAIN, P., VELETIC, I., FERRAJOLI, A., BURGER, J., O'BRIEN, S., BOSE, P., THOMPSON, P., JAIN, N., WIERDA, W.,

KEATING, M. J. & ESTROV, Z. 2017a. Constitutive Phosphorylation of STAT3 by the CK2-BLNK-CD5 Complex. *Mol Cancer Res,* 15**,** 610-618.
ROZOVSKI, U., HARRIS, D. M., LI, P., LIU, Z., JAIN, P., VELETIC, I., FERRAJOLI, A., BURGER, J., THOMPSON, P., JAIN, N., WIERDA, W., KEATING, M. J. & ESTROV, Z. 2017b. Activation of the B-cell receptor successively activates NF-kappaB and STAT3 in chronic lymphocytic leukemia cells. *Int J Cancer*.
ROZOVSKI, U., HARRIS, D. M., LI, P., LIU, Z., WU, J. Y., GRGUREVIC, S., FADERL, S., FERRAJOLI, A., WIERDA, W. G., MARTINEZ, M., VERSTOVSEK, S., KEATING, M. J. & ESTROV, Z. 2016. At High Levels, Constitutively Activated STAT3 Induces Apoptosis of Chronic Lymphocytic Leukemia Cells. *J Immunol,* 196**,** 4400-9.
ROZOVSKI, U., WU, J. Y., HARRIS, D. M., LIU, Z., LI, P., HAZAN-HALEVY, I., FERRAJOLI, A., BURGER, J. A., O'BRIEN, S., JAIN, N., VERSTOVSEK, S., WIERDA, W. G., KEATING, M. J. & ESTROV, Z. 2014. Stimulation of the B-cell receptor activates the JAK2/STAT3 signaling pathway in chronic lymphocytic leukemia cells. *Blood,* 123**,** 3797-802.
RUAN, J., HYJEK, E., KERMANI, P., CHRISTOS, P. J., HOOPER, A. T., COLEMAN, M., HEMPSTEAD, B., LEONARD, J. P., CHADBURN, A. & RAFII, S. 2006. Magnitude of stromal hemangiogenesis correlates with histologic subtype of non-Hodgkin's lymphoma. *Clin Cancer Res,* 12**,** 5622-31.
SAELAND, S., DUVERT, V., MOREAU, I. & BANCHEREAU, J. 1993. Human B cell precursors proliferate and express CD23 after CD40 ligation. *J Exp Med,* 178**,** 113-20.
SAIJO, K., MECKLENBRAUKER, I., SANTANA, A., LEITGER, M., SCHMEDT, C. & TARAKHOVSKY, A. 2002. Protein kinase C beta controls nuclear factor kappaB activation in B cells through selective regulation of the IkappaB kinase alpha. *J Exp Med,* 195**,** 1647-52.
SANO, S., ITAMI, S., TAKEDA, K., TARUTANI, M., YAMAGUCHI, Y., MIURA, H., YOSHIKAWA, K., AKIRA, S. & TAKEDA, J. 1999. Keratinocyte-specific ablation of Stat3 exhibits impaired skin remodeling, but does not affect skin morphogenesis. *EMBO J,* 18**,** 4657-68.
SANT, M., ALLEMANI, C., TEREANU, C., DE ANGELIS, R., CAPOCACCIA, R., VISSER, O., MARCOS-GRAGERA, R., MAYNADIE, M., SIMONETTI, A., LUTZ, J. M., BERRINO, F. & GROUP, H. W. 2010. Incidence of hematologic malignancies in Europe by morphologic subtype: results of the HAEMACARE project. *Blood,* 116**,** 3724-34.
SARI-HASSOUN, M., CLEMENT, M. J., HAMDI, I., BOLLOT, G., BAUVAIS, C., JOSHI, V., TOMA, F., BURGO, A., CAILLERET, M., ROSALES-HERNANDEZ, M. C., MACIAS PEREZ, M. E., CHABANE-SARI, D. & CURMI, P. A. 2016. Cucurbitacin I elicits the formation of actin/phospho-myosin II co-aggregates by stimulation of the RhoA/ROCK pathway and inhibition of LIM-kinase. *Biochem Pharmacol,* 102**,** 45-63.
SCARFO, L., FERRERI, A. J. & GHIA, P. 2016. Chronic lymphocytic leukaemia. *Crit Rev Oncol Hematol,* 104**,** 169-82.
SCHATTNER, E. J., MASCARENHAS, J., REYFMAN, I., KOSHY, M., WOO, C., FRIEDMAN, S. M. & CROW, M. K. 1998. Chronic lymphocytic leukemia B cells can express CD40 ligand and demonstrate T-cell type costimulatory capacity. *Blood,* 91**,** 2689-97.
SCHMID, C. & ISAACSON, P. G. 1994. Proliferation centres in B-cell malignant lymphoma, lymphocytic (B-CLL): an immunophenotypic study. *Histopathology,* 24**,** 445-51.
SCHMITT, C., ABT, M., CIORCIARO, C., KLING, D., JAMOIS, C., SCHICK, E., SOLIER, C., BENGHOZI, R. & GAUDREAULT, J. 2015. First-in-Man Study With Inclacumab, a Human Monoclonal Antibody Against P-selectin. *J Cardiovasc Pharmacol,* 65**,** 611-9.

SCHNELLER D1, M. G., SOUSEK A, PROELL V, VAN ZIJL F, ZULEHNER G, HUBER H, MAIR M, MUELLNER MK, NIJMAN SM, EFERL R, MORIGGL R, MIKULITS W. 2011. p19(ARF) /p14(ARF) controls oncogenic functions of signal transducer and activator of transcription 3 in hepatocellular carcinoma. *Hepatology,* 54**,** 164-172.

SCHUH, A., BECQ, J., HUMPHRAY, S., ALEXA, A., BURNS, A., CLIFFORD, R., FELLER, S. M., GROCOCK, R., HENDERSON, S., KHREBTUKOVA, I., KINGSBURY, Z., LUO, S., MCBRIDE, D., MURRAY, L., MENJU, T., TIMBS, A., ROSS, M., TAYLOR, J. & BENTLEY, D. 2012. Monitoring chronic lymphocytic leukemia progression by whole genome sequencing reveals heterogeneous clonal evolution patterns. *Blood,* 120**,** 4191-6.

SCHURINGA, J. J., SCHEPERS, H., VELLENGA, E. & KRUIJER, W. 2001. Ser727-dependent transcriptional activation by association of p300 with STAT3 upon IL-6 stimulation. *FEBS Lett,* 495**,** 71-6.

SCHUST, J. & BERG, T. 2004. A high-throughput fluorescence polarization assay for signal transducer and activator of transcription 3. *Anal Biochem,* 330**,** 114-8.

SCHUST, J., SPERL, B., HOLLIS, A., MAYER, T. U. & BERG, T. 2006. Stattic: a small-molecule inhibitor of STAT3 activation and dimerization. *Chem Biol,* 13**,** 1235-42.

SCIELZO, C., APOLLONIO, B., SCARFO, L., JANUS, A., MUZIO, M., TEN HACKEN, E., GHIA, P. & CALIGARIS-CAPPIO, F. 2011. The functional in vitro response to CD40 ligation reflects a different clinical outcome in patients with chronic lymphocytic leukemia. *Leukemia,* 25**,** 1760-7.

SEEKAMP, A., VAN GRIENSVEN, M., DHONDT, E., DIEFENBECK, M., DEMEYER, I., VUNDELINCKX, G., HAAS, N., SCHAECHINGER, U., WOLOWICKA, L., RAMMELT, S., STROOBANTS, J., MARZI, I., BRAMBRINK, A. M., DZIURDZIK, P., GASIOROWSKI, J., REDL, H., BECKERT, M. & KHAN-BOLUKI, J. 2004. The effect of anti-L-selectin (aselizumab) in multiple traumatized patients--results of a phase II clinical trial. *Crit Care Med,* 32**,** 2021-8.

SEIFFERT, M., SCHULZ, A., OHL, S., DOHNER, H., STILGENBAUER, S. & LICHTER, P. 2010. Soluble CD14 is a novel monocyte-derived survival factor for chronic lymphocytic leukemia cells, which is induced by CLL cells in vitro and present at abnormally high levels in vivo. *Blood,* 116**,** 4223-30.

SEIFFERT, M., STILGENBAUER, S., DOHNER, H. & LICHTER, P. 2007. Efficient nucleofection of primary human B cells and B-CLL cells induces apoptosis, which depends on the microenvironment and on the structure of transfected nucleic acids. *Leukemia,* 21**,** 1977-83.

SELLIER, H., REBILLARD, A., GUETTE, C., BARRE, B. & COQUERET, O. 2013. How should we define STAT3 as an oncogene and as a potential target for therapy? *JAKSTAT,* 2**,** e24716.

SEN, M., THOMAS, S. M., KIM, S., YEH, J. I., FERRIS, R. L., JOHNSON, J. T., DUVVURI, U., LEE, J., SAHU, N., JOYCE, S., FREILINO, M. L., SHI, H., LI, C., LY, D., RAPIREDDY, S., ETTER, J. P., LI, P. K., WANG, L., CHIOSEA, S., SEETHALA, R. R., GOODING, W. E., CHEN, X., KAMINSKI, N., PANDIT, K., JOHNSON, D. E. & GRANDIS, J. R. 2012. First-in-human trial of a STAT3 decoy oligonucleotide in head and neck tumors: implications for cancer therapy. *Cancer Discov,* 2**,** 694-705.

SERRANO, D., MONTEIRO, J., ALLEN, S. L., KOLITZ, J., SCHULMAN, P., LICHTMAN, S. M., BUCHBINDER, A., VINCIGUERRA, V. P., CHIORAZZI, N. & GREGERSEN, P. K. 1997. Clonal expansion within the CD4+CD57+ and CD8+CD57+ T cell subsets in chronic lymphocytic leukemia. *J Immunol,* 158**,** 1482-9.

SEYMOUR, J. F., MA, S., BRANDER, D. M., CHOI, M. Y., BARRIENTOS, J., DAVIDS, M. S., ANDERSON, M. A., BEAVEN, A. W., ROSEN, S. T., TAM, C. S., PRINE,

B., AGARWAL, S. K., MUNASINGHE, W., ZHU, M., LASH, L. L., DESAI, M., CERRI, E., VERDUGO, M., KIM, S. Y., HUMERICKHOUSE, R. A., GORDON, G. B., KIPPS, T. J. & ROBERTS, A. W. 2017. Venetoclax plus rituximab in relapsed or refractory chronic lymphocytic leukaemia: a phase 1b study. *Lancet Oncol*.

SFIKAKIS, P. P. & MAVRIKAKIS, M. 1999. Adhesion and lymphocyte costimulatory molecules in systemic rheumatic diseases. *Clin Rheumatol,* 18**,** 317-27.

SHAIN, K. H., DALTON, W. S. & TAO, J. 2015. The tumor microenvironment shapes hallmarks of mature B-cell malignancies. *Oncogene,* 34**,** 4673-82.

SHANAFELT, T. D., GEYER, S. M., BONE, N. D., TSCHUMPER, R. C., WITZIG, T. E., NOWAKOWSKI, G. S., ZENT, C. S., CALL, T. G., LAPLANT, B., DEWALD, G. W., JELINEK, D. F. & KAY, N. E. 2008. CD49d expression is an independent predictor of overall survival in patients with chronic lymphocytic leukaemia: a prognostic parameter with therapeutic potential. *Br J Haematol,* 140**,** 537-46.

SHARMA, S., ORLOWSKI, G. & SONG, W. 2009. Btk regulates B cell receptor-mediated antigen processing and presentation by controlling actin cytoskeleton dynamics in B cells. *J Immunol,* 182**,** 329-39.

SHI, X., ZHANG, H., PADDON, H., LEE, G., CAO, X. & PELECH, S. 2006. Phosphorylation of STAT3 serine-727 by cyclin-dependent kinase 1 is critical for nocodazole-induced mitotic arrest. *Biochemistry,* 45**,** 5857-67.

SHORTMAN, K. 1984. T-cell development in the thymus. *Nature,* 309**,** 583-4.

SHUKLA A, N. K. C., ADAM K AHRENS, CHRISTINE E CUTUCACHE, AMIT K MITTAL, PHILIP BIERMAN, DENNIS D WEISENBURGER, RUNQING LU AND SHANTARAM S JOSHI 2013. Stromal Tumor Microenvironment in Chronic Lymphocytic Leukemia: Regulation of Leukemic Progression. *Journal of Leukemias,* 1:113.

SIDDIQUEE, K., ZHANG, S., GUIDA, W. C., BLASKOVICH, M. A., GREEDY, B., LAWRENCE, H. R., YIP, M. L., JOVE, R., MCLAUGHLIN, M. M., LAWRENCE, N. J., SEBTI, S. M. & TURKSON, J. 2007. Selective chemical probe inhibitor of Stat3, identified through structure-based virtual screening, induces antitumor activity. *Proc Natl Acad Sci U S A,* 104**,** 7391-6.

SILVA, C. M. 2004. Role of STATs as downstream signal transducers in Src family kinase-mediated tumorigenesis. *Oncogene,* 23**,** 8017-23.

SLAGER, S. L., BENAVENTE, Y., BLAIR, A., VERMEULEN, R., CERHAN, J. R., COSTANTINI, A. S., MONNEREAU, A., NIETERS, A., CLAVEL, J., CALL, T. G., MAYNADIE, M., LAN, Q., CLARKE, C. A., LIGHTFOOT, T., NORMAN, A. D., SAMPSON, J. N., CASABONNE, D., COCCO, P. & DE SANJOSE, S. 2014. Medical history, lifestyle, family history, and occupational risk factors for chronic lymphocytic leukemia/small lymphocytic lymphoma: the InterLymph Non-Hodgkin Lymphoma Subtypes Project. *J Natl Cancer Inst Monogr,* 2014**,** 41-51.

SLAGER, S. L., CAPORASO, N. E., DE SANJOSE, S. & GOLDIN, L. R. 2013. Genetic susceptibility to chronic lymphocytic leukemia. *Semin Hematol,* 50**,** 296-302.

SNYDER, M., HUANG, X. Y. & ZHANG, J. J. 2011. Signal transducers and activators of transcription 3 (STAT3) directly regulates cytokine-induced fascin expression and is required for breast cancer cell migration. *J Biol Chem,* 286**,** 38886-93.

SONG, Y., QIAN, L., SONG, S., CHEN, L., ZHANG, Y., YUAN, G., ZHANG, H., XIA, Q., HU, M., YU, M., SHI, M., JIANG, Z. & GUO, N. 2008. Fra-1 and Stat3 synergistically regulate activation of human MMP-9 gene. *Mol Immunol,* 45**,** 137-43.

SPAARGAREN, M., BEULING, E. A., RURUP, M. L., MEIJER, H. P., KLOK, M. D., MIDDENDORP, S., HENDRIKS, R. W. & PALS, S. T. 2003. The B cell antigen receptor controls integrin activity through Btk and PLCgamma2. *J Exp Med,* 198**,** 1539-50.

SPANER, D. E., WANG, G., MCCAW, L., LI, Y., DISPERATI, P., CUSSEN, M. A. & SHI, Y. 2016. Activity of the Janus kinase inhibitor ruxolitinib in chronic lymphocytic leukemia: results of a phase II trial. *Haematologica,* 101**,** e192-5.

SPERTINI, O., FREEDMAN, A. S., BELVIN, M. P., PENTA, A. C., GRIFFIN, J. D. & TEDDER, T. F. 1991. Regulation of leukocyte adhesion molecule-1 (TQ1, Leu-8) expression and shedding by normal and malignant cells. *Leukemia,* 5**,** 300-8.

SPITZNER, M., ROESLER, B., BIELFELD, C., EMONS, G., GAEDCKE, J., WOLFF, H. A., RAVE-FRANK, M., KRAMER, F., BEISSBARTH, T., KITZ, J., WIENANDS, J., GHADIMI, B. M., EBNER, R., RIED, T. & GRADE, M. 2014. STAT3 inhibition sensitizes colorectal cancer to chemoradiotherapy in vitro and in vivo. *Int J Cancer,* 134**,** 997-1007.

STANKOVIC, T., WEBER, P., STEWART, G., BEDENHAM, T., MURRAY, J., BYRD, P. J., MOSS, P. A. & TAYLOR, A. M. 1999. Inactivation of ataxia telangiectasia mutated gene in B-cell chronic lymphocytic leukaemia. *Lancet,* 353**,** 26-9.

STEEBER, D. A., ENGEL, P., MILLER, A. S., SHEETZ, M. P. & TEDDER, T. F. 1997. Ligation of L-selectin through conserved regions within the lectin domain activates signal transduction pathways and integrin function in human, mouse, and rat leukocytes. *J Immunol,* 159**,** 952-63.

STEELE, A. J., PRENTICE, A. G., CWYNARSKI, K., HOFFBRAND, A. V., HART, S. M., LOWDELL, M. W., SAMUEL, E. R. & WICKREMASINGHE, R. G. 2010. The JAK3-selective inhibitor PF-956980 reverses the resistance to cytotoxic agents induced by interleukin-4 treatment of chronic lymphocytic leukemia cells: potential for reversal of cytoprotection by the microenvironment. *Blood,* 116**,** 4569-77.

STEVENSON, F. K., KRYSOV, S., DAVIES, A. J., STEELE, A. J. & PACKHAM, G. 2011. B-cell receptor signaling in chronic lymphocytic leukemia. *Blood,* 118**,** 4313-20.

STEVENSON, F. K., SAHOTA, S. S., OTTENSMEIER, C. H., ZHU, D., FORCONI, F. & HAMBLIN, T. J. 2001. The occurrence and significance of V gene mutations in B cell-derived human malignancy. *Adv Cancer Res,* 83**,** 81-116.

SWERDLOW, S. H., CAMPO, E., PILERI, S. A., HARRIS, N. L., STEIN, H., SIEBERT, R., ADVANI, R., GHIELMINI, M., SALLES, G. A., ZELENETZ, A. D. & JAFFE, E. S. 2016. The 2016 revision of the World Health Organization classification of lymphoid neoplasms. *Blood,* 127**,** 2375-90.

SZYDLOWSKI, M., JABLONSKA, E. & JUSZCZYNSKI, P. 2014. FOXO1 transcription factor: a critical effector of the PI3K-AKT axis in B-cell development. *Int Rev Immunol,* 33**,** 146-57.

TAKEDA, K. & AKIRA, S. 2001. Multi-functional roles of Stat3 revealed by conditional gene targeting. *Arch Immunol Ther Exp (Warsz),* 49**,** 279-83.

TAM, C. S., SHANAFELT, T. D., WIERDA, W. G., ABRUZZO, L. V., VAN DYKE, D. L., O'BRIEN, S., FERRAJOLI, A., LERNER, S. A., LYNN, A., KAY, N. E. & KEATING, M. J. 2009. De novo deletion 17p13.1 chronic lymphocytic leukemia shows significant clinical heterogeneity: the M. D. Anderson and Mayo Clinic experience. *Blood,* 114**,** 957-64.

TAUB, R. 2003. Hepatoprotection via the IL-6/Stat3 pathway. *J Clin Invest,* 112**,** 978-80.

TEFFERI, A. & PARDANANI, A. 2011. Serious adverse events during ruxolitinib treatment discontinuation in patients with myelofibrosis. *Mayo Clin Proc,* 86**,** 1188-91.

TELEN, M. J., WUN, T., MCCAVIT, T. L., DE CASTRO, L. M., KRISHNAMURTI, L., LANZKRON, S., HSU, L. L., SMITH, W. R., RHEE, S., MAGNANI, J. L. & THACKRAY, H. 2015. Randomized phase 2 study of GMI-1070 in SCD: reduction in time to resolution of vaso-occlusive events and decreased opioid use. *Blood,* 125**,** 2656-64.

TEN HACKEN, E., & BURGER, J. A. 2015 Microenvironment interactions and B-cell receptor signaling in chronic lymphocytic leukemia: implications for disease pathogenesis and treatment. *Biochim. Biophys*. 1863, 401–413.

TENG, Y., ROSS, J. L. & COWELL, J. K. 2014. The involvement of JAK-STAT3 in cell motility, invasion, and metastasis. *JAKSTAT,* 3**,** e28086.

THOMAS, M., CALAMITO, M., SRIVASTAVA, B., MAILLARD, I., PEAR, W. S. & ALLMAN, D. 2007. Notch activity synergizes with B-cell-receptor and CD40 signaling to enhance B-cell activation. *Blood,* 109**,** 3342-50.

TICCHIONI, M., ESSAFI, M., JEANDEL, P. Y., DAVI, F., CASSUTO, J. P., DECKERT, M. & BERNARD, A. 2007. Homeostatic chemokines increase survival of B-chronic lymphocytic leukemia cells through inactivation of transcription factor FOXO3a. *Oncogene,* 26**,** 7081-91.

TILL, K. J., LIN, K., ZUZEL, M. & CAWLEY, J. C. 2002. The chemokine receptor CCR7 and alpha4 integrin are important for migration of chronic lymphocytic leukemia cells into lymph nodes. *Blood,* 99**,** 2977-84.

TILL, K. J., SPILLER, D., HARRIS, R., CHEN, H., ZUZEL, M. & CAWLEY, J. C. 2005 CLL, but not normal, B cells are dependent on autocrine VEGF and alpha4beta1 integrin for chemokine-induced motility on and through endothelium. *Blood*. 105, 4813-9.

TRIMARCO, V., AVE, E., FACCO, M., CHIODIN, G., FREZZATO, F., MARTINI, V., GATTAZZO, C., LESSI, F., GIORGI, C. A., VISENTIN, A., CASTELLI, M., SEVERIN, F., ZAMBELLO, R., PIAZZA, F., SEMENZATO, G. & TRENTIN, L. 2015. Cross-talk between chronic lymphocytic leukemia (CLL) tumor B cells and mesenchymal stromal cells (MSCs): implications for neoplastic cell survival. *Oncotarget,* 6**,** 42130-49.

TSUBATA, T. & WIENANDS, J. 2001. B cell signaling. Introduction. *Int Rev Immunol,* 20**,** 675-8.

TSUKADA, N., BURGER, J. A., ZVAIFLER, N. J. & KIPPS, T. J. 2002. Distinctive features of "nurselike" cells that differentiate in the context of chronic lymphocytic leukemia. *Blood,* 99**,** 1030-7.

TU, L., POE, J. C., KADONO, T., VENTURI, G. M., BULLARD, D. C., TEDDER, T. F. & STEEBER, D. A. 2002. A functional role for circulating mouse L-selectin in regulating leukocyte/endothelial cell interactions in vivo. *J Immunol,* 169**,** 2034-43.

TURTLE, C. J., HAY, K. A., HANAFI, L. A., LI, D., CHERIAN, S., CHEN, X., WOOD, B., LOZANSKI, A., BYRD, J. C., HEIMFELD, S., RIDDELL, S. R. & MALONEY, D. G. 2017. Durable Molecular Remissions in Chronic Lymphocytic Leukemia Treated With CD19-Specific Chimeric Antigen Receptor-Modified T Cells After Failure of Ibrutinib. *J Clin Oncol***,** JCO2017728519.

UMEMOTO, E., TANAKA, T., KANDA, H., JIN, S., TOHYA, K., OTANI, K., MATSUTANI, T., MATSUMOTO, M., EBISUNO, Y., JANG, M. H., FUKUDA, M., HIRATA, T. & MIYASAKA, M. 2006. Nepmucin, a novel HEV sialomucin, mediates L-selectin-dependent lymphocyte rolling and promotes lymphocyte adhesion under flow. *J Exp Med,* 203**,** 1603-14.

VAISITTI, T., AYDIN, S., ROSSI, D., COTTINO, F., BERGUI, L., D'ARENA, G., BONELLO, L., HORENSTEIN, A. L., BRENNAN, P., PEPPER, C., GAIDANO, G., MALAVASI, F. & DEAGLIO, S. 2010. CD38 increases CXCL12-mediated signals and homing of chronic lymphocytic leukemia cells. *Leukemia,* 24**,** 958-69.

VALCECKIENE, V., KONTENYTE, R., JAKUBAUSKAS, A. & GRISKEVICIUS, L. 2010. Selection of reference genes for quantitative polymerase chain reaction studies in purified B cells from B cell chronic lymphocytic leukaemia patients. *Br J Haematol,* 151**,** 232-8.

VANNUCCHI, A. M. 2015. Ruxolitinib versus standard therapy for the treatment of polycythemia vera. *N Engl J Med,* 372**,** 1670-1.

VERMA, N. K., DOURLAT, J., DAVIES, A. M., LONG, A., LIU, W. Q., GARBAY, C., KELLEHER, D. & VOLKOV, Y. 2009. STAT3-stathmin interactions control microtubule dynamics in migrating T-cells. *J Biol Chem,* 284**,** 12349-62.

VERSTOVSEK, S., MESA, R. A., GOTLIB, J., LEVY, R. S., GUPTA, V., DIPERSIO, J. F., CATALANO, J. V., DEININGER, M., MILLER, C., SILVER, R. T., TALPAZ, M., WINTON, E. F., HARVEY, J. H., JR., ARCASOY, M. O., HEXNER, E., LYONS, R. M., PAQUETTE, R., RAZA, A., VADDI, K., ERICKSON-VIITANEN, S., KOUMENIS, I. L., SUN, W., SANDOR, V. & KANTARJIAN, H. M. 2012. A double-blind, placebo-controlled trial of ruxolitinib for myelofibrosis. *N Engl J Med,* 366**,** 799-807.

VLAD, A., DEGLESNE, P. A., LETESTU, R., SAINT-GEORGES, S., CHEVALLIER, N., BARAN-MARSZAK, F., VARIN-BLANK, N., AJCHENBAUM-CYMBALISTA, F. & LEDOUX, D. 2009. Down-regulation of CXCR4 and CD62L in chronic lymphocytic leukemia cells is triggered by B-cell receptor ligation and associated with progressive disease. *Cancer Res,* 69**,** 6387-95.

VON ANDRIAN, U. H. 1996. Intravital microscopy of the peripheral lymph node microcirculation in mice. *Microcirculation,* 3**,** 287-300.

VUILLIER, F., DUMAS, G., MAGNAC, C., PREVOST, M. C., LALANNE, A. I., OPPEZZO, P., MELANITOU, E., DIGHIERO, G. & PAYELLE-BROGARD, B. 2005. Lower levels of surface B-cell-receptor expression in chronic lymphocytic leukemia are associated with glycosylation and folding defects of the mu and CD79a chains. *Blood,* 105**,** 2933-40.

WALKER, K. F., LAPPIN, D. F., TAKAHASHI, K., HOPE, J., MACDONALD, D. G. & KINANE, D. F. 2000. Cytokine expression in periapical granulation tissue as assessed by immunohistochemistry. *Eur J Oral Sci,* 108**,** 195-201.

WALLS, E. V., DOYLE, M. G., PATEL, K. K., ALLDAY, M. J., CATOVSKY, D. & CRAWFORD, D. H. 1989. Activation and immortalization of leukaemic B cells by Epstein-Barr virus. *Int J Cancer,* 44**,** 846-53.

WALSBY, E., BUGGINS, A., DEVEREUX, S., JONES, C., PRATT, G., BRENNAN, P., FEGAN, C. & PEPPER, C. 2014. Development and characterization of a physiologically relevant model of lymphocyte migration in chronic lymphocytic leukemia. *Blood,* 123**,** 3607-17.

WALTER, H. S., RULE, S. A., DYER, M. J., KARLIN, L., JONES, C., CAZIN, B., QUITTET, P., SHAH, N., HUTCHINSON, C. V., HONDA, H., DUFFY, K., BIRKETT, J., JAMIESON, V., COURTENAY-LUCK, N., YOSHIZAWA, T., SHARPE, J., OHNO, T., ABE, S., NISHIMURA, A., CARTRON, G., MORSCHHAUSER, F., FEGAN, C. & SALLES, G. 2016. A phase 1 clinical trial of the selective BTK inhibitor ONO/GS-4059 in relapsed and refractory mature B-cell malignancies. *Blood,* 127**,** 411-9.

WANG, C., GAO, C., ZHUANG, J. L., DING, C. & WANG, Y. 2012. A combined approach identifies three mRNAs that are down-regulated by microRNA-29b and promote invasion ability in the breast cancer cell line MCF-7. *J Cancer Res Clin Oncol,* 138**,** 2127-36.

WANG, H., LAFDIL, F., WANG, L., PARK, O., YIN, S., NIU, J., MILLER, A. M., SUN, Z. & GAO, B. 2011. Hepatoprotective versus oncogenic functions of STAT3 in liver tumorigenesis. *Am J Pathol,* 179**,** 714-24.

WEKERLE, H. & KETELSEN, U. P. 1980. Thymic nurse cells--Ia-bearing epithelium involved in T-lymphocyte differentiation? *Nature,* 283**,** 402-4.

WEN, W., LIANG, W., WU, J., KOWOLIK, C. M., BUETTNER, R., SCUTO, A., HSIEH, M. Y., HONG, H., BROWN, C. E., FORMAN, S. J., HORNE, D., MORGAN, R., WAKABAYASHI, M., DELLINGER, T. H., HAN, E. S., YIM, J. H. & JOVE, R. 2014. Targeting JAK1/STAT3 signaling suppresses tumor progression and metastasis in a peritoneal model of human ovarian cancer. *Mol Cancer Ther,* 13**,** 3037-48.

WEN, Z., ZHONG, Z. & DARNELL, J. E., JR. 1995. Maximal activation of transcription by Stat1 and Stat3 requires both tyrosine and serine phosphorylation. *Cell,* 82**,** 241-50.

WENDLAND, M., WILLENZON, S., KOCKS, J., DAVALOS-MISSLITZ, A. C., HAMMERSCHMIDT, S. I., SCHUMANN, K., KREMMER, E., SIXT, M., HOFFMEYER, A., PABST, O. & FORSTER, R. 2011. Lymph node T cell homeostasis relies on steady state homing of dendritic cells. *Immunity,* 35**,** 945-57.

WHITFIELD, M. J., LEE, W. C. & VAN VLIET, K. J. 2013. Onset of heterogeneity in culture-expanded bone marrow stromal cells. *Stem Cell Res,* 11**,** 1365-77.

WIDNEY, D. P., GUI, D., POPOVICIU, L. M., SAID, J. W., BREEN, E. C., HUANG, X., KITCHEN, C. M., ALCANTAR, J. M., SMITH, J. B., DETELS, R. & MARTINEZ-MAZA, O. 2010. Expression and Function of the Chemokine, CXCL13, and Its Receptor, CXCR5, in Aids-Associated Non-Hodgkin's Lymphoma. *AIDS Res Treat,* 2010**,** 164586.

WILLIAM, J., EULER, C., CHRISTENSEN, S. & SHLOMCHIK, M. J. 2002. Evolution of autoantibody responses via somatic hypermutation outside of germinal centers. *Science,* 297**,** 2066-70.

WINKLER, D., SCHNEIDER, C., KROBER, A., PASQUALUCCI, L., LICHTER, P., DOHNER, H. & STILGENBAUER, S. 2005. Protein expression analysis of chromosome 12 candidate genes in chronic lymphocytic leukemia (CLL). *Leukemia,* 19**,** 1211-5.

WOYACH, J. A., BOJNIK, E., RUPPERT, A. S., STEFANOVSKI, M. R., GOETTL, V. M., SMUCKER, K. A., SMITH, L. L., DUBOVSKY, J. A., TOWNS, W. H., MACMURRAY, J., HARRINGTON, B. K., DAVIS, M. E., GOBESSI, S., LAURENTI, L., CHANG, B. Y., BUGGY, J. J., EFREMOV, D. G., BYRD, J. C. & JOHNSON, A. J. 2014a. Bruton's tyrosine kinase (BTK) function is important to the development and expansion of chronic lymphocytic leukemia (CLL). *Blood,* 123**,** 1207-13.

WOYACH, J. A., FURMAN, R. R., LIU, T. M., OZER, H. G., ZAPATKA, M., RUPPERT, A. S., XUE, L., LI, D. H., STEGGERDA, S. M., VERSELE, M., DAVE, S. S., ZHANG, J., YILMAZ, A. S., JAGLOWSKI, S. M., BLUM, K. A., LOZANSKI, A., LOZANSKI, G., JAMES, D. F., BARRIENTOS, J. C., LICHTER, P., STILGENBAUER, S., BUGGY, J. J., CHANG, B. Y., JOHNSON, A. J. & BYRD, J. C. 2014b. Resistance mechanisms for the Bruton's tyrosine kinase inhibitor ibrutinib. *N Engl J Med,* 370**,** 2286-94.

WOYACH, J. A., JOHNSON, A. J. & BYRD, J. C. 2012. The B-cell receptor signaling pathway as a therapeutic target in CLL. *Blood,* 120**,** 1175-84.

WOYACH, J. A., RUPPERT, A. S., GUINN, D., LEHMAN, A., BLACHLY, J. S., LOZANSKI, A., HEEREMA, N. A., ZHAO, W., COLEMAN, J., JONES, D., ABRUZZO, L., GORDON, A., MANTEL, R., SMITH, L. L., MCWHORTER, S., DAVIS, M., DOONG, T. J., NY, F., LUCAS, M., CHASE, W., JONES, J. A., FLYNN, J. M., MADDOCKS, K., ROGERS, K., JAGLOWSKI, S., ANDRITSOS, L. A., AWAN, F. T., BLUM, K. A., GREVER, M. R., LOZANSKI, G., JOHNSON, A. J. & BYRD, J. C. 2017. BTKC481S-Mediated Resistance to Ibrutinib in Chronic Lymphocytic Leukemia. *J Clin Oncol,* 35**,** 1437-1443.

WU, J., ZHANG, M. & LIU, D. 2016. Acalabrutinib (ACP-196): a selective second-generation BTK inhibitor. *J Hematol Oncol,* 9**,** 21.

XIE, T. X., WEI, D., LIU, M., GAO, A. C., ALI-OSMAN, F., SAWAYA, R. & HUANG, S. 2004. Stat3 activation regulates the expression of matrix metalloproteinase-2 and tumor invasion and metastasis. *Oncogene,* 23**,** 3550-60.

XU, D. & QU, C. K. 2008. Protein tyrosine phosphatases in the JAK/STAT pathway. *Front Biosci,* 13**,** 4925-32.

YAGO, T., TSUKUDA, M., TAJIMA, H., NISHI, T., KURATA-MIURA, K., OHKUBO, J. & MINAMI, M. 1997. Analysis of initial attachment of B cells to endothelial cells under flow conditions. *J Immunol,* 158**,** 707-14.

YAGO, T., WU, J., WEY, C. D., KLOPOCKI, A. G., ZHU, C. & MCEVER, R. P. 2004. Catch bonds govern adhesion through L-selectin at threshold shear. *J Cell Biol,* 166**,** 913-23.

YAHIAOUI, A., MEADOWS, S. A., SORENSEN, R. A., CUI, Z. H., KEEGAN, K. S., BROCKETT, R., CHEN, G., QUEVA, C., LI, L. & TANNHEIMER, S. L. 2017. PI3Kdelta inhibitor idelalisib in combination with BTK inhibitor ONO/GS-4059 in diffuse large B cell lymphoma with acquired resistance to PI3Kdelta and BTK inhibitors. *PLoS One,* 12**,** e0171221.

YIN, D., WAKIMOTO, N., XING, H., LU, D., HUYNH, T., WANG, X., BLACK, K. L. & KOEFFLER, H. P. 2008. Cucurbitacin B markedly inhibits growth and rapidly affects the cytoskeleton in glioblastoma multiforme. *Int J Cancer,* 123**,** 1364-75.

YOO, J. Y., HUSO, D. L., NATHANS, D. & DESIDERIO, S. 2002. Specific ablation of Stat3beta distorts the pattern of Stat3-responsive gene expression and impairs recovery from endotoxic shock. *Cell,* 108**,** 331-44.

YOUNG, L., SUNG, J., STACEY, G. & MASTERS, J. R. 2010. Detection of Mycoplasma in cell cultures. *Nat Protoc,* 5**,** 929-34.

YUAN, Z. L., GUAN, Y. J., CHATTERJEE, D. & CHIN, Y. E. 2005. Stat3 dimerization regulated by reversible acetylation of a single lysine residue. *Science,* 307**,** 269-73.

ZAMMARCHI, F., DE STANCHINA, E., BOURNAZOU, E., SUPAKORNDEJ, T., MARTIRES, K., RIEDEL, E., CORBEN, A. D., BROMBERG, J. F. & CARTEGNI, L. 2011. Antitumorigenic potential of STAT3 alternative splicing modulation. *Proc Natl Acad Sci U S A,* 108**,** 17779-84.

ZARNEGAR, B. J., WANG, Y., MAHONEY, D. J., DEMPSEY, P. W., CHEUNG, H. H., HE, J., SHIBA, T., YANG, X., YEH, W. C., MAK, T. W., KORNELUK, R. G. & CHENG, G. 2008. Noncanonical NF-kappaB activation requires coordinated assembly of a regulatory complex of the adaptors cIAP1, cIAP2, TRAF2 and TRAF3 and the kinase NIK. *Nat Immunol,* 9**,** 1371-8.

ZENZ, T., FROHLING, S., MERTENS, D., DOHNER, H. & STILGENBAUER, S. 2010. Moving from prognostic to predictive factors in chronic lymphocytic leukaemia (CLL). *Best Pract Res Clin Haematol,* 23**,** 71-84.

ZENZ, T., KROBER, A., SCHERER, K., HABE, S., BUHLER, A., BENNER, A., DENZEL, T., WINKLER, D., EDELMANN, J., SCHWANEN, C., DOHNER, H. & STILGENBAUER, S. 2008. Monoallelic TP53 inactivation is associated with poor prognosis in chronic lymphocytic leukemia: results from a detailed genetic characterization with long-term follow-up. *Blood,* 112**,** 3322-9.

ZHANG, H. F., CHEN, Y., WU, C., WU, Z. Y., TWEARDY, D. J., ALSHAREEF, A., LIAO, L. D., XUE, Y. J., WU, J. Y., CHEN, B., XU, X. E., GOPAL, K., GUPTA, N., LI, E. M., XU, L. Y. & LAI, R. 2016. The Opposing Function of STAT3 as an Oncoprotein and Tumor Suppressor Is Dictated by the Expression Status of STAT3beta in Esophageal Squamous Cell Carcinoma. *Clin Cancer Res,* 22**,** 691-703.

ZHANG, Q., NOWAK, I., VONDERHEID, E. C., ROOK, A. H., KADIN, M. E., NOWELL, P. C., SHAW, L. M. & WASIK, M. A. 1996. Activation of Jak/STAT proteins involved in signal transduction pathway mediated by receptor for interleukin 2 in malignant T lymphocytes derived from cutaneous anaplastic large T-cell lymphoma and Sezary syndrome. *Proc Natl Acad Sci U S A,* 93**,** 9148-53.

ZHANG, X., SUN, Y., PIREDDU, R., YANG, H., URLAM, M. K., LAWRENCE, H. R., GUIDA, W. C., LAWRENCE, N. J. & SEBTI, S. M. 2013. A novel inhibitor of STAT3 homodimerization selectively suppresses STAT3 activity and malignant transformation. *Cancer Res,* 73**,** 1922-33.

ZHANG, X., YUE, P., PAGE, B. D., LI, T., ZHAO, W., NAMANJA, A. T., PALADINO, D., ZHAO, J., CHEN, Y., GUNNING, P. T. & TURKSON, J. 2012. Orally bioavailable small-molecule inhibitor of transcription factor Stat3 regresses human breast and lung cancer xenografts. *Proc Natl Acad Sci U S A,* 109**,** 9623-8.

ZHAO, L., SHEY, M., FARNSWORTH, M. & DAILEY, M. O. 2001. Regulation of membrane metalloproteolytic cleavage of L-selectin (CD62l) by the epidermal growth factor domain. *J Biol Chem,* 276**,** 30631-40.

ZHAO, S. H., ZHAO, F., ZHENG, J. Y., GAO, L. F., ZHAO, X. J. & CUI, M. H. 2011. Knockdown of stat3 expression by RNAi inhibits in vitro growth of human ovarian cancer. *Radiol Oncol,* 45**,** 196-203.

ZHONG, Z., WEN, Z. & DARNELL, J. E., JR. 1994. Stat3: a STAT family member activated by tyrosine phosphorylation in response to epidermal growth factor and interleukin-6. *Science,* 264**,** 95-8.

ZHOU, T., GEORGEON, S., MOSER, R., MOORE, D. J., CAFLISCH, A. & HANTSCHEL, O. 2014. Specificity and mechanism-of-action of the JAK2 tyrosine kinase inhibitors ruxolitinib and SAR302503 (TG101348). *Leukemia,* 28**,** 404-7.

ZUCCHETTO, A., BOMBEN, R., DAL BO, M., BULIAN, P., BENEDETTI, D., NANNI, P., DEL POETA, G., DEGAN, M. & GATTEI, V. 2006. CD49d in B-cell chronic lymphocytic leukemia: correlated expression with CD38 and prognostic relevance. *Leukemia,* 20**,** 523-5; author reply 528-9.

ZUCCHETTO, A., VAISITTI, T., BENEDETTI, D., TISSINO, E., BERTAGNOLO, V., ROSSI, D., BOMBEN, R., DAL BO, M., DEL PRINCIPE, M. I., GORGONE, A., POZZATO, G., GAIDANO, G., DEL POETA, G., MALAVASI, F., DEAGLIO, S. & GATTEI, V. 2012. The CD49d/CD29 complex is physically and functionally associated with CD38 in B-cell chronic lymphocytic leukemia cells. *Leukemia,* 26**,** 1301-12.

ZUGOWSKI, C., LIEDER, F., MULLER, A., GASCH, J., CORVINUS, F. M., MORIGGL, R. & FRIEDRICH, K. 2011. STAT3 controls matrix metalloproteinase-1 expression in colon carcinoma cells by both direct and AP-1-mediated interaction with the MMP-1 promoter. *Biol Chem,* 392**,** 449-59.

Appendix 1: Mycoplasma testing of Hs5, HG3 and I83 cell lines

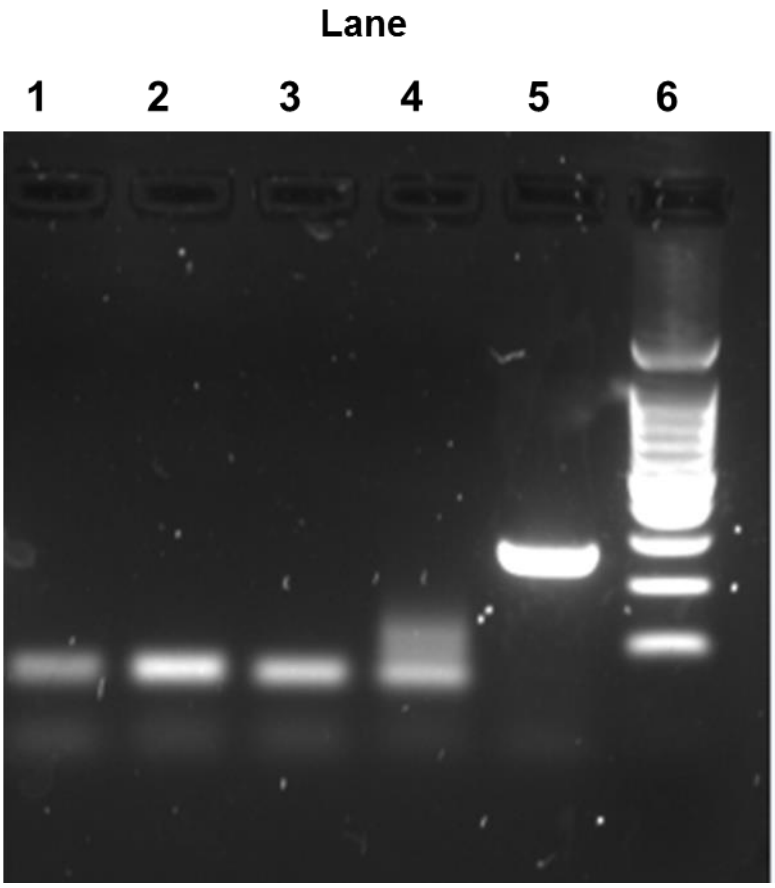

Agarose gel electrophoresis of PCR amplified products generated from Hs5, HG3 and I83 cell line supernatents. Equal volumes of PCR reactions containing Green GoTaq were loaded on a 2 % agarose gel and imaged under UV light. Lane 1, 2 and 3 show Hs5 BMSC, HG3 and I83 cell lines negative for mycoplasma. Lane 4 is the negative control, negative for mycoplasma and Lane 5 is the positive control showing a positive mycoplasma band at 270bp. Lane 6 contains the 100bp ladder.

Appendix 2: Effect of increasing concentrations of siRNA on transfection efficiency in CLL cells

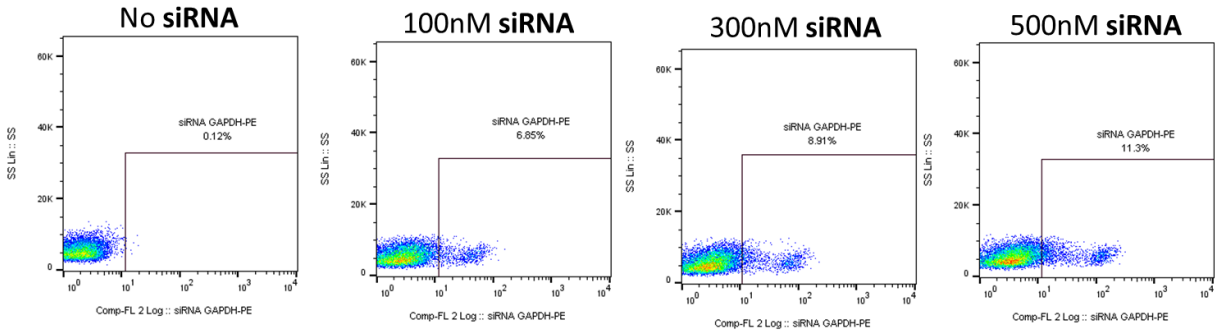

Dotplots showing the transfection efficiency in CLL cells using 100nM, 300nM and 500nM of fluorescent siRNA. Transfection efficiency was measured by the percentage of fluorescent siRNA positive cells indicated on the dotplots.

Appendix 3: Protein list and fold changes of phosphorylation for Proteome Profiler Phospho-Kinase Array

Fold changes in phosphorylation of proteins listed after 15 minutes BCR stimulation (IgM) compared to Untreated CLL cells

	Mean Intensity Units (average of duplicates)		Fold Change	
Protein (Phos Site)	**Untreated**	**IgM 15 minutes**	**≥2**	**≥1.5 <2**
p38 (T180,Y182)	4692	6748.5		
ERK1/2 (T202/Y204)	5393	18374	3.4	
JNK1/2/3 (T183/Y185)	7634.5	10069.5		
GSK-3 (S21/S9)	24980.5	38263		1.5
EGFR (Y1086)	3627.5	4663		
MSK1/2 (S376/S360)	28042	31716		
AMPK1 (T183)	14123.5	17446.5		
Akt1/2/3 S473	3347	14296.5	4.3	
TOR (S2488)	4193.5	3372		
CREB (S133)	43022	44403.5		
HSP27 (S78/S82)	7925.5	9571.5		
AMPK2 (T172)	13518	14297.5		
β-Catenin	3478.5	4214		
Src (Y419)	13231.5	11695		
Lyn (Y397)	10248.5	10852		
Lck(Y394)	3210.5	3366.5		
STAT2 (Y689)	22768	23824.5		
STAT5a(Y694)	9759	9311		
Fyn (Y420)	5704.5	4941.5		
Yes (Y426)	9189	9531		
Fgr(Y412)	3205	3913		
STAT6 (Y641)	16013	17061		
STAT5b (Y699)	12635	13307.5		
Hck (Y411)	8336.5	5779.5		
Chk-2 (T68)	9651	11348.5		
FAK (Y397)	18955.5	29214		1.5
PDGF R (Y751)	5350.5	5700.5		
STAT5 a/b (Y694/Y699)	12595.5	13736		
PRAS40 (T246)	21736.5	26074.5		
p53 (S392)	2700	2802		
Akt1/2/3 (T308)	9669.5	10988.5		
p53 (S46)	12628.5	11869.5		
p70 S6 Kinase (T389)	3561.5	8559.5	2.4	
p53 (S15)	1968	2992		
c-Jun (S63)	10023	13114		
p70 S6 Kinase (T421/S424)	12821	12806.5		
RSK1/2/3 (S380/S386/S377)	3683.5	4337.5		
eNOS (S1177)	2526.5	2933		
STAT3 (Y705)	3114.5	4658		
p27 (T198)	38050.5	39587		
PLC-γ1 (Y783)	1132	2618.5		
STAT3 (S727)	1296.5	2634	2	
WNK1 (T60)	24222	36568.5		1.5
PYK2 (Y402)	3524.5	5299		
HSP60	18557	34786		1.9

BCR stimulation was performed by incubating $2.5x10^7$ CLL cells with 10µg/ml $F(ab')_2$ IgM fragments for 15 minutes Protein was extracted and 400µg was loaded onto the membranes. Membranes were treated as per manufacturer's instructions. Blot intensities were calculated using Image J (V.1.5) with Protein Profiler add-on software.

Fold changes in phosphorylation of proteins listed after 4 hours BCR stimulation (IgM) compared to Untreated CLL cells

	Mean Intensity Units (average of duplicates)		Fold Change	
Protein (Phos Site)	**Untreated**	**IgM 4 hours**	**≥2**	**≥1.5 <2**
p38 (T180,Y182)	30180	39856		
ERK1/2 (T202/Y204)	38512	37256		
JNK1/2/3 (T183/Y185)	21874	30679		
GSK-3(S21/S9)	74292	79081		
EGFR (Y1086)	53059	62078		
MSK1/2 (S376/S360)	35195	43941		
AMPK1 (T183)	100695	61927		-1.6
Akt1/2/3 S473	6984	8084		
TOR (S2488)	13710	13446		
CREB (S133)	30829	7266	-4.2	
HSP27 (S78/S82)	29163	39131		
AMPK2 (T172)	60456	56863		
β-Catenin	2767	3747		
Src (Y419)	14529	20714		
Lyn (Y397)	97417	93624		
Lck(Y394)	5922	8451		
STAT2 (Y689)	76892	84671		
STAT5a(Y694)	45663	53695		
Fyn (Y420)	12447	22437		
Yes (Y426)	18975	27569		
Fgr(Y412)	3750	5155		
STAT6 (Y641)	54268	49833		
STAT5b (Y699)	48263	47150		
Hck (Y411)	13047	18618		
Chk-2 (T68)	36319	33968		
FAK (Y397)	7618	7174		
PDGF R (Y751)	13803	12484		
STAT5 a/b (Y694/Y699)	16904	19919		
PRAS40 (T246)	19866	18960		
p53 (S392)	2989	8169	2.7	
Akt1/2/3 (T308)	10725	21099		1.9
p53 (S46)	41176	55333		
p70 S6 Kinase (T389)	1555	5231	3.3	
p53 (S15)	3104	5181		1.7
c-Jun (S63)	12738	18870		
p70 S6 Kinase (T421/S424)	93751	111720		
RSK1/2/3 (S380/S386/S377)	5956	10042		
eNOS (S1177)	-301	71.5		
STAT3 (Y705)	8563	130914	15.2	
p27 (T198)	133576	150152		
PLC-γ1 (Y783)	2096	3132		
STAT3 (S727)	5031	135810	27	
WNK1 (T60)	153427	146722		
PYK2 (Y402)	4506	6740		
HSP60	14903	8397		1.8

BCR stimulation was performed by incubating $2.5x10^7$ CLL cells with 10μg/ml $F(ab')_2$ IgM fragments for 4 hours. Protein was extracted and 400μg was loaded onto the membranes. Membranes were treated as per manufacturer's instructions. Blot intensities were calculated using Image J (V.1.5) with Protein Profiler add-on software.

Fold changes in phosphorylation of proteins listed after 4 hours BCR stimulation (IgM) with Ruxolitinib pretreatment compared to BCR stimulated CLL cells

	Mean Intensity Units (average of duplicates)		Fold Change	
Protein (Phos Site)	**IgM 4 hours**	**IgM+Rux 4 hours**	**≥2**	**≥1.5 <2**
p38 (T180,Y182)	39856	41547.5		
ERK1/2 (T202/Y204)	37256	17598	-2.1	
JNK1/2/3 (T183/Y185)	30679	30731.5		
GSK-3(S21/S9)	79081	79770.5		
EGFR (Y1086)	62078	61723.5		
MSK1/2 (S376/S360)	43941	42725.5		
AMPK1 (T183)	61927	101039.5		1.6
Akt1/2/3 S473	8084	6887		
TOR (S2488)	13446	18266.5		
CREB (S133)	7266	15236.5	2	
HSP27 (S78/S82)	39131	26476.5		
AMPK2 (T172)	56863	66941.5		
β-Catenin	3747	2410		
Src (Y419)	20714	17368.5		
Lyn (Y397)	93624	89228.5		
Lck(Y394)	8451	8877.5		
STAT2 (Y689)	84671	79424		
STAT5a(Y694)	53695	56652.5		
Fyn (Y420)	22437	21985.5		
Yes (Y426)	27569	18144.5		
Fgr(Y412)	5155	4162		
STAT6 (Y641)	49833	45474		
STAT5b (Y699)	47150	47752.5		
Hck (Y411)	18618	17430		
Chk-2 (T68)	33968	38178		
FAK (Y397)	7174	6625.5		
PDGF R (Y751)	12484	11651.5		
STAT5 a/b (Y694/Y699)	19919	16179.5		
PRAS40 (T246)	18960	21311.5		
p53 (S392)	8169	10366.5		
Akt1/2/3 (T308)	21099	31654		
p53 (S46)	55333	84436.5		1.5
p70 S6 Kinase (T389)	5231	6574		
p53 (S15)	5181	6842.5		
c-Jun (S63)	18870	19046		
p70 S6 Kinase (T421/S424)	111720	116184.5		
RSK1/2/3 (S380/S386/S377)	10042	13449		
eNOS (S1177)	71.5	-320		
STAT3 (Y705)	130914	21145	-6	
p27 (T198)	150152	142917		
PLC-γ1 (Y783)	3132	3615.5		
STAT3 (S727)	135810	8178	-16	
WNK1 (T60)	146722	99962.5		
PYK2 (Y402)	6740	6449		
HSP60	8397	8957.5		

BCR stimulation was performed by incubating $2.5x10^7$ CLL cells with 10µg/ml $F(ab)_2$ IgM fragments or CLL cells were incubated with 1µM Ruxolitinib for 1 hour before stimulation. Protein was extracted and 400µg was loaded onto the membranes. Membranes were treated as per manufacturer's instructions. Blot intensities were calculated using Image J (V.1.5) with Protein Profiler add-on software.

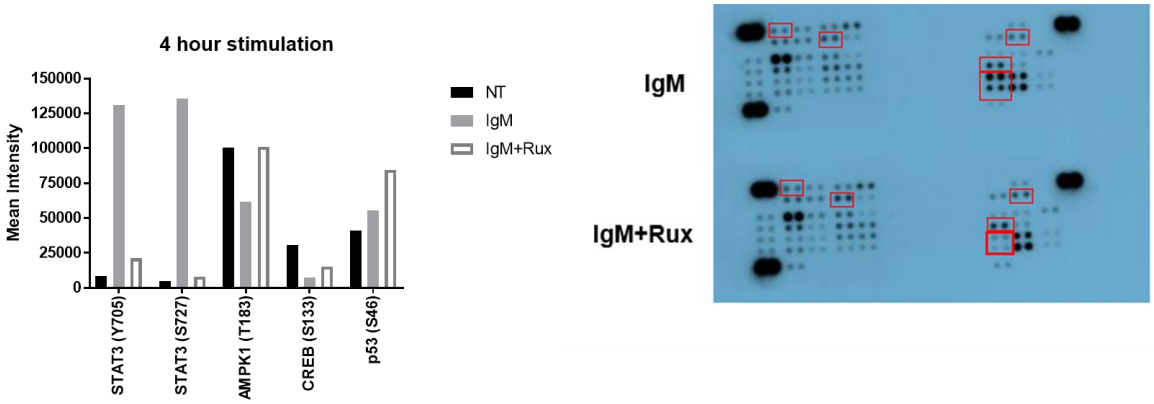

BCR stimulation was performed by incubating 2.5x10^7 CLL cells with 10µg/ml F(ab)$_2$ IgM fragments or CLL cells were incubated with 1µM Ruxolitinib for 1 hour before stimulation. Protein was extracted and 400µg was loaded onto the membranes. Membranes were treated as per manufacturer's instructions. Blot intensities were calculated using Image J (V.1.5) with Protein Profiler add-on software.

Appendix 4: List of genes and expression changes for the Taqman Extracellular Matrix and Adhesion Molecule Array

Fold changes in gene expression after 4 hours BCR stimulation (IgM) with Ruxolitinib pretreatment and BCR stimulated CLL cells compared to untreated

Gene	Fold Change after IgM stimulation (vs NT)	Fold Change after IgM+Ruxolitinib (vs NT)
COL4A2	4.0321	1.5049
COL7A1	2.0249	4.0432
CTNNA1	2.089	2.0887
ICAM1	3.9494	4.028
ITGA1	2.0173	2.0037
ITGA3	2.0151	1.99
SPP1	2.0633	1.0201
TNC	7.2177	7.739
COL5A1	-7.278	1.054
ECM1	-2.0308	1.0107
FN1	-2.16122	-2.0816
ITGA5	-2.0379	-2.008
ITGB5	-3.9872	-7.86782
KAL1	-6.93962	1.1081
MMP1	-6.2266	1.2026
MMP11	-3.9872	-3.96983
MMP2	-6.5616	-6.5018
TGFBI	-4.0883	-2.1023
THBS1	-4.086636	-2.0271
VCAN	-31.746031	-31.5457
18S	1.0152	0.9986
ACTB	0.9849	1.9751
ADAMTS1	0.9695	1.0189
ADAMTS13	1.0046	1.007
ADAMTS8	1.0033	1.0032
B2M	1.0009	1.0101
CD44	1	1.0019
CDH1	0.9875	0.994
CLEC3B	0.9928	1.003
CNTN1	1.0033	7.0982
COL11A1	1.0033	1.0032
COL12A1	0.5019	1.0026
COL14A1	1.0033	1.0032
COL15A1	1.011	1.0019
COL16A1	1.0033	1.0032
COL1A1	1.0292	1.0359
COL6A1	1.0259	1.0404
COL6A2	1.0098	0.9977
COL8A1	1.0033	1.0032
CTGF	1.0033	6.6155
CTNNB1	1.0008	2.0316
CTNND1	0.9964	2.0005
CTNND2	1.0033	1.0032
GAPDH	0.9932	0.993
GUSB	1.0195	1.0092
HAS1	1.8365	3.675
HMBS	1.0071	1.003

BCR stimulation was performed by incubating $2x10^7$ CLL cells with 10µg/ml $F(ab)_2$ IgM fragments or CLL cells were incubated with 1µM Ruxolitinib for 1 hour before stimulation. RNA was extracted and converted to cDNA 50g was loaded per well of the Taqman Array 96 well plate and was analysed on an ABI7500. Fold changes were calculated by the Comparative Ct ($2^{-\Delta\Delta Ct}$) relative quantitation method.

Fold changes in gene expression after 4 hours BCR stimulation (IgM) with Ruxolitinib pretreatment and BCR stimulated CLL cells compared to untreated

HPRT1	1.0039	1.0049
ITGA2	1.0027	1.0169
ITGA4	1.0066	2.0421
ITGA6	1.9942	1.0084
ITGA7	1.004	2.0245
ITGA8	1.0033	1.0032
ITGAL	1.0186	1.0226
ITGAM	0.9933	0.9929
ITGAV	1.0113	1.0013
ITGB1	1.0165	1.0234
ITGB2	1.0173	1.0181
ITGB3	1.007	1.0099
ITGB4	1.0826	1.1013
LAMA1	1.0033	1.0032
LAMA2	0.9786	-1.9725
LAMA3	1.3207	1.2751
LAMB1	1.0033	1.0032
LAMB3	1.0031	1.0044
LAMC1	0.9967	0.9964
MMP10	1.1824	1.3426
MMP12	1.0033	1.0032
MMP13	1.1748	1.1341
MMP14	1.0265	1.0154
MMP15	0.9922	0.999
MMP16	1.0033	1.0032
MMP3	1.0033	1.0032
MMP7	0.9917	0.9952
MMP8	1.0033	1.0032
MMP9	0.5016	0.5028
NCAM1	1	1.0006
PECAM1	1.002	1.0186
PGK1	0.9917	0.9948
PPIA	0.9939	0.9893
RPLP0	0.9904	0.9925
SELE	1.0033	1.0032
SELL	1.9459	-2.0049
SELP	1.0109	1.0204
SGCE	1.0324	1.0297
SPARC	0.4991	0.9934
SPG7	1.0063	1.0087
TBP	0.5033	0.5624
THBS2	1.0296	-6.8918
THBS3	0.9987	0.987
TIMP1	0.506	0.5069
TIMP2	0.5961	0.5635
TIMP3	0.9552	0.9576
UBC	2.0776	1.0048
VCAM1	0.9975	1.0057
VTN	0.9831	0.9813

BCR stimulation was performed by incubating $2x10^7$ CLL cells with 10µg/ml $F(ab)_2$ IgM fragments or CLL cells were incubated with 1µM Ruxolitinib for 1 hour before stimulation. RNA was extracted and converted to cDNA 50g was loaded per well of the Taqman Array 96 well plate and was analysed on an ABI7500. Fold changes were calculated by the Comparative Ct ($2^{-\Delta\Delta Ct}$) relative quantitation method.